Identification of mechanosensitive guanine nucleotide exchange factors (GEFs) : role in Vascular Homeostasis

Surya Prakash Rao Batta

DOCTORAT BIOLOGIE BRETAGNE SANTE LOIRE

Nantes Université

THESE DE DOCTORAT DE

NANTES UNIVERSITE

ECOLE DOCTORALE N° 605
Biologie Santé
Spécialité : Biologie Cellulaire, Biologie du Développement

Par

Surya Prakash Rao BATTA

Identification of Mechanosensitive Guanine Nucleotide Exchange Factors (GEFs)

Role in Vascular Homeostasis

Thèse présentée et soutenue à Nantes, le 16 Novembre 2022
Unité de recherche : L'Institut du Thorax, INSERM UMR1087 – CNRS UMR 6291

Rapporteurs avant soutenance :

Muriel LAFFARGUE Directeur de recherche et INSERM U1297
Stephan HUVENEERS Associate Professor et Amsterdam UMC, University of Amsterdam

Composition du Jury :

Président :	Julie GAVARD	Directeur de recherche et INSERM U1307, CNRS UMR6075
Examinateurs :	Muriel LAFFARGUE	Directeur de recherche et INSERM U1297
	Stephan HUVENEERS	Associate Professor et Amsterdam UMC, University of Amsterdam
	Julie GAVARD	Directeur de recherche et INSERM U1307, CNRS UMR6075
	Jean-Sebastien SILVESTRE	Directeur de recherche INSERM et Paris Cardiovascular Research Center
Dir. de thèse :	Vincent SAUZEAU	Chargé de recherche et INSERM UMR1087, CNRS UMR6291
Co-dir. de thèse :	Anne-Clémence VION	Chargée de recherche et INSERM UMR1087, CNRS UMR6291

Invité(s)

Gervaise LOIRAND	Directeur de recherche et INSERM UMR1087/CNRS6291
Hubert DESAL	Professeur des universités-Praticien hospitalier et CHU de Nantes
Daniel HENRION	Directeur de recherche INSERM et Université d'Angers

Acknowledgement

I would like to express my gratitude to all the people who helped and supported me during my PhD thesis period.

Specially, I would like to thank Dr. Anne-Clemence VION, Dr. Gervaise LOIRAND, Dr. Vincent SAUZEAU for giving a chance to pursue my PhD in their lab and bringing an end to my long journey towards a PhD degree.

I would also like to thank Dr. Muriel LAFFARGUE and Assoc.Prof. Stephan HUVENEERS for agreeing to be my thesis rapporteurs.

I thank to Dr. Julie GAVARD, Dr. Jean-Sebastien SILVESTRE, Prof. Hubert DESAL and Dr. Daniel HENRION for accepting to participate as my thesis jury members.

I would like to thank Prof. Chantal BOULANGER and Dr. Emmanuel LEMICHEZ for being my thesis committee members and their insight comments and support during my CSI.

I would also like to thank lab members for their support during the experiments and doctoral school administrative work, without that it would be hard for me to navigate through as a non-French speaking foreign student.

Also, I would like to thank the funding sources “NEXT” and “Genavie” for providing financial support during my PhD tenure.

I would like to thank the core facilities especially the microscope facility and lab kitchen for their support and help to conduct my research successfully.

Last but not least, I would thank Dr. Colin JAMORA who is not only my well-wisher and mentor but also supported me immensely throughout my research career.

Table of Contents

ABBREVIATIONS

α-SMA – Alpha Smooth Muscle Actin
ACE2 – Angiotensin converting enzyme 2
AKAP12 – A-Kinase Anchoring Protein 12
ALK1 – Activin A receptor like type1
AMPK – AMP-activated protein kinase
Arf – ADP-ribosylation factor
AT1R - Angiotensin II type1 receptor
BAECs – Bovine Aortic Endothelial Cells
BMP9 – Bone morphogenetic protein9
Caco2 – Cancer Coli intestinal epithelial cells
Cav1 – Caveolin1
CBF-1/RBP-Jk - Cp-binding factor 1 (CBF-1)/recombination signal sequence-binding protein-J kappa
Cdc42 – Cell division control protein 42 homolog
CRB3A – Crumbs homolog 3a
CREB – cAMP response element-binding protein
CS – cyclic stretch
DH – Dbl homology
ECs – Endothelial Cells
E2F1 – E2F transcription factor 1
E2F3 – E2F transcription factor 3
eNOS – Endothelial nitric oxide synthase
ERK – Extracellular signal-regulated kinase
ET-1 – Endothelin-1
FoxO1 – Forkhead box protein O1
FRET – Fluorescence resonance energy transfer
G-Protein – Guanine nucleotide binding protein
GADD45 – Growth Arrest and DNA Damage-inducible 45
GEF – Guanine Nucleotide Exchange Factor
GPCR – G-protein Coupled Receptor
HAECs - Human Aortic Endothelial Cells
HCAECs – Human Coronary Artery Endothelial Cells
HCE – Human Corneal Epithelial Cells
HDMEC – Human Dermal Microvascular Endothelial Cells
HEK – Human embryonic kidney
Hey ½ - Hes related family BHLH transcription factor with YRPW motif1/2
HMEC-human mammary epithelial cells
IAP-1&2 – Inhibitors of apoptosis
ICE-CPP32 – Interleukin-1β-converting enzyme-like and cysteine protease protein-32 like family
IFT88 – Intraflagellar Transport 88
IGF-1R – Insulin-like growth factor1 receptor
JACOP – Junction-associated-coiled-coil protein
JAM-A – Junctional adhesion molecule A
JNK – c-Jun N-terminal kinase
KLF2 – Kruppel-like factor2
Ldlr – Low density lipoprotein receptor
MLC – Myosin Light Chain

MMP – Matrixmetalloproteinases
NFkB – Nuclear Factor Kappa B
Notch1/3 – Neurogenic locus notch homolog protein 1/3
NRP2 – Neuropilin2
p21 – Protein 21 cyclin dependent kinase inhibitor
PBD – Pleckstrin Binding Domain
PDCD4 – Programmed cell death 4
PDK1 – 3-phosphoinositide-dependent protein kinase1
PECAM1 – Platelet and Endothelial Cell Adhesion Molecule1
PH – Pleckstrin homology
PI3K – Phosphoinositide 3-kinase
PKA – Protein Kinase A
PTEN – Phosphatase and tensin homolog
Rab – Ras-associated binding
Rac – Ras-related C3 botulinum toxin substrate
Ran – Ras-related nuclear protein
Ras – Rat sarcoma virus
RBD – Rhotekin Binding Domain
RhoA – Ras homolog family memberA
ROCK – Rho associated protein kinase
ROS – Reactive Oxygen Species
SM-22α - Smooth Muscle protein 22 alpha
SM-MHC – Smooth Muscle Myosin Heavy Chain
Smad6&7 – Supressor of mothers against decapentaplegic 6/7
SP1 – Specificity protein 1
SRE – Serum Response Element
SRF – Serum Response Factor
SS – Shear Stress
STAT1 – Signal transducer and activator of transcription 1
TGFβ – Transforming growth factor beta
TRAF2 – TNF receptor associated factor 2
TRP – Transient receptor potential
TRPA – Transient receptor potential subfamily A
TRPC – Transient receptor potential cation channels
TRPM – Transient receptor potential melastatin
TRPP2 – Transient receptor potential polycystic 2
TRPV – Transient receptor potential subfamily A
VE-cad – Vascular endothelial cadherin
VSMCs – Vascular Smooth Muscle Cells
WASP – Wiskott Aldrich syndrome protein

FIGURES

TABLES

Résumé de thèse en français

La mécano-transduction joue un rôle crucial dans la formation, le maintien et le remodelage du réseau vasculaire en fonction de l'évolution des besoins (Campinho et al., 2020). L'hémodynamique exerce deux types de forces : les contraintes de cisaillement et l'étirement qui sont principalement perçus par les cellules endothéliales (CE) et les cellules musculaires lisses vasculaires (VSMC) respectivement (Dessalles et al., 2021). Les CE et les VSMC perçoivent les changements de force hémodynamiques et s'adaptent pour maintenir le tonus vasculaire et promouvoir un remodelage vasculaire physiologique (Green et al., 2017). Malheureusement, les mécanismes qui favorisent cette adaptation peuvent également entraîner un remodelage pathologique lorsque l'altération des forces hémodynamiques devient chronique, comme dans des conditions d'hypertension (Baeyens et al., 2016; Carmeliet & Jain, 2000; Dajnowiec & Langille, 2007). Les forces hémodynamiques physiologiques maintiennent les cellules vasculaires dans un état sain quiescent et anti-inflammatoire. Cependant, les altérations hémodynamiques soit générant des contraintes hypo-physiologiques soit supra-physiologiques entraînent la prolifération des cellules vasculaires, un état pro-inflammatoire et favorisent leur dédifférenciation et la perméabilité vasculaire. Il a été démontré qu'elles sont associées à des pathologies vasculaires telles que l'athérosclérose ou encore l'anévrismes de l'aorte ou intracranien (Bennett et al., 2016 ; Deng et al., 2015; Marziano et al., 2021 ; Petsophonsakul et al., 2019).

Le cytosquelette cellulaire fournit un soutien structurel à la cellule et subit des modifications importantes en fonction du stimulus mécanique que la cellule perçoit. In-vivo, les régions aortiques qui reçoivent un flux physiologique élevé présentent des CE alignées dans le sens du flux, en comparaison, les cellules qui reçoivent un flux perturbé/faible sont désorganisées, démontrant ainsi l'effet des contraintes de cisaillement sur la réponse morphologique des CE (Hikita et al., 2018). Les cellules vasculaires expriment un large éventail de molécules mécano-sensibles allant des récepteurs de surface cellulaire aux protéines du cytosquelette. Parmis eux le complexe formé par les protéines PECAM1, VEGFRs et VE-cadherine a été fortement décrit comme participant à la régulation de nombreuses fonction mécano-sensibles et permet notamment d'établir le seuil de sensibilité physiologique d'un territoire vasculaire donné (Tzima et al., 2005). L'activation de ces molécules mécano-sensibles entraîne la

régulation de l'activité des petites GTPases, des protéines clés impliquées dans le remodelage du cytosquelette. Parmi les protéines de la famille Rho-GTPase, RhoA, Rac1 et Cdc42 ont été largement décrites pour leur rôle dans le remodelage du cytosquelette, permettant le maintien de la polarité cellulaire, la migration cellulaire et le control de la morphologie cellulaire (Etienne-Manneville & Hall, 2002). Par exemple, in-vitro, il a été démontré que les petites GTPases sont cruciales pour l'alignement des CE parallèlement à la direction du flux en condition physiologique (Tzima, 2006). Il est important de noter que l'altération de l'activité de ces petites GTPases a été associée à des maladies cardiovasculaires telles que l'hypertension (Lee et al., 2004).

Comme d'autres GTPases, les Rho-GTPases passent de la forme inactive liée au GDP à la forme active liée au GTP. Cette transition entre la forme inactive et la forme active est médiée par des facteurs d'échange de guanine (GEF), tandis que les protéines d'activation des GTPases (GAP) permettent le retour à la forme inactive liée au GDP. Outre les GEF et les GAP, les inhibiteurs de dissociation de guanine (GDI) régulent également l'activité des petites Rho-GTPases en les séquestrant dans le cytosol, réduisant ainsi leur accessibilité aux GEF à la membrane. En plus de cette régulation, il a été démontré que les Rho-GTPases sont régulées aux niveaux épigénétique, post-transcriptionnel et post-traductionnel (Chen et al., 2011; Hodge & Ridley, 2016; Liu et al., 2012; Yoon et al., 2007). Ainsi, l'expression et l'activation spécifiques dans certains types cellulaires, a des temps précis lors de l'embryogenese et au court du developpment déterminent la formation adéquate des vaisseaux sanguins (Kather & Kroll, 2013), leur perméabilité (Stockton et al., 2007), la migration des cellules vasculaires (Garrett et al., 2007), l'angiogenèse (Gambardella et al., 2010) et la transmigration des leucocytes (Van Rijssel et al., 2012).

Il existe près de 83 GEFs et 67 GAPs pour 20 Rho-GTPases et seulement 17 GAPs et 20 GEFs sont fortement exprimés dans l'endothélium (Van Buul et al., 2014 ; Vigil et al., 2010). Au cours des deux dernières décennies, l'implication de GEF tels que Arhgef1 (Guilluy et al., 2010), LARG (Wirth et al., 2008), ARHGEF11 (Zholdybayeva et al., 2018), ARHGEF12 (Zhang et al., 2015) et ARHGEF17 (Yang et al., 2018b) ont été décrites dans des maladies vasculaires pathologiques médiées par les contraintes de cisaillement,

telles que l'hypertension et l'anévrisme intracrânien. Bien que ces études soient peu nombreuses, elles laissent entrevoir l'association possible et l'implication de certains Rho-GEFs dans la pathogenèse des anévrismes intracrâniens. L'identification de ces GEFs nous aiderait donc à comprendre les mécanismes physiopathologiques de la formation des anévrismes intracrâniens.

Afin d'identifier les GEF mécano-sensibles, une analyse de séquençage ARN (3'SRP) a été réalisée à partir CE humaines et de VSMC aortiques primaires de rat soumises respectivement à différentes contraintes de cisaillement (physiologiques 16 dynes/cm2 et pathologiques 3,6 et 36 dynes/cm2) et différents degrés d'étirements cycliques (physiologiques 10%-1hz et pathologiques 20%-1hz). De plus, des artères provenant de rats spontanément hypertendus (SHR), de rats spontanément hypertendus sujets aux accidents vasculaires cérébrales (SHR-SP) et de rats wistar-kyoto (WKY, control normo-tendu) ont également été utilisés. A partir séquençage ARN sur les VSMCs, les ECs et les artères, nous avons pu identifier et valider avec succès trois GEFs : ARHGEF18, ARHGEF40 et Net1 ; dont les expressions étaient modulées en fonction des forces mécaniques subies par les cellules in-vitro ou in-vivo. Parmi les trois GEFs, nous nous sommes concentrés sur ARHGEF18 pour étudier son rôle dans la physiologie des CEs.

ARHGEF18, également connu sous le nom de p114-RhoGEF, est exprimé de manière ubiquitaire dans la plupart des types cellulaires et des tissus, avec une forte expression dans les reins et le pancréas, et une faible expression dans le cœur et le cerveau chez l'homme (Blomquist et al., 2000 ; Niu et al., 2003). Il a été démontré que ARHGEF18 interagit spécifiquement avec RhoA et active à la fois RhoA et Rac1 mais pas Cdc42 (Blomquist et al., 2000) (Herder et al., 2013 ; Niu et al., 2003). En tant que GEF spécifique de RhoA, il a été démontré qu'ARHGEF18 régule la phosphorylation de la MLC dépendante de RhoA-ROCK et la contractilité de l'actomyosine de manière spatio-temporelle (Terry et al., 2011). Dans les cellules épithéliales, il a été montré qu'ARHGEF18 est localisée aux jonctions serrées et joue un rôle dans leur maturation mais pas dans l'initiation de leur formation (Terry et al., 2011). Toujours dans les cellules épithéliales, ARHGEF18 exerce ses effets en interagissant avec de multiples partenaires protéiques tels que la myosine-IIA, ROCKII, Cinguline (Terry et al., 2011), LKB1 (X. Xu

et al., 2013) et EPB41L5 (Schell et al., 2017). L'extinction d'ARHGEF18 entraîne une discontinuité de la jonction ZO1 et une augmentation de la perméabilité (Terry et al., 2011) de la couche épithéliale ainsi qu'un réarrangement de la F-actine (Lu et al., 2017). L'extinction d'ARHGEF18 entraîne également une réduction de la migration des cellules épithéliales (Zaritsky et al., 2017). En plus de sa fonction dans l'activation de RhoA, le réarrangement du cytosquelette et la migration, il a été démontré que l'ARHGEF18 joue un rôle important dans la contraction des cellules épithéliales (Marivin et al., 2019) et le maintien de la polarité apico-basale en favorisant l'activation localisée de la signalisation RhoA-ROCK par interaction avec Patj et Ehm2 (Loie et al., 2015; Nakajima & Tanoue, 2011).

Bien que la fonction d'ARHGEF18 soit bien caractérisée dans les cellules épithéliales, très peu de travaux ont abordé le rôle d'ARHGEF18 dans les CE. Dans les CE, il a été montré qu'ARHGEF18 est localisé au niveau des jonctions serrées et qu'il est nécessaire pour la tension et l'intégrité de la jonction dans les CE microvasculaires (Tornavaca et al., 2015). In-vivo, la délétion complète d'ARHGEF18 entraîne une létalité embryonnaire (Beal et al., 2021). Cette létalité survient à cause d'un défaut de formation du placenta. Dans ce modèle, une vascularisation réduite et une augmentation d'hémorragies et d'œdèmes a été observés, suggérant une formation défectueuse du réseau vasculaire et de sa perméabilité en plus du rôle placentale.

D'un point de vue physiopathologique, ARHGEF18 a été identifiée comme surexprimée dans le cystadénocarcinome séreux ovarien, le carcinome épidermoïde et dans les cellules géantes tumorales polyploïdes induites par le chlorure de cobalt (F. Shi et al., 2021 ; C. Song et al., 2013 ; Q. Zhao et al., 2021). En outre, des mutations d'Arhgef18 ont été retrouvées dans la dégénérescence rétinienne adulte et chez des patients souffrant de fente orofaciale (Arno et al., 2017 ; El-Sibai et al., 2021).

Pour comprendre le rôle d'ARHGEF18 dans la réponse mécano-sensibles des CE, nous avons réalisé des expériences in vitro sur des CE sauvage, knockdown pour ARHGEF18 ou surexprimant ARHGEF18 sauvage ou GEF inactif. Nous avons montré que l'expression et l'activité d'ARHGEF18 sont modulées par le niveau de contraintes de

cisaillement appliqué. Il est intéressant de noter que l'activité d'ARHGEF18 est maximale lorsque les CE sont exposées à des contraintes physiologiques, ce qui suggère un rôle bénéfique de ce RhoGEF sur la biologie des CE. Cette activité élevée est associée à une expression plus faible de la protéine que dans les CE exposées à des contraintes de cisaillement pathologiques, suggérant qu'un défaut l'activation d'ARHGEF18 par en conditions pathologiques conduit à sa surexpression. Dans les CE, nous avons également démontré la spécificité d'ARHGEF18 pour RhoA. En effet, ARHGEF18 est incapable de se lier à Rac1 dans les CE, et ce quelques soit le niveau des contraintes de cisaillement. L'extinction d'ARHGEF18 dans les CE conduit à une baisse de l'activité total de RhoA, évaluée par précipitation d'affinité. Sachant qu'ARHGEF18 n'est pas le seul RhoGEF capable d'activer RhoA dans les CE, l'observation d'une réduction de l'activité de RhoA dans le lysat cellulaire total aurai pu etre manqué. Cela suggère donc qu'ARHEGF18 a un rôle essentiel dans l'activation de RhoA induite par les contraintes de cisaillement dans les CE. Dans les cellules épithéliales, ARHGEF18 peut se localiser à la fois aux jonctions adhérentes et aux jonctions serrées, en y étant recruté par Ga12 ou JAM-A respectivement (Acharya et al., 2018 ; Haas et al., 2020). Le seul autre article étudiant ARHGEF18 dans les CE a montré, par immunofluorescence, qu'ARHGEF18 est recruté aux jonctions serrées des CE microvasculaires dermiques par ZO-1 et JACOP (Tornavaca et al., 2015). Aucune de ces études n'a montré une interaction directe entre ARHGEF18 et ces protéines jonctionnelles. Nous n'avons malheureusement pas été en mesure de localiser ARHGEF18 in vitro dans les CE en immunofluorescence pour confirmer cette observation dans le teritoire artérielle. Cependant nous avons pu mettre en évidence que dans la rétine de souris adulte, ARHGEF18 est exprimer principalement dans les artères et non dans les veines ou dans le réseau capillaire. Cette observation suggère que l'expression d'ARHGEF18 est dépendante soit de la spécification artérielle soit des contraintes de cisaillement, les artères étant exposées à des niveaux de contraintes de cisaillement plus élevé que les veines ou les capillaires. De plus, nous avons réussi à co-précipiter ARHGEF18 avec ZO-1 et avec Claudine 5, montrant l'interaction directe d'ARHGEF18 avec deux protéines constituant les jonctions serrées dans les CE. De manière intéressante, dans les CE, ARHGEF18 n'interagit pas avec VE-Cadhérine, ce qui suggère que ARHGEF18 n'a pas de rôle direct sur l'établissement et la fonction des jonctions adhérentes. La surexpression du mutant Y260A-ARHGEF18

montre une rétention de ZO-1 dans le cytoplasme dans les cellules mutantes, ce qui suggère qu'ARHGEF18 participerait à la localisation de ZO-1 aux jonctions serrées dans les CE exposées à des contraintes de cisaillement physiologiques. Dans les cellules épithéliales, ARHGEF18 participe à l'adhésion cellulaire et à la migration collective via le control de la tension cellule-cellule (Terry et al., 2011) et le control de la communication à longue distance (Zaritsky et al., 2017). Dans nos mains, la migration et l'adhésion étaient également affectées dans les CE déficientes en ARHGEF18, ce qui suggère que des mécanismes similaires pourraient être en jeu. Il reste à déterminer si cela passe par des effecteurs similaires à ceux identifiés dans les cellules épithéliales, à savoir Patj, LKB1 et Lulu2.

Dans les CE, la tension cellule-cellule participe à la détection des contraintes de cisaillement permettant un comportement collectif des cellules. Nous avons pu démontrer que des CE déficientes en ARHGEF18 ne s'alignent plus dans le sens du flux en réponse à des contraintes de cisaillement physiologiques, réponse caractéristique de la santé endothéliale et du comportement collectif. Ces CE présentaient également une diminution de la localisation jonctionnelle de protéines de jonction serrée, ZO-1 et Claudin5. Nous avons pu également établir que ces CE déficientes en ARHGEF18 présentaient une déstabilisation de l'actine corticale. Il s'agit de la première observation montrant qu'un RhoGEF spécifique de RhoA peut contrôler la réponse des CE aux contraintes de cisaillement. Il est intéressant de noter que la perte d'ARHGEF18 ne perturbe pas seulement la jonction serrée dans des conditions de contraintes de cisaillement physiologiques mais altère également la formation et l'organisation des points focaux d'adhésions, ce qui suggère une communication croisée entre la jonction serrée et l'adhésion focale. En condition statique, nous avions déjà observé que les CE déficientes en ARHGEF18 adhéraient moins vite que les CE control. De manière intéressante, en observant l'adhésion unicellulaire des CE déficientes en ARHGEF18 sur un motif en L, nous avons pu mettre en évidence qu'elle forme des points focaux moins long que les CE control. Dans les ECs microvasculaires dermiques, ARHGEF18 participe au maintien de la vinculine jonctionnelle (Tornavaca et al., 2015). Comme la vinculine a été montrée comme un élément clé pour équilibrer la tension entre les adhésions focales et les jonctions d'adhérence (Birukova et al., 2016), il serait intéressant d'évaluer si

ARHGEF18 peut participer à la localisation de la vinculine au niveau des adhésions focales ou des jonctions serrées et donc favoriser leur stabilité. Pour comprendre plus finement comment ARHGEF18 participe à la réponse des CE aux contraintes de cisaillement, nous avons évalué l'effet de la délétion d'ARHGEF18 sur plusieurs voies de signalisation. Parmi les différentes voies de signalisation testées, seule p38 MAPK semble participer à l'effet d'ARHGEF18 puisque le l'éteintes d'ARHGEF18 réduit de manière significative le niveau de phosphorylation de p38 MAPK. L'inhibition de l'activité de p38 MAPK conduit à une perte d'alignement et une délocalisation de ZO-1 des jonctions similaires à ce qui est observé avec les CE déficientes en ARHGEF18. L'inhibition de p38 MAPK ne conduit cependant pas à la formation de gaps para-cellulaire contrairement au CE déficientes en ARHGEF18 suggérant que la signalisation en aval d'ARHGEF18 ne dépend pas entièrement de p38 MAPK. Les protéines RhoGEF ne sont pas seulement porteuses d'une activité GEF, mais présentent généralement des rôles supplémentaires en fonction de leur structure. Par exemple, il a été démontré que Trio, dans les CE, contribue à la localisation de Rac1 dans la cellule mais pas son activité bien qu'elle ait un domaine GEF spécifique pour Rac1 (Kroon et al., 2017). Dans nos mains, l'activité d'échange de nucléotides d'ARHGEF18 contribue à la formation des jonctions serrées car ZO-1 se délocalise des jonctions dans les CE exprimant le mutant GEF-inactif Y260A-ARHGEF18. De même que pour l'inhibition de p38 MAPK, la mutation Y260A ne conduit pas à la formation de gaps para-cellulaires, suggérant une fois de plus un rôle supplémentaire d'ARHGEF18 indépendant de son activité d'échange de nucléotides. Il est intéressant de noter que l'analyse RNA-seq des CE déficientes en ARHGEF18 a montré des altérations dans l'expression de nombreux marqueurs de l'inflammation. Nous avons donc commencé à investiguer le rôle potentiel d'ARHGEF18 dans la réponse anti-inflammatoire des CE soumises à des contraintes de cisaillement physiologique. Ainsi les CE déficientes pour ARHGEF18 présentent une diminution des niveaux de transcription de PTGS2 (codant pour la COX2, impliqué dans la synthèse des prostaglandines) en présence de TNFα sous contraintes de cisaillement physiologique en comparaison aux cellules contrôles.

En résumé, Nous avons pu mettre en évidence qu'ARHGEF18 est un RhoGEF dont l'expression et l'activité est dépendante des niveaux de contraintes de cisaillement.

ARHGEF18 participe à l'activation de RhoA et de p38 sous contraintes de cisaillement physiologiques et régule l'orientation des CE dans le sens du flux ainsi que la formation des jonction serrées via le son interaction directe avec ZO-1 et Claudine5. ARHGEF18 participe également à la formation des points focaux d'adhésion. Nous avons également montré que l'activité d'échange de nucléotide est essentielle à la formation des jonctions serrées sous flux.

Les travaux futurs viseront à mieux comprendre le rôle spécifique de ARHGEF18 dans la physiologie des cellules endothéliales et l'inflammation endothéliale in-vivo dans des conditions pathologiques.

INTRODUCTION

1. Mechanosignaling in Vascular system

1.1 History and importance of mechano-biology

Mechanotransduction plays a crucial part in shaping our life, from the way we hear the sound to how our organs are structured (Ingber, 2006). Nearly a century ago, a biologist, D'Arcy Thompson in his book "Growth and Form" proposed the relation between physics and/or mathematical principles in shaping the intricate structures we observe in living organisms (Thompson, 1917). Although, early mechanotransduction mostly stood for a physics and mathematical branch, it gained interest at cellular level with the early work of Sheetz and Singer showing that the two layers of erythrocyte membranes are connected through tension and altering one has an effect on the other (Sheetz & Singer, 1974), and with electron microscopy studies of microfilaments exhibiting tension during migration (Kolega, 1986). Another pioneering work by Huxley described the changes in structural actin and myosin arrangement in striated muscle in response to mechanical to tension (A. F. Huxley & Niedergerke, 1954; H. E. Huxley & Hanson, 1954). Even through, this early work showed the interaction between the mechanical forces and cells at the structural level, new technologies were needed to specifically measure the mechanical forces at the protein level. The introduction of technologies such as the atomic force microscopy in 1985 (Binnig et al.,), traction force microscopy (Oliver et al., 1995) and micropatterned substrates (Balaban et al., 2001; Tan et al., 2003) allowed to study the mechanical forces at focal adhesions at nanoscale as low as 10^{-18} N, as well as, identifying mechanosensitive proteins such as integrins *in-vitro* (N. Wang et al., 1993). Further advances in such technologies including tension-based FRET sensors improved the analysis of mechanical forces with spatio-temporal resolution (Y. Liu et al., 2013; Stabley et al., 2012).

During the course of evolution, organisms developed mechanisms to sense mechanical cues from the environment through cell surface molecules-to-organelle proteins. Even primitive organisms such as bacteria, uses pili or flagellum to sense a mechanical stimulus (Persat, 2017), and in eukaryotes, mechanotransduction relays on communication between cell surface, cytoskeleton protein and nuclear envelop proteins (Janota et al., 2020; Uray & Uray, 2021). Although, mechanotransducers can exert various

functions from adherent and structural proteins to ion channels, crosstalk between these proteins is essential for proper mechanotransduction and cellular homeostasis. For example, it has been shown that mechanical stimulation of focal adhesion complex resulted in the activation of mechanosensitive ion channels (Hayakawa, Tatsumi, and Sokabe 2008). In another study, Wang et al demonstrated a direct interaction and activity modulation of mechanosensitive ion channel Piezo with mechanosensory cadherin-β-catenin adhesion complex (J. Wang et al., 2022).

As the complexity increases with evolution, physical forces are integrated to properly establish highly ordered networks. One such network is the vascular network. During the animal development, blood vessels grow and form higher order networks to fulfill the energy need of the growing tissue/animal (Campinho et al., 2020). Although, mechanical forces are explicitly required for cellular function, initial stages of vascular network formation (vasculogenesis) mainly rely on the chemical signaling (e.g. Hedgehog, VEGF) (Swift & Weinstein, 2009). In the later stages (angiogenesis), blood flow is crucial for network development, maintenance and remodeling according to the changing needs (Campinho et al., 2020).

1.2 Hemodynamics

Hemodynamics deals with the mechanical properties related to blood flow. The synchronized heart contraction and relaxation cycles result in the flow of blood from arteries to capillaries and then to veins. As the heart pumps the blood out to the vascular system, it exerts three main physical forces on the on the vascular wall: shear stress, pressure and tensile strain (Dessalles et al., 2021) (Figure 1).

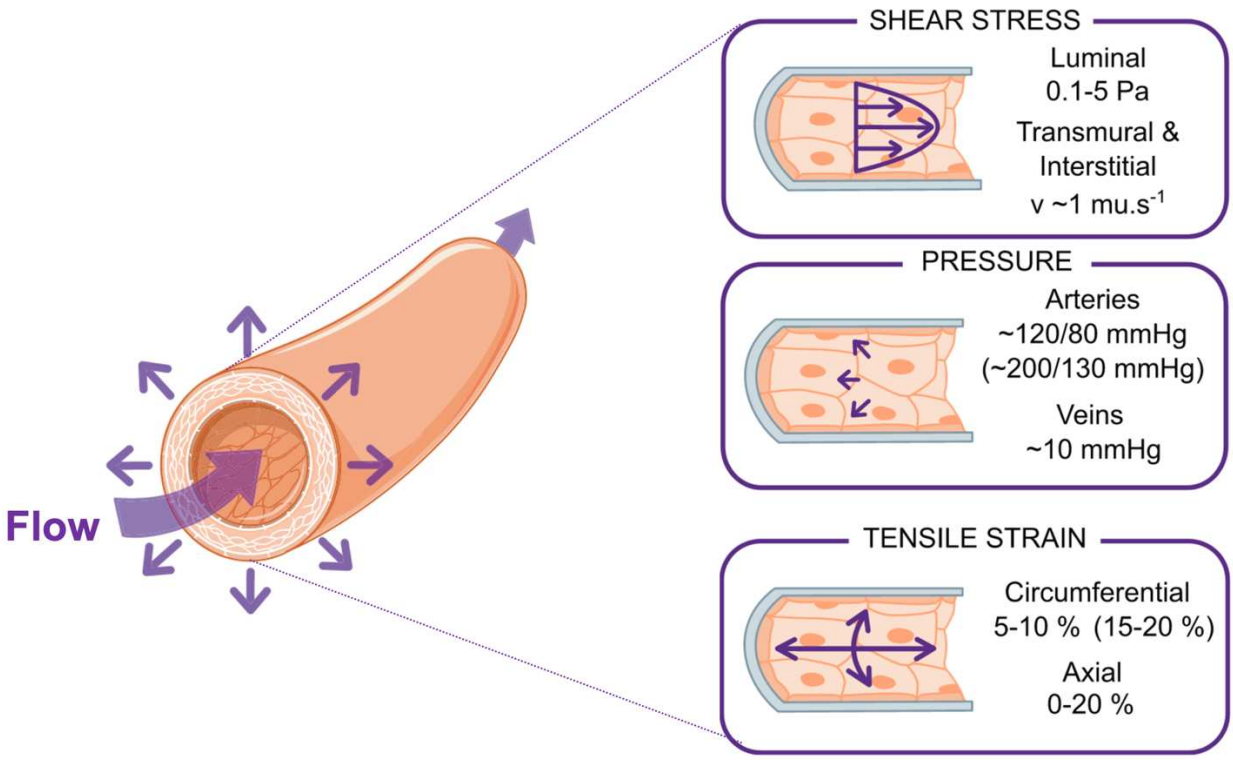

Figure 1: Schematic representation of blood flow mediated forces on vascular wall

ECs with in the lumen experience blood flow derived shear stress and pressure whereas VSMCs experience mainly the tensile strain. Physiological and pathological (parentheses) values are provided by each force is represented. (Adapted from Dessalles et al., 2021).

Shear stress (SS) is defined as the tangential frictional force applied on the luminal surface of vascular wall as a result of blood velocity and viscosity. It is calculated from following the Hagen-Poiseuille equation (Camasão & Mantovani, 2021):

$$\tau = 4q\mu/\pi r^3$$

where, τ = shear stress; q = flowrate; μ = viscosity of the fluid; r = radius of the vessel.

Pressure is defined as the force act on the vascular wall perpendicular to the direction of flow and is calculated using the following equation:

$$p = q.r$$

where, p = pressure, q = flow rate and r = radius of the vessel.

Tensile strain/stretch can be described as the ratio of the change in deformation to its original value. Tensile strain can be calculated from following equation (Camasão & Mantovani, 2021):

$$\sigma_c = Pr_i/t$$

where, σ_c = circumferential strain; P = Pressure applied by fluid; r_i = inner radius of the vessel; t = wall thickness.

The SS across the vascular tree varies depending on the type of the vessel (Figure 2). For example, SS in arteries ranges between 10 - 50 dynes/cm^2, and 1 - 20 dynes/cm^2 in veins (Papaioannou & Stefanadis, 2005).

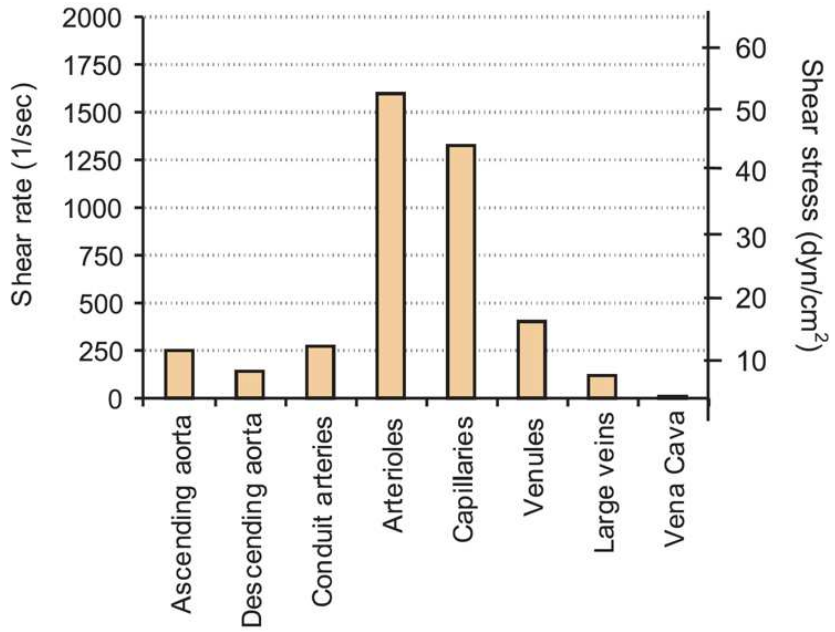

Figure 2: Graphical representation of shear stress across vascular tree.

Arterioles experience high shear stress values and Vena cava experience the lowest. Shear stress values measured by Lipowsky and his team in cat mesentery (Adapted from Papaioannou and Stefanadis 2005).

1.3 Role of hemodynamics in vascular homeostasis

The vascular system plays a crucial role in transporting essential nutrients and oxygen to all organs thereby supporting its function and viability (Carmeliet & Jain, 2000; Chilibeck et al., 1997). As the hemodynamic forces are not constant and vary across the vascular network, blood vessels are structurally adapted to cope up with these differences (Figure 3). For example, the largest blood vessel near the heart, the aorta, is thicker in size and contains more elastic tissue compared to capillaries, exposed to lesser hemodynamic forces (Humphrey & Schwartz, 2021; Tu & Chao, 2018).

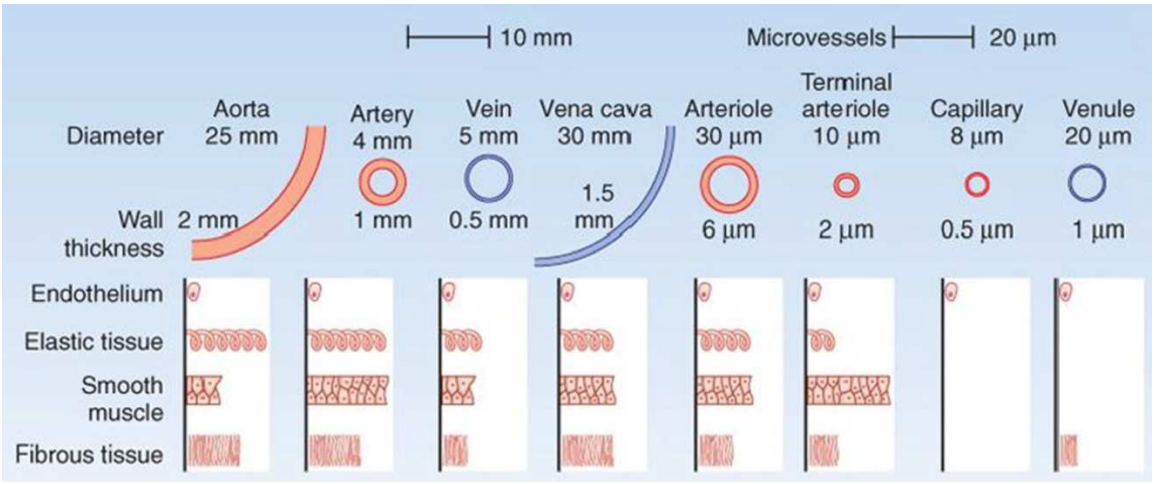

Figure 3: Schematic representation of blood vessel composition at various levels of vascular network.

Relative depiction of blood vessel diameter, thickness, and, quantity of elastic tissue, smooth muscle cells and fibrous tissue in different types of blood vessels (Adapted from Tu and Chao 2018).

In addition to its structural differences, the vascular system has a remarkable ability to adapt to the changing needs, for example, temporal and temporary vascular tone changes as a result of altered cardiac output during exercise to benefit the physiological health (Green et al., 2017). Unfortunately, mechanisms that promote vascular adaptation under physiological conditions can also result into pathological remodeling in case of chronic alteration in the hemodynamic conditions such as hypertension (Dajnowiec & Langille, 2007). Also, pathological altered vascular remodeling has been observed to support the new functional demands of pathological conditions such as solid cancers (Carmeliet & Jain, 2000). Although, chemical cues plays a crucial role in the maintenance of vascular homeostasis, the importance of flow-related mechanical forces in vascular homeostasis has been strengthened by the association of altered hemodynamics with vascular disorders (Baeyens et al., 2016).

Cells in the vascular wall, endothelial cells (ECs), vascular smooth muscle cells (VSMCs) and fibroblasts sense the alterations in hemodynamic forces and crosstalk between them helps regulating the vascular tone. ECs lining the vessel lumen and in direct contact with blood flow, experience SS due to the friction between the flowing blood and ECs (Davies, 1997; Stalcup et al., 1982). ECs also experience circumferential stretch due to the pulsatile nature of blood pressure (Lacolley, 2004). As embedded in the vascular extracellular matrix, VSMCs and fibroblasts primarily experience shear stretch

(Haga et al., 2007; X. Li et al., 2022), but also experience SS due to interstitial flow (Z. D. Shi et al., 2009; S. Tada & Tarbell, 2002).

1.4 Hemodynamics in vascular cell functions

Hemodynamics play an important role in vascular cell function. Hemodynamic forces under the physiological range keeps vascular cells in a healthy quiescence and anti-inflammatory state. However, alterations in the hemodynamics outside the physiological range results in vascular cell proliferation, pro-inflammatory and dedifferentiation state, and has been shown to associate with vascular pathologies such as atherosclerosis and aneurysms (Bennett et al., 2016; Deng et al., 2015; Marziano et al., 2021; Petsophonsakul et al., 2019). So, it is of much imperative that hemodynamic forces regulate ECs and VSMCs phenotype. Such alterations in the vascular cell function could affect the neighbouring cells thereby promoting the development and progression of the vascular diseases.

1.4.1. Effect of hemodynamics on ECs function

In-vivo, ECs continuously experience shear stress which has profound effect on its function. Early work using BAECs showed that ECs **proliferation** is regulated by SS and low SS is pro-proliferative whereas physiological or high SS has anti-proliferative affects (Levesque et al., 1990). This is through SS activated p53-p21 signaling pathway, which resulted in the inactivation of retinoblastoma protein by hypo-phosphorylation thereby G0/G1 cell cycle arrest (Lin et al., 2000) (Figure 4a). Interestingly, pathological SS such as turbulent flow increased ECs DNA synthesis as analyzed by radioactive thymidine incorporation (P. F. Davies et al., 1986).

Another important ECs function that is regulated by SS is **vascular barrier function** which is crucial to prevent leakage of flowing blood into the surrounding tissue. Alterations in vascular barrier occur under physiological conditions such as wound healing or in pathological conditions such as hemorrhages.

Endothelial barrier function is regulated through cell-cell junction modification. This occurs through phosphorylation mediated endocytosis of VE-cadherin (VE-cad), an adherent junctional transmembrane protein (Figure 4b). VE-cad has been shown to be

phosphorylated at multiple tyrosine and serine residues that could mediate endothelial cell-cell junction and vascular permeability (Dejana et al., 2008). Interestingly, VE-cad mediated permeability is vessel dependent, as VE-cad$^{Tyr658/685}$ phosphorylation is present only in veins, but not in arteries *in-vivo* (Orsenigo et al., 2012). Bradykinin induced permeabilization requires VE-cad$^{Tyr658/685}$ phosphorylation, indicating an additional factor such as phosphorylation VE-cad^{Serr665} (Gavard & Gutkind, 2006) may be needed to induce permeability in this territory (Orsenigo et al., 2012). Endothelial barrier permeability is tightly regulated and during any injury, ECs promote immune cells extravasation to reach the injured area. Using knock-in mouse models, it has been shown that the phosphorylation of VE-cad^{Tyr731} has an inhibitory affect and on-site leukocytes mediate the dephosphorylation thereby VE-cad internalization and permeability (Wessel et al., 2014). Another protein which is involved in vascular cell barrier function is vinculin, a cytoskeletal protein acts as a mechanosensory protein that senses the actin-based tensions. It has been shown that HUVECs treated with endothelial permeability and angiogenic factors such as VEGF, thrombin or TNFα resulted in actin-based remodeling of VE-cad adherens junctions and association of vinculin/F-actin at these junctions. Although, vinculin was shown not to be important for adherens junction formation, it plays important role in protecting from force dependent opening of adherens junctions through it interaction with VE-cad (Huveneers et al., 2012). This kind of vinculin-based protection of adherens junctions may play important role during immune cells extravasation under physiological context. Another junctional protein that is involved in the endothelial permeability is Claudin-5. Claudin 5 expression has been shown to regulated by both tight junction protein JAM-A (Kakogiannos et al., 2020) as well as adherens junction protein VE-cad (Taddei et al., 2008). The junctional stabilization of VE-cad clustering resulted in claudin-5 transcription through inhibition of FoxO1 by PI3K-AKT signaling mediated phosphorylation (Taddei et al., 2008). Interestingly, Claudin-5 knockout mice develops normally and showed neither edema nor blood leakage. However, Claudin-5 knockout results in vascular leakage of smaller molecules (<800 Daltons) only (Nitta et al., 2003) and may explain the normal development of knockout mice.

Hemodynamic forces affect vascular **permeability**. In this context, it has been showed using HUVECs and *in-vitro* experimental setup, SS modulates VE-cad$^{Tyr658/685}$ phosphorylation and is flow magnitude dependent. Lower SS (3.5 dynes/cm^2) increased VE-cad phosphorylation, which is reduced to basal level as the SS increases to 50 dynes/cm^2. Such phosphorylation is necessary but not enough for bradykinin induced permeability at least in the context of veins (Orsenigo et al., 2012). An interesting mechanism through which SS affect vascular permeability involves Notch signaling. In human dermal microvascular cells, it has been shown that SS activated Notch transmembrane domain forms a novel receptor complex VE-cad/LAR/Trio resulted in the activation of Rac1 and mediated junctional assembly and increased barrier function (Polacheck et al., 2017) (Figure 4c). In the pathological context, hypertension has been shown to downregulate Claudin5 expression and increased permeability in abdominal aortic coarctation induced arterial hypertension rat models (Mohammadi & Dehghani, 2014). In addition, low expression of Claudin5 has been shown to associate with disturbed flow and atherosclerosis vulnerable regions (Peter F. Davies et al., 2013).

In pathological context, mechanism that could compromise blood barrier is **vascular cell death**. Physiological SS supports ECs survival by inhibiting apoptosis through several mechanisms. Using HUVECs, it has been shown that SS inhibits TNFα mediated EC apoptosis through activation of PI3k-AKT pathway and subsequent phosphorylation of eNOS and inhibition of ICE-CPP32 (Dimmeler et al., 1997, 1998) (Figure 4d.ii). Another mechanism through which SS could potentially inhibit endothelial apoptosis is through inhibitor of apoptosis proteins (IAP-1&2). Research showed that, SS under the physiological range promotes IAP-1 &2 levels which resulted in the inhibition of caspase3 thereby apoptosis (X. Jin et al., 2002; Taba et al., 2003) (Figure 4d.iii).
SS also influence the **inflammatory** state of ECS. Pathological SS promotes endothelial inflammation through PECAM-1 mediated NFκB activation, which was substantially reduced by the knockdown of PECAM-1 in HUVECs (Feaver et al., 2013) (Figure 4d.i). The role of SS in endothelial inflammation was supported by the transcriptome study of ECs subjected to atheroprotective pulsatile SS and atheroprone oscillatory SS, wherein oscillatory SS has been shown to induce inflammatory markers such as VCAM1, IL-8, E-selectin (Maurya et al., 2021).

As SS regulates multiple functions of ECs, endothelial dysfunctions have been observed in the regions in the vascular tree that experience abnormal flow patterns such as aortic bifurcations and aortic arch, and are the sites for initiation of vascular diseases such as

atherosclerosis and intracranial aneurysm (Baeriswyl et al., 2019; Gimbrone & García-Cardeña, 2016).

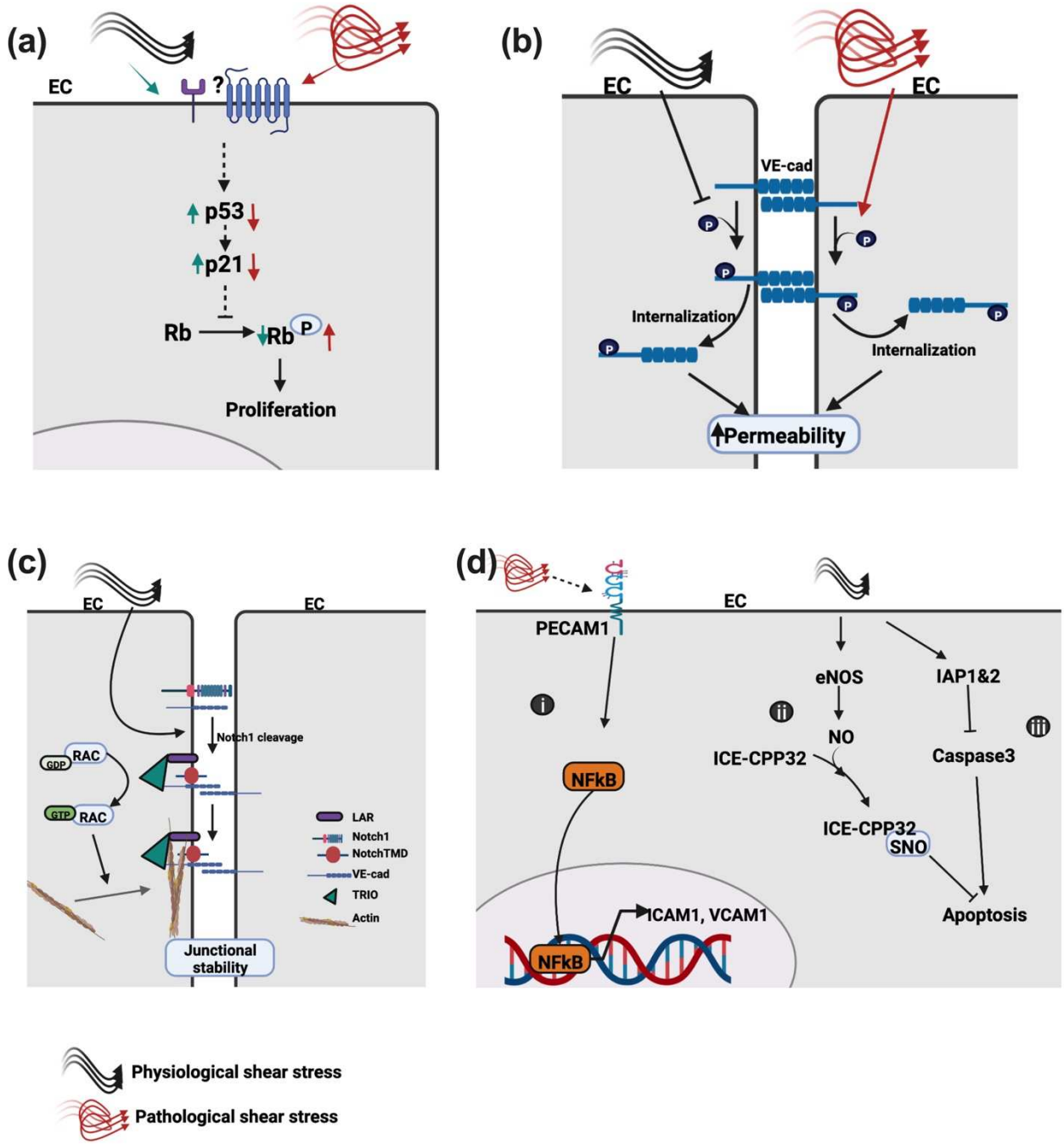

Figure 4: Effects of shear stress on ECs function

Physiological and pathological SS regulates ECs proliferation through modulation of retinoblastoma protein (Rb) phosphorylation through p53-p21 signaling cascade (a). Physiological and pathological SS regulates VE-cadherin phosphorylation mediated internalization thereby permeability (b). Physiological shear stress promotes Notch dependent junctional stability through junctional recruitment of LAR and TRIO. TRIO mediates cytoskeletal rearrangement through localized Rac activation, which results in junctional stability (c). Pathological SS activates PECAM-1 mediated NFkB signaling thereby expression of pro-inflammatory gene ICAM1 and VCAM1 (d.i). Physiological shear stress inhibits ECs apoptosis through nitrosylation of Interleukin-1β-converting enzyme-like and cysteine protease protein-32 like family (ICE-CPP32) (d.ii) and through production of inhibitor of apoptosis proteins (IAP1&2) (d.iii).

1.4.2. Effect of hemodynamics on VSMCs function

VSMCs reside in tunica media experience mainly cyclic stretch (CS) as a result of regular heart contractions.

In both *in-vivo* and *in-vitro* conditions, it has been shown that CS modulates VSMC **proliferation**. Subjecting rabbit aortic VSMCs to pathologic CS or altering the CS through induction of hypertension via abdominal aorta coarctation resulted in increased VSMC proliferation (Birukov et al., 1995; Qi et al., 2016). This increase in proliferation could be due to IGF-1R-PI3K signaling pathway, which was sensitive to mechanical stimulus. Under physiological CS conditions, IGF-1R signaling pathway could inhibit p53 stability thereby VSMC proliferation (J. Cheng & Du, 2007; Xiong et al., 2007) (Figure 5a). Another interesting mechanism through which CS regulate VSMC proliferation is through nuclear mechano-transductory complex protein Lamin A/C, Emerin. Pathological CS decreases LaminA/C and Emerin expressing which resulted in the removal of repressor effect on promoters that drives the expression of genes (E2F1, E2F3, SP1, STAT1) responsible for proliferation thereby VSMC proliferation (Qi et al., 2016) (Figure 5a).

CS also affects VSMC **apoptosis** through multiple signaling pathways. It has been shown that pathological CS promotes clustering of TNF-α receptor-1 (TNFR-1) which results int eh activation of TRAF2-JNK and p38 signaling thereby VSMC apoptosis (Sotoudeh et al., 2002) (Figure 5b.i). In addition, CS mediated downregulation Notch signaling has been shown to promote VSMCs apoptosis *in-vitro* (Morrow et al., 2005) (Figure 5b.iii). Conversely, *in-vitro* application of pathological strain upregulates miR21 (J. tao Song et al., 2012) and stretch induced chemokine (J. Zhao et al., 2017) mediated mechanisms to protect VSMCs from undergoing apoptosis (Figure 5b.ii). Such mechanisms may act as a protective shield in the presence of acute alterations in shear stretch, which could fail in chronic shear stretch altered conditions such as hypertension.

Interestingly, CS also influence the **inflammatory** status of VSMCs. Work done by Demicheva *et al* showed that altering the stretch values either by ligation of ear artery *in-vivo* or subjecting mouse and human VSMCs to pathological CS resulted in increase in AP-1 dependent monocyte chemoattractant protein (MCP-1) expression, which

attracts circulating monocytes to the site of vascular remodeling (Demicheva et al., 2008) (Figure 5c). At the site of vascular remodeling, macrophage secreted cytokines such as platelet-derived growth factor (PDGF) and IL-6 promotes VSMC phenotype switching from contractive to synthetic phenotype (Ashraf & Zen, 2021) (Figure 5c).

Under the physiological conditions, acute alterations in CS promotes VSMC phenotype switching that promote healthy vascular remodeling. However, conditions such as hypertension that result in chronic alteration result in pathological VSMC phenotype switching that promotes vascular disease formation and progression.

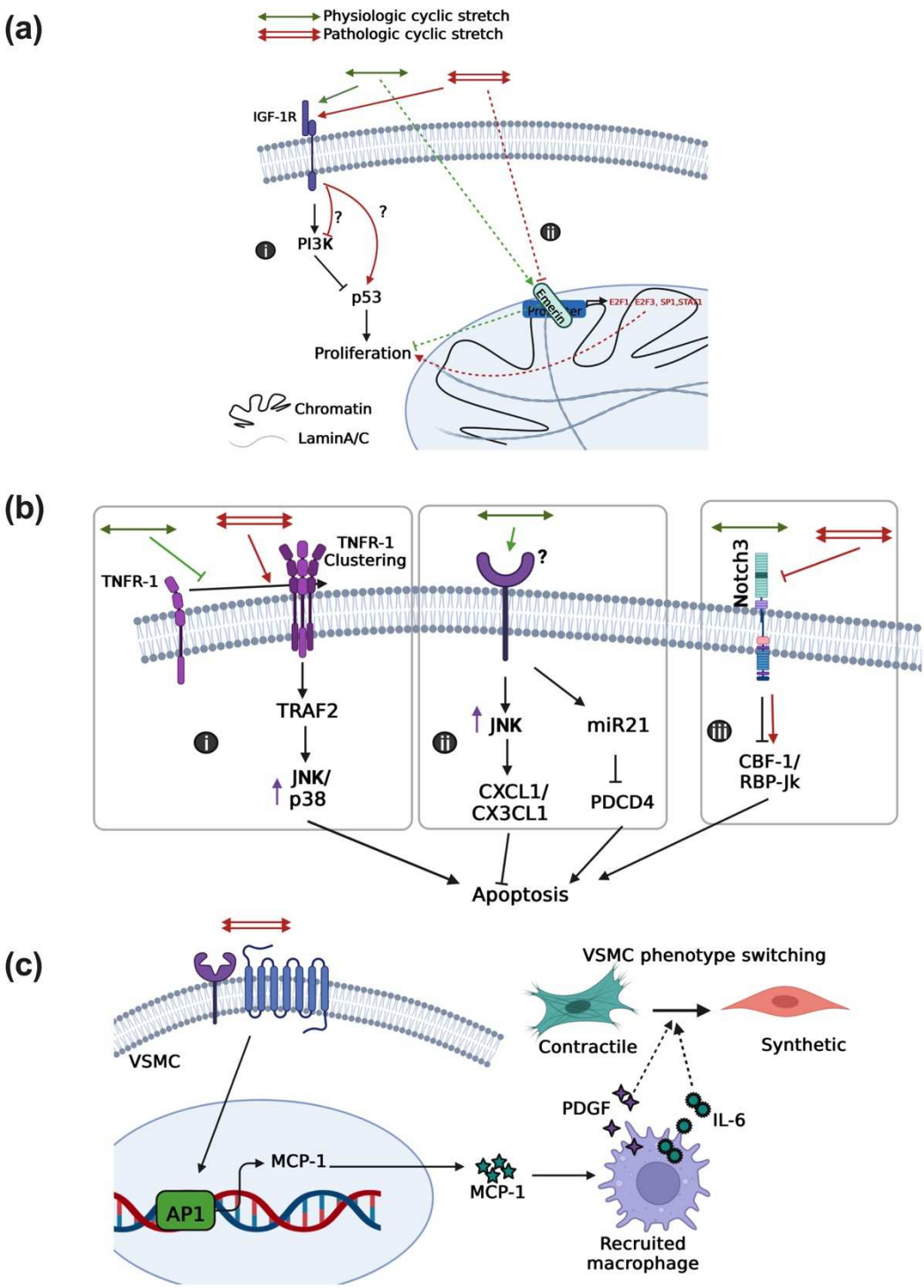

Figure 5: Effect of cyclic stretch on VSMCs function

Physiological and pathological CS modulates VSMC proliferation through IGF-1R mediated PI3k-p53 signaling pathway, as well as through regulation of LaminA/C and Emerin protein levels thereby controlling expression of proliferative genes at chromatin level (a). Pathological CS promotes VSMC apoptosis though TNFR-1 clustering mediated JNK/p38 signaling cascade (b.i) or through Notch3 downregulation, thereby promoting CBF-1/RBP-Jk mediated apoptosis (b.iii). Physiological CS inhibits VSMC apoptosis through upregulation of JNK signaling dependent anti-apoptotic cytokines CXCL1/CX3CL1 or by upregulation of miR21 that targets programmed cell death 4 (PDCD4) protein (b.ii). Pathological CS promotes inflammation through AP-1 mediated production of monocyte chemoattractant protein-1 (MCP-1). MCP-1 recruited macrophage derived PDGF and IL-6 promotes VSMC phenotype switching (c).

1.5 Mechanotransducers in vascular system

Vascular cells express a wide array of mechanosensitive molecules ranging from cell surface receptors to cytoskeletal proteins. Graphical representation of known mechanosensors are shown in the Figure 6.

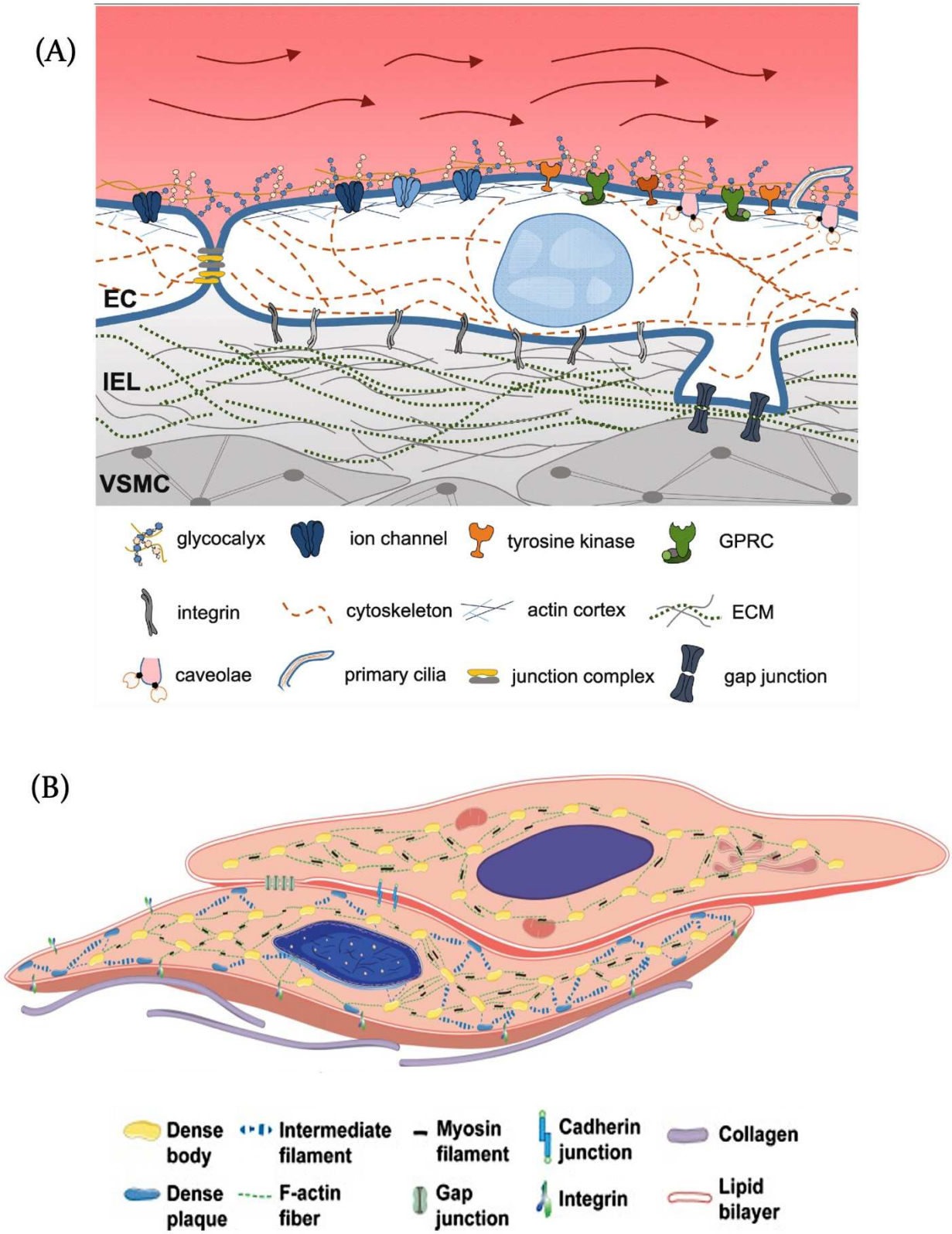

Figure 6: Schematic representation of mechanosensors in vascular cells.

Known mechanosensors from cell surface to extracellular matrix expressed in endothelial cells (A), and vascular smooth muscle cells (B) are represented.

Adopted from Fels & Kusche-Vihrog, 2020 & Ye et al., 2014

Glycocalyx is a negatively charged carbohydrate rich layer present on the luminal surface of the ECs consisting of glycoproteins and proteoglycans such as heparan, chondroitin sulfate and hyaluronic acid (Reitsma et al., 2007). The role of glycocalyx as a mechano-transducer came from initial studies wherein degrading the glycocalyx components by either heparinase or hyaluronidase, impaired SS mediated NO production (Florian et al., 2003; Mochizuki et al., 2003). The association of glycocalyx with SS sensing was further supported by the presence and altered glycocalyx thickness depending on the SS the ECs experienced in *in-vivo* and *in-vitro* conditions (Gouverneur et al., 2006; Van Den Berg et al., 2006). Interestingly, this effect of glycocalyx on NO production is mediated through activation of TRP channels and increasing the cytoplasmic calcium concentration by calcium ionophore (A23187) overcome the heparinase and hyaluronidase inhibition of NO synthesis (Dragovich et al., 2016). Decrease levels of glycocalyx has been associated with atheroprone regions in mouse internal carotid arteries compared to common carotid arteries (Van Den Berg et al., 2006). In mice models of carotid injury, deletion of syndecan-1, a major component of glycocalyx, increased intimal thickening and VSMC activation (Fukai et al., 2009).

Primary nonmotile cilia mechanosensory organelle are present in most cell types (Nauli et al., 2013). Cilia are extended-out microtubular structures that are connected to cytoskeletal microtubules (Egorova et al., 2012). In ECs the primary evidence of cilia as a mechanosensory to flow came from the study by Carlo Iomini, wherein subjecting ECs to laminar SS resulted in cilia disassembly (Iomini et al., 2004). ECs defective in cilia through mutations in associated proteins polaris and polysystin-1 results in decreased intracellular calcium and NO signaling (Nauli et al., 2008). Genetic deletion of IFT88, an essential ciliary protein, resulted in regression of retinal vascular network (A. C. Vion et al., 2018). However, in contrast, Dinsmore and Reiter reported no vascular defects in IFT88 endothelial-specific knockout adult mice (Dinsmore & Reiter, 2016). This contradiction could be due to the role of cilia at different developmental stages of vascular network. This was supported by the role of the cilium in EC response to SS and developmental morphogenesis. Deletion of IFT88 reduced the sensitivity of ECs to BMP9 specifically under low SS, which is perceived by ECs in immature and developing blood vessels (A. C. Vion et al., 2018). Although, IFT88 deletion resulted in proper

vascular network development with no major complications, it altered the vascular susceptibility to vascular diseases such as atherosclerosis. Endothelial-specific knockout of IFT88 resulted in significant increase in atherosclerotic lesions in $ApoE^{-/-}$ mice models (Dinsmore & Reiter, 2016).

Caveolae are plasma membrane invaginations formed from glycosphingolipids and cholesterol. Caveolae is present in most cell types and are coated with three types of proteins Caveolins(Cav)-1,-2&-3 (Echarri & Del Pozo, 2015). Caveolae are enriched with tyrosine kinases, GTP-binding proteins and calcium, and acts as sites of signal compartmentalization and integration (Anderson, 1998). In addition to act as a subcellular compartment, previous studies have supported the role of caveolae as mechanotransducers and in mechanosignaling. When ECs (BAEC) were subjected to SS, the number of caveolae increased, as well as ERK and AKT phosphorylation (Boyd et al., 2003; Rizzo et al., 2003). The role of caveolae as a mechanotransducer was further strengthened by the inhibition of Cav-1 using neutralizing antibody which blunt the SS-mediated ERK phosphorylation (Park et al., 2000). Complete genetic deletion of *Cav-1 in-vivo* resulted in impaired response of arteries to flow-mediated dilation, which was rescued by endothelial specific expression of Cav-1. In addition, the $Cav\text{-}1^{-/-}$ mice showed reduced flow-mediated eNOS activation which is demonstrated by reduced eNOS phosphorylation at position S1176 (J. Yu et al., 2006). In ECs, association of eNOS with caveolae has been shown to be important for flow-mediated eNOS activation (Rizzo et al., 1998). In VSMC, caveolae are shown to be involved in stretch induced Src, PI3K and Akt activation. Inhibiting Cav-1 using RNA interference or disrupting Caveolae using beta-cyclodextrin inhibits PI3K and AKT activation. Interestingly, CS increased the association of PI3K and Cav-1 complex with integrins (Sedding et al., 2005). In addition, Cav-1 could play a role in shear stretch mediated VSMCs proliferation, as $Cav\text{-}1^{-/-}$ mice showed increase VSMC proliferation upon carotid artery ligation compared to unligated artery (J. Yu et al., 2006). These studies show that caveolae acts as a mechanosensors by integrating mechanical cues in space and time.

Ion channels are involved in multiple functions ranging from osmoregulation to neuronal signaling. The mechano-sensitivity of ion channels were first described in bull

frog auditory epithelial cells in 1979 (Corey & Hudspeth, 1979). In ECs, the first SS sensitive K^+ channels were described in BAECs in 1988 (Olesen et al., 1988). In vasculature, Piezo1, a mechanically activated non-selective cation channels, is expressed in both ECs and VSMCs. Endothelial-specific deletion of piezo1 resulted in embryonic death due to defects in vascular remodeling. Knocking down of piezo1 in HUVECs resulted in defective EC alignment to SS (Ranade et al., 2014). Moreover, it has been shown that in ECs, SS activation of piezo1 resulted in the release of ATP which in turn result in the activation of Gq/11 coupled purinergic P2Y2 receptor leading to AKT and eNOS activation thereby flow mediated vasodilation (S. P. Wang et al., 2016). In addition to its role in SS-mediated vasodilation, role of peizo1 in endothelial inflammation has been reported. In HUVECs, knocking down of piezo1 resulted in reduced disturbed flow induced NFkB nuclear localization and endothelial inflammation. Moreover, endothelial-specific knockout of *Piezo1* resulted in reduced atherosclerosis progression in *Ldlr* knockout mice model (Albarrán-Juárez et al., 2018). In VSMCs, Piezo1 plays a dispensable role in vascular tone regulation via increasing cytosolic calcium and transglutaminase activity (Retailleau et al., 2015).

Other important ion channels involved in maintaining vascular physiology are transient receptor potential (TRPs) channels. Although many TRPs have been identified (TRPCs,TRPVs, TRPMs, TRPAs, TRPPs,) only few of them (TRPC1, 5, 6; TRPV1, 2, 4; TRPM3, 7; TRPA1; TRPP2) have shown to be mechanosensitive (Inoue et al., 2009). TRPs show their effect by modulating Ca^{+2} influx and Ca^{+2}-calmodulin complex activation. In ECs, inhibition of TRPV4 using specific inhibitor ruthenium red, inhibited endothelium-derived hyperpolarizing factor (EDHF) mediated flow-induced vasodilation. Similar response was observed *in-vivo*, as knock out of TRPV4 abrogated EDHF mediated response to increased luminal flow in mice model (Loot et al., 2008). TRPP2 has been shown to localize cilium and acts as a mechanosensor. In ECs, knockdown of TRPP2 resulted in dampened flow induced NO production (Aboualaiwi et al., 2009). Interestingly, it has been shown that only heteromeric composition of the channels (TRPP2, TRPC1 and TRPV4) were able to mediate flow ionic currents (Du et al., 2014). In VSMCs, TRP channel mediated Ca+2 influx results in activation of myosin light chain kinase and smooth muscle cell contraction (Earley & Brayden, 2015).

Integrins are heterodimeric transmembrane adhesion molecules composed of one α- and one β- subunits. In mammals, there are 19 α and 8 β subunits, in combination giving rise to 25 different receptors (Humphries, 2000). In the cytoplasmic side, integrin interacts with focal adhesion proteins thereby connecting the extracellular environment to cell through cytoskeletal components (Burridge, 2017; Schumacher et al., 2021).The role of integrins as mechanotransducers came from the early work by Ning Wang, where they showed that application of mechanical forces using anti-integrin β1 receptor antibody coated magnetic beads to capillary ECs resulted in cytoskeletal stiffening and increased focal adhesion formations, which was disrupted in the presence of RGD peptide (N. Wang et al., 1993). In addition, mechanical stimulation of NIH3T3 cells by stretching resulted in the conformational change of integrins αVβ3 from low to high affinity. This conformational change is mediated through PI3K activity as inhibition of PI3K activity using specific inhibitors LY-294002 reduced conformational activation (Katsumi et al., 2005; Tzima et al., 2005). Integrins also play a role in SS induced ECs cell alignment by regulating the activity of RhoA. In BAECs, SS activates RhoA and this activation was shown to be inhibited by pretreatment of fibronectin surface with anti-fibronectin neutralizing antibody interferes fibronectin-integrin interactions (Tzima et al., 2001). *In-vitro* experiments using HAECs showed that atherogenic turbulent flow-mediated integrin activation resulted in increased NFkB signaling and ICAM1 and VCAM1 expression. In addition, inhibition of αV-integrin activation using a peptide inhibitor reduced the atherosclerotic burden in $ApoE^{-/-}$ mice model (Jie Chen et al., 2015). However, β1 integrin-mediated endothelial flow-sensing requires functional caveolae. As pretreatment of BAECs with filipin that binds to cholesterol and disrupts β1 caveolae structure, inhibited integrin mediated SS induced eNOS and AKT phosphorylation (B. Yang & Rizzo, 2013). Thus, cooperation between mechanosensors play an important role in efficient mechano-transduction process. Interestingly, integrins do also signals to the cell about the directionality of the force. Recent work by Ioannis Xanthis in HUVECs showed that β1 integrin is responsible for flow direction sensing of ECs and the resulting cytoskeletal rearrangement and transcription (Xanthis et al., 2019).

GPCRs and G-proteins plays important role in vascular cell physiology. One of such GPCR is angiotensin-II type-1 receptor (AT1R). The role of AT1R as a mechanosensor came from early studies using HEK293 overexpression and rat cardiomyocytes models. Subjecting either AT1R overexpressing HEK293 cells or primary rat cardiomyocytes to CS significantly increased ERK phosphorylation and is mediated through activation of $G\alpha_{q/11}$, which was inhibited by candesartan, an angiotensin receptor blocker (Zou et al., 2004). Similar observations were made in rat arterial smooth muscle cells, wherein subjecting arterial smooth muscle cells to 20% stretch resulted in increased ERK phosphorylation as well as myocardin, a smooth muscle specific transcription factor, which was inhibited by Losartan, an angiotensin receptor blocker (Chiu et al., 2013). Identified through RNAi screen in the breast cancer cell line MDA-MB-231, GPR68 was shown to be SS sensitive. *In-vivo* GPR68 is expressed in ECs of small diameter arteries and endothelial specific $GPR68^{-/-}$ mice exhibited defective flow-mediated dilation. It acts upstream of eNOS, however the exact mechanism is still not known (J. Xu et al., 2018). G-proteins such as $G\alpha_{q/11}$ have been shown to be mechanosensitive (Dela Paz et al., 2017). $G\alpha_{q/11}$ acts as G-protein for multiple GPCRs such as bradykinin receptor B2 in BAECs (Chachisvilis et al., 2006) and sphingosine-1-phosphate receptor3 (S1P3) in HCAECs (Dela Paz et al., 2017). In ECs, the mechanosensory role of Gαq/11 was further supported by its association with PECAM1, one of the molecules of endothelial mechanosensory complex (Dela Paz et al., 2014; Otte et al., 2009; Yeh et al., 2008).

PECAM-1 is a transmembrane homophilic adhesion protein interacts with β- and γ-catenins and may interact with cytoskeleton (Ilan et al., 2000). PECAM-1 is expressed in mesodermal cells including ECs. Using BAECs, studies have shown that shear stress as well as osmotic shock induces PECAM-1 phosphorylation and subsequent ERK1/2 activation (Harada et al., 1995; Osawa et al., 2002). Interestingly, tweezing PECAM-1 using specific antibody coated magnetic beads resulted in PECAM-1 and ERK1/2 phosphorylation (Osawa et al., 2002). Mounting experimental evidences show that PECAM-1 indeed acts as a mechanosensory in EC and is a crucial component of the endothelial mechanosensing complex VE-cad/PECAM1/VEGFRs (Shay-Salit et al., 2002; Tzima et al., 2005).

Tyrosine kinase receptors are single transmembrane, multidomain proteins that undergoes autophosphorylation upon activation through ligand binding, which results in the concomitant activation of downstream signal transducers such as MAP kinases. The tyrosine kinase receptor to angiopoietin-1 and -2 (Ang-1 and Ang-2) Tie2 plays important role in cardiac development and angiogenesis during embryogenesis (Jeansson et al., 2011; Maisonpierre et al., 1997; Suri et al., 1996). In ECs, the mechanosensitive aspect of Tie2 was described using HUVECs. It has been shown that subjecting HUVECs to laminar SS resulted in ligand independent Tie2 phosphorylation which was directly proportional to the SS applied (Jong Lee & Young Koh, 2003). Other tyrosine kinase receptors that plays prominent role in vascular physiology is the VEGFR family (Simons et al., 2016). Using BAECs, Jin *et al*, showed ligand independent activation of VEGFR2. In their work, subjecting BAECs to SS resulted in VEGFR2 phosphorylation as well as activation of downstream signaling components such as AKT and eNOS, which was inhibited by the VEGFR2 inhibitors (Z. G. Jin et al., 2003). Moreover, study reported the mechanosensitive role of VEGFR3 in regulating the fluid shear stress set point thereby vessel diameter (Baeyens et al., 2015). In addition to mechanosensory role, VEGFR3 as a mechanotransducer was studied in mouse embryo, wherein the level of VEGFR3 phosphorylation in lymphatic ECs correlates with interstitial fluid pressure. Although this phosphorylation of VEGFR3 is mediated through β1-integrin signaling, it is necessary for fluid pressure mediated lymphatic ECs proliferation (Planas-Paz et al., 2012).

In ECs, mechanosensitive PECAM1 and VEGFRs form an **endothelial mechanosensory complex** along with endothelial specific cadherin, VE-cad, which was first described by Martin Schwartz and his group in 2005 (Tzima et al., 2005). Although members of other cadherin family are shown to be mechanosensitive (Bard et al., 2008; Ko et al., 2001), experiments to prove the mechanosensitive nature of VE-cad were unfruitful. Stimulation of VE-cad with magnetic beads coated with anti-VE-cad antibody failed to elicit PI3k activity in BAECs. Interestingly, stimulation of PECAM1 in the same way resulted in increased PI3K activity, which was reduced or blunted in ECs lacking VE-cad compared to wild type BAECs. Moreover, loss of either PECAM1 or VE-cad resulted in failure of VEGFR2 phosphorylation and activation upon flow stimulation

in BAECs (Tzima et al., 2005). Despite the lack of mechanosensitivity nature, VE-Cad plays an irreplaceable role in endothelial mechanosensing and as an adapter protein in mechanosensory complex that helps in the association of PECAM1 and VEGFRs. Although, primarily it has been shown that the mechanosensory complex has VEGFR2 as one of its components, later work by Coon *et al* showed that VEGFR3 could replace VEGFR2 in the complex. While VEGFR2 and VEGFR3 showed redundancy *in-vitro* settings, the physiological function of mechanosensitive VEGFR3 is interesting. The protein expression levels of VEGFR2 is the same in ECs of various blood vessels, whereas VEGFR3 expression varies and is dependent on the type of vessel, having high expression in lymphatic and low in arteries (Baeyens et al., 2015; Witmer et al., 2002). Mechanistically, VEGFR3 replacement of VEGFR2 in the complex determines the fluid SS set point, defined as "*a theoretical model of regulation of a biological process in which a biological variable remains in a determined range of values despite the environmental changes that modify the initial value of the variable*" (Roux et al., 2020). In case of ECs, set point refers to the wall SS. Overexpressing VEGFR3 in ECs of aorta *in-vivo*, which are exposed to high flow, resulted in lowering of the arterial SS set point thereby adaptation of ECs in order to reach the low optimal set point thus increasing lumen diameter (Baeyens et al., 2015).

1.6 Mechanosignaling in vascular system

Following the mechanical stimulation of the previously cited sensors, both cytoskeleton and biochemical signaling in vascular cells get activated. As ECs are in proximity to the blood stream, they are the first ones to respond to the altered hemodynamics.

ECs respond to flow in a temporal fashion. Their early response includes activation of ion channels and GPCRs; followed by modulation of signaling pathways and cytoskeletal rearrangement, gene transcription and finally cellular changes such as cell alignment (Peter F. Davies et al., 1997) (Figure 7). Cells adopt a rapid response such as NO and prostaglandin secretion in case of short acute alterations in SS which regulate VSMCs contraction thereby vasodilation or vasoconstriction and stabilization of blood flow (Koller et al., 1994; Koller & Kaley, 1991). As the cytoskeleton gives structural support to the cell, it always exists in a "pre-tensed" state. Due to their "pre-tensed" nature,

alterations in cytoskeleton upon SS sensing can be seen within minutes despite the stabilization of cytoskeletal network and cell alignment relative to the mechanical force takes time (6 h to 72 h in ECs depending on the force applied) (Helmke et al., 2001; Osborn et al., 2006). In addition, the cytoskeletal proteins plays important role in the mechano-transduction process through converging the stimulus perceived from cell surface, cell junctions and focal adhesions, which results in the altered biochemical signaling, transcription and cellular phenotype (Peter F. Davies, 2009).

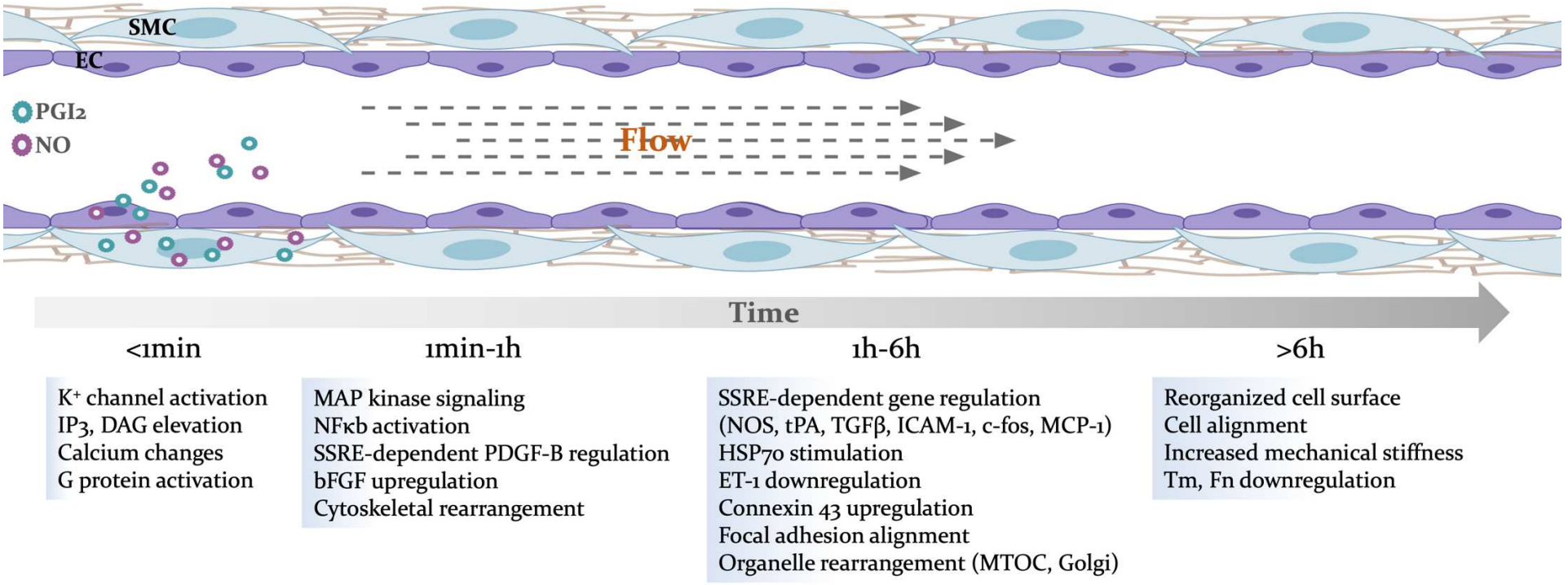

Figure 7: Kinetics of signaling events activated by shear stress in vascular cells.

Picture represents the early, middle and late responses of vascular cell to shear stress ranging from ion channel activation to cytoskeletal rearrangement mediated cell alignment (Adapted from Davies. P.F et al 1997).

Mechanical stimulation of cell surface mechano-sensors such as integrins, GPCRs, ion-channels, TRKs results in activation of multiple signaling cascades responsible for cell adjustment and survival.

1.6.1. PI3K/AKT signaling

PI3K/AKT signaling is one of the key signaling networks which are activated by hemodynamic forces (Figure 8). PI3Ks are membrane bound kinases, when activated they mediate the conversion of PIP2 to PIP3 which interacts and mediates AKT phosphorylation through PKD1 and downstream signaling events (Morello et al., 2009). Initial work in 1998, showed that HUVECs subjected to laminar SS showed an increase in AKT phosphorylation which was substantially inhibited using PI3K inhibitors such as wortmannin and LY294002 (Dimmeler et al., 1998). The activated AKT then phosphorylates eNOS at S1177 which resulted in its activity and NO production (Dimmeler et al., 1998, 1999). This PI3K-AKT activation could be through SS activated cell surface receptors such as VEGFR2 (Z. G. Jin et al., 2003) and PECAM1 (Osawa et al., 2002), and activation of receptor bound Shc (K. Den Chen et al., 1999)or Src kinases(Tzima et al., 2005) (Okuda et al., 1999). Interestingly, it has been showed that SS-mediated AKT phosphorylation requires VE-cad as VE-cad null ECs fail to activate AKT under shear stress (Shay-Salit et al., 2002). Moreover, SS-induced AKT activation has been shown to play role in inflammation. Subjecting HUVECs to low shear stress resulted in PI3K independent activation of AKT and ICAM1 expression by promoting interferon regulatory factor 3 (IRF3) activation (L. Zhu et al., 2021).

In VSMCs, activated PI3K phosphorylates L-type calcium channels resulted in influx of calcium thereby vasoconstriction (Morello et al., 2009). In 1998, Takashi Seki and collaborators showed that Ang-II stimulated Ca^{+2} currents in rat aortic smooth muscle cell line A7r5 which was significantly suppressed by lavendustin-A, a selective inhibitor of tyrosine protein kinase and Ly-294002, an inhibitor of PI3K, both of which are downstream intracellular effectors of AT1R (Seki et al., 1999). As AT1R have shown to be mechanosensitive, similar PI3K-mediated Ca^{+2} currents may be at play upon mechanical stimulus (Figure 9). On the other hand, PI3K-AKT signaling may promote VSMC proliferation through mTOR signaling as inhibiting AMPK through either RNAi or

specific inhibitor resulted in increased PDGF induced pulmonary arterial smooth muscle cell proliferation (Y. Song et al., 2016). Similar role of PI3K/AKT/mTOR signaling has been reported in stretch-induced bladder smooth muscle cell proliferation (Adam et al., 2003).

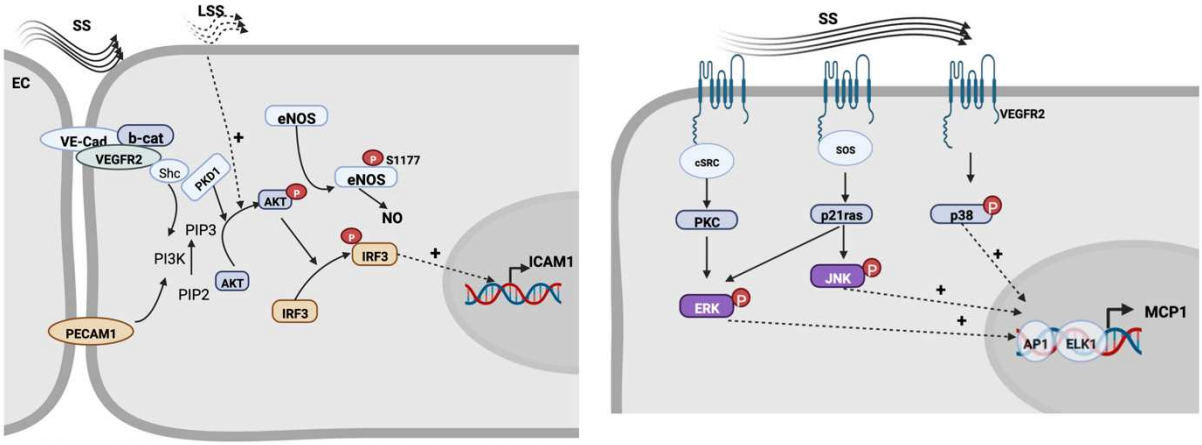

Figure 8 Signaling mechanisms mediate by mechanical forces in ECs

In ECs, Shear stress mediates activation of PI3K/AKT signaling through VEGFR2 and PECAM1 which in turn activates eNOS through phosphorylation at ser1177 position. PI3K/AKT signaling also activates interferon regulatory factor 3 which results in the increased transcription of inflammatory cell adhesion molecules such as ICAM1 (left). Shear stress also activates several surface reports including VEGFR2 which results in the activation of secondary messengers such as ERK, JNK an p38 which result in transcriptional activation (right).

1.6.2. MAPK signaling

MAPK signaling has been shown to be modulated by hemodynamic forces and been shown to activate MAPK signaling molecules such as MEKK-JNK and MEKK-ERK (Tseng et al., 1995) (Y. S. Li et al., 1996) (Figure 8). In HUVECs, SS induces ERK phosphorylation through c-SRC, PKC dependent pathways, as inhibiting either c-SRC by Herbimycin A or PKC by phorbol 12, 13 dibutyrate (PDBU) completely abrograted shear stress induced ERK phosphorylation (Takahashi & Berk, 1996). In addition to c-SRC, SOS (Son of Sevenless)-dependent activation of $p21^{ras}$ has been described in the activation of MEKK-JNK and MEKK-ERK (Jalali et al., 1998; Y. S. Li et al., 1996). In addition to PI3K/AKT signaling, Shay-salit and collaborators showed that in BAECs, shear stress also induces p38 activation. Such activation requires VE-cad as VE-cad null ECs fail to induce shear stress mediated p38 phosphorylation (Shay-Salit et al., 2002). These signaling events mediate the transcription of shear stress induced gene such as MCP-1 and c-fos through activation of AP-1/TRE and SRC/ELK1 responsive elements respectively (K. Den Chen et al., 1999; Hsieh et al., 1993; Shyy et al., 1994)

In the context of VSMCs, application of CS to rat VSMCs shown to induce both ERK and JNK activation (Reusch et al., 1997). This induction could be mediated though mechanosensitive integrins, as applying CS through magnetic beads coated integrin antibody results in increased ERK activation (Goldschmidt et al., 2001). In human aortic VSMC, it has been shown that pathological CS resulted in increased in p38 phosphorylation and ATF3 mediated inhibition of ACE2 transcription thereby regulating VSMC cell functions such as proliferation (X. Liu et al., 2021) (Figure 9). Although, CS activates much of the MAPK signaling molecules, the specific inhibition of p38 using the specific inhibitor SB203580 prevents CS mediated VSMC alignment (Q. Chen et al., 2003).

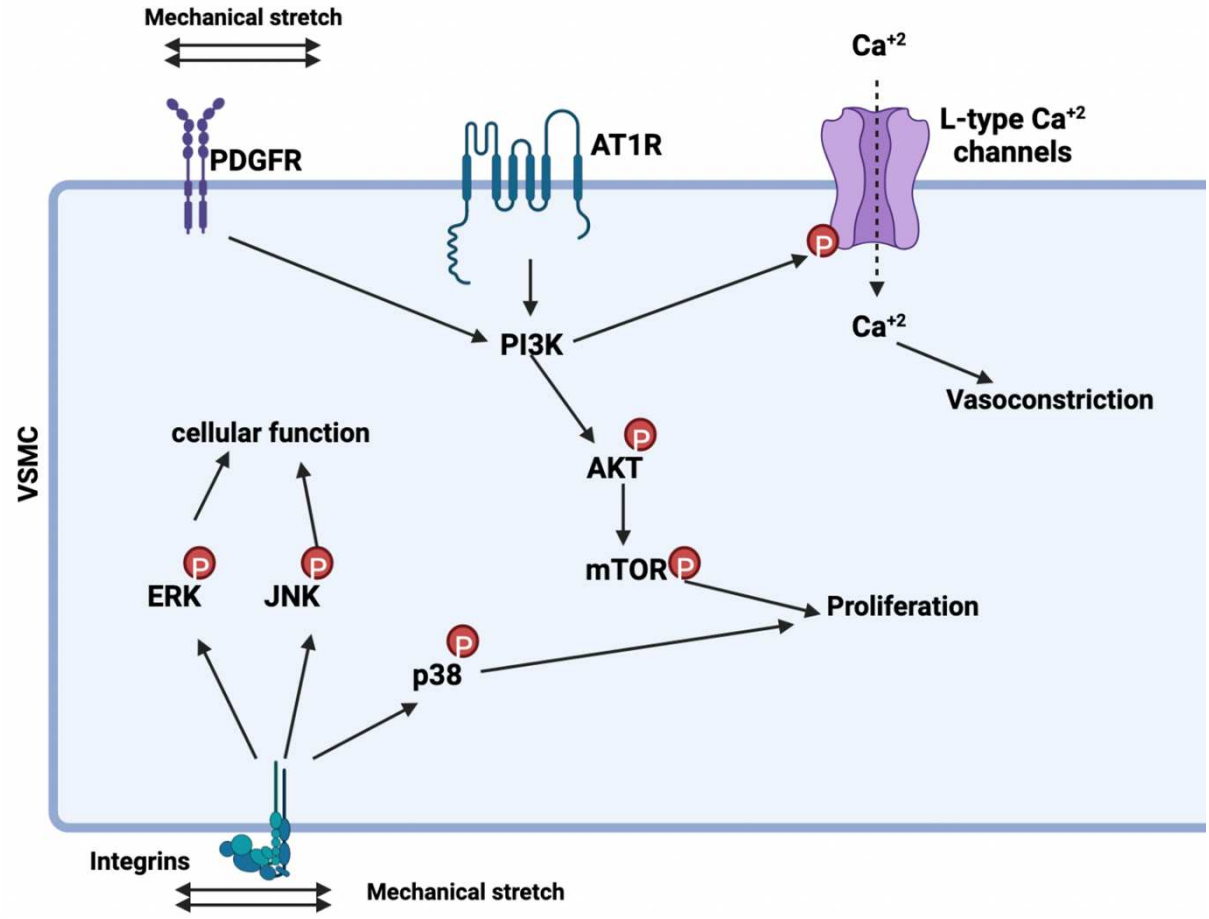

Figure 9: Signaling mechanisms mediate by mechanical forces in VSMCs

In VSMCs, mechanical activation of PDGFR and AT1R results in the activation of PI3K/AKT signaling which results in the regulation of proliferation. Activated PI3K also activates L-type Ca+2 channels thus modulating vasoconstriction. Mechanical activation of integrin signaling result in the activation of ERK, JNK and p38 thereby regulating cellular functions.

1.6.3. eNOS signaling between EC-VSMCs

Blood flow-mediated SS promotes activation of mechanosensitive receptors on EC surface, which results in the production of prostaglandins and NO (Figure 7), which regulates smooth muscle cell contraction, there by vascular tone (Figure 11). In ECs, NO is produced by eNOS through the conversion of L-arginine to L-citrulline and have been shown to increase with both SS and CS (Awolesi et al., 1995; Ayajiki et al., 1996). eNOS is constitutively expressed, its activity is regulated by intracellular calcium and Ca^{+2}-calmodulin interaction (Busse & Mülsch, 1990). However, early experiments in porcine aortic ECs and HUVECs showed that SS-mediated NO production is independent of calcium and is regulated through intracellular pH and tyrosine phosphorylation (Ayajiki et al., 1996). Tyrosine phosphorylation promotes eNOS interaction with Caveolin-1 through the reductase domain which renders eNOS in inactive state (Fleming & Busse, 1999; García-Cardeña et al., 1996; Ghosh et al., 1998) (Figure 10). *In-situ* flow experiments showed that SS increased the activity of caveolae-associated eNOS as well as promotes the dissociation of eNOS from caveolae and eNOS interaction with calmodulin (Rizzo et al., 1998). SS modulates activity of eNOS through promoting the interaction with HSP90 (García-Cardeña et al., 1998) as well as by phosphorylating eNOS at Ser^{1177} (Ser^{1179} in bovine) through PKA and AKT dependent as well as c-Src dependent activation of MEK1/2 and ERK1/2 signaling mechanisms (Boo et al., 2002; Boo & Jo, 2003; Davis et al., 2001; Dimmeler et al., 1999) (Figure 8 & 10). Using BAECs, it's been shown that SS upregulates eNOS transcription through nuclear transcription factor NFκB (Davis et al., 2004; Y. Zhao et al., 2015a).

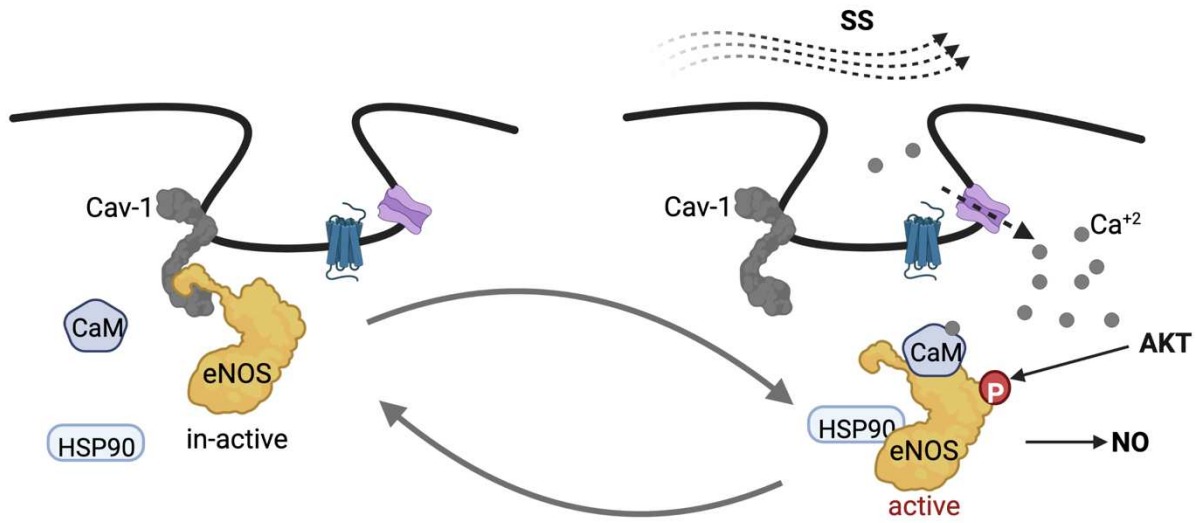

Figure 10: Shear stress regulation of eNOS at Caveolae

In Caveolae, eNOS binds to caveolin-1 through its reductase domain. Such interaction keeps eNOS in an in-active state. Upon shear stress stimulus, eNOS release from Caveolin-1 and gets activated through its interaction with Ca^{+2} calmodulin and AKT dependent phosphorylation at ser1177. The activated eNOS mediates the production of Nitrous Oxide.

Endothelial NO diffuses into surrounding matrix embedded SMCs. In SMCs, NO mediates vasodilation through the remodeling of acto-myosin complex (Figure 11). This is mediated through activation of soluble guanylyl cyclase activity followed by increase intracellular cGMP, which result in activation of cGMP-dependent protein kinase G and subsequent uptake of cytosolic calcium into sarcoplasmic reticulum. NO and PKG activated signaling pathways results in the decreased phosphorylation of MLC20, thereby, reducing actin/myosin interaction and contraction. (Arnold et al., 1977; Carvajal et al., 2000; Y. Zhao et al., 2015b) (Figure 11).

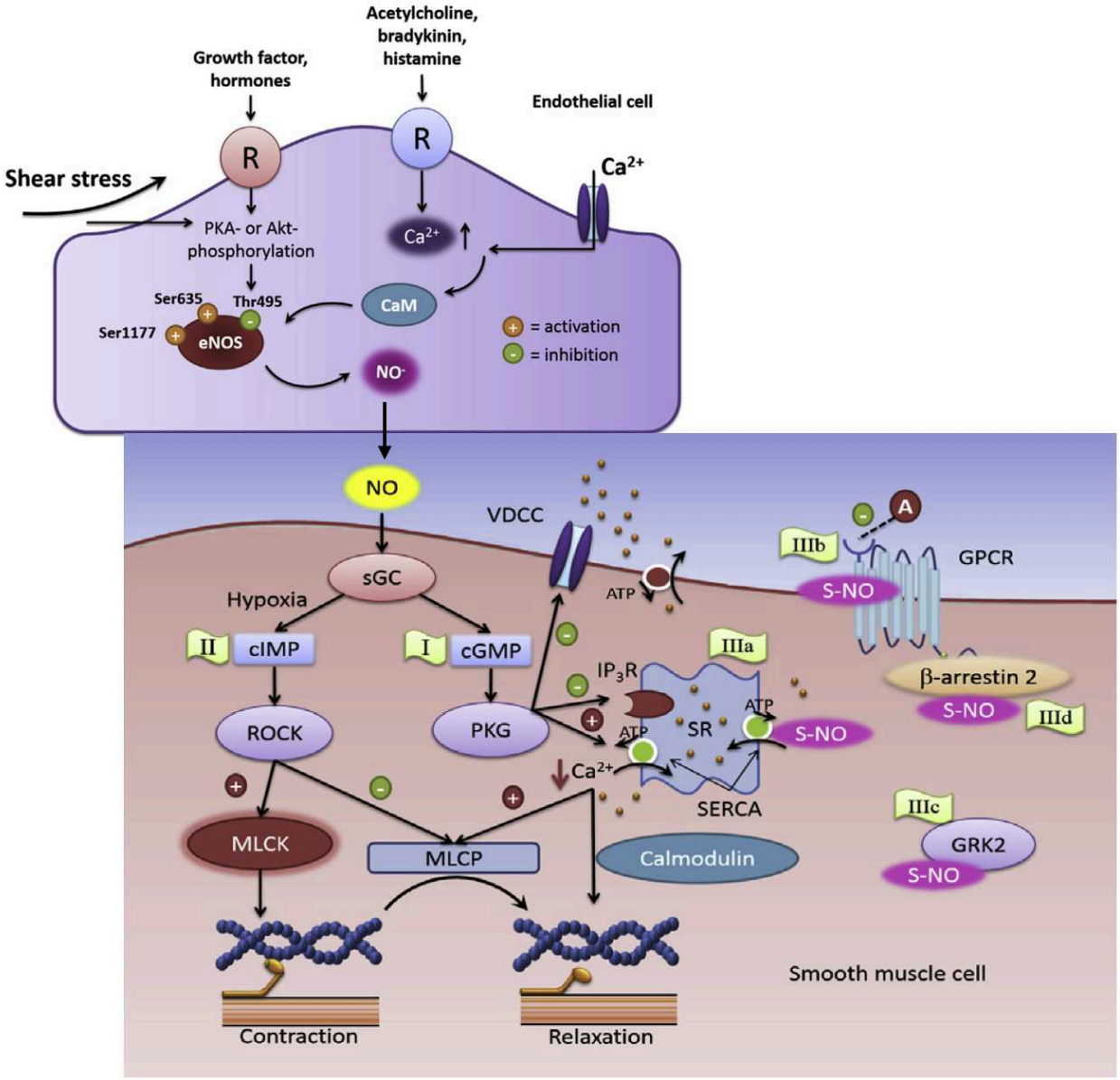

Figure 11: eNOS-NO signaling between ECs & VSMCs

In ECs, shear stress dependent and independent signaling mechanisms leads to eNOS activation either through interacting with Ca^{+2}-calmodulin or through phosphorylation at Ser1177 and 635. Phosphorylation at Thr495 acts as inhibitory. The activated eNOS mediates the production of NO. Produced NO diffuse into nearby VSMCs and promotes vasodilation through the activation of soluble Guanylyl cyclase and cGMP dependent mechanisms. (Adapted and modified from Y. Zhao et al., 2015a*).*

Integrins could acts as a shear stress mechanosensors and could be responsible for shear stress mediated eNOS signaling, as blocking of integrin signaling by blocking antibody significantly inhibited the shear stress mediated vasodilation in porcine coronary arteries (Muller et al., 1997). Among the endothelium derived vasodilatory molecules, NO signaling plays significant role in flow mediated vasodilation. Under physiological

condition, NO is continuously produced in ECs through SS sensing mechanisms and is important to maintain basal vascular tone as well as modifying the vascular in response to acute alterations in SS (Stoner et al., 2012).

1.6.4. Mechanotransduction in vascular homeostasis and diseases

Mechanical stimulus plays a prominent role in vascular development and homeostasis, whereas, chronic alterations in mechanical stimulus from physiological range results in maladaptation of vascular cell signaling, ultimately leading to vascular pathologies.

Flow-mediated mechanosignaling is important for arterio-venous specification of endothelial progenitor cells (EPCs), as subjecting EPCs to SS resulted in upregulation of arterial specific markers (ephrinB2, Notch1/3, Hey1/2 and ALK1), and downregulation of venous specific marker (ephrinB4, NRP2) in a SS and time-dependent manner (Obi et al., 2009). On the other hand, SS stimulates the expression KLF2, a key transcription factor involved in anti-inflammatory state of ECs (Dekker et al., 2002; SenBanerjee et al., 2004). This was further supported by the association of high and low expression of KLF2 in atheroprotective and proatherogenic regions respectively, described in human and murine carotid arteries (Dekker et al., 2005).

ECs and VSMCs respond to mechanical stimulus by modulating their signaling mechanisms to maintain vascular network in physiological healthy condition. In contrast, unability to respond to aberrant hemodynamic forces or dysfunctionality of ECs and VSMCs could favor vascular diseases such as hypertension, atherosclerosis and aneurysms.

In case of **hypertension**, eNOS-NO signaling plays crucial role, as it is one of the main endothelial factors which maintain vascular tone. The importance of eNOS signaling came from mice studies wherein genetic ablation of eNOS resulted in substantial increase in blood pressure and hypertension (Shesely et al., 1996). However, delivering eNOS through blood cell by transplanting bone marrow from wildtype mice was sufficient to rescue from hypertension (Wood et al., 2013). As eNOS -NO signaling is important for vascular tone maintenance, defective signaling in both ECs and in VSMCs have been identified in vascular pathologies such as hypertension (Giaid & Saleh, 1995;

Schermuly et al., 2008; Y. Y. Zhao et al., 2009). Importantly, hypertension mediated CS could switch VSMC phenotype from contractile to proliferative and secretory as shown using *in-vitro* and *in-vivo* studies (Qi et al., 2016; W. Bin Wang et al., 2019). Such dysfunctional signaling results in the progression of hypertension with increased arterial stiffness and hyperplasia.

Atherosclerosis forms predominantly at the arch and branch sites where vascular cells experience disturbed flow and low SS (VanderLaan et al., 2004). It has been shown that disturbed flow causes EC dysfunction by increasing ECs proliferation (Chien, 2008; P. F. Davies et al., 1986), downregulation of vasoprotective eNOS and KLF2 expression as well as increased expression of inflammatory molecules (VCAM1 and ICAM1) and ROS generation (Nam et al., 2009). Disturbed flow and low SS could induce pro-inflammatory state by promoting TNFα stimulated interaction of TRAF-2 with TNFR and downstream activation of p38 and JNK, thereby VCAM1 expression, which was shown to be inhibited by physiological SS (Nagel et al., 1999; Yamawaki et al., 2003). Interestingly, it has been shown that turbulent SS causes vessel dysfunction through downregulation of Smad6 and Smad7, which are shown to be negative regulators of the TGFβ signaling (Toppert et al., 1997). This supports the importance of laminar SS in vascular physiology by regulating the TGFβ signaling which is important for proper vessel formation as well as dysfunction (Goumans et al., 2009).

Another vascular disease that is associated with altered hemodynamics is **intracranial aneurysm,** which is characterized by abnormal bulging and weakening of cerebral arteries in the Circle of Willis. Both high and low SS has been shown to associate with development and progression of aneurysm (Meng et al., 2014). Regions with high SS are the sites of aneurysm formation, whereas low SS has been associated with aneurysm rupture once the aneurysm is formed (Jou et al., 2008). Although the exact molecular mechanisms have not been yet identified, endothelial dysfunction has been reported at early stage of the disease. In experimentally induced cerebral aneurysm model, reduced eNOS at the site of aneurysm formation was reported (Aoki et al., 2011). Furthermore, dysfunctional ECs express PGE receptor subtype2 which promotes macrophage infiltration, subsequent NF-kB signaling and aneurysm formation (Aoki et al., 2017). In

addition to endothelial dysfunction, phenotype switching of VSMC from contractile to secretory has been observed in human tissue samples which would secrete proinflammatory cytokines and MMPs and contribute to aneurysm development (N. Nakajima et al., 2000).

2. Small GTPases and Mechanotransduction

2.1 Introduction about Rho-GTPases

First identified in 1985 (Madaule & Axel, 1985), the small GTPase-Rho (Ras-homology) proteins form a subfamily within the superfamily of Ras-like proteins which also includes Ras, Rab, Arf and Ran families. The Rho-GTPase subfamily consists of 20 proteins (Figure 12). The common characteristics are the presence of G domains, Rho insert region and C-terminal hypervariable region. G-domains are necessary for guanine nucleotide binding, Rho insert region is essential for guanine nucleotide exchange factor (GEF) binding, and the C-terminal hypervariable region is subjected to post-translation modifications that regulate Rho-GTPase localization and activity (Freeman et al., 1996; Schaefer et al., 2014; Vega & Ridley, 2008).

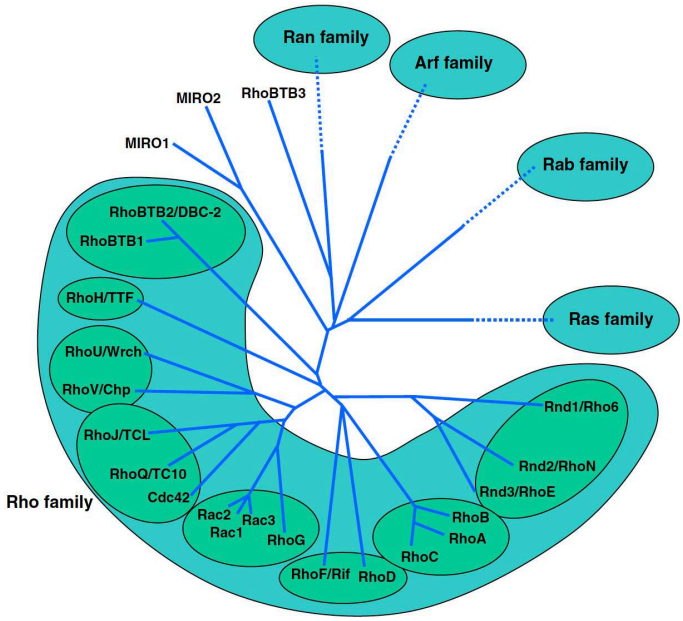

Figure 12: Phylogenetic tree showing the mammalian Ras GTPases superfamily

The 20 Rho GTPase family members are grouped into eight subfamilies (Adapted from Vega .F.M and Ridley .A.J 2008)

Like other monomeric GTPases, Rho-GTPases switch in between inactive GDP-bound form and active GTP-bound form. The transition between the inactive and active form is mediated by guanine nucleotide exchange factors (GEFs), while and GTPases activating proteins (GAPs) allow the return to the inactive GDP-bound form. In addition to GEFs and GAPs, guanine nucleotide dissociation inhibitors (GDIs) also regulate small Rho-GTPases activity by sequestering inactive GDP-bound Rho-GTPases within the cytosol, thereby preventing their accessibility to GEFs at the membrane. As an additional layer of regulation, post-translational modifications such as lipid modifications (for example: prenylation, palmitoylation), phosphorylation, sumoylation and ubiquitylation serves the Rho-GTPase activation in a spatiotemporal way (Hodge & Ridley, 2016). Moreover, Rho-GTPases are known to be regulated at epigenetic and post-transcriptional levels, via miRNAs (Ji Chen et al., 2011; M. Liu et al., 2012; Yoon et al., 2007) (Figure 13).

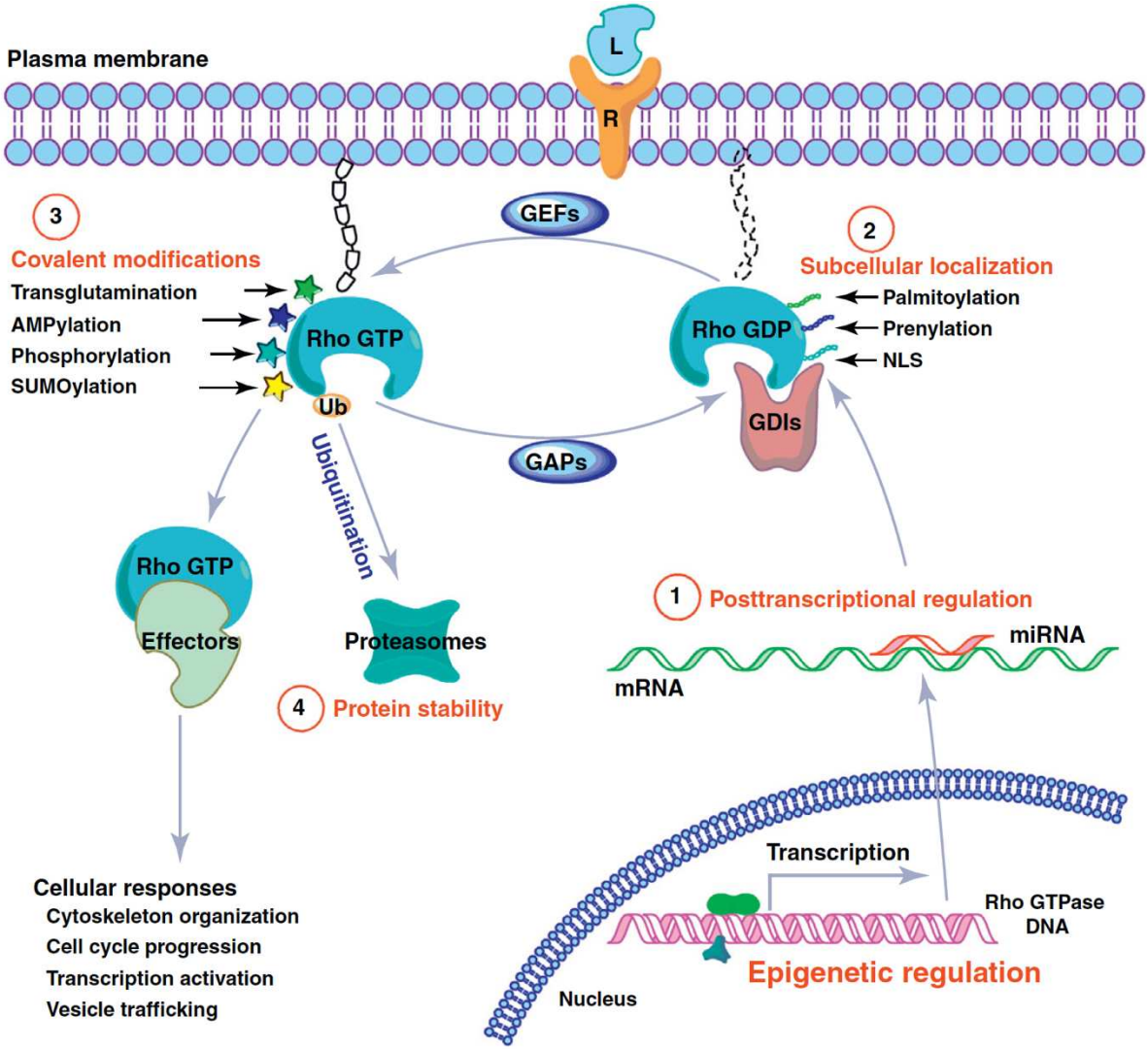

Figure 13: Overview of Rho-GTPase regulatory mechanisms

Rho-GTPase are regulated at multiple levels (1) post-transcriptional regulation through miRNA mediated RNA degradation; (2) subcellular localization through post-translational modifications such as palmitoylation, prenylation and NLS; (3) activity through covalent modifications; and (4) protein stability, (Adapted from Liu et al. 2012)

2.2 Rho-GTPases in EC and VSMC biology

Among Rho-GTPase family members, RhoA, Rac1 and Cdc42 are well characterized for their role in cell polarity maintenance, migration and morphology (Etienne-Manneville & Hall, 2002). Although, RhoA, Rac1 and Cdc42 all act on actin cytoskeleton, the outcome serves different purposes: RhoA induces actin-myosin filaments assembly (stress fibers), Rac1 induces actin-rich surface protrusions (lamellipodia), and Cdc42 promotes filopodia, actin-rich finger-like membrane protrusions (Kozma et al., 1995; Ridley et al., 1992; Ridley & Hall, 1992). Each of these processes plays an important role

during cell migration, as Rac1-mediated lamellipodia promotes pulling force, RhoA-mediated stress fibers promote traction force, and Cdc42-generated filopodia initiates the migration and its direction. However, co-ordination between these processes is essential for a proper cell migration (Raftopoulou & Hall, 2004).

In addition, the pretensed cytoskeleton provides structural support and undergoes drastic structural changes relative to the mechanical stimulus. Cells such as ECs and VSMCs that experience mechanical stimulation to a larger extent rely on efficient Rho-GTPases signaling for cytoskeleton integrity and arrangement in response to the perceived force. For example, it has been shown *in-vitro* that small-GTPases are crucial for EC alignment parallel to physiological laminar flow direction, the primary response of ECs to SS (Tzima, 2006). This process involves rearrangement of microfilaments and microtubules (Girard & Nerem, 1995; Levesque & Nerem, 1985; Malek & Izumo, 1996). *In-vivo*, aortic regions expose to high physiological flow showed well aligned ECs compared to cells exposed to disturbed/low SS, thus demonstrating the effect of SS on EC shape (Hikita et al., 2018)(Figure 14).

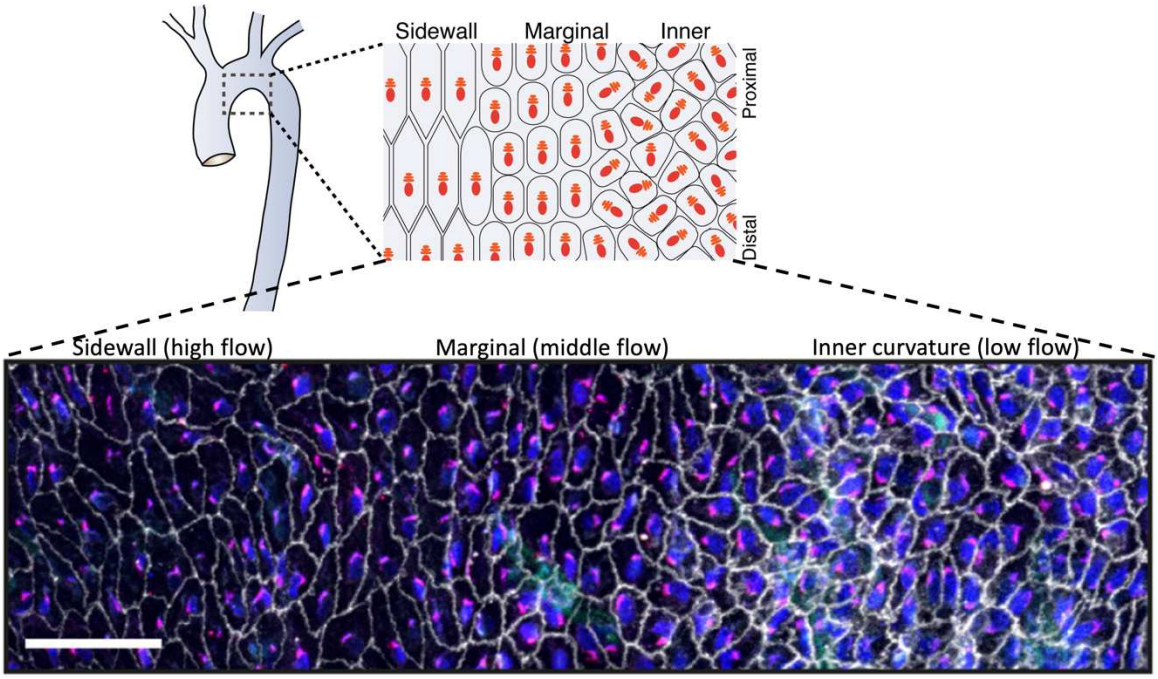

Figure 14: Differential alignment of ECs in response to different flow magnitudes

En face confocal microscopy of the aortic arch form the inner curvature showed the ECs to perceived flow. polarity marker Golph4 (red), VE-cad (white). (Adapted and modified from Hikita et al. 2018)

The response of Rho-GTPase to SS has been described as biphasic in *in-vitro* conditions (Wojciak-Stothard & Ridley, 2003) (Figure 15).

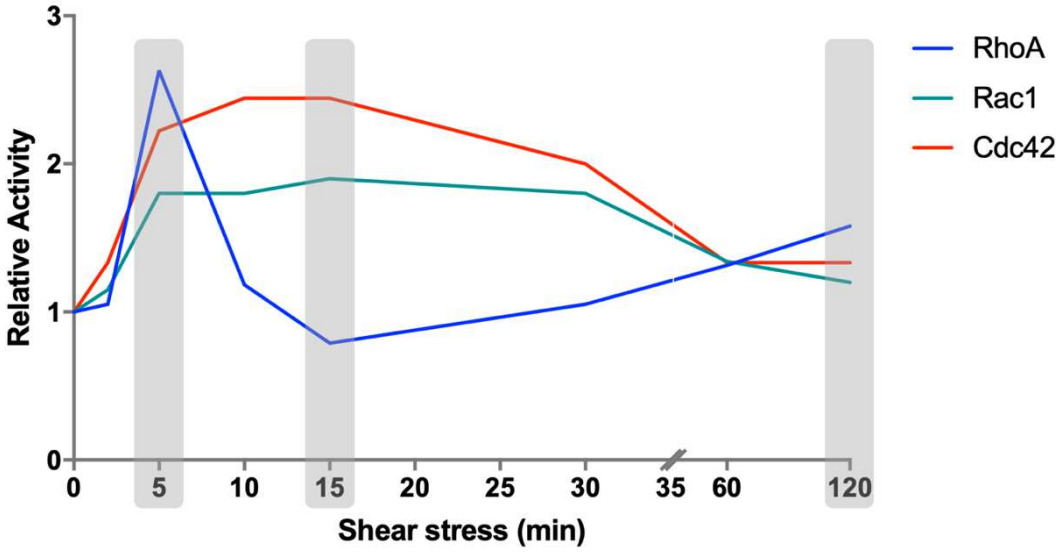

Figure 15: Kinetics of small-GTPase activation upon shear stress stimulus in HUVECs

Relative activity of RhoA, Rac1 and Cdc42 in HUVECs subjected to laminar shear stress (3 dyn/cm^{2}). Within 5 min of shear stress stimulus, RhoA activity reaches to a peak maximum of approx.2.5 fold. Rac1 and Cdc42 activity slowly increases and reaches a maximum peak at 15min when RhoA activity is at its low. By the time 2hrs upon shear stress stimulation, a second wave of RhoA activity starts whereas Rac1 and Cdc42 is at tis minimum. (arbitrary values obtained from Wojciak-Stothard & Ridley, 2003).

RhoA regulates multiple signaling pathways primarily through its kinase effector ROCK (Bishop & Hall, 2000; Kilian et al., 2021). Activated ROCK phosphorylates MLCP leads to its inactivation, thus resulted in enhanced MLC phosphorylation and this phosphorylation promotes actin-myosin interaction and subsequent contraction (Loirand et al., 2006). RhoA-ROCK signaling also activates LIMK1/2 which inactivates Cofilin through phosphorylation. This result in reduced actin depolymerization thereby promoting polymerization of G-actin into F-actin (Kauskot et al., 2016). Polymerization of G-actin into F-actin results in the release of G-actin bound MKL1 which localizes into nucleus and mediates serum response factor (SRF) target gene expression (Miralles et al., 2003; Vartiainen et al., 2007).

In ECs, the early onset of RhoA activation in response to SS occurs at 5 min, followed by a reduction back to basal level within 15 min. Then the RhoA activity slowly increases again and reaches a maximum at 2 h. (Figure 15) During this biphasic response, ECs reduce stress fibers, retract and polarize along the direction of the flow. SS exposure for long time results in the establishment of stress fibers and cell alignment parallel to the

flow direction. Although ECs overexpressing constitutively active form of RhoA showed stress fiber formation, they failed to align to the flow direction (Wojciak-Stothard & Ridley, 2003). This indicates that timely on/off activation of RhoA is necessary for proper ECs response to flow and alignment. In addition, SS mediated RhoA-ROCK activation is important for EC planar polarity (Hikita et al., 2018). Pharmaceutical inhibition of ROCK showed disruption of spatial localization of PAR-3/aPKCλ and aPKCλ/ GSK3β complex, thereby impairing endothelial polarity. In human saphenous endothelial cells and BAECs, inhibition of ROCK using hydroxy-fasudil, a ROCK inhibitor, resulted in increased AKT and eNOS phosphorylation and NO release. This effect was inhibited by PI3 kinase inhibitor, LY294002, indicating the regulation of PI3K/AKT/eNOS signaling by RhoA (Wolfrum et al., 2004). This could be through PTEN, which was shown to be activated by ROCK in neutrophils (Z. Li et al., 2005).
In VSMCs, RhoA has been shown to mediate PDGF-bb-induced VSMCs proliferation through activation of ERK1/2 signaling (Kamiyama et al., 2003).

In ECs, SS activates **Rac1** in a spatio-temporal manner, and Rac1 activation occurs as early as 5min upon SS stimulus and reaches its maximum at 15min (Wojciak-Stothard and Ridley 2003) (Figure 15). Active Rac1 is localized at the rear end of the cell in respect to flow direction (Tzima et al. 2002). However, Rac1 activation requires newly formed SS-induced newly formed integrin-ECM interactions, as inhibiting them reduced Rac1 activation. Interestingly, overexpression of either dominant negative or dominant active Rac1 do not promote SS induced ECs alignment. These studies showed that the localized activation, rather than overall Rac1 activity is important for SS-mediated cell alignment (Tzima et al. 2002).
Though much of the Rac1 mediated signaling has been identified in non-vascular cells, similar conserved mechanisms might exist in ECs. Rac1 is involved in multiple signaling mechanisms. For example, in MEFs and HMECs, Rac1 contributes to GPCR-mediated PI3K-AKT signaling by promoting membrane localization of p110β, a PI3K isoform, where it potentiates AKT activation (Cizmecioglu et al., 2016). In addition to PI3K-AKT signaling, Rac1 has also been shown to activate p38 (S. Zhang et al., 1995), JNK (Dérijard et al., 1995; Han et al., 1996; Jiang et al., 1996) and ERK (Eblen et al., 2002) through PAK1-mitogen activated protein kinase kinase (MKK) signaling pathway. Rac1 also regulates

NADPH redox pathway by directly interacting with and activating p67phox, a subunit of NADPH oxidase complex (Abo et al., 1992; Diekmann et al., 1994; Sulciner et al., 1996). In addition to the RhoA-ROCK signaling, Rac1 was also shown to activate LIMK1/2 through PAK1 thereby promoting F-actin polymerization (Kauskot et al., 2016; N. Yang et al., 1998).

Cdc42 activity matches Rac1 activity with an increase within 5min of shear stress, and, reaches a maximum at 15min, and maintains at a low level at later time points (Figure 15). Although, Cdc42 is known to regulate cell polarity, overexpression of dominant negative mutant does not affect SS- mediated ECs orientation. However, ECs expressing dominant negative Cdc42 showed reduced cell elongation to the SS (Wojciak-Stothard & Ridley, 2003). In BAECs, using dominant negative mutants of Cdc42, it had been shown that Cdc42 is essential for the positioning of microtubule organizing center upon SS stimulation (Tzima et al., 2003). Similar to Rac1, Cdc42 has also been shown to activate JNK and p38 kinases in overexpression cell culture systems (Coso et al., 1995; Minden et al., 1995). This was further supported by Cdc42 and RhoA involvement in SS-mediated activation of JNK signaling pathway in BAECs (S. Li et al., 1999). Such activation of JNK signaling could be independent of PAK1 as observed in COS7 and HEK 293T cells (Teramoto et al., 1996).

Overall, this demonstrates the complex regulation of cell signaling by small GTPases. In the context of ECs and shear stress, orchestration between RhoA, Rac1 and Cdc42 activity is essential for proper EC alignment and polarity.

In addition to the above mentioned RhoGTPases, other GTPases from Rho sub family such as RhoG, RhoJ and RhoQ have been shown to be involved in vascular cell biology. Few such small-RhoGTPases are discussed below.

In ECs, **RhoG** activity has been implicated in leukocyte transmigration. Binding of leukocyte to ICAM1 results in the activation of RhoG in ECs through interaction with RhoG specific SH3-containing GEF (SGEF or Arhgef26). Interestingly, cortactin, a cortical actin binding protein, has been shown to be required for this activation (Schnoor et al., 2011) and knocking down of either RhoG or SGEF significantly reduced trans-endothelial migration (Van Buul et al., 2007). In addition to its role in leukocyte

trans-endothelial migration, RhoG has been shown to be involved in VEGF-Trio mediated arterial remodeling in zebrafish model, through its involvement in endothelial size regulation via cytoskeletal remodeling. Although RhoG activation has not been studied, overexpression of an active form of RhoG increases endothelial cell size similar to trio overexpression (Van Buul et al., 2007). The increase in endothelial size was accompanied by increased focal adhesions. This may be due to upregulated Rac1 activity but not RhoG as another work in cancer cells showed increased focal adhesions upon RhoG knockdown (Zinn et al., 2019). Recently, RhoG has been shown to be involved in VEGF mediated VEGFR micropinocytosis and dependent angiogenic signaling. This RhoG activity is depend on its activator Arhgef26. Knocking down of either Arhgef26 or RhoG showed similar defects *in-vitro* angiogenic assay. Interestingly, Arhgef26$^{-/-}$ mice showed reduced atherosclerotic plaques compared to wild type mice in adeno-associated virus-induced murine atherosclerosis model (A. Vion, 2022; Q. M. Zhu et al., 2021). These results suggest a crucial role for RhoG in atherosclerotic plaque formation *in-vivo*.

RhoJ, also known as TC10-like (TCL), belongs to the Cdc42 subfamily that shares similarity with RhoQ and Cdc42. Aspenstrom and collaborators showed that overexpressing constitutively active RhoJ mutant in Cos7 cells resulted in formation of lamellipodia, actin bundles and focal adhesions (Aspenström et al., 2004). In addition to its role in cytoskeletal organization, RhoJ has been shown to play an important role in endocytosis. RhoJ is expressed in most cell types and its expression is regulated by ERG (ETS-related gene) transcription factor which is abundant in ECs (Yuan et al., 2011). Knocking down of RhoJ using siRNA resulted in reduced ECs migration, proliferation and tube-formation. Using mice retinal angiogenesis model, it has been shown that RhoJ activation is involved in retinal angiogenesis. While VEGF promotes endothelial filopodia formation in sprouting vessels, Sema3E and its receptor PlexinD1 counteracts it by activating RhoJ thereby causing filopodia retraction in those sprouting vessels maintaining a balance and a patterning of the network (Fukushima et al., 2011). Additionally, in ECs, RhoJ regulates FMNL3(Formin Like 3) mediated EC lumen formation through polarized trafficking of podocalyxin (Richards et al., 2015). Another important function of RhoJ in angiogenesis came from recent work by Sundararaman *et al*, where they showed that RhoJ positive endocytic vesicles are enriched in α5β1

integrins (Sundararaman et al., 2020). Using *in-vitro* EC culture experiment, others showed that, knocking down of RhoJ results in increased extracellular fibronectin, a major ligand for α5β1 integrins (Astrof & Hynes, 2009). Overexpression of dominant active RhoJ led to an increased cycling of α5β1 endocytosis. Accordingly, *In-vivo* knockout of RhoJ was responsible for reduced retinal vascular out growth and increased fibronectin deposition (Astrof & Hynes, 2009).

RhoQ, formerly called TC10, has been shown to be primarily expressed in heart and skeletal muscle as analyzed by northern blot analysis (Neudauer et al. 1998). RhoQ shares similarity with protein sequence with Cdc42 and has been shown to interact with known Cdc42 effectors such as WASP and PAK thus modulating cytoskeletal organization (Aspenström et al., 2004; Neudauer et al., 1998). Overexpression of dominant active RhoQ in NIH3T3 fibroblasts resulted in longer peripheral extensions, reduced stress fibers and loss of cortical actin compared to cells expressing dominant active Cdc42. However, it had no effect on membrane ruffle formation unlike Cdc42 (Kanzaki et al., 2002; Neudauer et al., 1998). In ECs, RhoQ also shown to induces podosomes formation (Billottet et al., 2008). *In-vivo*, knocking out of RhoQ resulted in reduced retinal vascular network. Mechanistically, DLL4/Notch signaling induces RhoQ expression (Kofler et al., 2011) and RhoQ exerts its effect on DLL4/Notch signaling through mediating the nuclear localization of Notch Intracellular Domain (NICD), as knocking down of RhoQ resulted in reduced nuclear NICD and increased NICD in lysosomes for degradation (Bridges et al., 2020).

2.3 Rho-GTPase signaling in pathophysiology

RhoA signaling plays prominent role in vascular pathophysiology. Increased activation of RhoA has been observed in Ang-II treated VSMCs and aortas of hypertensive rat models such as spontaneously hypertensive stroke prone rats (SHR-SP) (Kataoka et al., 2002; Seko et al., 2003). In addition, inhibition of RhoA/ROCK signaling by the Rho-kinase inhibitor Y27632, repressed MCP-1 and TGFB1 expression as well as early inflammation, vascular remodeling and vascular lesions in L-NAME-induced hypertensive rat model (Kataoka et al., 2002). Similar role of RhoA has been described in SHR rats, wherein inhibition of Rho-kinase by fasudil prevented hypertension-

mediated vascular remodeling (Mukai, 2002). In the pathogenesis of abdominal aortic aneurysm, it has been shown that inhibition of Rho-kinase with fasudil significantly reduced the thickening of aorta, formation and severity of Ang-II induced aneurysm formation in ApoE$^{-/-}$ mice. This is through inhibiting VSMCs apoptosis and ECM degradation through MMP secretion (Y. Wang et al., 2005). RhoA signaling has been shown to involve in ET-1 induced Cardiac hypertrophy. Koichiro *et al*, showed that inhibiting Rho/ROCK pathway using either specific inhibitor Y27632 or overexpression of dominant negative ROCK1 inhibited ET-1 induced hypertrophic genes such as atrial natriuretic peptide and brain natriuretic peptide in neonatal rat ventricular cardiomyocytes (Kuwahara et al., 1999). Later, it was shown that Rho/ROCK signaling activates ERK1/2 which directly or indirectly phosphorylates and activates the transcription factor GATA4 which mediates the transcription of hypertrophic genes (Yanazume et al., 2002).

Shear stress and AT1R signaling induces ROS production which is important for vascular tone maintaining by activation p38-eNOS signaling pathway (Bretón-Romero et al., 2012; Eguchi et al., 2018). This could be through by **Rac1** which promotes NADPH complex formation by interacting with p67^{phox} subunit thereby ROS production (Sumimoto, 2008). Under pathological conditions such as hypertension, Ang-II-AT1R signaling increases ROS production and vascular cell dysfunction (Eguchi et al., 2018). *In-vivo*, chronic infusion of Ang-II induced aneurysm formation in LDLR$^{-/-}$ mice, which was abrogated by endothelial specific knockout AT1R (Rateri et al., 2011). The role of Rac1 in aneurysm formation was described by Marinković and his group, wherein inhibition of Rac1 activity using specific inhibitor 6-Mercaptopurine resulted in reduced incidence of aneurysm formation as well as pro-inflammatory JNK signaling activation in ApoE$^{-/-}$ mice (Marinković et al., 2013). Moreover, *in-vitro* inhibition of Rac1 using 6-Mercaptopurine inhibited TNFα induced JNK and NFkB mediated inflammatory gene expression in HUVECs (Marinković et al., 2014), indicating the role of Rac1 in JNK and NFkB signaling under different physiological context. During immune cell transmigration through ECs, attachment of immune cell triggers ICAM1 and VCAM1 clustering which results in the formation of transmigratory cup, a cup like membrane protrusions at the interface of immune cell and ECs (Barreiro et al., 2002). This

transmigratory cup formation requires GEF Trio mediated activation of Rac1, as inhibition of Trio using ITX3 or silencing of Rac1 resulting in similar and reduced membrane protrusion and neutrophil transmigration (Van Buul et al., 2007; van Rijssel et al., 2012). In ECs, Rac1 activity is necessary for shear stress induced NFkB mediated ICAM1 expression, as cells overexpressing dominant negative mutant of Rac1 fail to induce ICAM1 under shear stress (Tzima et al., 2002). Interestingly, shear stress induced ICAM1 is influenced by the extracellular matrix, as, it was shown that cells plated on fibronectin coating induced ICAM1 expression whereas collagen coating did not (Orr et al., 2005). In VSMCs, Rac1-PAK1 signaling has been shown to regulate *in-vivo* VSMC proliferation and migration in balloon injury mice model of neointima formation as overexpressing dominant negative PAK resulted in inhibition of neointima formation (D. Wang et al., 2009).

Although there is no direct evidence for the role of **Cdc42** in vascular pathologies has been reported yet, its association with vascular malformations came from *in-vivo* animal model studies and its important role in postnatal blood vessel development (Barry et al., 2015; Yoshida et al., 2021). Endothelial specific deletion of Cdc42 resulted in defective ECs migration and capillary-venous malformations (Laviña et al., 2018). Moreover, loss of Cdc42 leads to increase in MEKK3-MEK5-ERK5 signaling mediated-overexpression of KLF2/4 and cerebral cavernous malformations (Castro et al., 2019).

2.4 GEFs in EC physiology

There are nearly 83 GEFs and 67 GAPs for 20 Rho-GTPase and only 17 GAPs and 20 GEFs are shown to be highly expressed in endothelium (Table 1 & 2) (Van Buul et al., 2014; Vigil et al., 2010).

Table 1: List of GEFs highly expressed in endothelial cells

Highest expressed GEFs transcripts in HUVECs were shown in the 3rd column relative to the average expression level in Roth-504 Affymetrix data sets (Adapted from Van Buul et al., 2014; Vigil et al., 2010)

Gene name	Alternative names	Relative expression in HUVEC	Rho GTPase targets	Function
NME1	NB; AWD; NBS; GAAD; NDKA; NM23; NDPKA; NDPK-A; NM23-H1	21.68		
ECT2	ARHGEF31	19.95	RhoA, Rac1, Cdc42	
FGD5	ZFYVE23	16.42	Cdc42	Involved in VEGF-induced endothelial cell adhesion signaling, cell-cell junction stabilization and associated with vascular development.[52, 118–120.]
DNMBP	TUBA; ARHGEF36; RP11–114F7.3	12.63	Cdc42	
RGNEF	RIP2; p190RHOGEF	12.08	RhoA	
DOCK6	AOS2, ZIR1	8.45	Rac1, Cdc42	
DOCK4	WUGSC:H_GS034D21.1	8.36	Rac1, Rac2	
ARHGEF15	E5; ARGEF15; Ephexin5; Vsm-RhoGEF	8.29	Cdc42, RhoA	Mediator of VEGF-induced retinal angiogenesis.[57,134]
FGD6	FYVE, RhoGEF and PH domain-containing protein 6	7.49		
BCR		7.39	RhoA	
ARHGEF7	β-pix, RP11–494P5.1, COOL-1, COOL1, Nbla10314, P50, P50BP, P85, P85COOL1, P85SPR, PAK3, PIXB	7.32	Rac1, Cdc42	Mediator of VEGF-induced permeability.[138]
VAV2	vav 2 guanine nucleotide exchange factor	7.23	Rac1, RhoA, RhoG, Cdc42	Mediator of growth factor- or mechanotransduction-induced signaling in control of cell-cell adhesion, migration and angiogenesis.[141-143,145,147,148]
ITSN1	ITSN, SH3D1A, SH3P17	7.18	Cdc42	Pro-survival mediator and promotes vascular integrity.[150,151]
ARHGEF10	GEF10	7.00	RhoA, RhoB, RhoC	
FARP1	RP11–111L24.1, CDEP, PLEKHC2, PPP1R75	6.43	Rac1	
TRIO	ARHGEF23, tga	6.43	Rac1, RhoG, RhoA	Regulator of endothelial docking structures during transmigration of leukocytes.[160]
PLEKHG4	ARHGEF44, PRTPHN1, SCA4	6.26	Rac1, Cdc42, RhoA	
ALS2	ALSJ; PLSJ; IAHSP; ALS2CR6	6.25	Rac1	
DOCK9	RP11–155N3.2, ZIZ1, ZIZIMIN1	5.93	Cdc42	
PLEKHG1	D10Ertd733e, Gm521, mKIAA1209	5.53		
ARHGEF12	Larg, RO2792	5.08	RhoA, RhoC	Mediator of Semaphorin 4D and S1P-induced endothelial signaling.[165,166]

Table 2: List of GAPs highly expressed in endothelial cells

Highest expressed GAPs transcripts in HUVECs were shown in the 3rd column relative to the average expression level in Roth-504 Affymetrix data sets (Adapted from Van Buul et al., 2014; Vigil et al., 2010)

Gene name	Alternative names	Relative expression in HUVEC	Rho GTPase targets	Function
DEPDC1	DEP.8; SDP35; DEPDC1A; DEPDC1-V2	40.60		
ARHGAP24	FilGAP, RC-GAP72, RCGAP72, p73, p73RhoGAP	25.86	Rac1, Cdc42	Regulates endothelial cell migration, tubulogenesis and angiogenesis.[46]
ARHGAP29	PARG1, RP11–255E17.1	24.97	RhoA	Regulates endothelial adhesion, spreading and polarization during vascular lumen formation and endothelial barrier function.[53, 54.]
ARHGAP18	MacGAP, SENEX, bA307O14.2	21.52	RhoA	Role in endothelial capillary tube formation and barrier protective function.[56]
DEPDC1B	XTP1; BRCC3	20.19		
ARAP3	CENTD3, DRAG1	16.69	RhoA	Adhesion and migration of endothelial cells during (lymph) angiogenesis.[59,63,64]
ARHGAP22	RhoGAP2, RhoGap22, p68RacGAP	11.16	Rac1	Role in endothelial capillary tube formation.[48]
ARHGAP11a	GAP (1–12); rho GTPase-activating protein 11A; rho-type GTPase-activating protein 11A	10.73		
ARHGAP28	Rho GTPase activating protein 28	10.14		
RACGAP1	CYK4, HsCYK-4, ID-GAP, MgcRacGAP	9.97	Rac1, Cdc42	
DLC1	Deleted in Liver Cancer 1, ARHGAP7, HP, STARD12, p122-RhoGAP	7.54	RhoA, RhoB, RhoC, Cdc42	
ARHGAP17	PP367; RICH1; WBP15; MST066; MST110; NADRIN; PP4534; RICH1B; MSTP038; MSTP066; MSTP110	7.39	Rac1, Cdc42, RhoA	
BCR		7.39	RhoA, Rac, Cdc42	
ARHGAP31	AOS1, CDGAP	6.47	Rac1, Cdc42	
ARHGAP19	rho GTPase-activating protein 19	6.40	RhoA	
MYO9B	myosin-lxb, CELIAC4, MYR5	5.87	RhoA	
RALBP1	RIP1, RLIP1, RLIP76	5.20	Rac1, Cdc42	Role in tumor-associated angiogenesis.[98]

These GEFs and GAPs have been shown to regulate Rho-GTPase-dependent processes such as permeability (Stockton et al., 2007), migration (Garrett et al., 2007), angiogenesis (Gambardella et al., 2010) and leukocyte transmigration (Van Rijssel et al., 2012). Angiogenesis and maintenance of functional blood vessels is a complex process, and, timely dependent orchestrated activation of small-GTPases is crucial, in addition to the factors such as ligand-receptor signaling, and ion channel mediated Ca^{+2} signaling (Adams & Alitalo, 2007; Urade et al., 2022). GEFs, GAPs and GDIs regulate spatio-

temporal activation of small-GTPases. Developmental timing and cell specific expression of such regulators determines proper blood vessel formation (Kather & Kroll, 2013). One such GEF is **FGD5**, a cdc42 specific GEF whose expression is specific to vascular endothelial cells. In mice embryo, FGD5 expression is high during early embryonic stage and reduces at postnatal day 8. Knockdown of FGD5 in HUVECs inhibited VEGF mediated EC migration and tube formation (Kurogane et al., 2012). In addition, adenoviral overexpression of FGD5 resulted in EC apoptosis through Hey1-p53 signaling pathway in mice retina models (C. Cheng et al., 2012).

Trio is a RhoGEF that gained attention these past few years in vascular biology. Trio is a RhoGEF with three enzymatic domains (two GEF domains and Ser/Thr kinase domain). The two GEF domains GEF1 and GEF2 interact with and activate the Rac1/RhoG and RhoA respectively. Overexpression of TrioGEF1 and GEF2 resulted in membrane ruffles, lamellipodia and actin stress fiber formation respectively (Bellanger et al., 1998). In ECs, during the process of leukocyte trans-endothelial migration, Trio is recruited to ICAM1 at the leukocyte docking site where it activates Rac1 and RhoG which are important for ICAM1 clustering and membrane protrusions respectively (Van Rijssel et al., 2012). Under SS conditions, Trio has been shown to play a role in EC alignment independently of its GEF activity (Kroon et al., 2017). Flow results in the localization of active Rac1 downstream to the flow direction. Knocking down of Trio does not affect the Rac1 activity but results in loss of Rac1 polarization and failure of ECs to align parallel to the flow. Further experiments using GEF domain mutants showed that Trio indeed acts as a scaffold protein in mediating Rac1 polarization (Kroon et al., 2017). The role of Trio in endothelial cell-cell junction formation and maintenance as well as in vascular permeability cannot be overlooked. *In-vitro*, during the formation of adherent junctions, Trio is recruited to VE-cadherin and promotes local Rac1 activity thereby contributing to adherent junction stability. Interestingly, knockdown of Trio resulted in failure of endothelial adherent junction to re-assemble in response to the thrombin treatment (Timmerman et al., 2015). Similar work by Mikelis *et al*, showed that the inflammatory molecule histamine resulted in the activation of RhoA via Gα11/q-Trio activation, which leads to endothelial barrier disruption (Mikelis et al., 2015). In addition to inflammation-induced permeability, Trio's role in SS mediated barrier integrity has been explored. Work by Polacheck *et al*, They showed that SS-activated

Notch resulted in the formation of novel transmembrane complex consisting of Notch1, VE-cad, LAR and Trio; which activates junctional Rac1 thereby promoting barrier integrity (Polacheck et al., 2017). These studies suggest a crucial role of Trio in flow mediated EC orientation as well as in barrier restoration upon inflammatory stimulus under physiological conditions.

While not being a RhoGEF, **EPAC1** (Exchange protein activated by cAMP-1) is a guanine nucleotide exchange factor, shown to regulate multiple functions of shear stress mediated endothelial functions. In human arterial ECs, knocking down EPAC1 reduces shear stress induced Rap1 activation as well as shear stress induced genes such as KLF2, eNOS and thrombomodulin. In addition, using knockdown approaches, it was shown that EPAC1 mediates adherent junction stability through VE-cad/VEGFR2/PECAM1 mechanosensory complex (Rampersad et al., 2016). In line with this observation, EPAC1 knockout mice showed fragmented VE-cad junctions and increased permeability as analyzed by measuring trans-endothelial resistance. Knockout of EPAC1 reduced Rap1 activity but no significant effect on RhoA and Rac1 activity was observed (García-Ponce et al., 2020).

Unlike other GEFs, **GEF-H1** has been shown to interact with microtubules. In bound state, GEF-H1 stays inactive and any mechanical alterations to microtubular network such as depolymerization results in the release of GEF-H1 and thus actives it (Birkenfeld et al., 2008). Birukova and collaborators showed that subjecting human pulmonary ECs to cyclic stretch resulted in the depolymerization of microtubular network and activation of RhoA and stretch induced cell permeability. The increased RhoA activity was due to free active GEF-H1, as knocking down of GEF-H1 diminished stretch induced RhoA signaling and permeability (Birukova et al., 2010). Similar work in the context of GEF-H1 and thrombin induced permeability supports the role of GEF-H1 in vascular permeability (Birukova et al., 2006). In addition to the role of GEF-H1 in mechanical and inflammation mediated vascular permeability, GEF-H1 has been shown to be involve in leukocyte trans-endothelial migration process as well. Knock-out of GEF-H1 resulted in reduced neutrophil infiltration to the inflamed site. Although GEF-H1 deletion did not affect neutrophil migration under static conditions, GEF-H1 null neutrophils showed

defective crawling under sheer stress (Fine et al., 2016). In addition, stimulation of ECs with the proinflammatory molecule LPS induces the expression of GEF-H1 as well as increase in the phosphorylation of p65 and p38. Knocking down of GEF-H1 or RhoA significantly reduces this p38 and p65 phosphorylation. Through RhoA mediated p38 activation, GEF-H1 regulates NF-κB transactivation and secretion of inflammatory cytokines such as IL-8, IL-6 and TNFα (Guo, Tang, et al., 2012; Guo, Xing, et al., 2012).

SmallGTPase activity has been shown to be altered in cardiovascular diseases such as hypertension. In hypertension, increased RhoA/ROCK signaling has been observed in VSMCs (Lee et al., 2004). Work by Guilluy *et al*, identified **Arhgef1** (also known as p115 or Lsc) as a intracellular mediator of vasoconstrictor action of Ang-II (Guilluy et al., 2010). Treating rat vascular smooth cells with Ang-II resulted in activation of Arhgef1 through phosphorylation at Tyr738 which was mediated by Jak2. This induction is unique as Ang-II failed to activate other well-known Rho-GEFs such as Arhgef11 and Arhgef12. In mice model, VSMC specific deletion of Arhgef1 resulted in inhibition of Ang-II mediated vascular contraction and resistance to Ang-II induced hypertension. Interestingly, Arhgef1-mediated vasoconstriction is specific for Ang-II as Arhgef1 null mice arteries have no observable difference in endothelin-1 and phenylephrine-induced vasoconstriction. Moreover, RhoA/Rho-kinase activation has been reported in human patients of hypertension and similar Ang-II mediated signaling mechanism may have been the underlying cause of such activation (Carbone et al., 2015). Although the above described activation of Arhgef1 is through the interaction of Ang-II with AT1R, the mechanosensitive nature of AT1R described by Zou *et al* could result in the activation of Arhgef1 thus suggesting a potential role of Arhgef1 in mechanotransduction during hypertension (Mederos Y Schnitzler et al., 2011; Zou et al., 2004).

Another GEF that is mechanically activated and involved in hypertension is **LARG** (also known as Arhgef12). Using knockout mice models, it has been shown that LARG is involved in salt induced-hypertension but not in maintaining normal blood pressure. This LARG activity is downstream of G-protein G12-13, as smooth muscle specific knockdown of G12-13 gave similar phenotype as LARG knockout (Wirth et al., 2008). Integration of LARG in mechanotransduction signaling pathway came from the work in

fibroblasts, as mechanical stimulation of integrins using magnetic beads resulted in the activation and recruitment of LARG to focal adhesion complexes. This activation of LARG is mediated by non-receptor tyrosine protein kinase Fyn. The recruited LARG mediates the RhoA signaling thereby causing cellular stiffness (Guilluy, Swaminathan, et al., 2011). Interestingly, in ECs, application of mechanical forces to ICAM1 using magnetic beads resulted in its clustering, reproducing the natural effect of immune cell adhesion and prompted RhoA activation. This ICAM1 clustering was associated with LARG activation which activity was proportional to the mechanical strength applied to the ECs. Knocking down of LARG in ECs resulted in decreased leukocyte rolling and endothelial transmigration (Lessey-Morillon et al., 2014).

Hypertension has been shown to associate with cerebral arterial and intracranial aneurysms in human patients as well as its enlargement and rupture (Rooprai et al., 2022; Spittell, 1983; Tada et al., 2014; Takagi & Umemoto, 2017; Taylor et al., 1995). This was further strengthened by the development and progression of aneurysms induced laboratory animal models (Gertz et al., 2013; Lysgaard Poulsen et al., 2016; Strange et al., 2020).

In the past decade, association of ARHGEF11 (Zholdybayeva et al., 2018), ARHGEF12 (Zhang et al., 2015) and ARHGEF17 (Yang et al., 2018b) with intracranial aneurysm (IAs) has been described. In their paper, Zholdybayeva *et al,* identified single nucleotide polymorphism in the intronic sequence of *ARHGEF11* genomic DNA from Kazakh population with IAs (Zholdybayeva et al., 2018). Another study using human IA rupture samples identified microRNAs that target *ARHGEF12* (M. Zhang et al., 2015). Another recent study described the association of mutations in *ARHGEF17* with intracranial aneurysm in Chinese patients (Yang et al. 2018). In their study, they have identified at least 5 missense mutations in patients with IA that might affect the interaction of ARHGEF17 with its interacting partners. Inhibition of *arhgef17* expression using morpholinos results in intracranial hemorrhage which was rescued by expression of human *ARHGEF17* in zebrafish model.

Although, these studies are handful, they impart the association and involvement of Rho-GEFs in IAs. Many GEFs may be involved in the pathogenesis of IAs and identifying

such GEFs would help us in understanding the pathophysiological mechanisms of IA formation.

3. ARHGEF18

ARHGEF18, also known as p114-RhoGEF, is a 114kDa Rho GEF, first cloned (clone ID: KIAA0521) by Ohara's group as a part of 'predicting and analysis of coding sequences of unidentified human genes', and was then identified and characterized by Blomquist (Blomquist et al., 2000; Ishikawa et al., 1998). ARHGEF18 is ubiquitously expressed in most cell types and tissues. With a high expression in kidney and pancreas, and a low expression in heart and brain in humans (Blomquist et al., 2000; Niu et al., 2003).

3.1 Structure

ARHGEF18 gene encodes for three different isoforms; isoform-1, -2 and -3 and a smaller ARHGEF18 transcript was detected in skeletal muscle (Blomquist et al., 2000). ARHGEF18 isoform-2, 1015 amino acids in length, is considered as the canonical form and is expressed in most cell types. Isoform-1 differs from isoform-2 by additional 158 amino acids at the N-terminus. However, no special domains have been attributed to these additional amino acids. Isoform-3, also known as LOCGEF-X3 is shown to be expressed exclusively in eosinophils through a leukocyte-specific transcriptional initiation site, that results in 1361 amino acids ARHGEF18. ARHGEF18 isoform regulates the cell polarity in activated eosinophils and leukocytes (Turton et al., 2018). All three isoforms contain Dbl homology (DH) domain followed by a pleckstrin homology (PH) domain, which are characteristics of GEFs and differ in amino acid number at the N-terminus (Figure 16). Of the three, the canonical isoform-2 is well characterized.

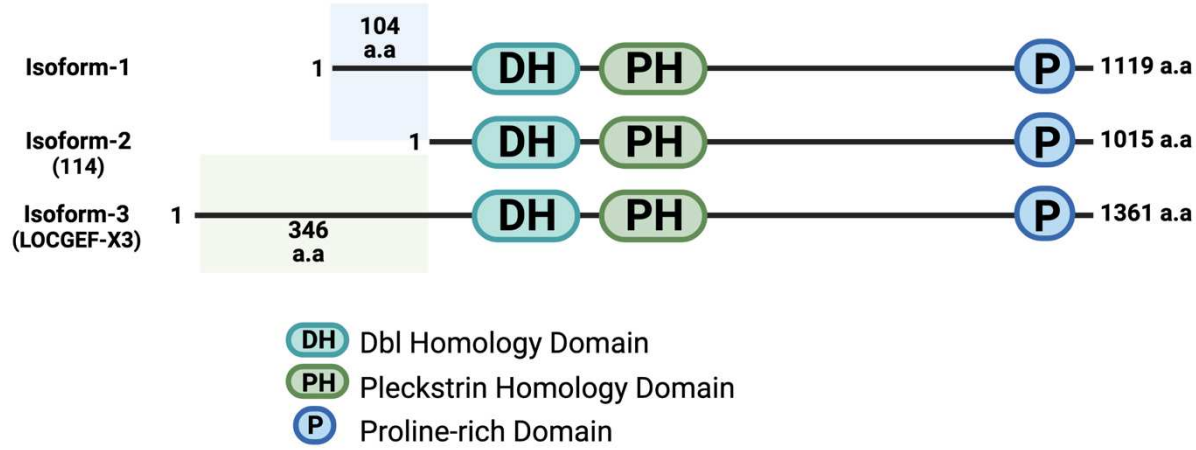

Figure 16: Structure of Arhgef18 isoforms

Schematic representation of all three isoforms of Arhgef18 with known DH, PH and proline-rich domains. All three isoforms are identical except at the N-terminus.

3.2 Interaction with small-GTPases:

The amino acid sequence of ARHGEF18 shows similarities to GEFs specific for RhoA but not Rac and Cdc42. *In-vitro* radioactive GTP[S] labelling experiments using purified recombinant ARHGEF18 and small GTPases showed that ARHGEF18 activity is specific towards RhoA but not Rac1 or Cdc42 (Blomquist et al., 2000). In contrast, others showed that overexpression of ARHGEF18 increased both RhoA and Rac1 activity (Herder et al., 2013; Niu et al., 2003). Although, no direct transfer of radioactive GTP to Rac1 was observed in Arhgef18 overexpression by Blomquist, increased activity in Rac1 observed by Niu could be due to the crosstalk between RhoA and Rac1 signaling networks. This activation was further supported by increased Rac1 mediated ROS production and increased membrane localization of $p67^{phox,}$ a NADPH oxidase subunit in Arhgef18 overexpressing NIH3T3 cells (Niu et al., 2003). Direct interaction of ARHGEF18 with RhoA but not Rac1 was further supported by mass-spectrometry analysis (Paul et al., 2017). Knocking down of ARHGEF18 in human corneal epithelial cells (HCEs) significantly reduced active RhoA, without affecting Rac1 and Cdc42 activity, and overexpression increases both active RhoA and phosphorylated MLC (Terry et al., 2011). At the junctions, ARHGEF18 regulates RhoA-ROCK activity and actomyosin contractility in a spatio-temporal manner, thereby, junctional stability. In support of this, ARHGEF18 has been shown to promote actomyosin-driven movement, which is

dependent on RhoA activity, and does not affect lamellipodia-driven migration, which depends on Rac activity (Terry et al., 2012).

3.3 Role of Arhgefi8 in epithelial cells

Consistent with the role of active RhoA in stress fiber formation, overexpression of Arhgefi8 in human bladder carcinoma J82 cells induced stress fiber formation (Blomquist et al., 2000), and this was further supported by the work where overexpression of DH/PH domain of Arhgefi8 is sufficient to induce stress fiber formation, but not the Proline rich C-terminal domain (Niu et al., 2003). Overexpression of Arhgefi8 mediates the SRF responsible SRE transcription which was inhibited by Clostridium botulinum C3 transferase, a specific ADP-ribosylates which inactivates Rho proteins but not Rac and Cdc42 (Blomquist et al., 2000). This action of Arhgefi8 was shown to be mediated through G-protein $G_{\beta\gamma}$ subunit through several multiple interactions with multiple domains of Arhgefi8 as analyzed *in-vitro* by overexpressing various domains of Arhgefi8 (Niu et al., 2003). Another important protein that may regulate the Arhgefi8 localization is Sept9b. Arhgefi8 has been shown to interact with septin9b, a cytoskeletal component using yeast two hybrid system and overexpression of septin9b in cell culture system reduced both RhoA-activation as well as active RhoA mediated stress fiber formation (Mostowy & Cossart, 2012; Nagata & Inagaki, 2005). This could be one of the several mechanisms of spatio-temporal regulation of Arhgefi8 mediated RhoA activation. In podocytes, Arhgefi8 interacts with EPB41L5 and regulates the actomyosin activation and focal adhesion maintenance which are required for podocyte physiological function (Schell et al., 2017) (Figure 17) and Knocking down of Arhgefi8 leads to significant rearrangement of F-actin in podocytes (Lu et al., 2017). GPCR independent activation of Arhgefi8 during neurulation in frog and zebrafish embryos has been reported. This is mediated by a cytoplasmic protein DAPLE which activates $G_{\beta\gamma}$ subunit of G-proteins which in turn activates Arhgefi8 and RhoA-ROCK signaling and apical cell constriction (Marivin et al., 2019).

In the context of **cell-cell junction**, using epithelial cells (Caco-2 & HCE), ARHGEF18 is shown to be localized at tight-junction but not adherent-junction, and is required for

junctional maturation but not for junction initiation and spreading (Terry et al., 2011). Knocking down of ARHGEF18 results in discontinuous junctional ZO1 and increased permeability. At tight junctions, ARHGEF18 forms a junctional complex with myosin-IIA, ROCKII and Cingulin. Cingulin acts as an adaptor protein and regulates the localization of ARHGEF18 to matured junctions (Terry et al., 2011). Another protein, LKB1, a ser/thr kinase, has been shown to interact with Arhgef18 and disruption of this interaction by overexpression of dominant negative mutants also resulted in punctation of junctional ZO1, indicating the importance of ARHGEF18 at tight junctional stability (X. Xu et al., 2013) (Figure 17). In a RNA interference screen to identify GEFs responsible for epithelial cell migration in scratch wound assay, Arhgef18 has been shown to be responsible for mediating the long distance signaling during collective cell migration (Zaritsky et al., 2017). During migration, Arhgef18 mediates double phosphorylation of MLC at the cell-cell junctions. Silencing of Arhgef18 results in reduced junctional double phosphorylated myosin but not at the leading edge (Terry et al., 2012). In epithelial cells, knocking down of Arhgef18 results in redistribution of myosin from junctions to stress fibers along with phosphorylated MLC, without apparent effect on total phospho-MLC and MLC phosphatase (Terry et al., 2011).

In the context of **apico-basal cell polarity and morphogenesis**, RhoA activation plays important role in developmental signaling pathways such as Wnt-planar cell polarity pathway. In N1E-115 mouse neuroblastoma cells, Arhgef18 mediates Wnt-3a induced RhoA activation via interaction with both Dvl and Daam1 proteins, thus playing significant role in mammalian embryo development (Takuji Tsuji, 2010) (Figure 17). In 3D culture systems, silencing of ARHGEF18 resulted in epithelial cysts with multiple lumen without affecting the polarity (Terry et al., 2011). This was further supported by Kim and collaborators, using the MDCK-HGF induced lumen formation model they demonstrated that knocking down of Arhgef18 results in multiple lumen formation and this effect was due to low RhoA and ROCK-I activity and reduced epithelial cell movement during lumen formation (Kim et al., 2015). On the other hand, in epithelial cells, Arhgef18 is recruited to the apical cell-cell boundary by an apical polarity regulator

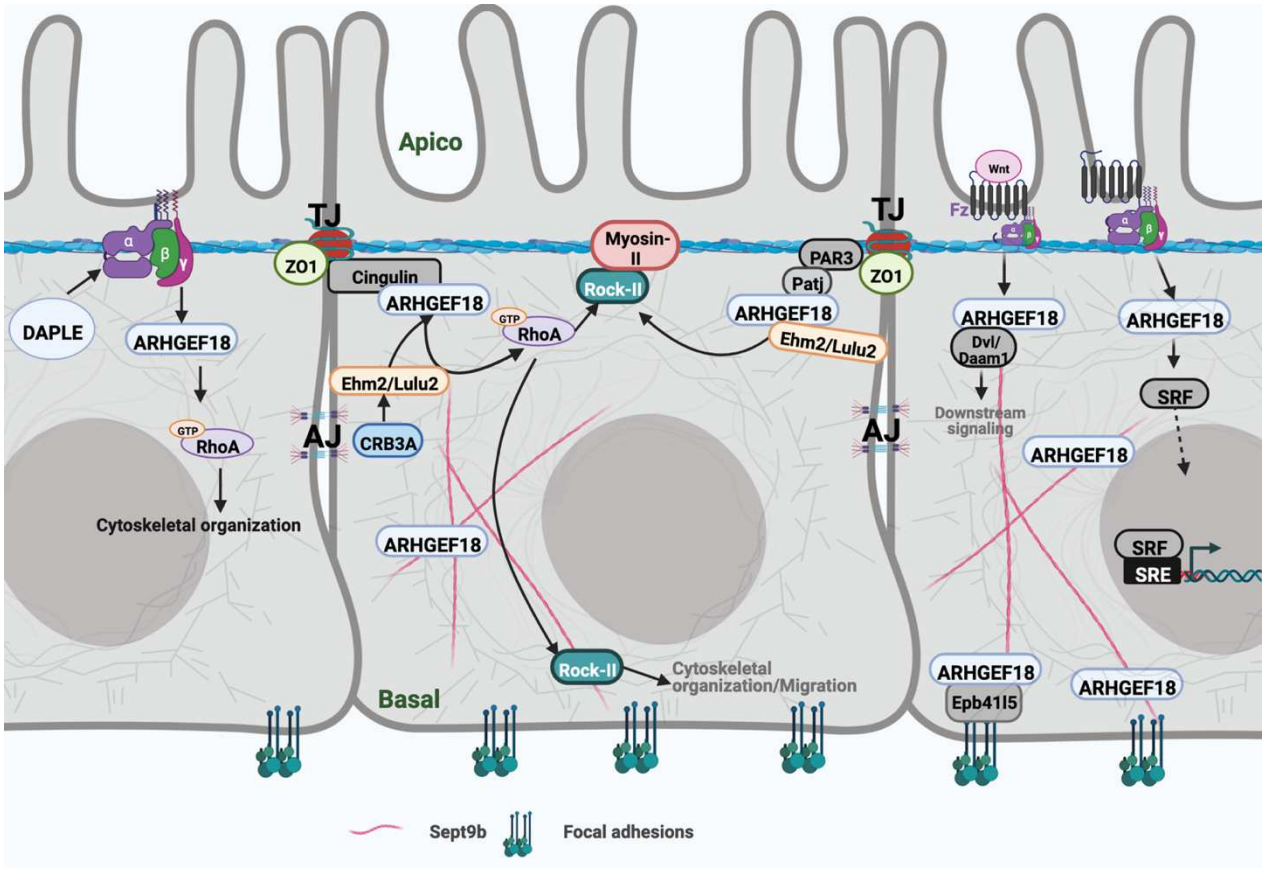

Figure 17: Schematic representation of Arhgef18 signaling in epithelial cells

In epithelial cells, Arhgef18 interacts with multiple partners and regulate RhoA-ROCK dependent cytoskeletal re-arrangement, migration, apico-basal polarity and transcription.

Patj through interaction with PDZ binding domain, where it was activated by Lulu2 which results in local activation of RhoA and circumferential actomyosin belt (H. Nakajima & Tanoue, 2011). Consistently with the role of Arhgef18 in apico-basal polarity maintenance *in-vitro*, knocking down of Arhgef18 results in the loss of apico-basal polarity in retinal and neuro epithelial cells in medaka fish and also increased proliferation of retinal progenitor cells (Herder et al., 2013). In HeLa cells, ARHGEF18 is important for Crumb homolog 3A (CRB3A) induced epithelial cell phenotype with well-established circumferential actin cytoskeleton and is mediated though Ehm2-Arhgef18 dependent RhoA-ROCK2 signaling (Loie et al., 2015).

In epithelial cells, ARHGEF18 maintains tight junctional stability as well as apico-basal cell polarity through interacting with various partners and regulating cytoskeletal dynamics through localized activation of RhoA-ROCK signaling.

3.4 Role of Arhgefi8 in endothelial cells

Although, function of Arhgefi8 is well characterized in epithelial cells, very little work has addressed the role of Arhgefi8 in ECs. In ECs, Arhgefi8 has been shown to localized at tight junctions and required for junctional tension and integrity in microvascular ECs (Tornavaca et al., 2015). *In-vivo*, complete deletion of Arhgefi8 resulted in embryonic lethality (Beal et al., 2021). Despite the role of Arhgefi8 in junctional integrity, endothelial specific Arhgefi8 knockout mice develop normally undermining the importance of Arhgefi8 in other cell types such as VSMCs. This is partially supported by the reduced vasculature, increased hemorrhage and oedema observed in Arhgefi8$^{-/-}$ Arhgefi8$^{-/-}$ embryos, which resembles the phenotypes of defective vascular network formation and compromised vascular permeability.

In ECs, ARHGEF18 has been shown to localize to the tight junctions and involved in maintaining junctional tension.

3.5 Arhgefi8 as a part of mechanotransduction complex.

The work that supports the role of ARHGEF18 in mechanotransduction came in 2015, using endothelial cells (HDMEC), Tornavaca showed that Arhgefi8 is recruited to tight junctions by ZO-1 and JACOP (Figure 18 top). Silencing ARHGEF18 results in loss of junctional vinculin, thereby, compromised VE-cadherin mediated endothelial cell-cell tension (Tornavaca et al., 2015). In Caco-2 cells, ARHGEF18 is responsible for the tension-mediated activation of RhoA signaling at adheren junctions by recruitment through Ga12, which activates mDia and F-actin (Acharya et al., 2018). Similar function of ARHGEF18 in RhoA activation-mediated junctional tension at adheren junctions during cell migration was reported. Such localized RhoA activation is necessary for junctional stability through E-cadherin recruitment thereby protection against mechanical stress during migration (Gupta et al., 2021). In epithelial (MDCK) cells, Haas *et al* identified the role of Arhgefi8 in extracellular matrix stiffness mediated tight junctional remodeling (Figure 18 bottom). They showed that knocking down of Arhgefi8 resulted in disassembly of tight junctions on hard surfaces such as hydrogels with stiffness of 40kPa and glass coverslips but not on the hydrogels with low stiffness (1kpa).

This works through junctional localization of Arhgef18 and could be mediated through stiffness-activated integrin signaling. This junctional localization of Arhgef18 is regulated by JAM-A thereby formation of appropriate focal adhesions (Haas et al., 2020). These reports established ARHGEF18 as a part of mechanotransduction complex. The recruitment of ARHGEF18 to the tight and adheren cell-cell junction was regulated by interaction with multiple proteins, wherein it regulates localized RhoA activity thereby junctional tension and maintaining junctional stability.

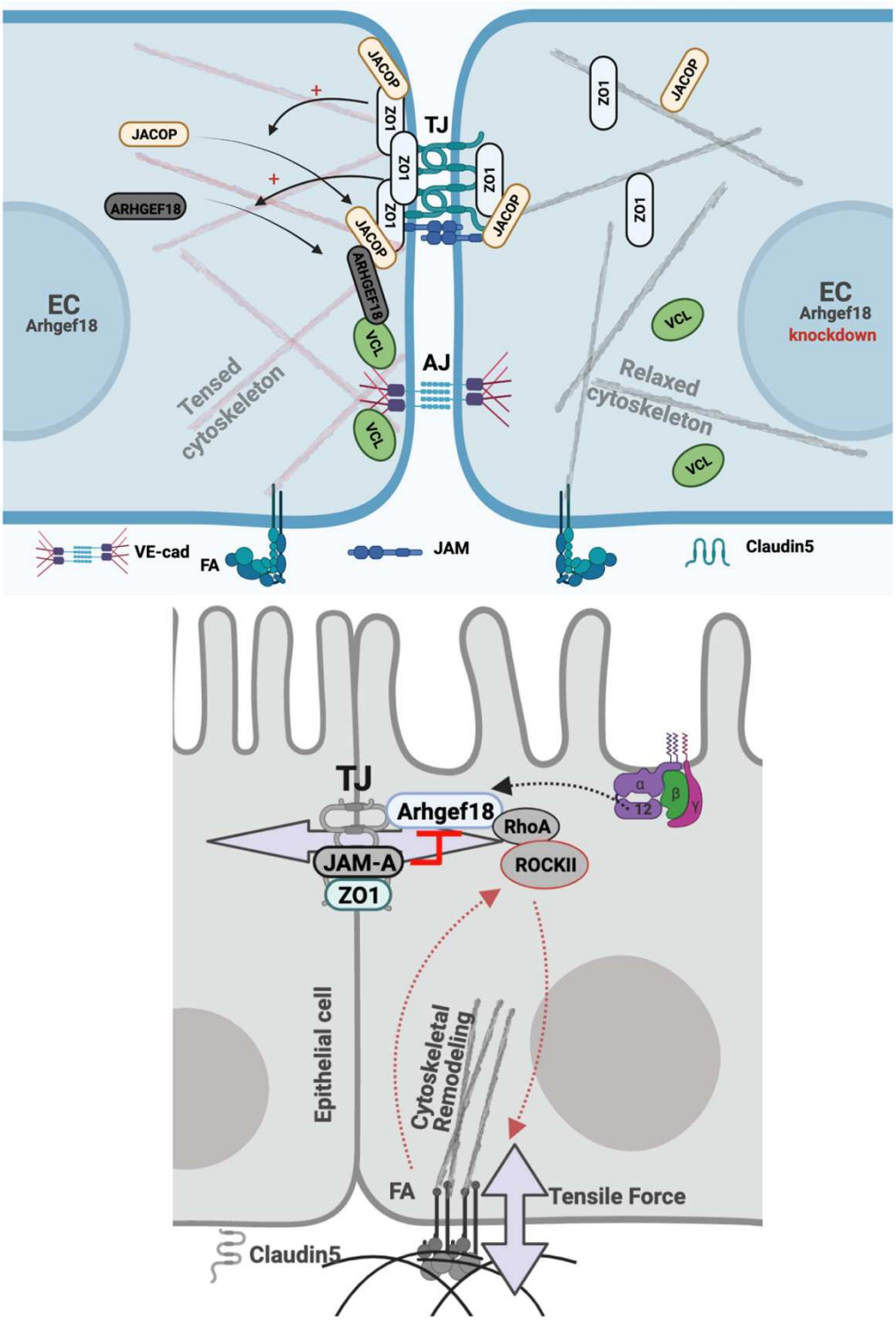

Figure 18: Schematic representation of Arhgef18 in mechanotransduction pathway

Top: Arhgef18 recruited to tight junction by ZO1 along with JACOP, where it interacts with vinculin and mediates VE-cad based actin based cytoskeletal tension. Knockdown of Arhgef18 resulted in reduced junctional localization of ZO1, JACOP and Vinculin, and, altered cytoskeletal tension.

Bottom: Arhgef18 mediates stiffness induced cytoskeletal and focal adhesion remodeling which is finetuned by JAM-A which negatively regulates the recruitment of Arhgef18 to tight junction. Gα12 mediated signaling might induce Arhgef18 localization (Adapted and modified from Haas et a.l,2020 & Acharya et al., 2018).

3.6 Role of ARHGEF18 in pathophysiology

An insight of ARHGEF18 role in pathological conditions came from multiple studies that reported mutations and overexpression of ARHGEF18 in human diseases.

Increased expression of ARHGEF18 was observed in Ovarian serous cystadenocarcinoma (OSCC), squamous-cell carcinoma (SCC) and in Cobalt chloride induced polyploid tumor giant cells (F. Shi et al., 2021; C. Song et al., 2013; Q. Zhao et al., 2021). In SCC, increased expression of ARHGEF18 was found to be associated with lymph node metastasis, which supports its role in promoting myosin-dependent amoeboid-like locomotion which was mainly used by tumor cells (C. Song et al., 2013; Terry et al., 2012).

Mutations in Arhgef18 has been found in adult-onset retinal degeneration and in orofacial cleft patients (Arno et al., 2017; El-Sibai et al., 2021). In adult-onset retinal degeneration, multiple mutations such as c.808A>G (p.Thr270Ala), c.2738_2761del (p.Arg913_Glu920del) and other nonsense mutation were found. Of the mutations, p.Thr270Ala mutation showed a reduced GEF activity and p.Arg913_Glu920del has not shown any defect in GEF activity. Overexpression of p.Thr270Ala mutant showed altered cortical actomyosin cytoskeletal rearrangement. The effect of other mutations in ARHGEF18 function and it relevance in the pathogenesis of retinal degeneration is not known (Arno et al., 2017).

In orofacial cleft patients, mutation in Arhgef18 coding sequence (G>A) has been identified in fibroblastic cells of orofacial cleft patients. These nucleotide transition results in change in amino acid p.Arg495Gln. This mutation falls in DH/PH domain of Arhgef18 and could result in reduced GEF activity. However, no functional studies has been done to characterize this mutation (El-Sibai et al., 2021).

Association of single nucleotide polymorphism in the intron and 3'UTR of ARHGEF18 has been demonstrated in Systemic Capillary Leak Syndrome and Chinese population with the risk of non-idiopathic pulmonary arterial hypertension respectively. However, how these SNP affects the Arhgef18 mRNA stability and/or translation has not been

reported (D. Li et al., 2018; Xie et al., 2013). Work by Frauenstein *et al*, found a dampened TLR2 mediated NFkB activation in human monocytes knockdown for Arhgef18 indicating an important role of ARHGEF18 in NFkB mediated inflammatory process. (Frauenstein et al., 2021).

These studies shed light on the importance of ARHGEF18 in human physiology and its alterations in pathological conditions. Moreover, ARHGEF18 could be key molecule underlying the pathogenesis of many inflammatory diseases.

OBJECTIVES

From the afore-discussed literature based on *in-vitro* studies and involvement of altered hemodynamics in human pathological conditions, it is evident that blood flow-mediated mechanical forces are pivotal for vascular cell identity, vascular network formation and vascular homeostasis. Hemodynamic regulated cytoskeletal organization plays important role in vascular cell health as ECs which experience turbulent blood flow exhibit omnidirectional cytoskeletal network and are the one prone to exhibit a pro-inflammatory profile and are proatherogenic.

Small-GTPases such as RhoA, Rac1 and Cdc42 regulate the cytoskeletal dynamics and rearrangement in response to the external signal. GEFs mediates the rate limiting step in the regulation of small-GTPases activity and contributes to their precise activation in a spatio-temporal manner, and, thus evolved as master regulators. Identifying how hemodynamic forces modulate the expression and activity of these master regulators in vascular cells could help us to better understand vascular pathophysiology.

Based on this, my PhD thesis is focused on two main objectives:

1) Identify the mechanosensitive GEFs in ECs and VSMCs *in-vitro*.
2) Functionally characterize the identified mechanosensitive GEFs in vascular cell physiology *in-vitro* and *in-vivo*.

RESULTS

1. Identification of mechanosensitive GEFs in ECs and VSMCs *in-vitro*

In order to identify mechanosensitive GEFs, a 3'seq-RNA Profiling (3'SRP) analysis was performed using HUVECs and primary rat aortic VSMCs were subjected to shear stress and cyclic stretch respectively. In addition, different types of arteries from spontaneously hypertensive (SHR), spontaneously hypertensive stroke prone (SHR-SP) rats and wistar-kyoto (WKY) rats were also used. SHR and SHR-SP rats develops hypertension and SHR-SP present cerebral stroke without a well-defined genetic cause and external stimulus. WKY rats served as wild type normotensive control. As VSMCs contribute to higher percentage of total cell population in arteries, the arteries from SHR and SHR-SP rats served as an *in-vivo* source of VSMCs that experience pathological shear stretch.

1.1 3'SRP analysis of VSMCs

1.1.1. Materials and Methods

VSMC isolation and culture: Primary rat VSMC were isolated from 4-week-old Wistar rats as follows. Rats were sacrificed according to the institutional animal handling ethics. Then the thoracic aorta was dissected out and endothelial cells were removed by gently scraping the aortic lumen with forceps. The remaining aortic tissue was then sliced into small pieces, and digested with collagenase type-11 (L5004176; Worthington) at a concentration of 1.5mg/ml for 2 h at 37°C. After the digestion, collagenase was inactivated with serum, the tissue was spun down and plated in a 6 well plate in the presence of complete medium (DMEM+10%FCS+P/S). The VSMCs which migrated out from the tissue, were cultured in complete medium and were used for experiments in between passage 2 & 4.

Application of cyclic stretch: For cyclic stretch experiments, rat aortic VSMCs were plated on fibronectin (1:400 dilution, FC010; Merck Millipore) coated silicone plates (MCFX-424; World Precision Instruments) at a density of 50,000 cells/cm^2. Once reaching 100% confluency, cells were subjected to physiological stretch (10%, 1Hz) and pathological stretch (20%, 1Hz) conditions for 30 min and 24 h using mechanoculture FX (CellScale) stretching device.

Artery tissue samples: 12-month-old WKY, SHR, SHR-SP rats (Charles River) were sacrificed according to the institutional animal handling ethics. Cerebral and mesenteric arteries were isolated and used for RNA extraction and 3'SRP analysis

RNA extraction: RNA from *in-vitro* samples (static and stretch applied VSMCs) were extracted using Nucleospin XS kit (Macherey-Nagel) according to the product manual. For the isolation of RNA from cerebral and mesenteric arteries, tissues were frozen in liquid nitrogen and crushed into powder using motar and pestle. The powdered tissue was then subjected to two stage purification. First, the RNA was separated from protein and DNA using TRIzol (Ref.15596018, Thermofischer). Then, the upper aqueous phase containing RNA which was obtained from trizol purification, was mixed with ethanol (1:3 ratio), added to the RNA purification columns from Nucleospin XS plus kit (Macherey-Nagel) and processed according to the product manual. The purity of the RNA was measured using nanodrop and samples with an absorbance of 1.8 (at 260/280) and above 2.0 (at 260/230) were used for 3'SRP analysis.

3'SRP analysis was performed according to the 3′-Digital Gene Expression (3′-DGE) approach developed by the Broad institute (Charpentier et al., 2021). The libraries were prepared from 10 ng of total RNA in a volume of 4µl. The mRNA poly(A) tails were tagged with universal adapters, well-specific barcodes and unique molecular identifiers (UMIs) were used during template-switching reverse transcription. Barcoded cDNAs from multiple samples were then pooled, amplified and fragmented using a transposon-fragmentation approach which enriches for 3'ends of cDNA : 200ng of full-length cDNAs were used as input to the Nextera™ DNA Flex Library Prep kit (ref #20018704, Illumina) and Nextera™ DNA CD Indexes (24 Indexes, 24 Samples) (ref #20018707, Illumina) according to the manufacturer's protocol (Nextera DNA Flex Library Document, ref #1000000025416 v04, Illumina).

Size library was controlled on 2200 Tape Station Sytem (Agilent Technologies). A library of 350-800 bp length was run on a NovaSeq 6000 using NovaSeq 6000 SP Reagent Kit 100 cycles (ref #20027464, Illumina) with 17*-8-105* cycles reads.

Bioinformatics protocol: Raw fastq pairs matched the following criteria: the 16 bases of the first read correspond to 6 bases for a designed sample-specific barcode and 10 bases for a unique molecular identifier (UMI). The second read (104 bases) corresponds to the captured poly(A) RNAs sequence.

Bioinformatics steps were performed using a snakemake pipeline (https://bio.tools/3SRP). Samples demultiplexing was performed with a python script. Raw paired-end fastq files were transformed into a single-end fastq file for each sample. Alignment on refseq reference transcriptome, available from the UCSC download site, was performed using bwa. Aligned reads were parsed and UMIs were counted for each gene in each sample to create an expression matrix containing the absolute abundance of mRNAs in all samples. Reads aligned on multiple genes or containing more than 3 mismatches with the reference were discarded. The expression matrix was normalized and differentially expressed genes (DEG) were searched using the R package deseq2 (Love et al., 2014). If DEG were found, functional annotation was performed using the R package ClusterProfiler (Wu et al., 2021; G. Yu et al., 2012). GO and KEGG enrichment analysis, as well as Gene Set Enrichment Analysis (GSEA), provided insights into solving biological hypothesis.

cDNA synthesis and qRT-PCR analysis: For VSMC and rat arteries samples, cDNA was synthesized using M-MLV reverse transcriptase (28025013; Invitrogen), random primers (48190011; Invitrogen) and 500ng of RNA according to the manual. qRT-PCR was performed using SYBR green (Eurogentec) and gene specific primers (Table 3) on real time PCR machine (Applied biosystems) according to the standard protocol.

Table 3: List of qRT-PCR primers used to validate 3'SRP genes in VSMCs

Primer Name	Sequence
Net1-Fw	5'- TGGATGAGAAGCAGAAGGAC -3'
Net1-Rv	5'- TAAACCTGGTAGGAGTGGC -3'
Fn1-Fw	5'- CGAGGTGACAGAGACCACAA -3'
Fn1-Rv	5'- CTGGAGTCAAGCCAGACACA -3'
Col1A1-Fw	5'- TACAGCACGCTTGTGGATGG -3'

Col1A1-Rv	5'- CAGATTGGGATGGAGGGAGTT -3'
IGF1-Fw	5'- CCTACAAAGTCAGCTCGTTC -3'
IGF1-Rv	5'- GTCTTGTTTCCTGCACTTCC -3'
GAPDH-Fw	5'-AACCCATCACCATCTTCCAG-3'
GAPDH-Rv	5'-CCAGTAGACTCCACGACATAC-3'

1.1.2. Results

3'SRP analysis allowed the identification of several mechanosensitive GEFs in VSMCs *in-vitro* and *in-vivo*. In cerebral arteries, significant variation in the transcript levels of 3 GEFs, 7 GAPs and 1 guanine nucleotide releasing factor were observed between WKY, SHR and SHR-SP samples (Figure 19).

To validate the 3'SRP results by **qRT-PCR**, *Net1* was chosen as its expression was increased in cerebral arteries of SHR and SHR-SP rats compared to WKY control rats. In addition, a similar expression pattern in mesenteric arteries was observed, as well as a high basal expression of *Net1* in cerebral arteries was seen compared to mesenteric arteries (Figure 20). qRT-PCR analysis did not validate the increased transcription of *Net1* in SHR and SHR-SP cerebral arteries compared to WKY controls, but confirmed the transcript fold difference between mesenteric and cerebral arteries (Figure 22a).

In rat VSMCs that underwent physiological (10%; 1Hz) and pathological (20%; 1Hz) cyclic stretch, very few GEFs/GAPs were significantly altered between physiological and pathological stretch conditions. At the shorter time point (30min), *Arhgef31* transcript was significantly downregulated and *Arhgap10* was significantly upregulated in pathological cyclic stretch compared to physiological cyclic stretch conditions. However, no difference was observed between the two conditions at longer time point i.e., 24h (Figure 21). Also, *Vav1* transcript level was increased upon 20% stretch at 24h compared to the 10% condition (Figure 21).

Though, it was only a trend in the 3'SRP results, **qRT-PCR** validation of the primary rat aortic VSMCs samples showed a significant induction of *Net1* transcript levels in pathological stretch (20%; 1HZ) condition compared physiological stretch (10%; 1Hz) (Figure 22b). In parallel to *Net1*, we did saw an increase in the expression of previously

known stretch regulated genes such as *FN1*, *Col1A1* and *IGF1* under pathological stretch (20%; 1HZ) condition compared physiological stretch (10%; 1Hz) (Figure 22b).

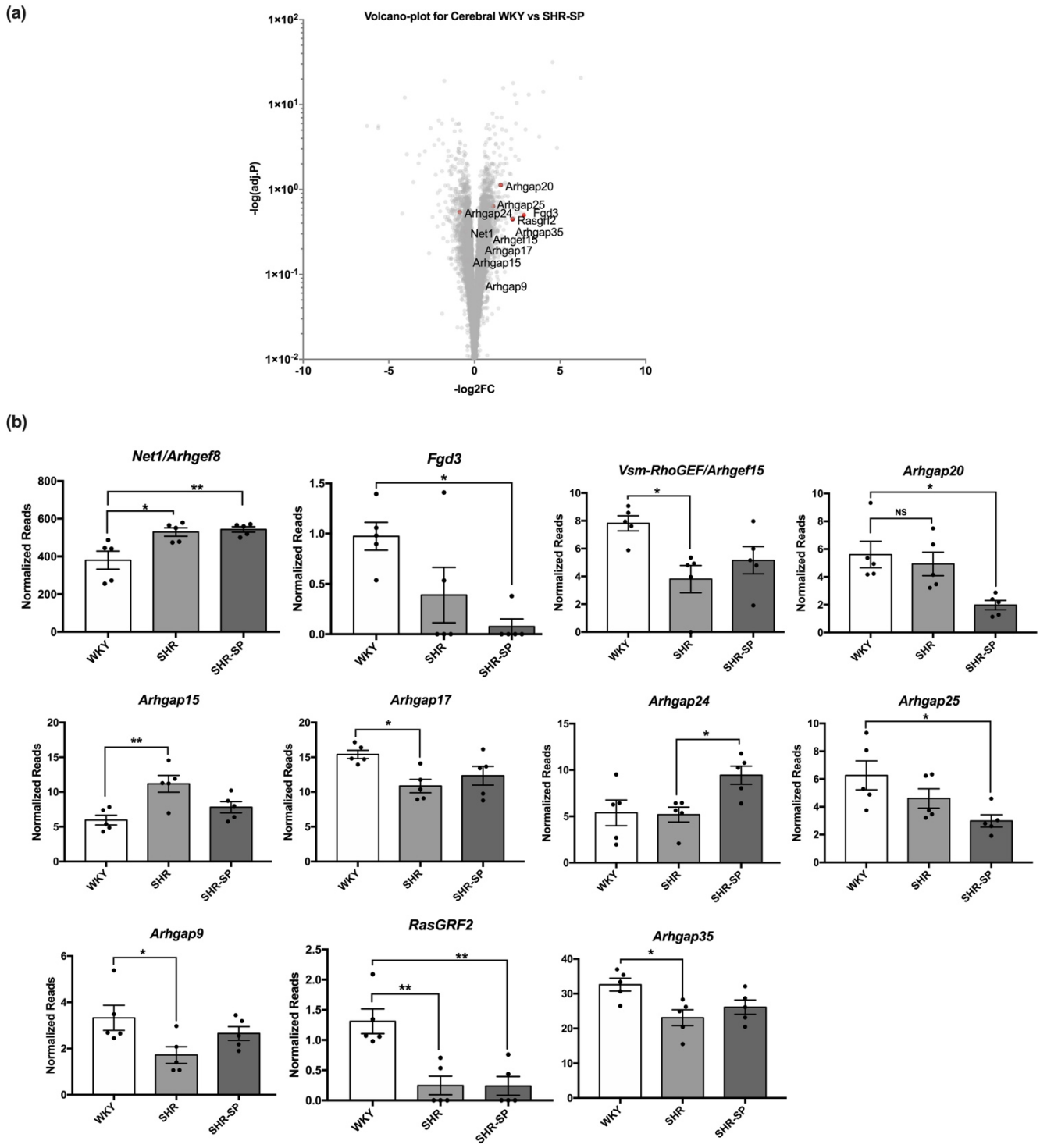

Figure 19: 3'SRP analysis of RNA from WKY, SHR, SHR-SP rat cerebral arteries

*Volcano plot shows the altered GEFs and GAPs expression between WKY and SHR-SP cerebral arteries (a); qRT-PCR validation of GEFs/GAPs significantly altered in 3'SRP analysis between WKY, SHR, SHR-SP cerebral arteries (b). Statistical significance was calculated by One-way ANOVA followed by Tukey's multiple comparison test. *p<0.03, **<0.002, ***p<0.0002*

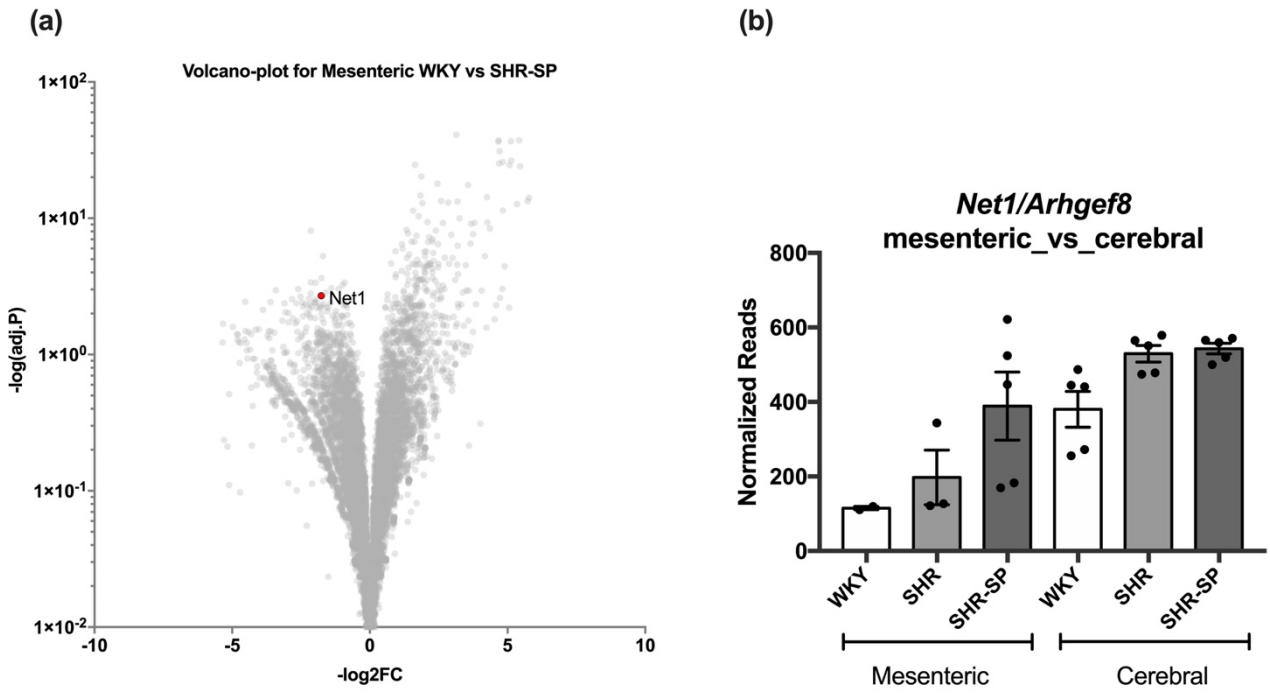

Figure 20: Comparative 3'SRP analysis of Net1 expression in mesenteric and cerebral arterial tissue

Volcano plot shows the altered gene expression at transcript level between WKY and SHR-SP mesenteric arteries (a); bar diagram shows the number of Net1 transcript reads in mesenteric and cerebral arteries of WKY, SHR, SHR-SP rats (b).

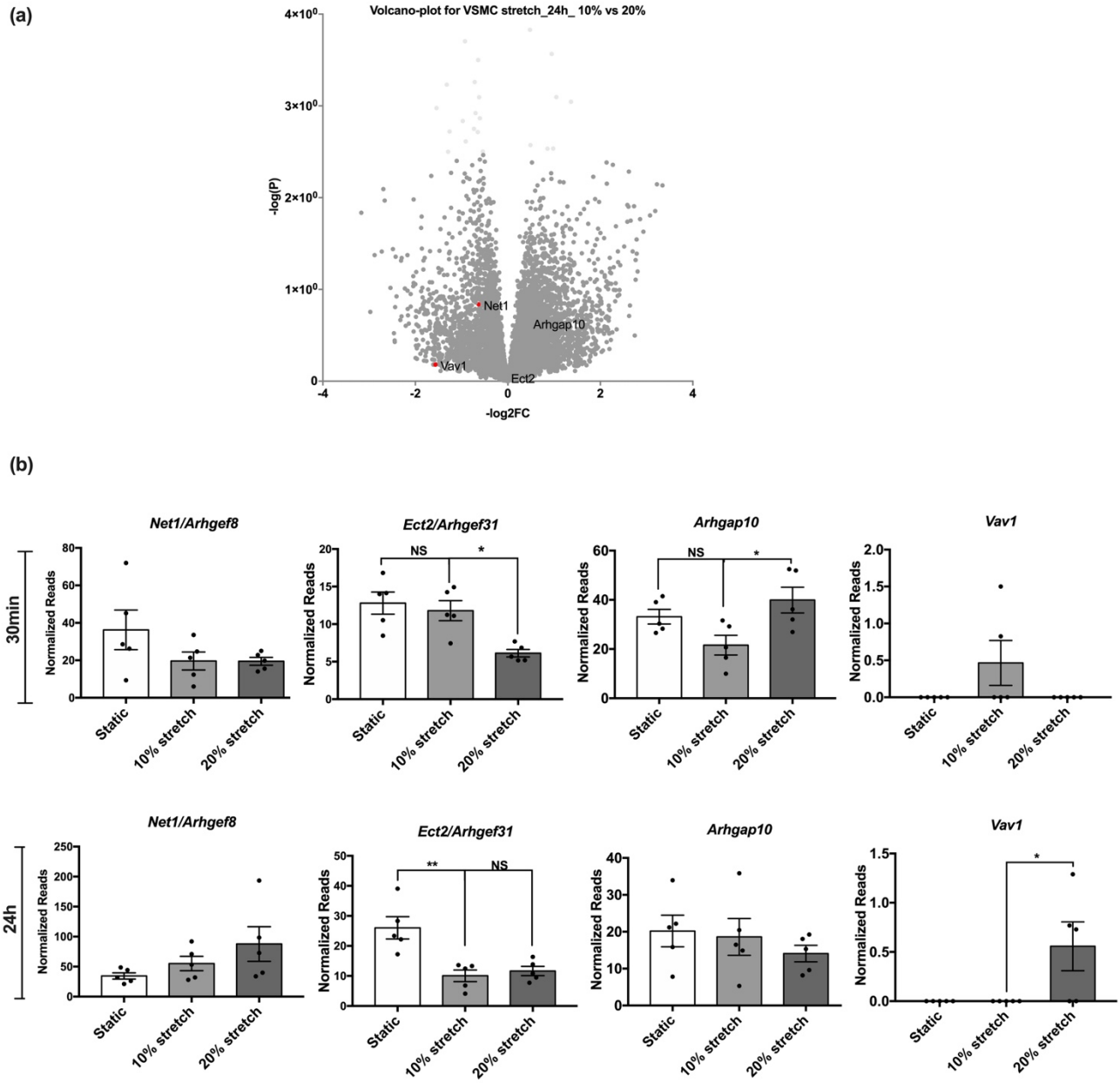

Figure 21: 3'SRP analysis of rat aortic VSMCs subjected to various stretch conditions

*Volcano plot shows the altered gene expression in VSMCs subjected to 10% and 20% cyclic stretch for 24hrs (a); bar diagram shows significantly altered GEFs/GAPs between 10% and 20% cyclic stretch applied for 30min (top) and 24h (bottom) time point (b). One-way ANOVA followed by Tukey's multiple comparison test. *p<0.03, **<0.002, ***p<0.0002*

.

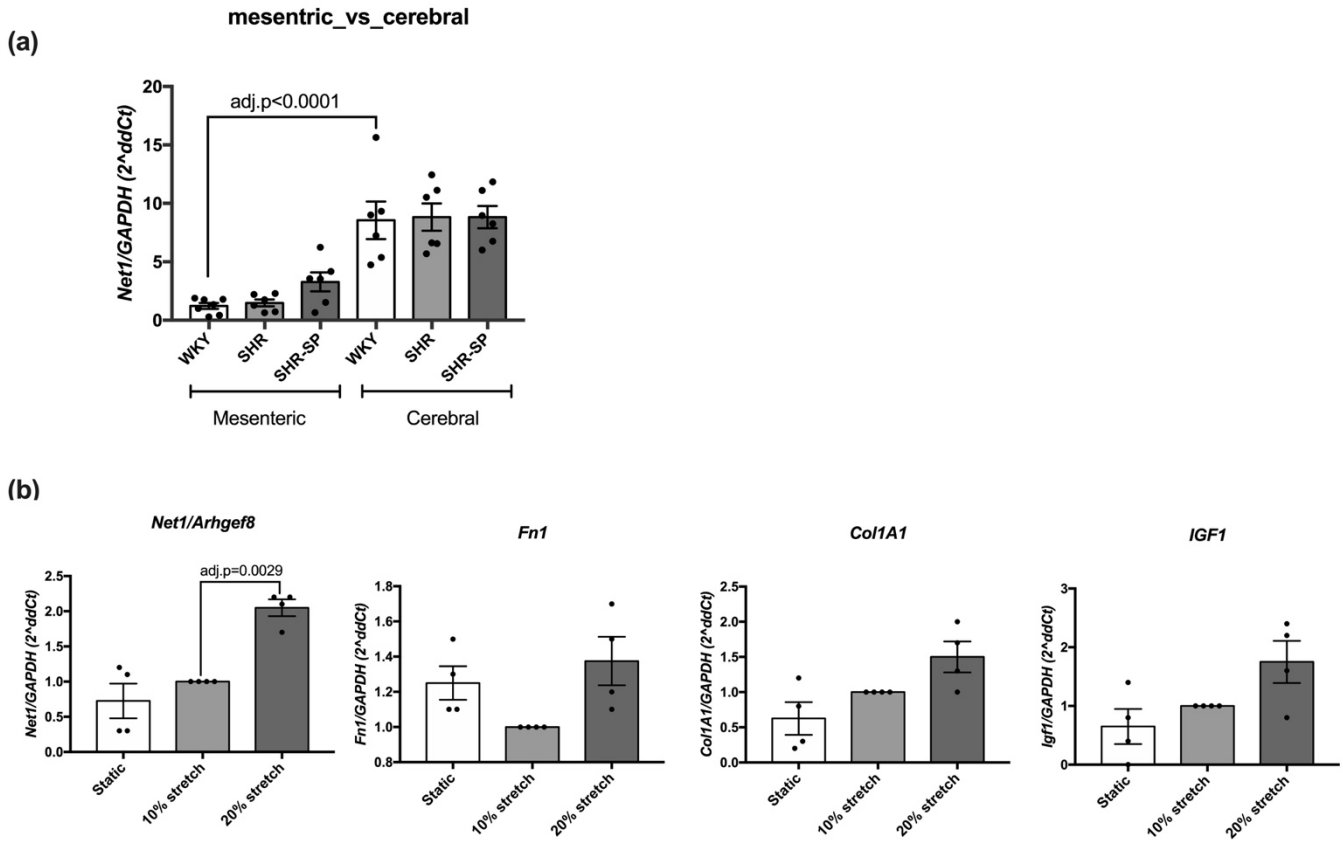

Figure 22: qRT-PCR validation of Net1 gene expression

*Bar diagram represents the fold difference in Net1 transcript between mesenteric and cerebral arteries of WKY, SHR, SHR-SP rats (a) and Net1, Fn1, Col1A1, IGF1 in VSMCs subjected to physiological (10%; 1Hz), and pathological (20%; 1Hz) stretch conditions for 24 h (b). One-way ANOVA followed by Tukey's multiple comparison test. *p<0.03, **<0.002, ***p<0.0002*

1.2 3'SRP analysis of ECs

1.2.1. Materials and Methods

Detailed information on materials and methods which was used could be found in the following accompanied article. Briefly, HUVECs (p2-p4) were subjected to physiological [16 dynes/cm² (HSS)] and pathological [3.6 dynes/cm² (LSS) & 36 dynes/cm² (HSS)] shear stress for 24 h. RNA was extracted and 3'SRP analysis was performed. Genes that showed significant changes in their transcript levels relative to the shear stress applied were then validated by qRT-PCR using gene specific primers (Table 4).

Table 4: qRT-PCR primers used to validate 3'SRP results in ECs

Gene name	Taqman probes ID
ARHGEF18	Hs00248726_m1
ARHGEF40	Hs01554494_m1
KLF2	Hs00360439_g1
ARHGEF26	Hs00248943_m1
ARHGEF37	Hs01049681_m1
SOS2	Hs01127273_m1
TRIO	Hs01125865_m1
GAPDH	Hs04420697_g1
UBC	Hs00824723_m1
HPRT	Hs02800695_m1

1.2.2. Results

Our **3'SRP analysis** revealed changes in gene expression in ECs upon SS application for 24h. Statistical analysis had identified 6 GEFs and 4 GAPs whose expression was modulated relative to the SS applied (Figure 23). Of the identified GEFs and GAPs, *ARHGEF18*, *ARHGEF40*, *ARHGEF26*, *ARHGEF37*, *SOS2* and *TRIO* were selected for further validation by qRT-PCR, as they play an important role in endothelial cell biology as well as cell-cell junction maintenance. In **qRT-PCR analysis**, only two GEFs, *ARHGEF18* and *ARHGEF40,* presented the same expression pattern as observed in 3'SRP with statistical significance. *ARHGEF18* transcript level was inversely proportional to the

SS applied and showed a high transcript under static conditions and was reduced as the SS value increased. Furthermore, opposite expression pattern was observed for *ARHGEF40* with low expression under static condition and an increased expression relative to the SS (Figure 24).

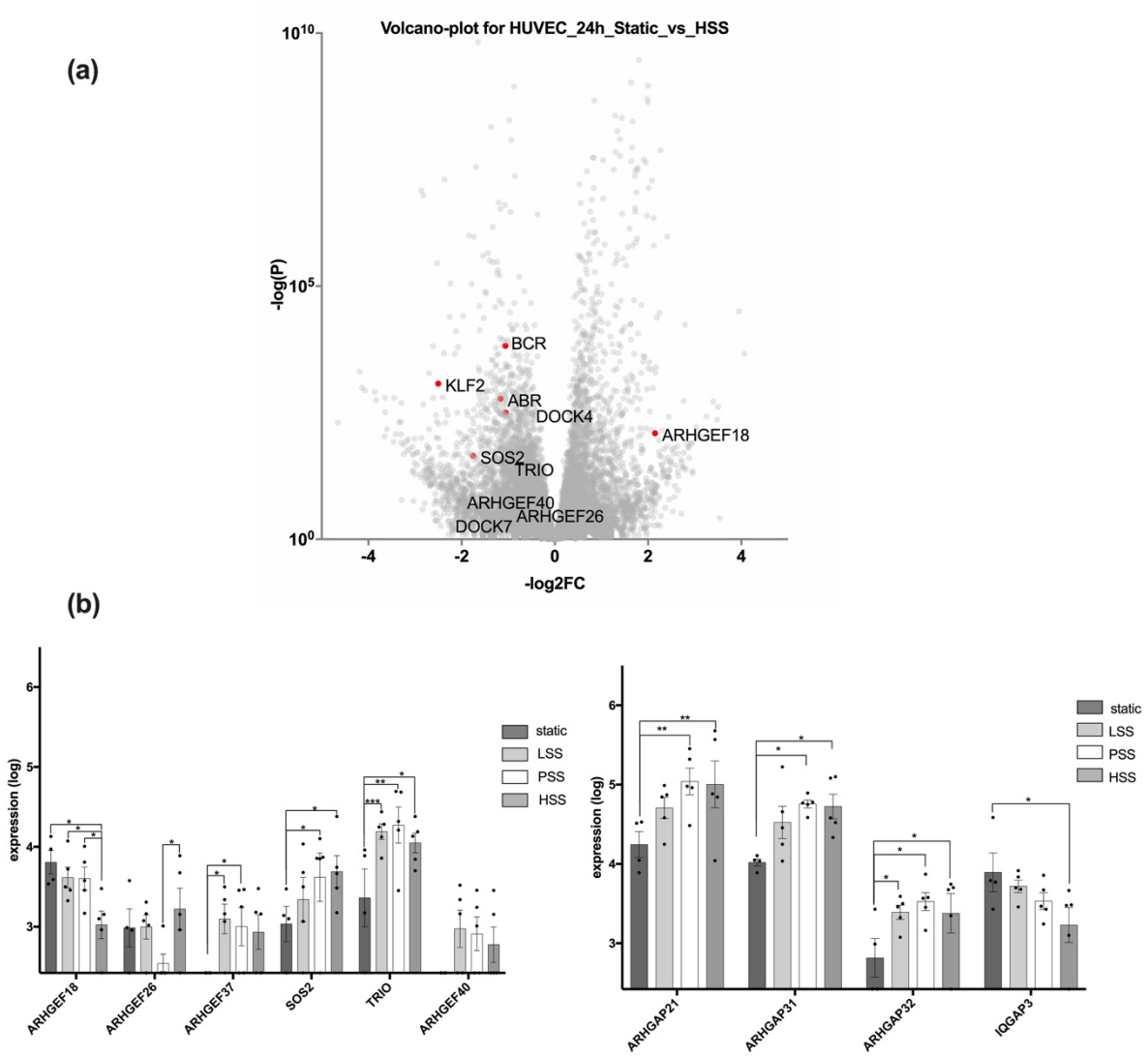

Figure 23: 3'SRP analysis of RNA from HUVECs subjected to physiological and pathological shear stress

*Volcano plot shows altered GEFs expression in HUVECs subjected to HSS relative to static conditions (a). Bar graph represents reads of statistically significant GEFs (top) and GAPs(bottom) from 3'SRP analysis between various shear stress conditions (b). Statistical significance was calculated by Two-way ANOVA followed by Tukey's multiple comparison test. *p<0.03, **<0.002, ***p<0.0002*

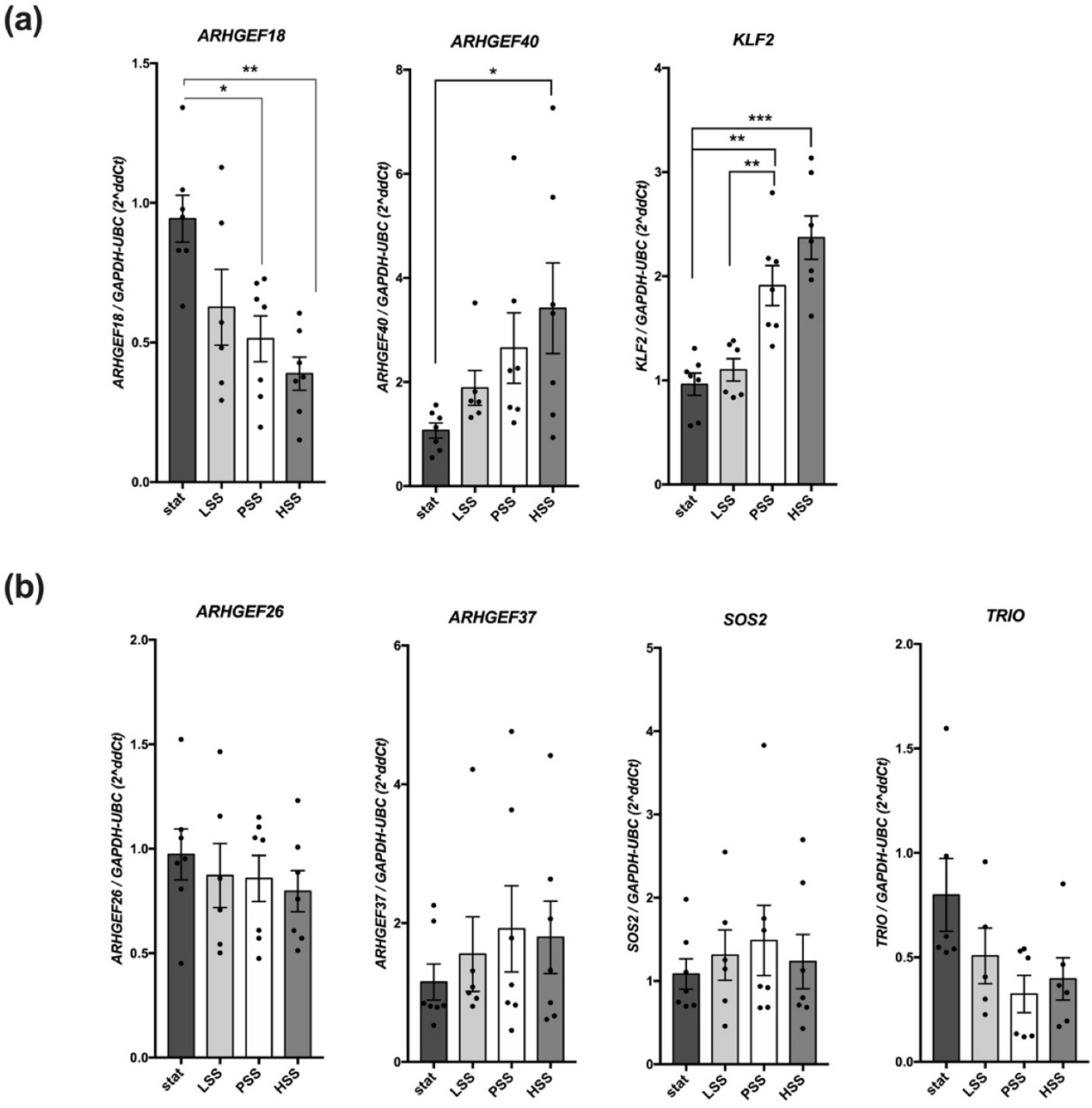

Figure 24: qRT-PCR validation of GEFs expression in HUVECs under various shear stress conditions

*Bar graph represents GEFs expression significantly altered and were successfully validated by qRT-PCR. KLF2 expression serves as a positive control for responsiveness of HUVECs to shear stress (a). Bar graph represents GEFs whose expression was not successfully validated by qRT-PCR (b). Statistical significance was calculated by One-way ANOVA. *p<0.03, **<0.002, ***p<0.0002*

1.3 Take-home message from 3'SRP analysis

From the 3'SRP analysis on VSMCs, ECs and arteries, we were able to successfully validate **three GEFs** whose expression was modulated related to the mechanical forces the cells experienced *in-vitro* or *in-vivo*.

Net1 transcript level was increased in primary rat aortic VSMCs exposed to 20% cyclic stretch *in-vitro*. Net1, a RhoA specific GEF (Alberts & Treisman, 1998), was shown to be involved in developmental processes such as mesendoderm formation (Wei et al., 2017) as well as in tumor angiogenesis (Y. Zhang et al., 2017). However, previous work from our lab demonstrated that complete deletion Net1 in mice showed no defect in vascular development without any cardiovascular phenotype (unpublished data).

ARHGEF18 transcript level was SS dependent and its mRNA level was inversely correlated with the magnitude of shear stress applied on ECs. ARHGEF18 is a RhoA specific GEF and well characterized for its role in epithelial cell cytoskeletal organization, migration and maintenance of apico-basal polarity. However, very little is known in the context of ECs and vascular physiology.

ARHGEF40 expression was also modulated by SS in ECs and is directly proportional to SS magnitude. A quick pubmed search resulted in just 13 articles since the time of its discovery in 2005 (Tse et al., 2005), where it was described as a RhoA GEF and it role was described in mechano-transduction mediated cytoskeletal rearrangement (Fujiwara et al., 2016), epithelial cell tube morphology (Nishimura et al., 2018), along with a significant role in cancer cell proliferation and migration (Gu et al., 2022).

Taken into consideration about the previously published work and availability of molecular tools to successfully study the role of GEF *in-vitro* and *in-vivo*, ARHGEF18 was chosen to study its role in the mechanosensitivity of ECs and angiogenesis.

2. Functional characterization of mechanosensitive ARHGEF18 in shear stress mediated EC signaling

2.1 Role of ARHGEF18 in ECs physiology under longer shear stress conditions (24 h)

To understand the role of ARHGEF18 in SS-induced ECs response, we performed *in-vitro* experiments using ECs (HUVECs) under static and SS conditions. The results are described in the form of an article in the following pages onwards.

In brief, we showed that SS affected the transcription level of *AHRGEF18*. To understand how SS modulates the activity and expression of ARHGEF18 in ECs, active GEF trapping experiments were performed using nucleotide free mutants of $RhoA^{G17A}$ and $Rac1^{G15A}$. Under the SS conditions tested (static, 3.6 dynes/cm^2, 16 dynes/cm^2 and 36 dynes/cm^2), ARHGEF18 interacted only with RhoA but not Rac1. In addition, we observed a decrease in ARHGEF18 activity under pathological SS conditions (3.6 dynes/cm^2 and 36 dynes/cm^2) compared to physiological SS condition (16 dynes/cm^2). Interestingly, knocking down of ARHGEF18 using RNAi resulted in a reduced RhoA and Rac1 activity.
At cellular level, under static conditions, ARHGEF18 silenced ECs showed a reduction in cell adhesion, focal adhesion maturation, migration and an increased network forming capacity compared to control cells as assayed by *in-vitro* assays. However, silencing ARHGEF18 did not affect ECs permeability. Under physiological SS conditions, knocking down of ARHGEF18 resulted in an impaired ECs alignment parallel to the direction of flow and a reduction in focal adhesion points as well as localization of tight junction proteins ZO1 and CLDN5 at cell-cell junctions. Similar results were also obtained using GEF mutant ($ARHGEF18^{Y260A}$) overexpressing cells.
At molecular level, we observed that knocking down of ARHGEF18 resulted in inhibition of shear stress mediated p38 activation and this response was dependent on the GEF activity as cell overexpressing GEF mutant ($ARHGEF18^{Y260A}$) also resulted in similar results. p38 specific inhibition exhibited similar defective ZO1 localization and cytoskeletal arrangement similar to ARHGEF18 knockdown cells.
These results indicate that ARHGEF18 is mediating its effect through p38 signaling pathway and is GEF activity dependent.

ARHGEF18 participates in Endothelial Cell Mechano-sensitivity in Response to Flow

Surya Prakash Rao Batta[1], Marc Rio[1], Corentin Lebot[1], Céline Baron-Menguy[1], Robin Le Ruz[1], Gervaise Loirand[1], Anne-Clémence Vion[1]

[1]Université de Nantes, CHU Nantes, CNRS, INSERM, l'institut du thorax, F-44000 Nantes, France.

*** Correspondance:**
Anne-Clémence Vion
anne-clemence.vion@univ-nantes.fr

Keywords: endothelial cell, shear stress, guanine exchange factor, mechano-transduction

Abstract

Hemodynamic forces play an important role in vascular network development and homeostasis. In physiological condition, shear stress generated by laminar flow promotes endothelial cells (EC) health and induces their alignment in the direction of flow. In contrast, altered hemodynamic forces induce endothelial dysfunction and lead to the development of vascular disorders such as atherosclerosis and aneurysms. Following mechano-sensor activation, Rho protein-mediated cytoskeletal rearrangement is one of the first steps in transforming flow-induced forces into intracellular signals in EC via guanine nucleotide exchange factors (RhoGEFs) that mediate the spatio-temporal activation of these Rho proteins. Here we identified ARHGEF18 as a flow-sensitive RhoGEF specifically activating RhoA. Both ARHGEF18 expression and activity were controlled by shear stress level. ARHGEF18 promotes EC adhesion, focal adhesion formation and migration. ARHGEF18 localized to the tight junction by interacting with ZO-1 and participated to shear stress-induced EC elongation and alignment via its nucleotide exchange activity and the activation of p38 MAPK. Our study therefore characterized ARHGEF18 as the first flow-sensitive RhoA GEF in ECs, whose activity is essential for the maintenance of intercellular junctions and a properly organized endothelial monolayer under physiological flow conditions.

Introduction

Mechano-sensitivity and mechano-transduction play crucial roles in shaping life. Cells, individually or collectively, need to respond appropriately to mechanical cues coming from their environment to adapt and survive, and to ensure healthy tissue development and homeostasis[4]. In the vascular system, endothelial cells (ECs) are exposed constantly to mechanical strains exerted by blood flow[5,6]. ECs are thus able to sense small variations in the direction, magnitude, and regularity of blood flow-induced shear stress[7,8] and consequently modulate their functions to generate adapted response. This leads, for instance, to arteriogenesis[9], vasculature patterning[10,11] and acute regulation of vessel tone,[12] which are critical for both the development and maintenance of a healthy cardiovascular system. On the opposite, failure of ECs to adapt to changes in blood flow or chronic exposure to abnormal flow is the cause of vascular diseases such as hypertension, atherosclerosis[6,13,14] or intracranial aneurysm formation[15].

In physiological condition, shear stress generated by laminar flow as observed in linear parts of the vascular tree, promotes ECs health and induces their alignment in the direction of flow[16,17]. To do so, ECs use several mechano-sensing mechanisms. Well-studied examples are ion channels[18], primary cilia expressed at the apical surface of cells[19,20], but also include mechano-sensing complexes at cell-cell interface such as the PECAM-1/VEGFRs/VE-cadherin complexe[13] and at cell membrane-extracellular matrix attachment such as focal adhesions and integrins[21]. These sensors and complexes play an essential role in transforming flow-induced physiological forces into intracellular signals ultimately leading to various cellular response ranging from chemokine release, Nitric Oxide production to cell proliferation and junction reorganization Rho protein-mediated actin cytoskeleton reorganization is one of the first steps of this process[22–26], as supported by the overexpression of dominant-negative mutants of RhoA or Rac1 in ECs that prevent their correct elongation and alignment[27]. An increase in Rho protein activity is rapidly induced in ECs upon shear stress exposure, with two peaks of activity at 5 min and 2 hours for RhoA [27,28], and a maximal Rac1 and cdc42 activation at 15 min[16,21]. At longer time point, Rho-GTPases activity is not completely lost but preserves a basal level suggesting their involvement not only in establishing the alignment but also in maintaining it. Shear stress not only controls Rho-GTPases activity but also their localization. Upon physiological shear stress exposure, these Rho-GTPases translocate within minutes, from the cytosol to the plasma membrane where they can meet their partners and act on the cytoskeleton[29]. Activation of Rho proteins consists in their transition from an inactive state (GDP-bound) to an active state (GTP-bound)[30]. By promoting the release of GDP followed by GTP loading, the guanine nucleotide exchange factors of Rho proteins, the RhoGEFs, induced Rho protein activation[31]. The peculiar interest of RhoGEFs is their tissue-specific expression and their signal/temporal-specific activation[32] which place them at the control center of the broad effects of Rho-GTPases in cell biology. Some of those RhoGEFs have been described to be exclusively expressed in ECs, such as FGD5[33],to participate in ECs mechano-sensitivity. The RhoGEFs Tiam1 and Vav2 have been shown to be involved in the rapid activation of Rac1 upon shear stress[34]. The RhoGEF Trio keeps Rac1 active at the downstream side of the EC and is essential for long term flow-induced cell alignment[35] as well as barrier integrity through the formation of a NOTCH1/VE-Cadh/LAR/Trio complex[36]. Lastly, ARHGEF12 has been implicated in force sensing through ICAM and participates in leukocytes rolling and transmigration on ECs[37].

Here, using unbiased RNA screening in ECs, we identify that ARHGEF18 expression and activity are flow sensitive. We demonstrate that ARHGEF18 is a RhoA-specific RhoGEF interacting with ZO1 in ECs. We show that ARHGEF18 participates in ECs alignment in response to flow by controlling p38 MAPK activity, tight junction and focal adhesion formation through its guanine nucleotide exchange activity.

Results

Shear stress regulates ARHGEF18 expression and activity

In order to identify RhoGEFs expression modulated by shear stress (SS), we performed a 3'RNA profiling on endothelial cells (EC) exposed to different SS levels (no flow, Static, 0 dyn/cm^2; pathological Low SS, 3,6 dyn/cm^2, (LSS); physiological SS, 16 dyn/cm^2 (PSS) and pathological High SS, 36 dyn/cm^2, (HSS)) (Fig 1A, MA plot of static vs PSS condition). The identification of *KLF2* as a flow-dependent gene the expression of which was significantly increased by HSS validated our experimental conditions (Fig 1A). Among the genes with differential expression, we identified several RhoGEFs but only *ARHGEF18* expression decreases with increased SS (Fig 1A and suppl 1A). We then confirmed this decrease in *ARHGEF18* mRNA expression in EC with increased SS by qPCR, using *KLF2* mRNA expression as an internal control (Fig 1B and Fig suppl 1B). Surprisingly, contrary to the observed down-regulation of

ARHGEF18 mRNA with increased SS, ARHGEF18 protein level increased in pathological SS conditions (LSS and HSS) compared to physiological condition (PSS) (Fig 1C), suggesting an additional post-transcriptional effect of SS on ARHGEF18 protein level. We then examined the sensitivity of ARHGEF18 activity to SS by pull-down assay using nucleotide-free $RhoA^{G17A}$ and $Rac1^{G15A}$ mutants to trap active RhoGEF[38]. Interestingly, under static condition, we were able to trap ARHGEF18 with the $RhoA^{G17A}$ mutant but not with the $Rac1^{G15A}$ mutant indicating a basal nucleotide exchange activity of ARHGEF18 on RhoA but not on Rac1 (Fig 1D and E (lane1, static condition)), confirming ARHGEF18 specificity for RhoA[39].
As we were unable to trap ARHGEF18 with $Rac1^{G15A}$ mutant, we validated the efficiency of this pull-down assay by blotting proteins that have coprecipitated with Rac^{G15A} with an antibody to Vav, known as a Rac GEFs in EC[40]. We were able to detect Vav in the coprecipitated proteins, thus validating this pull-assay and confirming that ARHGEF18 did not interact with Rac1 (Fig suppl 1C). Interestingly, the amount of ARHGEF18 captured by the $RhoA^{G17A}$ mutant was high in ECs exposed to physiological SS (PSS) compared to pathological SS (LSS and HSS) thus revealing a high exchange activity of ARHGEF18 on RhoA in physiological flow condition that is reduced in pathological shear stress situations (Figure 1D, lane 2 to 4)). As in static condition, $Rac1^{G15A}$ mutant was unable to trap ARHGEF18 in ECs exposed to SS (Figure 1E). Overall, this demonstrates that ARHGEF18 is a RhoGEF specific for RhoA in ECs whose expression and activity are modulated by flow. Though its protein expression is reduced in ECs exposed to physiological SS, its activity is high. In contrast, pathological SS condition presented a higher level of ARHGEF18 protein which is not associated with any gain in activity.

ARHGEF18 is expressed in arterial EC and localizes to tight junction

In epithelial cells, ARHGEF18 has been shown to participate in tight junction formation[41]. We thus assessed the possible interaction of ARHGEF18 with proteins involved in EC junctions. Co-immunoprecipitation of the VE-cadherin complex did not allow the detection of ARHGEF18 in the immunoprecipitated fraction (Fig 1F, left). In contrast, ARHGEF18 was present in the immunoprecipitated fraction of the ZO-1 complex (Fig 1F, right). We next used immunofluorescence staining of retinas from adult mice to verify the expression of ARHGEF18 *in vivo* in the vasculature. Using isolectin B4 staining to label ECs, we identified ARHGEF18 expressed in the arteries of the retina but not in the veins or in the capillaries (Fig 1G). Interestingly the staining was stronger in arteries close to the optic nerve (Fig 1D, artery first order) and fainted as the arteries caliber decreased and as the network ramified to become capillary (Fig suppl 1E). Altogether, these data showed that ARHGEF18 is expressed in arterial EC *in vivo* and localizes to the tight junction by interacting with ZO-1.

ARHGEF18 participates in ECs adhesion and migration

We next assessed the functional role of ARHGEF18 in ECs adhesion and migration, two processes that depend on the dynamic organization of the actin cytoskeleton and the activity of the Rho proteins. We used siRNA silencing and shRNA silencing strategies to turn off the expression of ARHGEF18 protein in ECs. siRNA silencing reduced the expression of ARHGEF18 by 72%(Fig suppl 2A) and shRNAs by 90% with the two shRNAs selected, namely shA18.1 and shA18.4 (Fig suppl 2B). We first evaluated the consequence of ARHGEF18 loss on RhoA activity by pull-down assay using GST-RBD beads. Under physiological SS, RhoA activity was decreased by 30% with both shA18.1 and shA18.4 shRNA expressing ECs (Fig suppl 2C), which was in line with the specificity of ARHGEF18 for RhoA.
We first observed that ARHGEF18 silencing decreased cell-surface interaction analyzed by real-time impedance measurement (Fig 2A and Fig 2D). Both adhesion, corresponding to the linear phase of impedance rise (Fig 2A,B and Fig 2D,E), and spreading of ECs, represented by the maximal value of impedance (Fig 2C and 2F), were decreased. This was observed with siRNA (approximately 25% decrease) as well as with shRNA silencing (approximately 50% decrease). To further characterize this effect at single-cell level, ECs were plated onto fibronectin-coated L-shaped that overcomes the variability in cell morphology by forcing cells to seed individually and to adopt a normalized geometry and allowing a better comparison and quantification of focal adhesion number and size. Both with siRNA (Fig 2G) and with shRNA (Fig 2H) strategies, silencing of ARHGEF18 led to a significant decrease in focal adhesion number compared to control condition (siCTR or shNT respectively). Specifically, the number of focal adhesion site longer than 5um were decreased with both siRNA and shRNA targeting ARHGEF18 compared to their respective control suggesting a defect in focal adhesion maturation.
Basal adhesion as well as maintenance of proper cell-to-cell contact are also a key element in cell migration. Therefore, we investigated if ARHGEF18 would participate in ECs migration. In a wound

healing assay, we observed that the closure of the wound was slowed down in ARHGEF18 silenced ECs compared to control ECs (Fig 2I,J,K) suggesting that ARHGEF18 is involved in collective cell migration. Overall, we identified that ARHGEF18 promotes adhesion, focal adhesion sites formation and migration in ECs *in vitro*.

ARHGEF18 participates in ECs response to flow

As we identified that ARHGEF18 was particularly active when ECs were exposed to physiological SS (Fig 1D) we investigated if ARHGEF18 could contributed to ECs physiological response to flow. First, As expected, control ECs (shNT) aligned and elongated in the direction of flow, harbored continuous VE-cadherin junction with junction-associated lamellipodia formation at the front and rear of the cells, continuous ZO-1 staining as well as cortical actin cables (Fig 3A, upper panel). On the opposite, ECs deficient in ARHGEF18 (shA18.1 and shA18.4) failed to elongate and align in the flow direction under physiological SS(Fig 3B and Fig suppl 3B), leading to a significant decrease in the flow-response index which integrates both the aspect ratio of each cell (major axis length / minor axis lenght) and its angle with the flow direction. Additionally, ARHGEF18 silencing (shRNA strategy) was not affecting the proliferation rate of ECs under PSS, ruling out a possible contribute of proliferation on cell shape in our experimental setting (Fig suppl 3A). VE-cadherin was still present at junctions in ARHGEF18 deficient ECs but the number of gaps in-between cells significantly increased compared to control ECs (Fig 3A, C and Fig suppl 3B). ZO-1 localization at junction appeared disrupted and was significantly decrease compared to control condition (Fig 3A,D; Fig suppl 3B). In the same line, cortical actin was significantly less abundant in ECs deficient in ARHGEF18 compared to control (Fig 3A,E; Fig suppl 3B). As tight junctions are also composed of Claudins, we then assessed the effect of ARHGEF18 loss on Claudin 5 localization, the most abundant Claudin in ECs. To do so, we took advantage of mosaic experiment were the shRNA expression (shA18.1) was not induced in all ECs. Interestingly, we observed that the intensity of the peak of claudin5 at junction (colocalizing with VE-cadherin) in-between a control ECs and an EC expressing the shRNA (GFP tagged) (Fig 3F and 3G middle graph) was decreased compared to the intensity of the peak of claudin5 in-between two control ECs (not expressing the shRNA, Fig 3F and 3G upper graph, Fig suppl 3D). This peak was almost absent in-between two ECs expressing the shRNA (both GFP tagged) (Fig 3F and 3G lower graph, Fig suppl 3D). Additionally, we observed a slight decrease in Claudin 5 expression by western Blot in ECs expressing the shRNA sh18.1 and a significant decrease in ECs expressing the shRNA sh18.4 (Fig suppl 3E) suggesting that loss of ARHGEF18 lead to tight junction destabilization under physiological SS which could affect Claudin 5 protein expression or stability. Finally, as focal adhesions were affected by ARHGEF18 loss under static condition (Fig 2G,H) and as focal adhesion participate in ECs response to SS[24], we analyzed the effect of ARHGEF18 depletion on paxillin expression and localization in ECs exposed to physiological SS. Interestingly, while Paxillin staining revealed that focal adhesion appeared long and mostly collectively oriented in almost all control ECs (classified as paxillin High), ARHGEF18 deficient ECs had less of these “paxillin High” ECs and presented significantly more ECs with short and disorganized focal adhesions (classified as paxillin Low) (Fig 3H, I and Fig suppl 3F,G). Quantification confirmed the significant change in the shape of focal adhesion/paxillin staining induced by ARHGEF18 depletion in EC in PSS condition (Fig 3I and Fig suppl 3G). Surprisingly, this change of paxillin was not associated with modification of paxillin phosphorylation level, assessed by western blot, in ECs deficient in ARHGEF18 compared to control (Fig suppl 3H). Altogether, these data showed that ARHGEF18 contributed to ECs response to physiological SS by promoting tight junction formation and actin recruitment at cell-cell junction and preventing paracellular gaps formation but also by participating in focal adhesion sites organization but without affecting Paxillin phosphorylation.

p38 MAPK mediates ARHGEF18 effects in flow response of ECs

Several intracellular pathways have been shown to control ECs adhesion and tight junction formation as well as ECs migration, among them Akt, p38 MAPK and ERK1/2 activation play a central role in controlling focal adhesion and actin remodeling[44–48]. Additionally, p38 MPAK and ERK1/2 activity can be controlled by RhoGTPases[49,50]. Thus, we explored the possible implication of p38 MAPK, Akt and ERK1/2 in ARHGEF18-mediated effect on ECs. As expected[51], physiological SS increased p38 phosphorylation in ECs exposed to physiological SS (Fig 4A). ARHGEF18 silencing led to a significant decrease in p38 phosphorylation (Fig 4A; Fig suppl 4A). On the contrary, ERK1/2 phosphorylation and Akt phosphorylation levels remained unchanged in ECs deficient in ARHGEF18 compared to control ECs (Fig suppl 4B and suppl 4C respectively). In order to understand if p38 MAPK participated in ARHGEF18-mediated flow response of ECs, we inhibited p38 pharmacologically using SB239063 (100

nM). As previously shown[52], p38 inhibition significantly reduced ECs elongation and orientation in the flow direction under physiological SS (Fig 4B) thus mimicking ARHGEF18 silencing. We then investigated the effect of p38 inhibition on tight junction and focal adhesion formation induced by physiological SS. As observed in ARHGEF18-depleted EC, p38 MAPK inhibition significantly decreased the amount of ZO-1 at tight junctions, which appeared discontinuous (Fig 4C,D), and slightly but significantly reduced the amount of actin at cell junction (Fig 4 D,E). Surprisingly, these effects were not accompanied with increased gaps number in-between ECs suggesting that part of the effect of ARHGEF18 on EC junctions were not mediated by p38. Paxillin staining also revealed that p38 MAPK inhibition under physiological SS led to the loss of focal adhesion organization similar to that observed with ARHGEF18 silencing (Fig 4F,G). These data suggest that ARHGEF18 participate to EC elongation and alignment in response to PSS by controlling tight junction and focal adhesion via the activation of p38 MAPK.

GEF activity of ARHGEF18 is important for p38 activation and flow response of ECs

To dig further into the mechanism of action of ARHGEF18, we wanted to define whether its role in p38 activation and EC response to PSS was due to its ability to induce guanine nucleotide exchange on Rho proteins. We thus generated ECs over-expressing the Y260A-ARHGEF18 inactive mutant (FlAG tagged) that has no guanine nucleotide exchange factor activity[39], These ECs also expressed shRNA targeting the endogenous form of ARHGEF18 to eliminate potential effects due endogenous ARHGEF18 activity. We validated our constructs, by checking in a pull-down assay the inability of the Y260A-ARHGEF18 mutant to interact with the nucleotide free RhoA ($RhoA^{G17A}$), while the WT-ARHGEF18 generated a strong interaction (Fig 5A). Under physiological SS, p38 MAPK phosphorylation was reduced in Y260A-ARHGEF18 expressing ECs compared to ECs over-expressing the WT form (Fig 5B). This effect was associated with a failure of Y260A-ARHGEF18 expressing ECs to elongate and align in the direction of the flow while ECs expressing the WT form elongated and aligned properly in response to physiological SS (Fig 5C and D). Additionally, no gaps were observed in ECs monolayer expressing either the WT or GEF mutant ARHGEF18 under physiological SS, confirming that ARHGEF18 must have another function to regulate gap formation. To assess the involvement of the GEF activity of ARHGEF18 in tight junction formation, we took advantage of mosaic experiment were the Y260A-ARHGEF18 inactive mutant was not expressed in all ECs. In those experiment, examination of tight junction by ZO-1 staining show a strong peak of ZO-1, colocalized with VE-cadherin at junction in-between two control ECs (Fig 5E and 5F left graph), which was decreased at the junction in-between a WT EC and a Y260A-ARHGEF18 expressing EC (Fig 5E and 5F middle graph) and almost absent at the junction of two Y260A-ARHGEF18 expressing ECs (Fig 5E and 5F right graph). We also observed that the intracellular staining of ZO-1 was increased in Y260A-ARHGEF18 expressing EC compared to control ECs (Fig 5E and F). In these experiments, we also observed a slight decrease in VE-cadherin staining intensity in-between control and GEF-mutant ECs or in-between 2 GEF-mutant ECs, something we did not observed with ARHGEF18 silencing. Lastly, in ECs with low and local over-expression of the GEF-mutant, we observe a focal loss of ZO-1 together with a dissolution of the VE-cadherin junction (Fig 5E, lower panel). Overall, these data highlight the requirement of the nucleotide exchange activity of ARHGEF18 for the activation of p38 MAPK and the subsequent EC response to physiological flow.

Discussion

Our present work identifies a new SS-sensitive RhoGEF in ECs: ARHGEF18. ARHGEF18, also known as p114-RhoGEF, has been described mostly in epithelial cells where it controls cell tight junction maturation and apicobasal polarity establishment[39,53] via RhoA and Rac1 activation[54–56]. At the junction of epithelial cells, ARHGEF18 is shown to localized at tight junctions where it regulates RhoA-Rock activity and actomyosin contractility in spatio-temporal manner[39]. ARHGEF18 has also been shown to participate in long range communication of epithelial cell to pass the pulling force information from leading cells to neighboring cells in a wound closure assay, suggesting a potential mechano-sensitive role of this protein[41]. In this work, focusing on endothelial cells, we showed that ARHGEF18 expression and activity is modulated by the magnitude of SS applied. Interestingly, ARHGEF18 activity is at its highest when ECs are exposed to physiological SS suggesting a beneficial role of this Rho-GEF on ECs biology. This high activity is associated with a lower expression of the protein than in pathological SS, suggesting the failure in ARHGEF18 activation by pathological SS leads to its over-expression. Data from epithelial cells and GTP transfer experiments were in favor of a specificity of ARHGEF18 for the

RhoGTPase RhoA[54]. In ECs, we also demonstrated this specificity for RhoA, as ARHGEF18 was unable to bind to Rac1 in any SS condition. ARHGEF18 is not the only RhoGEF able to activate RhoA in ECs, therefore the effect at the total cellular level, as assessed by pulldown, could have been missed. The observation of a reduction of RhoA activity in total cell lysat is thus strongly in favor of an essential role of ARHGEF18 in the SS-induced activation of RhoA in ECs. From works done in epithelial cells, it appears that ARHGEF18 can localize to both adherent and tight junction, being recruited there by Gα12 or JAM-A respectively[58,59]. The only other article studying ARHGEF18 in ECs showed ARHGEF18 recruitment to tight junction of dermal microvascular ECs by both ZO-1 and JACOP[60]. In both cell type, this localization of ARHGEF18 was responsible for establishing cell tension at junction. None of these studies showed a direct interaction between ARHGEF18 and those junctional proteins. Unfortunately, we were unable to stain for ARHGEF18 *in vitro* in ECs, and could not observe ARHGEF18 at junctions in ECs nor evaluate the influence of SS on this localization. However, we successfully co-precipitated ARHGEF18 and ZO-1, showing the direct interaction of these 2 proteins in ECs implying the junctional localization of ARHGEF18. Interestingly, in ECs, ARHGEF18 is not interacting with VE-Cadherin, suggesting that ARHGEF18 does not directly impact adherent junctions. Our data from the over-expression of the Y260A-ARHGEF18 mutant showed a trapping of ZO-1 within the cytoplasm in mutant cells, suggesting that in opposition to what has been shown in microvascular ECs under static condition where ZO-1 acts upstream to ARHGEF18 bringing it to tight junctions, ARHGEF18 would participate in ZO-1 localization to tight junction in ECs under physiological SS. Additionally, we successfully stained the vasculature of the retina in mice, showing that ARHGEF18 was indeed expressed in ECs *in vivo*, but also that it expression correlates with arterial specification, ie. strongly expressed in more mature arteries (close to the optic nerve) and weakly expressed in less mature arteries (distant from the optic nerve). This observation could mean either a role of arterial specification in ARHGEF18 expression or a role of SS as arteries from different caliber are exposed to different SS level. In epithelial cell, ARHGEF18 contribution to cell-cell tension[39] and long range communication[41] participates in cell adhesion and collective migration. In our hands, migration and adhesion were also affected in ARHGEF18-silenced ECs, suggesting that similar mechanisms could be at play. Whether it goes through similar effectors as the one identified in epithelial cell, namely Patj, LKB1 and Lulu2 is still to determined.

In ECs, cell-cell tension participates in SS sensing allowing collective behavior[61]. Interestingly ARHGEF18 silencing leads to a loss of ECs alignment in response to physiological SS, a hallmark of endothelial health and collective behavior. This is accompanied by a loss of the tight junction proteins (ZO-1 and Claudin5) at junctions and a destabilization of cortical actin. This is the first observation showing that a RhoA-specific RhoGEF can control EC response to flow. Interestingly, loss of ARHGEF18 not only disrupts tight junction under physiological SS but also impairs focal adhesion formation and organization, suggesting a cross-talk between tight junction and focal adhesion. We also observed a loss in focal adhesion in single cell adhesion experiment suggesting a direct role of ARHGEF18 on focal adhesion. In dermal microvascular ECs, ARHGEF18 participate in the maintenance of junctional vinculin[60]. As vinculin has been shown as a key element to balance tension between focal adhesions and adherens junctions[62], it would be interesting to evaluate if ARHGEF18 can participate in vinculin localization at focal adhesion or tight junctions and therefore promote their stability. Among the different signaling pathways tested, only p38 MAPK seems to participate in the effect of ARHGEF18 as ARHGEF18 silencing reduces p38 MAPK phosphorylation level and inhibiting p38 MAPK activity reproduces most of the effect of ARHGEF18 silencing. The only effect that was not seen with p38 MAPK inhibition but observed with ARHGEF18 silencing was the formation of paracellular gaps, suggesting that ARHGEF18 downstream signaling does not fully depend on p38 MAPK. RhoGEF proteins not only carry GEF activity but usually display additional roles depending on their structure. As an example, Trio has been shown in ECs to contribute to Rac1 localization within the cell but not to Rac1 activity while having a GEF domain specific for Rac1[35]. In our hands, nucleotide exchange activity of ARHGEF18 contributes to tight junction formation as ZO-1 mis-localizes from junctions in Y260A-ARHGEF18 expressing ECs. In the same line as p38 MAPK inhibition, the Y260A mutation does not trigger paracellular gaps, suggesting once more an additional role of ARHGEF18 independent of its nucleotide exchange activity. Interestingly, in mice, complete deletion of ARHGEF18 resulted in embryonic lethality[63]. ARHGEF18 null embryos showed reduced vasculature, increased hemorrhage and oedema, which is in line with our *in vitro* observation. Future work will aim at better understanding the specific role of ARHGEF18 in endothelial cell *in vivo* both in physiology and pathologies.

Acknowledgments
We thank Dr. Vincent Sauzeau and Dr. Thibaut Quillard for helpful comments on the manuscript. We are most grateful to the Genomics Core Facility GenoA, member of Biogenouest and France Genomique and to the Bioinformatics Core Facility BiRD, member of Biogenouest and Institut Français de Bioinformatique (IFB) (ANR-11-INBS-0013) for the use of their resources and their technical support. We acknowledge the IBISA MicroPICell facility (Biogenouest), member of the national infrastructure France-Bioimaging supported by the French national research agency (ANR-10-INBS-04). This work was supported by the NeXT initiative (A.-C. Vion, S. Batta and C. Lebot), the French national research agency (ANR) (A.-C. Vion) and the local fund Genavie (S. Batta). The authors declare no competing financial interests. Author contributions: S. Batta performed experiments, analyzed the results, and wrote the manuscript. M. Rio, C. Lebot, C. Baron-Menguy performed experiments and analyzed results, R. Leruz performed experiments. G Loirand reviewed the manuscript. A.-C. Vion designed the study, performed experiments, analyzed the results, and wrote the manuscript.

Tables

Table 1: shRNA sequences used in this study

Name	Sense (5'->3')	Antisense (5'->3')	Target
shNT (non-target)	CAAATCACAGAATCGTCGTAT	ATACGACGATTCTGTGATTTG	None
shArhgef18.1	GGCCACAATGAAGCTGTTAGT	ACTAACAGCTTCATTGTGGCC	Exon
shArhgef18.2	CAAAACTTGATCAAGAAAATT	AATTTTCTTGATCAAGTTTTG	Exon
shArhgef18.3	CGGGCTACGACTGCACAAACA	TGTTTGTGCAGTCGTAGCCCG	Exon
shArhgef18.4	AAGACAAGATGTCCTTTATGA	TCATAAAGGACATCTTGTCTT	Exon
shArhgef18.5	CGATTTTATTTGTAAAGTTGA	TCAACTTTACAAATAAAATCG	3'UTR
shArhgef18.6	GAGCAAATGTTCCTATTTTCG	CGAAAATAGGAACATTTGCTC	3'UTR

Table 2: Primers and oligos used to amplify Arhgef18

Oligo name	Oligo sequence (5'->3')
Arhgef18_Fw	ACAGCTCTGCGATCGCCACCATGACGGTCTCTCAGAAAGGG
Arhgef18_Rev	GCTGTCTCGAGAATTAAGAAGAAGATGACGTCTTCTTTGC
ORF18-Oligo1	ATGACGGTCTCTCAGAAAGGG
ORF18-Oligo2	GTACGTCGGTCAGCAGGATAG
ORF18-Oligo3	CTCACCTTCCGCAAGGAAGAC
ORF18-Oligo4	GAAGTTGCGTTGCCGCTCCTG
ORF18-Oligo5	CCCACCAGGACAGCTATGTG
ORF18-Oligo6	GAAGAAGATGACGTCTTCTTTGCTGG

Figure 1

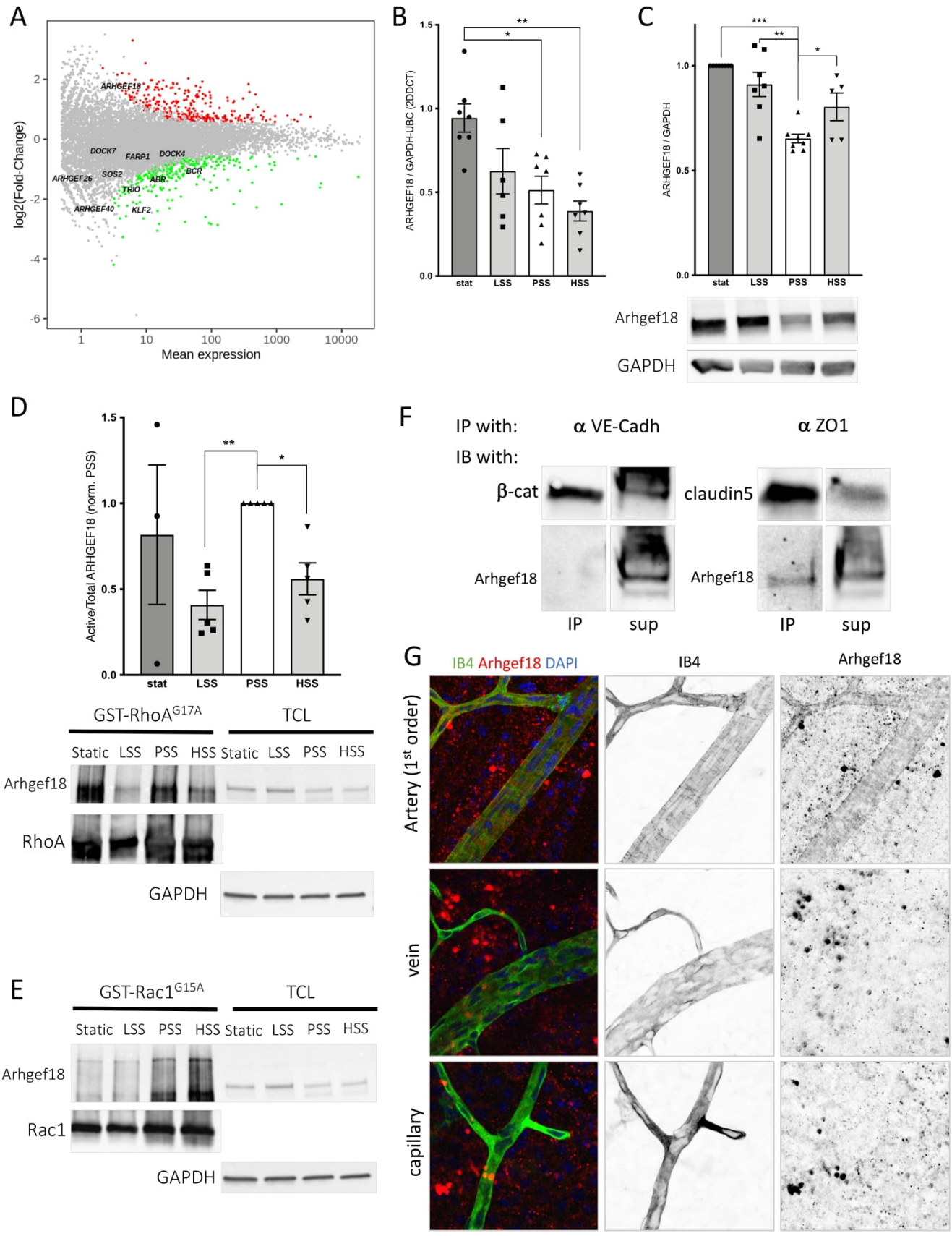
A
log2(Fold-Change)
Mean expression
ARHGEF18
DOCK7
FARP1
DOCK4
ARHGEF26
SOS2
ABR
BCR
TRIO
ARHGEF40
KLF2
B
ARHGEF18 / GAPDH-UBC (2DDCT)
stat
LSS
PSS
HSS
C
ARHGEF18 / GAPDH
Arhgef18
GAPDH
D
Active/Total ARHGEF18 (norm. PSS)
GST-RhoA^{G17A}
TCL
Static LSS PSS HSS Static LSS PSS HSS
Arhgef18
RhoA
GAPDH
E
GST-Rac1^{G15A}
TCL
Static LSS PSS HSS Static LSS PSS HSS
Arhgef18
Rac1
GAPDH
F
IP with:
α VE-Cadh
α ZO1
IB with:
β-cat
claudin5
Arhgef18
Arhgef18
IP
sup
IP
sup
G
IB4 Arhgef18 DAPI
IB4
Arhgef18
Artery (1st order)
vein
capillary

Figure 2

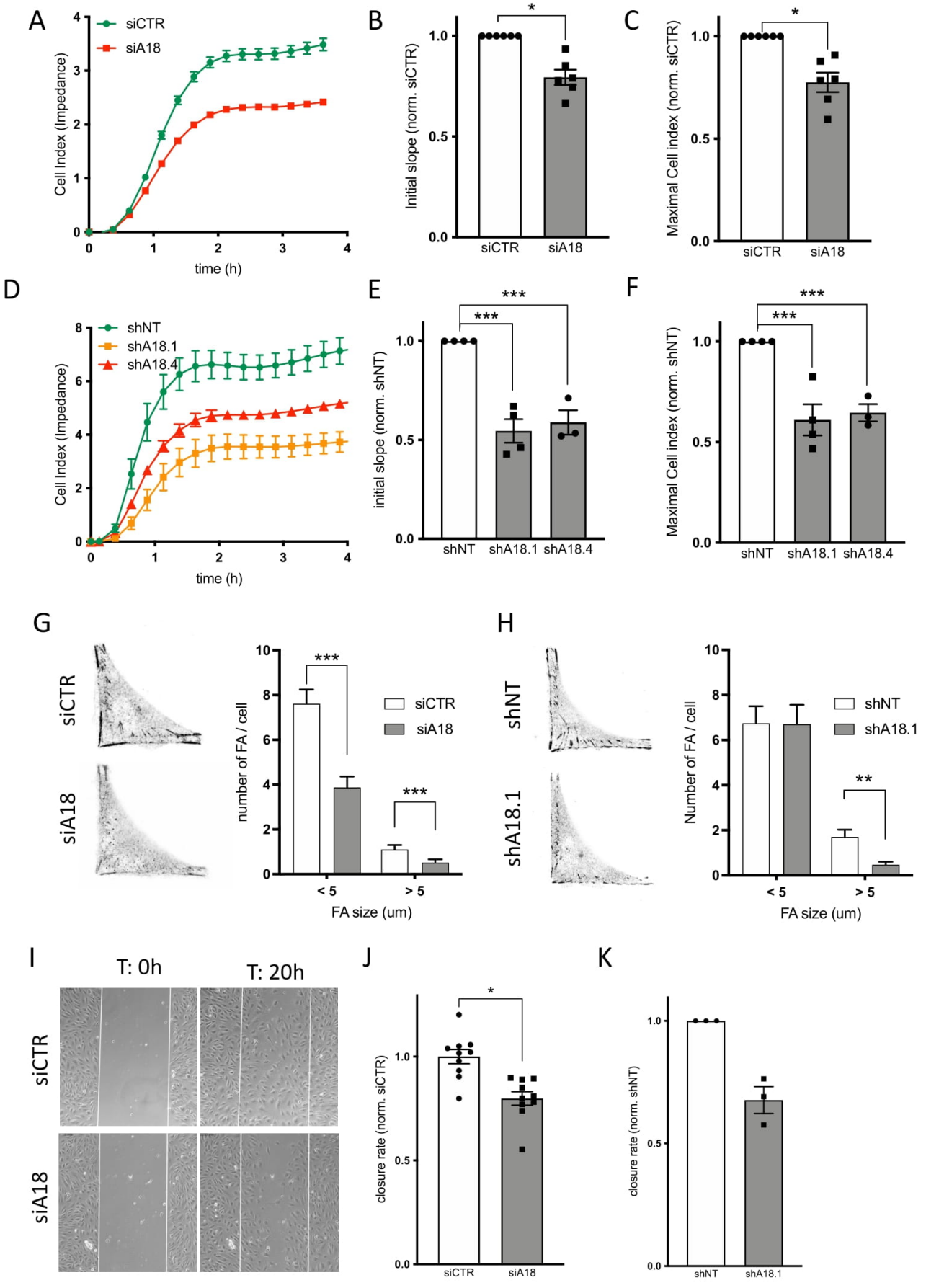
A
siCTR
siA18
Cell Index (Impedance)
time (h)
B
Initial slope (norm. siCTR)
siCTR
siA18
C
Maximal Cell index (norm. siCTR)
D
shNT
shA18.1
shA18.4
E
initial slope (norm. shNT)
F
Maximal Cell index (norm. shNT)
G
number of FA / cell
FA size (um)
H
Number of FA / cell
I
T: 0h
T: 20h
J
closure rate (norm. siCTR)
K
closure rate (norm. shNT)

Figure 3

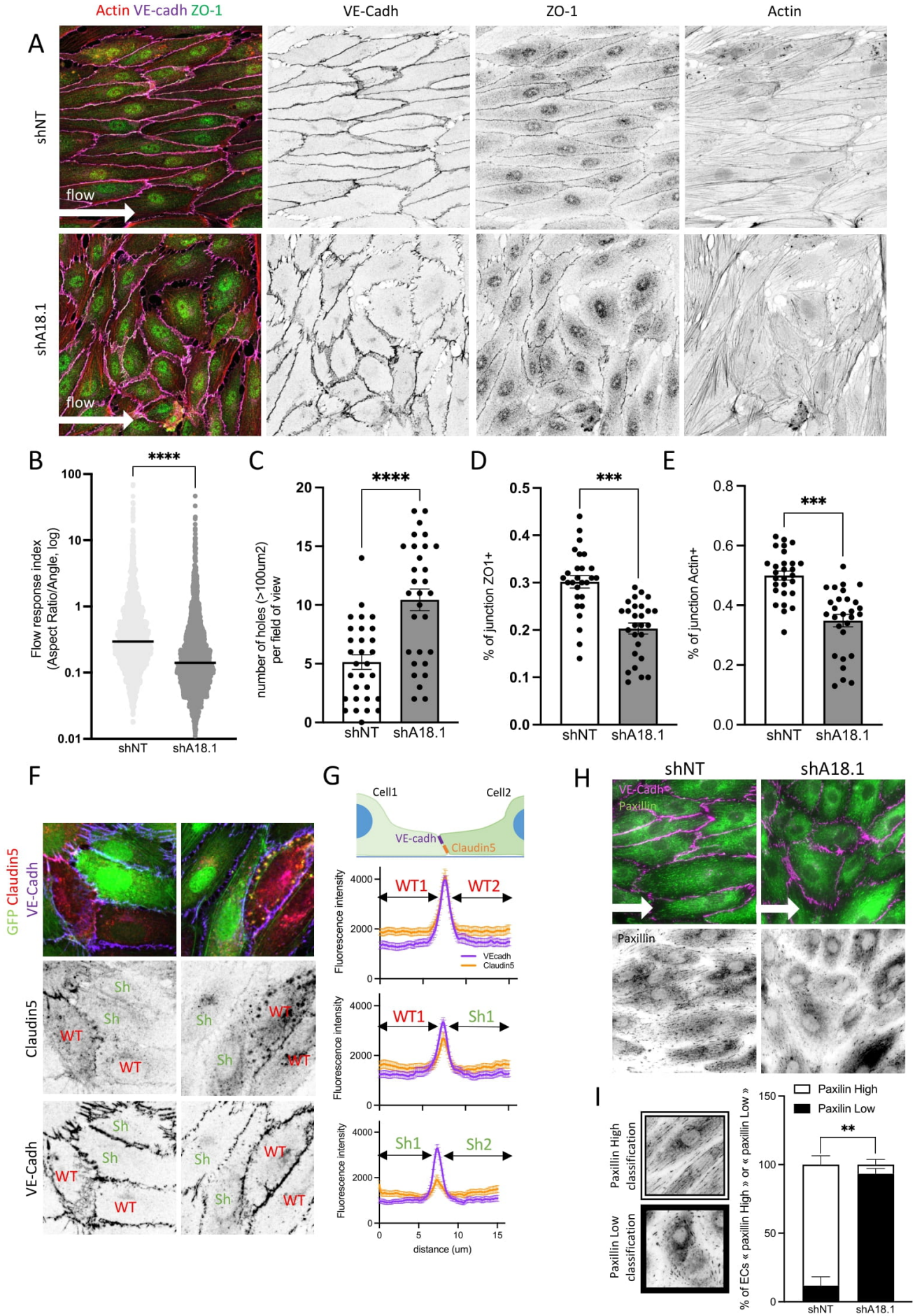
Actin VE-cadh ZO-1
VE-Cadh
ZO-1
Actin
A
shNT
shA18.1
flow
flow
B
****
Flow response index (Aspect Ratio/Angle, log)
100
10
1
0.1
0.01
shNT
shA18.1
C
****
number of holes (>100um2) per field of view
20
15
10
5
0
shNT
shA18.1
D
***
% of junction ZO1+
0.5
0.4
0.3
0.2
0.1
0.0
shNT
shA18.1
E
***
% of junction Actin+
0.8
0.6
0.4
0.2
0.0
shNT
shA18.1
F
GFP Claudin5
VE-Cadh
Claudin5
VE-Cadh
Sh
WT
G
Cell1
Cell2
VE-cadh
Claudin5
Fluorescence intensity
WT1
WT2
VEcadh
Claudin5
WT1
Sh1
Sh1
Sh2
distance (um)
H
shNT
shA18.1
VE-Cadh
Paxillin
Paxillin
I
Paxillin High classification
Paxillin Low classification
% of ECs « paxillin High » or « paxillin Low »
Paxilin High
Paxilin Low
**
150
100
50
0
shNT
shA18.1

Figure 4

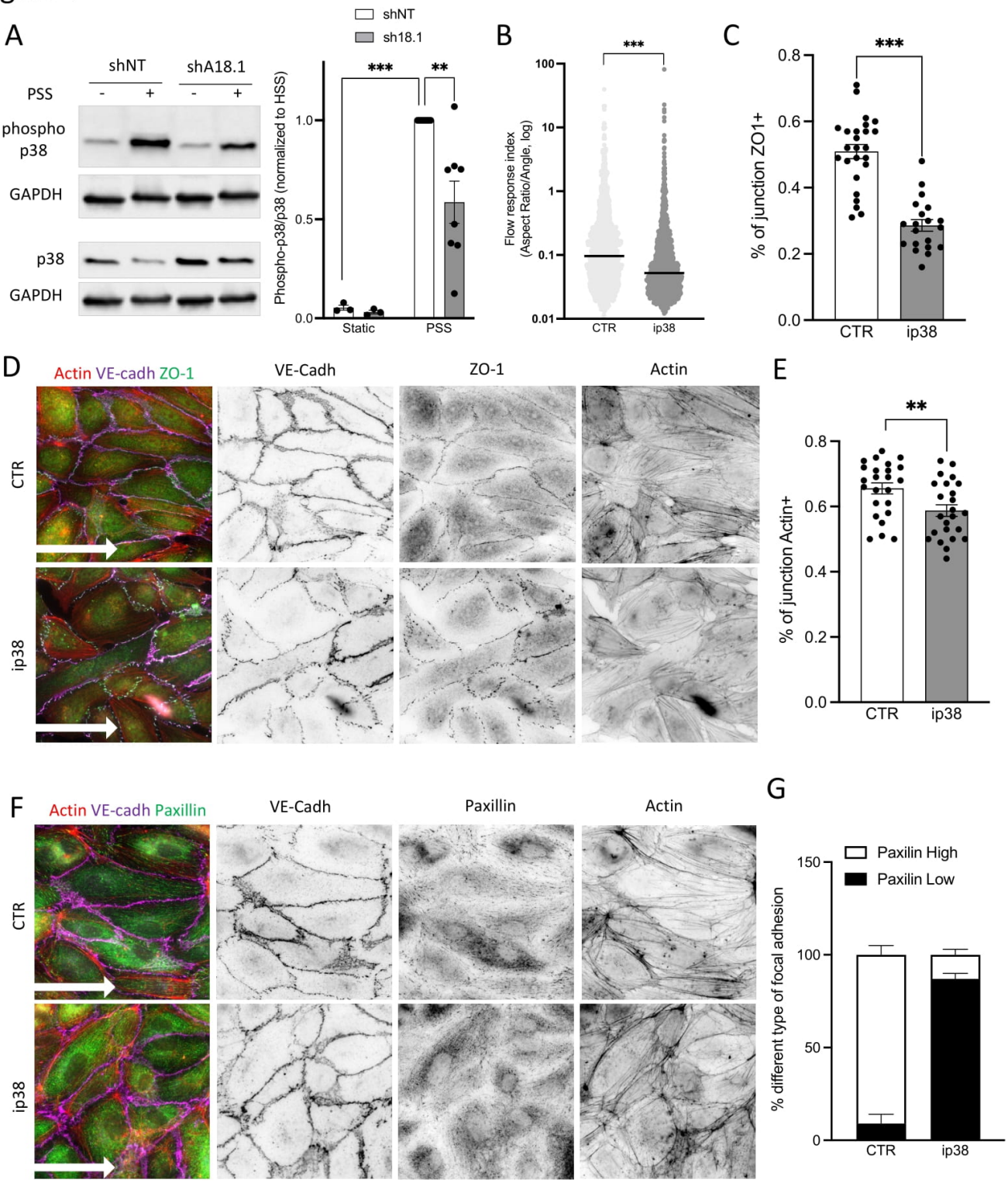
A
shNT
shA18.1
PSS
- + - +
phospho p38
GAPDH
p38
GAPDH
shNT
sh18.1
Phospho-p38/p38 (normalized to HSS)
***
**
Static
PSS
B
***
Flow response index (Aspect Ratio/Angle, log)
CTR
ip38
C
***
% of junction ZO1+
CTR
ip38
D
Actin VE-cadh ZO-1
VE-Cadh
ZO-1
Actin
CTR
ip38
E
**
% of junction Actin+
CTR
ip38
F
Actin VE-cadh Paxillin
VE-Cadh
Paxillin
Actin
CTR
ip38
G
Paxilin High
Paxilin Low
% different type of focal adhesion
CTR
ip38

Figure 5

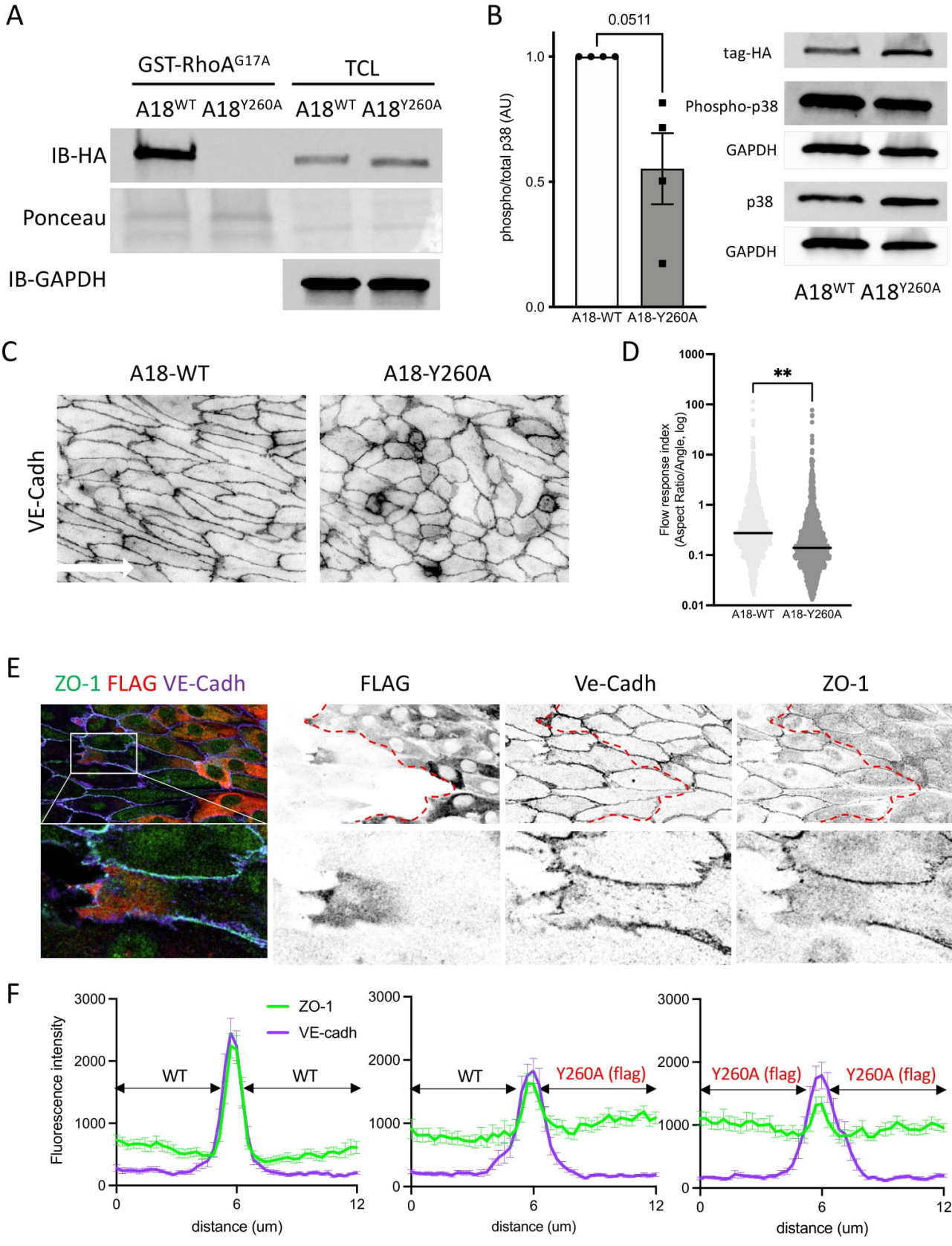
A
GST-RhoA^{G17A}
TCL
A18^{WT} A18^{Y260A} A18^{WT} A18^{Y260A}
IB-HA
Ponceau
IB-GAPDH
B
0.0511
phospho/total p38 (AU)
1.0
0.5
0.0
A18-WT A18-Y260A
tag-HA
Phospho-p38
GAPDH
p38
GAPDH
A18^{WT} A18^{Y260A}
C
A18-WT
A18-Y260A
VE-Cadh
D
**
Flow response index
(Aspect Ratio/Angle, log)
1000
100
10
1
0.1
0.01
A18-WT A18-Y260A
E
ZO-1 FLAG VE-Cadh
FLAG
Ve-Cadh
ZO-1
F
Fluorescence intensity
3000
2000
1000
0
ZO-1
VE-cadh
WT
WT
Y260A (flag)
Y260A (flag)
Y260A (flag)
0
6
12
distance (um)

Figures Legends

Figure 1: ARHGEF18 expression and activity is shear-stress dependent and bound to RhoA but not RAC1. **A.** MA plot comparing gene expression between static condition and high shear stress. 24h of SS. Green dots: up-regulated genes in HSS condition; red dots: down-regulated genes in HSS condition. N=4. **B.** qPCR analysis of Arhgef18 RNA expression level. 24h of SS, LSS: low shear stress; PSS: physiological shear stress; HSS: high shear stress. N>5. *p<0.05; **p<0.01; One-way ANOVA. **C.** Western-Blot analysis of ARHGEF18 protein expression level (left, quantification; right, representative blot). 24h of SS, LSS: low shear stress; PSS: physiological shear stress; HSS: high shear stress. N>5. *p<0.05; **p<0.01; ***p<0.001; One-way ANOVA. **D.** Quantification and representative blot of ARHGEF18 binding on nucleotide-free RhoA (GST-RhoA^{G17A}) by pull-down assay. 24h of SS, LSS: low shear stress; PSS: physiological shear stress; HSS: high shear stress. N=5. *p<0.05; **p<0.01; ***p<0.001; One-way ANOVA. **E.** Representative blot of ARHGEF18 binding on nucleotide-free Rac1 (GST-Rac1^{G15A}) by pull-down assay. 24h of SS, LSS: low shear stress; PSS: physiological shear stress; HSS: high shear stress. Representative of N=3. **F.** Representative blot from Co-immunoprecipitation of ARHGEF18 with VE-cadherin (left) or ZO-1 (right). Co-immunoprecipitation efficiency was assessed by the presence of β-catenin and Claudin 5 in the immunoprecipitated fraction of VE-cadherin complex and ZO-1 complex respectively (upper lanes). Static condition. Representative of N=2. **G.** Immunofluorescent staining of ARHGEF18 in mouse retina. Retinas from 4 weeks-old animals. Green: Isolectin B4; Representative of N=5.

Figure 2: ARHGEF18 participates to endothelial cell adhesion and migration. **A.** Representative curves of impedance measurement during adhesion of HUVECs. Green: non-targeting siRNA (siCTR); red: siRNA targeting arhegf18 RNA (siA18). . **B.** Quantification of adhesion speed (slope of the linear part of the curve) of HUVECs transfected with a control siRNA (siCTR) or with an siRNA targeting Arhgef18 (siA18). N=6. *p<0.05; Wilcoxon T-test. **C.** Quantification of maximal adhesion (plateau of the curve) of HUVECs transfected with a control siRNA (siCTR) or with an siRNA targeting Arhgef18 (siA18). N=6. *p<0.05; Wilcoxon T-test. **D.** Representative curves of impedance measurement during adhesion of HUVECs. Green: non-targeting shRNA (shNT); red and orange: shRNAs targeting arhgef18 RNA (shA18.4 andshA18.1 respectively). **E.** Quantification of adhesion speed (slope of the linear part of the curve) of HUVECs expressing a non-targeting shRNA (shNT) or a shRNA targeting Arhgef18 (shA18.1 or A18.4). N<3. ***p<0.001; One-way ANOVA. **F.** Quantification of maximal adhesion (plateau of the curve) of HUVECs expressing a non-targeting shRNA (shNT) or a shRNA targeting Arhgef18 (shA18.1 or A18.4). N<3. ***p<0.001; One-way ANOVA. **G.** Representative images of HUVECs adhesion on L-shaped micropattern immune-stained for paxillin (siRNA transfected HUVECs) and Quantification of focal adhesion number and size. N=39 (cells) from 4 different experiments. ***p<0.001; 2-way ANOVA. **H.** Representative images of HUVECs adhesion on L-shaped micropattern immune-stained for paxillin. (shRNA expressing HUVECs) and Quantification of focal adhesion number and size. N=51 (cells) from 4 different experiments. ***p<0.001; 2-way ANOVA. **I.** Representative images of wound assay experiment (phase contrast images) at starting point (T:0h) and 20h post wound. siRNA transfected HUVECs. **J.** Quantification of closure speed of HUVECs transfected with a control siRNA (siCTR) or with an siRNA targeting Arhgef18 (siA18). N=10. *p<0.05; paired T-test. **K.** Quantification of closure speed of HUVECs expressing a control shRNA (shNT) or a shRNA targeting Arhgef18 (shA18.1). N=3.

Figure 3: ARHGEF18 participates in ECs response to flow, tight junction formation and focal adhesion formation. **A.** Representative images of HUVECs expressing a non-targeting shRNA (shNT) or a shRNA targeting Arhgef18 (shA18.1), exposed to physiological SS and stained for ZO-1 (green), VE-cadherin (magenta) and actin (red). Flow direction is indicated by the arrow. **B.** Quantification of cell orientation and elongation with the flow in HUVECs expressing a non-targeting shRNA (shNT) or a shRNA targeting Arhgef18 (shA18.1), exposed to physiological SS. 24h of SS. Each dot represents a cell. N=5 with in-between 200 and 600 cells analyzed by experiment. ***p<0.001; Mann-Whithney T-test. **C.** Quantification of number of holes in-between cells in HUVECs expressing a non-targeting shRNA (shNT) or a shRNA targeting Arhgef18 (shA18.1), exposed to physiological SS. 24h of SS. N=3, 10 areas analyzed by experiment. ***p<0.001; Unpaired T-test. **D.** Quantification of ZO-1 localized at junction in HUVECs expressing a non-targeting shRNA (shNT) or a shRNA targeting Arhgef18 (shA18.1), exposed to physiological SS. 24h of SS. N=3, 9 areas analyzed by experiment. ***p<0.001; Unpaired T-test. **E.** Quantification of Actin localized at junction in HUVECs expressing a non-targeting shRNA (shNT) or a shRNA targeting Arhgef18 (shA18.1), exposed to physiological SS. 24h of SS. N=3, 9 areas analyzed by experiment. ***p<0.001; Unpaired T-test. **F.** Representative images of Claudin5 staining in a mix population of WT cells (GFP negative, non-green, indicated as “WT” on images) and cells expressing a shRNA targeting Arhgef18 (shA18.1, GFP positive, green, indicated as “KO” on images), exposed to physiological SS. Green: GFP; red: Claudin5; Magenta: VE-cadherin. **G.** Quantification of the Claudin5 staining at junction using plot profile analysis. N=3, 12 couple of cells analyzed per experiment. **H.** Representative images of Paxillin staining in HUVECs expressing a non-targeting shRNA (shNT) or a shRNA targeting Arhgef18 (shA18.1), exposed to physiological SS. Flow direction is indicated by the arrow. Green: paxillin; magenta: VE-cadherin. **I.** Quantification of focal adhesion type by hand classification of paxillin staining within each cell based on the representative images for each category on the left (white box: paxillin high = numerous, elongated and aligned focal adhesions; black box: paxillin low = few, short and misaligned focal adhesions). N=4. Quantified blindly.

Figure 4: p38 mediates ARHGEF18 effects in flow response of ECs. A. Quantification of p38 phosphorylation by Western blot in HUVECs expressing a non-targeting shRNA (shNT) or a shRNA targeting Arhgef18 (shA18.1), under static condition or exposed to physiological SS (PSS). Static: N=3; PSS: N=8. **p<0.01; ***p<0.001 2-way ANOVA**. B.** Quantification of cell orientation and elongation with the flow in HUVECs treated with an inhibitor for p38 (SB239063, 100nM, ip38) or vehicle (CTR), exposed to physiological SS. 24h of SS. Each dot represents a cell. N=4 with in-between 200 and 450 cells analyzed by experiment. ***p<0.001; Mann-Whitney T-test. **C.** Quantification of Actin localized at junction in HUVECs treated with an inhibitor for p38 (SB239063, 100nM, ip38) or vehicle (CTR), exposed to physiological SS. 24h of SS. N=2, 10 to 14 areas analyzed by experiment. **p<0.01; Unpaired T-test. **D.** Representative images of HUVECs treated with an inhibitor for p38 (SB239063, 100nM, ip38) or vehicle (CTR) exposed to physiological SS. 24 and stained for ZO-1 (green), VE-cadherin (magenta) and actin (red). Flow direction is indicated by the arrow. **E.** Quantification of ZO-1 localized at junction in HUVECs treated with an inhibitor for p38 (SB239063, 100nM, ip38) or vehicle (CTR) exposed to physiological SS. 24h of SS. N=2, 10 to 15 areas analyzed by experiment. ***p<0.001; Unpaired T-test. **F.** Representative images of Paxillin staining in HUVECs treated with an inhibitor for p38 (SB239063, 100nM, ip38) or vehicle (CTR), exposed to physiological SS. Flow direction is indicated by the arrow. Green: paxillin; magenta: VE-cadherin; red: Actin. **G.** Quantification of focal adhesion type by hand classification of paxillin staining within each cell based on the representative images for each category on the left (white box: paxillin high = numerous, elongated and aligned focal adhesions; black box: paxillin low = few, short and misaligned focal adhesions). N=2. Quantified blindly.

Figure 5: GEF activity of ARHGEF18 is important for p38 activation and flow response of ECs. A. Representative blot of ARHGEF18 binding on nucleotide-free RhoA (GST-RhoA^{G17A}) by pull-down assay with HUVECs exposed to physiological SS, over-expressing WT form (A18^{WT}) or mutant form (A18^{Y260A}) of ARHGEF18. **B.** Quantification of p38 phosphorylation by Western blot in HUVECs exposed to physiological SS, over-expressing WT form (A18^{WT}) or mutant form (A18^{Y260A}) of ARHGEF18. N=4. Paired T-test. **C.** Representative images of HUVECs HUVECs exposed to physiological SS, over-expressing WT form (A18^{WT}) or mutant form (A18^{Y260A}) of ARHGEF18 and stained VE-cadherin. Flow direction is indicated by the arrow**. D.** Quantification of cell orientation and elongation with the flow in HUVECs exposed to physiological SS, over-expressing WT form (A18^{WT}) or mutant form (A18^{Y260A}) of ARHGEF18. Each dot represents a cell. N=1 with in-between 1000 and 1350 cells analyzed by experiment. **p<0.01; Unpaired T-test. E. Representative images of ZO-1 staining in a mix population of WT cells (FLAG negative, non-red) and cells over-expressing the mutant form (A18^{Y260A}) of ARHGEF18 (FLAG positive, red), exposed to physiological SS. Green: ZO-1; red: FLAG; Magenta: VE-cadherin. F. Quantification of the ZO-1 staining at junction using plot profile analysis. N=1, 25 couples of cells analyzed per experiment.

Material and Methods

Cell culture and microfluidic chamber experiments
HUVECs (passage 2 to 6; PromoCell) were routinely cultured in EBM media supplemented with the provided growth factors kit (Promocell). For flow experiments dedicated to Pull-down/Co-IP/WB lysate collection, cells were cultured on 0.2% gelatin-coated slides (Menzel Glazer) and unidirectional laminar shear stress was applied using peristaltic pumps (Gilson) connected to a glass reservoir (ELLIPSE) and the chamber containing the slide. For flow experiments dedicated immunofluorescence staining, cells were cultured on 0.2% gelatin-coated 0.4 ibidi slides (IBIDI) and unidirectional laminar shear stress was applied using the pumping system and control unit form IBIDI. Local shear stress was calculated using Poiseuille's law and averaged to 3.6 dyn/cm^2 (pathological low shear stress: LSS) 16 dyn/cm^2 (physiological shear stress: PSS) or 36 dyn/cm^2 (pathological high shear stress: HSS). For p38 MAPK inhibition studies, confluent HUVEC were pretreated with p38 MAPK specific inhibitor (100nM, SB239063; TOCRIS) for at least 1hr prior to physiological SS, treatment was maintained during the flow stimulation.

Mice
Retinas from Wild Type C57/BL6 mice were collected on euthanized mice at 4-week-old in PFA 4% and used for immunofluorescent staining.

3'Sequencing RNA Profiling:
Experimental protocol: The protocol was performed according to the 3′-digital gene expression (3′-DGE) approach developed by the Broad institute as described in https://doi.org/10.21203/rs.3.pex-1336/v1. The libraries were prepared from 10 ng of total RNA in 4µl. The mRNA poly(A) tails were tagged with universal adapters, well-specific barcodes and unique molecular identifiers (UMIs) during template-switching reverse transcription. Barcoded cDNAs from multiple samples were then pooled, amplified and tagmented using a transposon-fragmentation approach which enriches for 3'ends of cDNA : 200ng of full-length cDNAs were used as input to the Nextera™ DNA Flex Library Prep kit (ref #20018704, Illumina) and Nextera™ DNA CD Indexes (24 Indexes, 24 Samples) (ref #20018707, Illumina) according to the manufacturer's protocol (Nextera DNA Flex Library Document, ref #1000000025416 v04, Illumina).
Size library was controlled on 2200 Tape Station Sytem (Agilent Technologies). A library of 350-800 bp length was run on a NovaSeq 6000 using NovaSeq 6000 SP Reagent Kit 100 cycles (ref #20027464, Illumina) with 17*-8-105* cycles reads.
Bioinformatics protocol: Raw fastq pairs match the following criteria: the 16 bases of the first read correspond to 6 bases for a designed sample-specific barcode and 10 bases for a unique molecular identifier (UMI). The second read (104 bases) corresponded to the captured poly(A) RNAs sequence.
Bioinformatics steps were performed using a snakemake pipeline (https://bio.tools/3SRP). Samples demultiplexing was performed with a python script. Raw paired-end fastq files were transformed into a single-end fastq file for each sample. Alignment on refseq reference transcriptome, available from the UCSC download site, was performed using bwa. Aligned reads were parsed and UMIs were counted for each gene in each sample to create an expression matrix containing the absolute abundance of mRNAs in all samples. Reads aligned on multiple genes or containing more than 3 mismatches with the reference were discarded. The expression matrix was normalized and differentially expressed genes (DEG) were searched using the R package deseq2 (doi: 10.1186/s13059-014-0550-8). If DEG were found, functional annotation was performed using the R package ClusterProfiler (doi: 10.1016/j.xinn.2021.100141 / doi: 10.1089/omi.2011.0118).

Generation of Lentiviral vectors:
For RNA interference, the sequence for non-target shRNA was previously described (KY Lee et al 2016) (Table 1). For Arhgef18, specific sense and anti-sense DNA sequences were identified using free online services (http://sidirect2.rnai.jp/; http://web.stanford.edu/group/markkaylab/cgi-bin/)[1] (Gu et al. 2014). The sequences that met the optimal criteria were selected and synthesized as oligos in the form of miR-E backbone. The oligos were then amplified using the primers miRE-fw (5'-TGAACTCGAGAAGGTATATTGCTGTTGACAGTGAGCG-3'), miRE-Rv (5'-TCTCGAATTCTAGCCCCTTGAAGTCCGAGGCAGTAGGC-3') and Q5 Hot Start High-Fidelity DNA polymerase (NEB M049S). The final amplicon was then digested and cloned into LT3GEPIR in-between XhoI and EcoRI restriction sites as previously described[2]. The cloned shRNAs were sequence confirmed using the primer miRseq5 (5'-TGTTTGAATGAGGCTTCAGTAC-3'). The resultant lentiviral vector drives the expression of shRNA along with EGFP under TRE3G promoter, a doxycycline inducible promoter.

For Arhgef18 overexpression constructs, Arhgef18 was amplified from HUVEC cDNA by overlap-extension PCR using the following oligos and primers (Table 2). The resultant amplicon was digested and clone into LT3(AsiSI)N1-GPIR (modified LT3GEPIR) vector in between AsiSI and EcoRI restriction sites. The resultant vector LT3N1-GPIR-Arhgef18 encodes Arhgef18-EGFP fusion protein under TRE3G promoter. GEF mutant version of Arhgef18 was generated by site directed mutagenesis of tyrosine to alanine at amino acid position 260 using primers A18-Y260A-SDM-Fr (5'-CATAACCAAAGCCCCAGTGCTGGTG-3'), A18-Y260A-SDM-Rev (5'-CGTTGTGTAACCAGGAGAATG-3') and Q5 site directed mutagenesis kit (NEB E0554). This LT3N1-GPIR-Arhgef18 vectors were further modified to substitute EGFP with 3XHA-FLAG tag, shArhgef18.6 to target endogenous Arhgef18 and P2A sequence to replace IRES using standard molecular cloning techniques. The resultant vector is designated as Arhgef18-HA/FLAG_shArhgef18.6.

Lentivirus production, transduction and induction of gene of interest vectors

Lentivirus vector carrying either the shRNA or Arhgef18 ORF was transfected into HEK293T cells along with packaging vectors psPAX2 and pVSVG2 (provided by Prof. Dr.Utz Fischer's lab) using polyethylenimine (764965; Sigma-Aldrich) transfection agent. After overnight incubation, the medium was replaced with fresh medium (DMEM+10%serum+PenStrep). Forty-eight hours and 72 h after transfection, viral supernatant was collected, filtered through 0.22 µm filter and used to infect HUVECs (passage 2) in the presence of polybrene (8 µg/ml, H9268; Sigma-Aldrich). The transduced HUVECs were selected with puromycin (8ug/ml, P8833; Sigma-Aldrich) for 48 h and maintained in the presence of puromycin (1µg/ml). The induction of either shRNA or full length Arhgef18 was performed at least 2days before the experiment by supplementing the medium with doxycycline (1µg/ml, D9891; Sigma-Aldrich) and maintained throughout the experimental procedure.

Pulldown Assay

Pulldown of active small GTPases (RhoA/Rac) or active Arhgef18 was done as previously described[3]. Briefly, HUVECs (WT, shRNA or A18-Y260A) subjected to various shear stress conditions for indicated time, were lysed in either RBD lysis buffer (50 mM Tris-HCl (pH 7.6), 500 mM NaCl, 1% (vol/vol) Triton X-100, 0.1% (wt/vol) SDS, 0.5% (wt/vol) deoxycholate and 10 mM MgCl2) or GEF lysis buffer (20 mM HEPES pH 7.5, 150 mM NaCl, 5 mM $MgCl_2$, 1% (vol/vol) Triton X-100, 1 mM DTT) supplemented with protease and phosphatase inhibitor cocktail. Cell debris was removed by centrifugation and equal volumes of cell lysate was incubated with 25-50 ug of either GST-RBD/PBD for active small-GTPases; or GST tagged RhoAG17A/Rac1G15A for active GEF pulldown for 45min. After incubation, beads were washed twice in respective wash buffers. Captured proteins were detected using Western Blot.

Co-immunoprecipitation assay

HUVECs (WT) subjected to various shear stress conditions for indicated time, were lysed in RBD lysis buffer (50 mM Tris-HCl (pH 7.6), 500 mM NaCl, 1% (vol/vol) Triton X-100, 0.1% (wt/vol) SDS, 0.5% (wt/vol) deoxycholate and 10 mM MgCl2) supplemented with protease and phosphatase inhibitor cocktail. Lysis buffer was homogenized passing through a 32-gauge syringe needle and cellular debris were removed by centrifugation (5 min, 10000 rpm). A small amount of the lysate was collected in order to assess the presence of the protein in the total cell lysate. Beads were first equilibrated in RBD buffer and then coated with 0.5 µg of the following antibodies: Claudin5 (genentex), ZO-1 (Thermofisher), VE-cadherin (R&D systems), Paxillin (Abcam). Cell lysats were then incubated with the coated beads, supernatants and immunoprecipitats (washed 3 times) were stored to proceed for Western blot.

Micropatterning assay

Pattern shape was design with FIJI software to have a L shaped pattern 50x50µm long and 6µm large. PDMS stencils were placed in IBIDI wells and cleaned in a Plasma cleaner for 5 min. A hydrophobic treatment was done using PLL PEG (Poly-lysine Polyethylene glycol 100µg/ml) for 30min. Wells were washed 3 times with PBS. Patterns were then prepared using the Primo device (Alveole). Briefly, the wells with PLPP (photoinitiator, Alveole) were placed under a microscope with the PRIMO device. focus was adjusted to UV reflection and the patterning sequence was launched with 1200mJ/mm2 UV exposure. Once patterned, wells were profusely washed with PBS and then coated with fibronectin (10µg/ml). Six hundred cells were seeded per well for 1h, then washed and the remaining cells were left to adhere for 12 h.

Western blotting

HUVECs were washed with cold PBS and scraped off in NETF buffer supplemented with protease and phosphatase inhibitors. Lysates were centrifuged and protein supernatant was quantified using the

Lowry protein assay (Bio-Rad). Lysates were reduced in lamelli buffer and electrophoresis was performed using precast SDS-PAGE gels (Biorad) and transferred on to PVDF membranes (Biorad). Equal loading was checked using Ponceau red solution. Membranes were then blocked in 5% milk and probed with primary antibodies over-night (see below) and respective secondary antibodies (1:3000). The membranes were developed using ECL (Biorad) using the Chemidoc imaging system (Biorad). After initial immunodetection, membranes were re-probed with anti–GAPDH antibody. The protein bands were quantified using fiji and expressed as a relative value to either GAPDH or as the ratio of phosphorylated to total protein. The following antibodies were used: ARHGEF18 (1/500; GTX102223; Genetex), p38 (1:500; 9212, CST), Phospho-p38 (1:500; 9211, CST) ERK1/2 (1:500; 4695, CST), phospho-ERK1/2 (1:500; 9101, CST), Akt (1:500; 9272, CST), phospho-Akt (1:500; 9271, CST), Claudin5 (1:500; 34-1600, Invitrogen), RhoA (1:500; 2117, CST), Rac1 (1:500; 2465, CST), Vav (1:250; ab92890; abcam), GST (1:2000; PC53-100UG; Oncogene), paxillin (1:500; ab32084; abcam), phospho-paxillin (1:500; ab194738; abcam), GAPDH (1:1000; MAB374, MerckMillipore).

In vitro Immunofluorescence staining
HUVECs were fixed with 4% PFA in PBS for 10 min at room temperature (RT). Blocking/ permeabilization was performed using blocking buffer consisting of 5% BSA (Sigma-Aldrich), 0.5% Triton X-100 (Sigma-Aldrich), 0.01% sodium deoxycholate (Sigma-Aldrich), and 0.02% sodium azide (Sigma-Aldrich) in PBS at pH 7.4 for 45 min at RT. Primary antibodies were incubated at the desired concentration in 1:1 Blocking buffer/PBS at RT for 2 hours and secondary antibodies (Life Technologie, Alexa, 1/500) were incubated at the desired concentration in 1:1 blocking buffer/PBS for 1 hour at RT. DAPI (Sigma-Aldrich, 1/10000, 5 min) was used for nuclear labeling and phaloidin488 (life technologies, 1/500, 45min) was used to labelled polymerized actin. The following antibodies were used in vitro: VE-Cadherin (1/1000, RandD), ZO-1 (1/500, 61-7300, life technologies), claudin5 (MAB19903, Abnova, 1/500), paxillin (Abcam, 1/1000),

In vivo Immunofluorescence staining
Retinas were fixed with 4% PFA in PBS overnight at 4°C. Blocking/ permeabilization was performed using blocking buffer consisting of 1% FBS, 3% BSA (Sigma-Aldrich), 0.5% Triton X-100 (Sigma-Aldrich), 0.01% sodium deoxycholate (Sigma-Aldrich), and 0.02% sodium azide (Sigma-Aldrich) in PBS at pH 7.4 for 1 hour at RT. Anti-ARHGEF18 antibody was incubated at 1/400 in 1:1 Blocking buffer/PBS overnight at 4°C and secondary antibody (anti-rabbit 568, life technologies, 1/400) was incubated in 1:1 blocking buffer/PBS for 2 hours at RT. DAPI (Sigma-Aldrich, 1/10000, 5 min) was used for nuclear labeling and Isolectin B4 488 (life technologies, 1/400, 1h) was used to labelled endothelial cells. Retinas were mounted in Mowiol.

Impedance-based assay
Cell adhesion assay was performed using xCELLigence RTCA instrument (Roche). Briefly, HUVECs (P4-P6) expressing either shNT (non-target), sh18.1 or sh18.4 were plated in E-plate 96 well (5232368001; Agilent) at a density of 20,000cells/well. Cell adhesion was measured as electrical impedance between electrodes and represented as cell index value over a period of time.

Wound healing assay
Confluent monolayer of HUVECs were scratched using a pipette tip. Cell debris were washed and the medium was replaced with fresh complete medium. Cell migration was videorecorded under optimal conditions (37^{o}C and 5%CO2) using an inverted Ti Eclipse microscope equipped with a 10x/0.25 phase contrast objective and a DS-Qi2 CMOS camera (Nikon France, Champigny Sur Marne). Images were recorded every 5 minutes during 24h. Wound area was manually measured at different time points using Fiji and rate of wound closure was calculated by area relative to time.

Proliferation assay
Proliferation assay was performed using the Edu-click647 kit (BCK-EdU647; Base Click). HUVECs expressing the shRNAs were plated in µ-Slide VI 0.4 (80606; IBIDI) at a density of 30,000cells per channel in starving medium (EBM+0.5%serum+doxy+puro). After 16 h, cells were stimulated with complete medium (EBM+2%serum+doxy+puro) in the presence of EdU (5uM) under static or flow for 8 h. Cells were fixed in 4%formaldehyde for 10 min, stained for EdU and nuclei were labeled with DAPI (62248; Thermofisher) according to the kit manual. DAPI+ and EdU+ cells were counted using Fiji.

Microscope image acquisition
Images from fluorescently labeled HUVECs were acquired using a confocal A1 SIM microscope (Nikon)

equipped with a Plan-Apochromat 20×/0.8 NA Ph2 objective or with a 60x/1.4 plan apochromat objective; or using an Eclipse Ti2 inverted microscope (Nikon). Images were taken at room temperature using NIS Element software. Images of Retinas and Aortas were taken using a LFOV FLIM inverted confocal microscope (Nikon) equipped with a Plan-Apochromat 20×/0.8 NA Ph2 objective or with a Plan-Apochromat 60×/1.4 NA DIC objective. The microscope was equipped with a photon multiplier tube detector. Images were taken at room temperature using NIS element software (Nikon).

Flow-induced orientation analysis

Cell shape was quantified using a dedicated FIJI macro. Basically, VE-Cadherin staining was detected in order to segment the border of each endothelial cell. Based on this segmentation a skeleton was built and aspect ratio (major axis lenght by minor axis lenght, AR) as well as the angle between the flow direction and the main axis was determined for all entire ECs visible on the image. Flow index corresponding to the ratio of AR and the angle was calculated for each EC. Flow index thus integrates both the elongation and the alignment of endothelia cells: The higher the flow index is, the better the cell response to the flow. Based on the VE-cadherin staining, gaps in the endothelial monolayer were quantified manually, only gaps with an area above 100um were taken in account.

Cell junction activity analysis

ZO-1 intensity at the junctions was quantified using FIJI. Briefly, an enlarged mask from the VE-Cadherin segmentation previously described was generated and applied on the ZO-1 staining image, percentage of the ZO-1 staining in this area was extracted for each image. Actin cable formation was measured by the intensity of the phalloidin staining at the junctions using the same enlarged mask applied on the Actin staining image (FIJI). Both analyses were made automatically by FIJI with identical parameter for mask enlargement and threshold values. Claudin5 localization at junction was quantified using a mix of ECs expressing or not the shRNA targeting ARHGEF18. Using FIJI, Intensity plots for both Claudin5 and VE-cadherin staining were obtained by drawing a line of approximately 15um in between two cells.

Basal adhesion analysis

For micropatterning images, paxillin channel was thresholded and the focal adhesion length was quantified for each focal adhesion detected. The focal adhesions were then classified by size within each cell. Quantification was done blindly.

For shear stress exposed ECs, focal adhesion type was assessed qualitatively by classifying blindly (by 2 operators) the overall aspect of Paxillin staining in the cell. Cells with long, numerous and parallel focal adhesions were classified 1 and cells with short, few and disorganized focal adhesions were classified 0.

Statistical analysis

Statistical analysis was performed using GraphPad Prism software. For in vitro and in vivo experiments, when only 2 conditions were compared, a paired T-test or a Wilcoxon T-test were used depending on the distribution of the data. For multiple comparison an ordinary one-way ANOVA (data distribution was assumed to be normal) was used, followed by a Tukey test. Details of the statistical test used for each experiment can be found in the figure legends.

Bibliography

1. Ui-Tei, K. *et al.* Guidelines for the selection of highly effective siRNA sequences for mammalian and chick RNA interference. *Nucleic Acids Res.* **32**, 936–948 (2004).
2. Fellmann, C. *et al.* An optimized microRNA backbone for effective single-copy RNAi. *Cell Rep.* **5**, 1704–1713 (2013).
3. Guilluy, C., Dubash, A. D. & García-Mata, R. Analysis of RhoA and Rho GEF activity in whole cells and the cell nucleus. *Nat. Protoc.* **6**, 2050–2060 (2011).
4. Ingber, D. E. Cellular mechanotransduction: putting all the pieces together again. *FASEB J. Off. Publ. Fed. Am. Soc. Exp. Biol.* **20**, 811–827 (2006).
5. Ballermann, B. J., Dardik, A., Eng, E. & Liu, A. Shear stress and the endothelium. *Kidney Int. Suppl.* **67**, S100-108 (1998).
6. Hahn, C. & Schwartz, M. A. Mechanotransduction in vascular physiology and atherogenesis. *Nat. Rev. Mol. Cell Biol.* **10**, 53–62 (2009).
7. Wang, C., Baker, B. M., Chen, C. S. & Schwartz, M. A. Endothelial cell sensing of flow direction. *Arterioscler. Thromb. Vasc. Biol.* **33**, 2130–2136 (2013).
8. Givens, C. & Tzima, E. Endothelial Mechanosignaling: Does One Sensor Fit All? *Antioxid. Redox Signal.* **25**, 373–388 (2016).
9. Galie, P. A. *et al.* Fluid shear stress threshold regulates angiogenic sprouting. *Proc. Natl. Acad. Sci. U. S. A.* **111**, 7968–7973 (2014).
10. Franco, C. A. *et al.* Non-canonical Wnt signalling modulates the endothelial shear stress flow sensor in vascular remodelling. *eLife* **5**, e07727 (2016).
11. Daems, M., Peacock, H. M. & Jones, E. A. V. Fluid flow as a driver of embryonic morphogenesis. *Dev. Camb. Engl.* **147**, dev185579 (2020).
12. Lu, D. & Kassab, G. S. Role of shear stress and stretch in vascular mechanobiology. *J. R. Soc. Interface* **8**, 1379–1385 (2011).
13. Tzima, E. *et al.* A mechanosensory complex that mediates the endothelial cell response to fluid shear stress. *Nature* **437**, 426–431 (2005).
14. Chiu, J.-J. & Chien, S. Effects of disturbed flow on vascular endothelium: pathophysiological basis and clinical perspectives. *Physiol. Rev.* **91**, 327–387 (2011).
15. Chalouhi, N., Hoh, B. L. & Hasan, D. Review of cerebral aneurysm formation, growth, and rupture. *Stroke* **44**, 3613–3622 (2013).
16. Tzima, E. *et al.* Activation of Rac1 by shear stress in endothelial cells mediates both cytoskeletal reorganization and effects on gene expression. *EMBO J.* **21**, 6791–6800 (2002).
17. Pan, S. Molecular mechanisms responsible for the atheroprotective effects of laminar shear stress. *Antioxid. Redox Signal.* **11**, 1669–1682 (2009).
18. Hoger, J. H., Ilyin, V. I., Forsyth, S. & Hoger, A. Shear stress regulates the endothelial Kir2.1 ion channel. *Proc. Natl. Acad. Sci. U. S. A.* **99**, 7780–7785 (2002).
19. Vion, A.-C. *et al.* Primary cilia sensitize endothelial cells to BMP and prevent excessive vascular regression. *J. Cell Biol.* **217**, 1651–1665 (2018).
20. Van der Heiden, K. *et al.* Endothelial primary cilia in areas of disturbed flow are at the base of atherosclerosis. *Atherosclerosis* **196**, 542–550 (2008).
21. Goldfinger, L. E. *et al.* Localized alpha4 integrin phosphorylation directs shear stress-induced endothelial cell alignment. *Circ. Res.* **103**, 177–185 (2008).
22. Tzima, E. Role of small GTPases in endothelial cytoskeletal dynamics and the shear stress response. *Circ. Res.* **98**, 176–185 (2006).
23. Boon, R. A. *et al.* KLF2-induced actin shear fibers control both alignment to flow and JNK signaling in vascular endothelium. *Blood* **115**, 2533–2542 (2010).
24. Girard, P. R. & Nerem, R. M. Shear stress modulates endothelial cell morphology and F-actin organization through the regulation of focal adhesion-associated proteins. *J. Cell. Physiol.* **163**, 179–193 (1995).

25. Levesque, M. J. & Nerem, R. M. The elongation and orientation of cultured endothelial cells in response to shear stress. *J. Biomech. Eng.* **107**, 341–347 (1985).
26. Malek, A. M. & Izumo, S. Mechanism of endothelial cell shape change and cytoskeletal remodeling in response to fluid shear stress. *J. Cell Sci.* **109 (Pt 4)**, 713–726 (1996).
27. Wojciak-Stothard, B. & Ridley, A. J. Shear stress-induced endothelial cell polarization is mediated by Rho and Rac but not Cdc42 or PI 3-kinases. *J. Cell Biol.* **161**, 429–439 (2003).
28. Tzima, E., del Pozo, M. A., Shattil, S. J., Chien, S. & Schwartz, M. A. Activation of integrins in endothelial cells by fluid shear stress mediates Rho-dependent cytoskeletal alignment. *EMBO J.* **20**, 4639–4647 (2001).
29. Li, S. *et al.* Distinct roles for the small GTPases Cdc42 and Rho in endothelial responses to shear stress. *J. Clin. Invest.* **103**, 1141–1150 (1999).
30. Etienne-Manneville, S. & Hall, A. Rho GTPases in cell biology. *Nature* **420**, 629–635 (2002).
31. Rossman, K. L., Der, C. J. & Sondek, J. GEF means go: turning on RHO GTPases with guanine nucleotide-exchange factors. *Nat. Rev. Mol. Cell Biol.* **6**, 167–180 (2005).
32. Cook, D. R., Rossman, K. L. & Der, C. J. Rho guanine nucleotide exchange factors: regulators of Rho GTPase activity in development and disease. *Oncogene* **33**, 4021–4035 (2014).
33. Cheng, C. *et al.* Endothelial cell-specific FGD5 involvement in vascular pruning defines neovessel fate in mice. *Circulation* **125**, 3142–3158 (2012).
34. Liu, Y. *et al.* A novel pathway spatiotemporally activates Rac1 and redox signaling in response to fluid shear stress. *J. Cell Biol.* **201**, 863–873 (2013).
35. Kroon, J. *et al.* Flow-induced endothelial cell alignment requires the RhoGEF Trio as a scaffold protein to polarize active Rac1 distribution. *Mol. Biol. Cell* **28**, 1745–1753 (2017).
36. Polacheck, W. J. *et al.* A non-canonical Notch complex regulates adherens junctions and vascular barrier function. *Nature* **552**, 258–262 (2017).
37. Lessey-Morillon, E. C. *et al.* The RhoA guanine nucleotide exchange factor, LARG, mediates ICAM-1-dependent mechanotransduction in endothelial cells to stimulate transendothelial migration. *J. Immunol. Baltim. Md 1950* **192**, 3390–3398 (2014).
38. García-Mata, R. *et al.* Analysis of activated GAPs and GEFs in cell lysates. *Methods Enzymol.* **406**, 425–437 (2006).
39. Terry, S. J. *et al.* Spatially restricted activation of RhoA signalling at epithelial junctions by p114RhoGEF drives junction formation and morphogenesis. *Nat. Cell Biol.* **13**, 159–166 (2011).
40. Garrett, T. A., Van Buul, J. D. & Burridge, K. VEGF-induced Rac1 activation in endothelial cells is regulated by the guanine nucleotide exchange factor Vav2. *Exp. Cell Res.* **313**, 3285–3297 (2007).
41. Zaritsky, A. *et al.* Diverse roles of guanine nucleotide exchange factors in regulating collective cell migration. *J. Cell Biol.* **216**, 1543–1556 (2017).
42. Loie, E., Charrier, L. E., Sollier, K., Masson, J.-Y. & Laprise, P. CRB3A Controls the Morphology and Cohesion of Cancer Cells through Ehm2/p114RhoGEF-Dependent Signaling. *Mol. Cell. Biol.* **35**, 3423–3435 (2015).
43. Kim, M., M Shewan, A., Ewald, A. J., Werb, Z. & Mostov, K. E. p114RhoGEF governs cell motility and lumen formation during tubulogenesis through a ROCK-myosin-II pathway. *J. Cell Sci.* **128**, 4317–4327 (2015).
44. Rousseau, S. *et al.* Vascular endothelial growth factor (VEGF)-driven actin-based motility is mediated by VEGFR2 and requires concerted activation of stress-activated protein kinase 2 (SAPK2/p38) and geldanamycin-sensitive phosphorylation of focal adhesion kinase. *J. Biol. Chem.* **275**, 10661–10672 (2000).

45. Kanaji, N. *et al.* The p38 mitogen-activated protein kinases modulate endothelial cell survival and tissue repair. *Inflamm. Res. Off. J. Eur. Histamine Res. Soc. Al* **61**, 233–244 (2012).
46. Lee, J. *et al.* p85 beta-PIX is required for cell motility through phosphorylations of focal adhesion kinase and p38 MAP kinase. *Exp. Cell Res.* **307**, 315–328 (2005).
47. Ni, Y. *et al.* TNFα alters occludin and cerebral endothelial permeability: Role of p38MAPK. *PloS One* **12**, e0170346 (2017).
48. Langille, B. L. Morphologic responses of endothelium to shear stress: reorganization of the adherens junction. *Microcirc. N. Y. N 1994* **8**, 195–206 (2001).
49. Bahrami, S. & Drabløs, F. Gene regulation in the immediate-early response process. *Adv. Biol. Regul.* **62**, 37–49 (2016).
50. Kilian, L. S., Voran, J., Frank, D. & Rangrez, A. Y. RhoA: a dubious molecule in cardiac pathophysiology. *J. Biomed. Sci.* **28**, 33 (2021).
51. Sumpio, B. E. *et al.* MAPKs (ERK1/2, p38) and AKT can be phosphorylated by shear stress independently of platelet endothelial cell adhesion molecule-1 (CD31) in vascular endothelial cells. *J. Biol. Chem.* **280**, 11185–11191 (2005).
52. Azuma, N. *et al.* Role of p38 MAP kinase in endothelial cell alignment induced by fluid shear stress. *Am. J. Physiol. Heart Circ. Physiol.* **280**, H189-197 (2001).
53. Nakajima, H. & Tanoue, T. Lulu2 regulates the circumferential actomyosin tensile system in epithelial cells through p114RhoGEF. *J. Cell Biol.* **195**, 245–261 (2011).
54. Blomquist, A. *et al.* Identification and characterization of a novel Rho-specific guanine nucleotide exchange factor. *Biochem. J.* **352 Pt 2**, 319–325 (2000).
55. Herder, C. *et al.* ArhGEF18 regulates RhoA-Rock2 signaling to maintain neuro-epithelial apico-basal polarity and proliferation. *Dev. Camb. Engl.* **140**, 2787–2797 (2013).
56. Niu, J., Profirovic, J., Pan, H., Vaiskunaite, R. & Voyno-Yasenetskaya, T. G Protein betagamma subunits stimulate p114RhoGEF, a guanine nucleotide exchange factor for RhoA and Rac1: regulation of cell shape and reactive oxygen species production. *Circ. Res.* **93**, 848–856 (2003).
57. Lawson, C. D. & Burridge, K. The on-off relationship of Rho and Rac during integrin-mediated adhesion and cell migration. *Small GTPases* **5**, e27958 (2014).
58. Acharya, B. R. *et al.* A Mechanosensitive RhoA Pathway that Protects Epithelia against Acute Tensile Stress. *Dev. Cell* **47**, 439-452.e6 (2018).
59. Haas, A. J. *et al.* Interplay between Extracellular Matrix Stiffness and JAM-A Regulates Mechanical Load on ZO-1 and Tight Junction Assembly. *Cell Rep.* **32**, 107924 (2020).
60. Tornavaca, O. *et al.* ZO-1 controls endothelial adherens junctions, cell-cell tension, angiogenesis, and barrier formation. *J. Cell Biol.* **208**, 821–838 (2015).
61. Carvalho, J. R. *et al.* Non-canonical Wnt signaling regulates junctional mechanocoupling during angiogenic collective cell migration. *eLife* **8**, (2019).
62. Birukova, A. A., Shah, A. S., Tian, Y., Moldobaeva, N. & Birukov, K. G. Dual role of vinculin in barrier-disruptive and barrier-enhancing endothelial cell responses. *Cell. Signal.* **28**, 541–551 (2016).
63. Beal, R., Alonso-Carriazo Fernandez, A., Grammatopoulos, D. K., Matter, K. & Balda, M. S. ARHGEF18/p114RhoGEF Coordinates PKA/CREB Signaling and Actomyosin Remodeling to Promote Trophoblast Cell-Cell Fusion During Placenta Morphogenesis. *Front. Cell Dev. Biol.* **9**, 658006 (2021).

2.2 Complementary results

2.2.1. Effect of ARHGEF18 silencing on capillary formation and ECs permeability in static conditions

2.2.1.1 Materials and Methods

Network formation assay was performed on Matrigel (354230; Corning) in 96 well plate. HUVECs were plated on Matrigel at a density of 15000 cells per well in complete medium. The network formation was photographed at 20 min interval for 24 h using JuLi Stage microscope and was analyzed using Fiji macro (Angiogenesis analyzer).

For **permeability assay**, HUVECs expressing shRNAs were plated onto 0.4mm trans-well inserts (353095; Corning) coated with 0.2% gelatin (G1393; Sigma-Aldrich). Once the cells formed a confluent monolayer, fluorescent dextran dyes 3 kDa and 70 kDa (D3329, D1540 respectively; Thermofisher) were added to the top chamber at a concentration of 1mg/ml. Medium from lower chamber was collected at different time points. Fluorescence was measured using Varioskan LUX (Thermofisher; Excitation at 595nm and emission at 615nm for 3kDA dextran; Excitation at 570nm and emission at 590nm for 70kDa dextran).

2.2.1.2 Results

Matrigel assay showed that, compared to control ECs, ARHGEF18-deficient ECs formed a denser capillary network (Figure 25 a) with a decrease in mean mesh size (Figure 25 b) and an increase in number of connections (Figure 25 c). This observation suggests that the number of loops formed was increased without significant increase in tube length.

From dextran transwell permeability assay, we observed that ARHGEF18 silencing did not affect permeability as both smaller molecules (3kDa) and large (70kD) molecules dextran beads crossed the endothelial layer at the same speed in shNT, shA18.1 and shA18.4 expressing conditions (Figure 25 d). This suggests that the loss of ARHGEF18 expression did not affect ECs permeability.

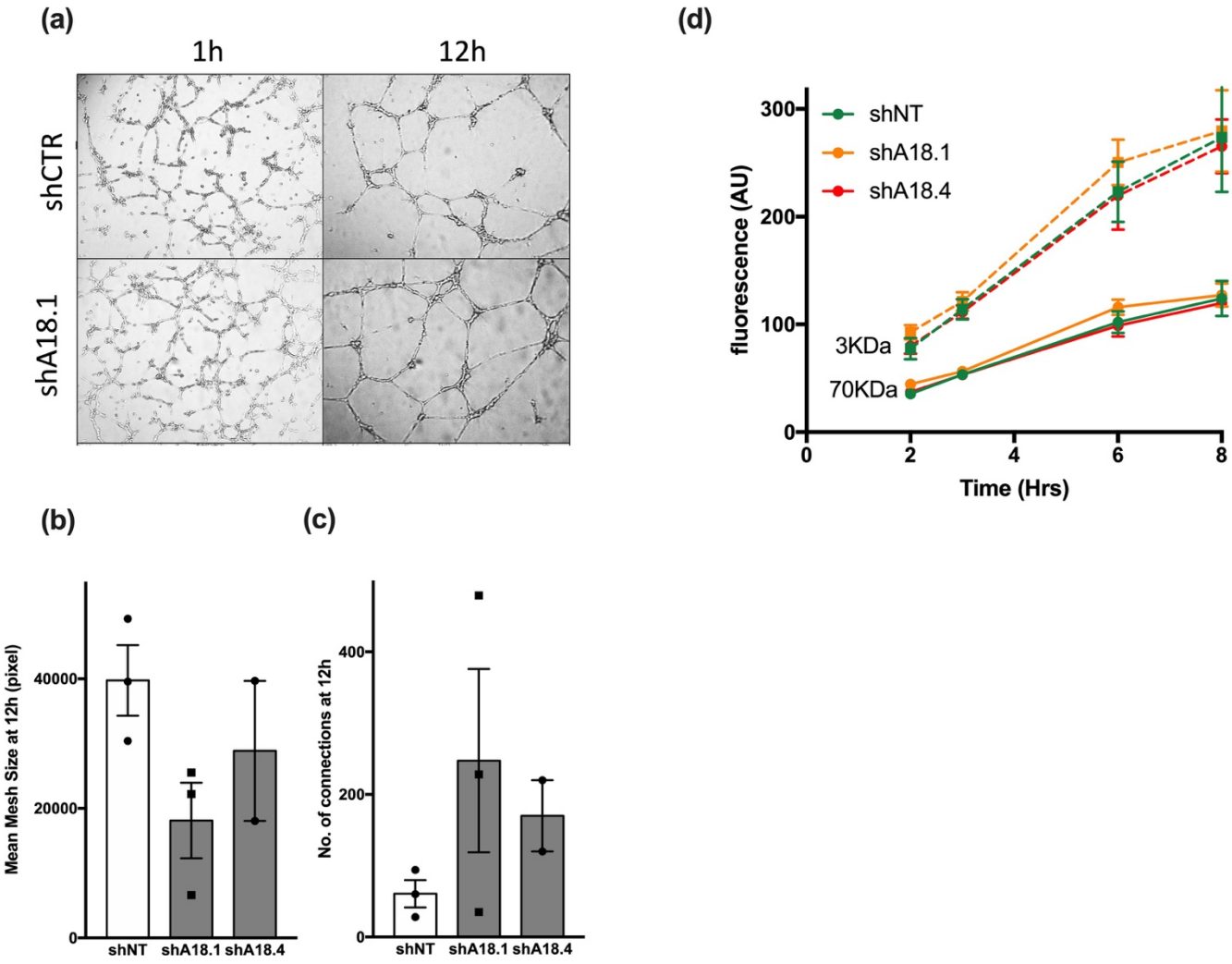

Figure 25: Effect of ARHGEF18 on HUVECs network forming capability and permeability

Representative image of matrigel network formation of HUVECs expressing either non-target (shCTR) or ARHGEF18 specific shRNAs (shA18.1) at 1 h and 12 h post-seeding(a), Quantification of mean mesh size (b) and number of connections in HUVECs expressing non-targeted(shNT) or ARHGEF18-targeted shRNAs (sh18.1 and shA18.4) (c). Permeability of control (shNT) and ARHGEF18 shRNA (shA18.1, shA18.4) expressing HUVEC monolayers on transwell membrane under static conditions (d). Permeability was assessed by the measurement of fluorescence of FITC-conjugated 3 kDa – and 70 kDa-dextrans in the lower chamber at different time-points after its addition to the upper chamber at to min. Data are expressed as mean+/-SEM.

2.2.2. Effect of ARHGEF18 silencing on RhoA and Rac1 activity under physiological shear stress

To determine if ARHGEF18 affects the activity of RhoA and Rac1, confluent monolayers of control and ARHGEF18-depleted ECs were subjected to physiological (16 dynes/cm^2) SS condition for 24 h, then lysed to measure RhoA and Rac1 activity pulldown

experiments using Rho-binding domain of rhotekin and PAK, respectively. were performed using GST-RBD and GST-PBD Sepharose beads. Western blot analysis showed a significant reduction in active RhoA and Rac1 in ARHGEF18-deficient ECs compared to controls (Figure 26). This suggest that ARHGEF18 modulate the activity of both RhoA and Rac1 in ECs under SS.

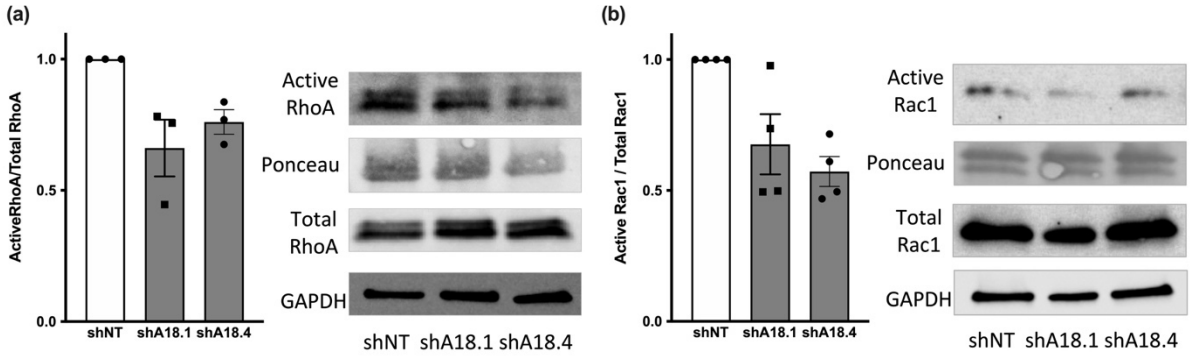

Figure 26: Effect of ARHGEF18 knockdown on RhoA and Rac1 activity under physiological shear stress conditions

Quantification and representative immunoblot of RhoA (a) Rac1 (b) and GAPDH in lysates of HUVECs expressing either non-targeting (shNT) or ARHGEF18 specific shRNAs (shA18.1, shA18.4) under physiological SS (16 dynes/cm^2) for 24 h. Data were expressed as mean+/-SEM.

2.2.3. Shear stress mediated ARHGEF18 activity at short time points

As observed before, pathological SS decreases the activity of ARHGEF18 at 24 h. However, *in-vitro*, SS activates small-GTPases and downstream signaling networks as early as 5 min (Iring et al., 2019; Shay-Salit et al., 2002; Wojciak-Stothard & Ridley, 2003). To analyze how SS modulate the ARHGEF18 activity at shorter time points, active GEF pulldown experiments using GST-RhoA^{G17A} were performed on HUVECs subjected to physiological (16 dynes/cm^2) and pathological shear stress (3.6 dynes/cm^2 and 36 dynes/cm^2) conditions for 0 min, 5 min, 30 min and 6 h. Although we were able to capture active ARHGEF18 at all time-points, we did not see any difference in the activity between physiological and pathological shear stress conditions (Figure 27).

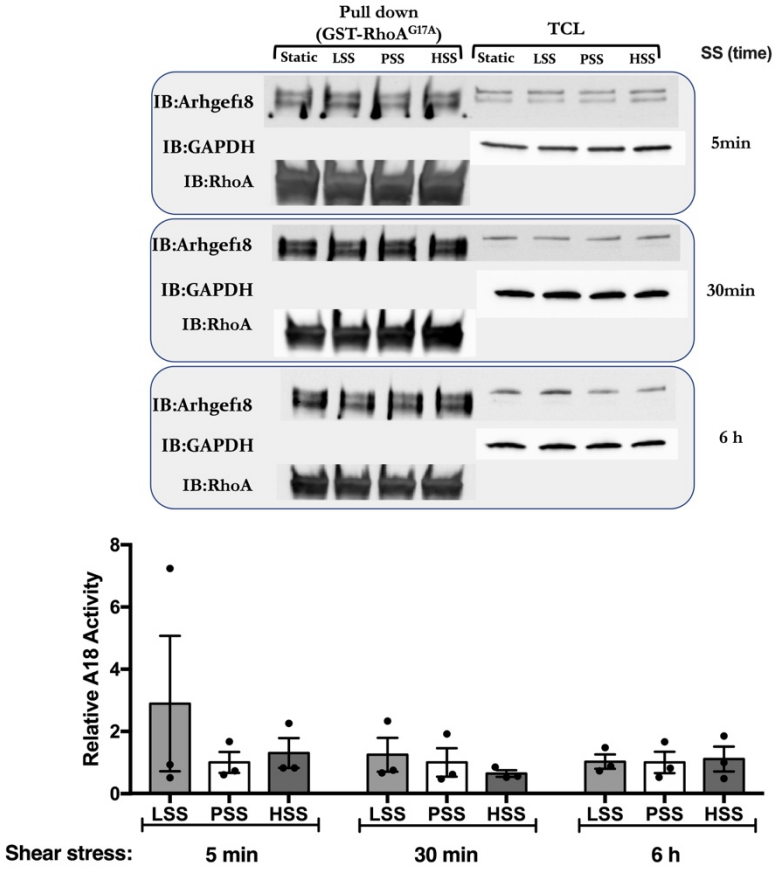

Figure 27: ARHGEF18 activity under various shear stress conditions at short time-points

Representative immunoblots of ARHGEF18, RhoA and GAPDH in GST-RhoA^{G17A} pulldown fractions and total cell lysates of HUVECs subjected to static, physiological SS (PSS) and pathological SS (LSS, HSS) for 5 min, 30 min and 6 h time points (top). Quantification of relative ARHGEF18 activity in HUVECs subjected LSS, PSS and HSS conditions for 5 min, 30 min and 6 h time points. Data were expressed as mean+/-SEM.

2.2.4. Effect of ARHGEF18 silencing on shear stress activated signaling networks at short time points

Although we did not observe any alterations in ARHGEF18 activity under SS conditions at short time points tested, ARHGEF18 was still active under such conditions and could mediate SS induced signaling mechanisms in ECs. To understand how ARHGEF18 affects SS activated signaling network at early time points, control and ARHGEF18-depleted ECs were subjected to physiological SS (36 dynes/cm² for 0 min, 5 min, 30 min), then lysed and western blot analysis was performed to study the alterations in previously known SS-mediated signaling mechanisms such as AKT, ERK, SRC, and p38. Of the signaling mechanisms tested, ARHGEF18 silencing did not affect the activation

of any tested signaling molecules at early timepoints 0 min and 5 min (Figure 28). However, at 30 min, we observed a tendency of decrease in SS induced p38 and paxillin phosphorylation in ARHGEF18 knockdown ECs compared to control cells (Figure 28).

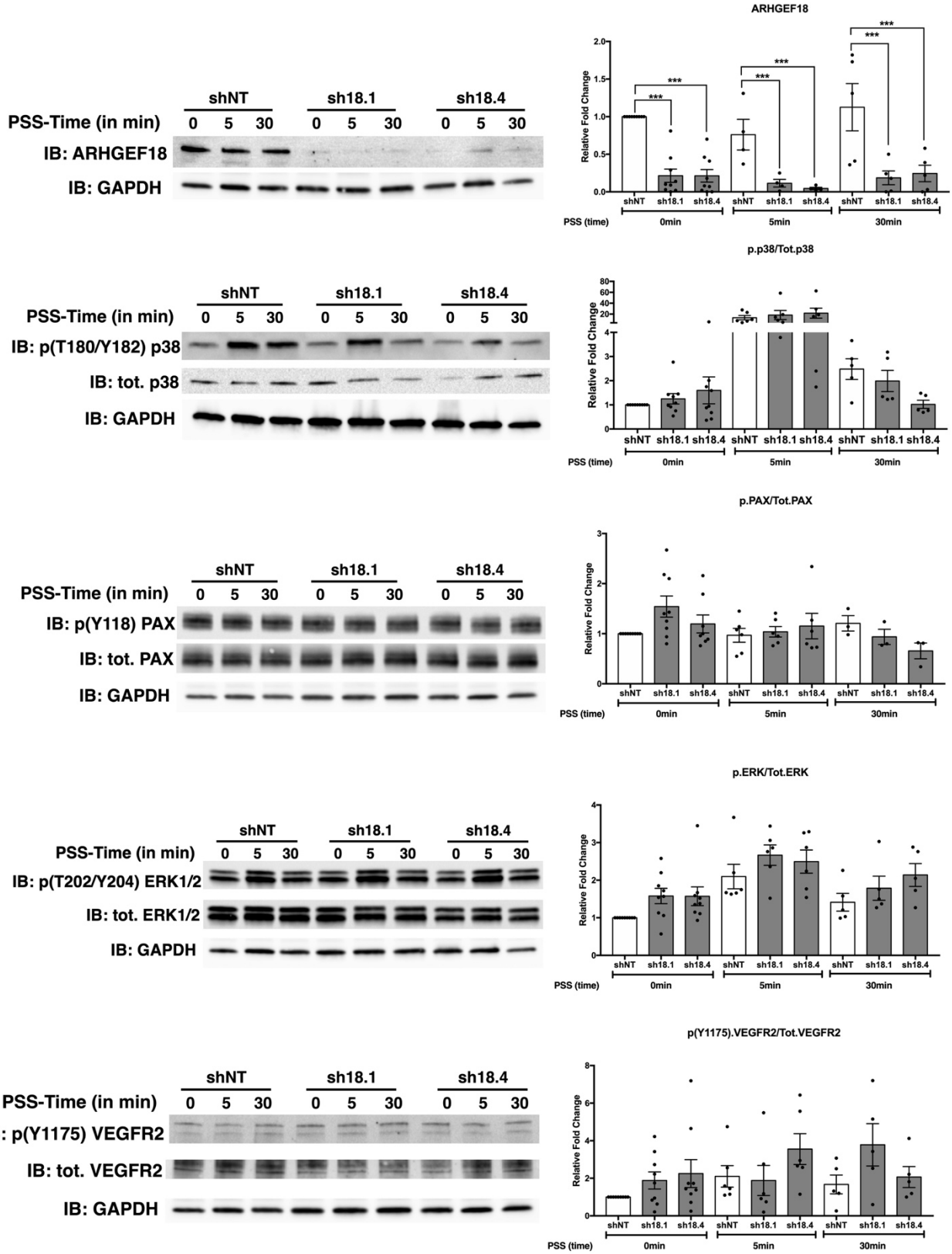

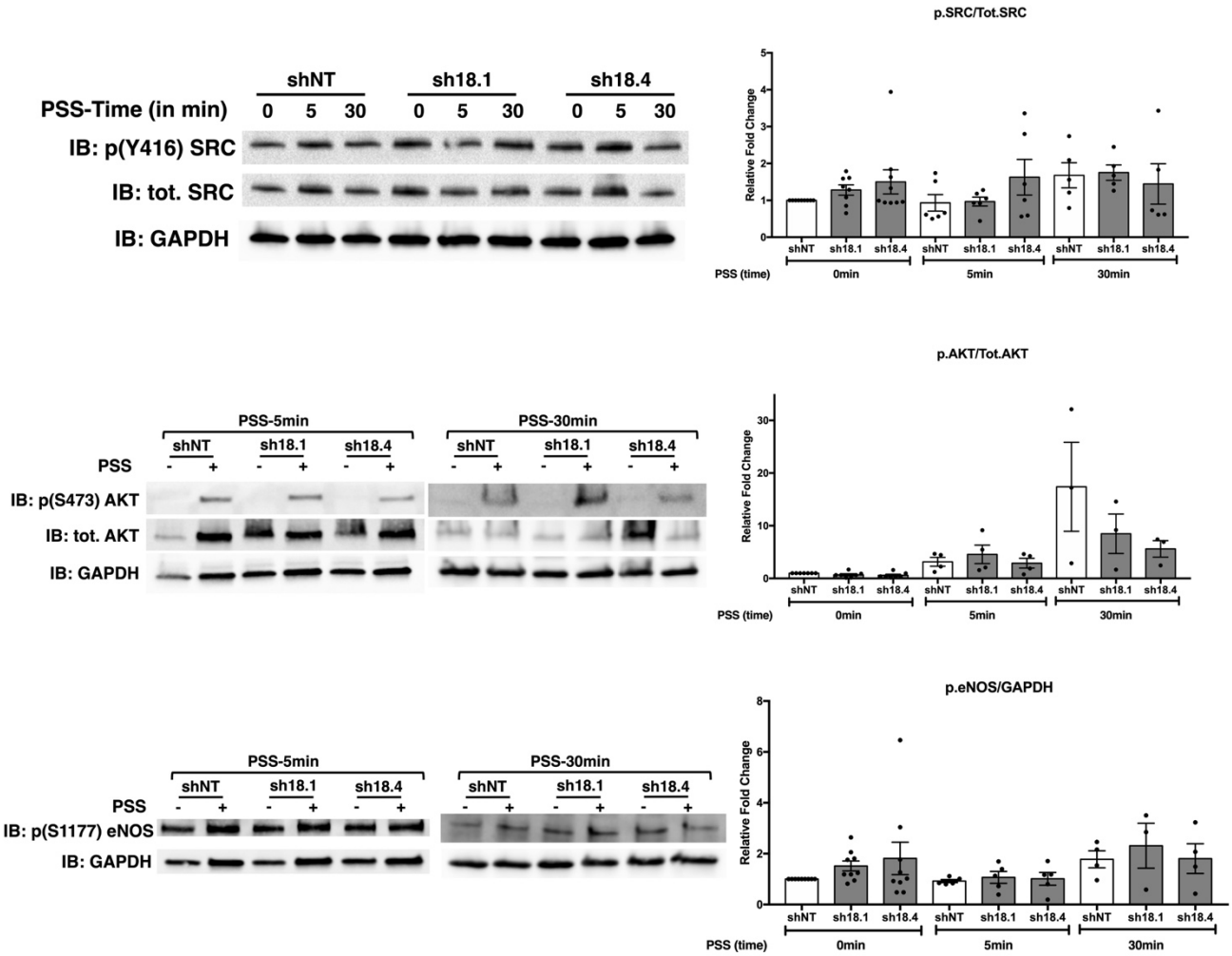

Figure 28: Effect of ARHGEF18 silencing on shear stress activation of ERK, SRC and VEGFR2 at short time points

*Representative immunoblots of ARHGEF18, phospho-p38, total-p38, phospho-paxillin, total-paxillin, phospho-ERK1/2, total-ERK1/2, phospho-VEGFR2, total-VEGFR2, phospho-SRC, total-SRC, phospho-AKT, total-AKT, phospho-eNOS and GAPDH in total cell lysates of HUVECs expressing either non-targeting (shNT) or ARHGEF18 specific shRNAs (shA18.1, shA18.4) under physiological SS (PSS) for 0 min 5 min and 30 min time points (left). Quantification of relative fold change of ARHGEF18, phospho-p38, phospho-paxillin, phospho-ERK1/2, phospho-VEGFR2, phospho-SRC, phospho-AKT and phospho-eNOS in expressing either non-targeting (shNT) or ARHGEF18 specific shRNAs (shA18.1, shA18.4) under physiological SS (PSS) for 0 min 5 min and 30 min time points (right). Data were expressed as mean+/-SEM. Statistical significance was calculated by 2way ANOVA followed by Tukey's multiple comparison test. *p<0.03, **<0.002, ***p<0.0002*

2.2.5. Role of ARHGEF18 in ECs inflammation

Altered SS and inflammation has been known to associate with various vascular pathologies (Cecchi et al., 2011; Sullivan et al., 2000). In addition, p38 signaling has been shown to be involved in vascular inflammation (Elkhawad et al., 2012). As our data suggested that ARHGEF18 regulates SS mediated p38 activation, we went on to

investigate the role of ARHGEF18 in EC inflammation under SS. For this purpose, we chose TNFα as an inflammatory stimulus, which has been shown to play crucial role in vascular inflammation (Brånén et al., 2004) as well as its ability to modulate p38 signaling (Mukaro et al., 2018). Confluent control and ARHGEF18-deficient ECs monolayers were subjected to physiological (16 dynes/cm^2) SS condition in the absence and presence of TNFα at a concentration of 2ng/ml for 24hrs. Knocking down of ARHGEF18 did not have much effect on TNFα-induced expression of cell adhesion molecules such as ICAM1 and VCAM1 transcripts. Interestingly, knocking down of ARHGEF18 resulted in a significant reduction in TNFα induced *PTGS2* (which encodes for COX2) transcript level (Figure 29 a). However, we failed to recapitulate the similar phenotype at the protein level (Figure 29 b). TNFα induced *PTGS2* transcript level is dampened by loss of ARHGEF18, indicating a possible pathway wherein ARHGEF18 acting downstream of TNFα in TNFα-*PTGS2* signaling axis. To understand whether TNFα affects ARHGEF18 activity, active GEF pull down experiments were performed using nucleotide free mutant of RhoA^{G17A}, on cell lysates obtained from ECs treated with TNFα under physiological shear stress for 10 min and 6 h. Although we did not see any change in the activity of ARHGEF18 in TNFα treated cell for 10min compared to control cells, at 6hr time point, we did observe a tendency of decrease in ARHGEF18 activity upon TNFα stimulation compared to control cells under physiological SS condition (Figure 30). These data suggest a role of ARHGEF18 in TNFα mediated *PTGS2* transcription.

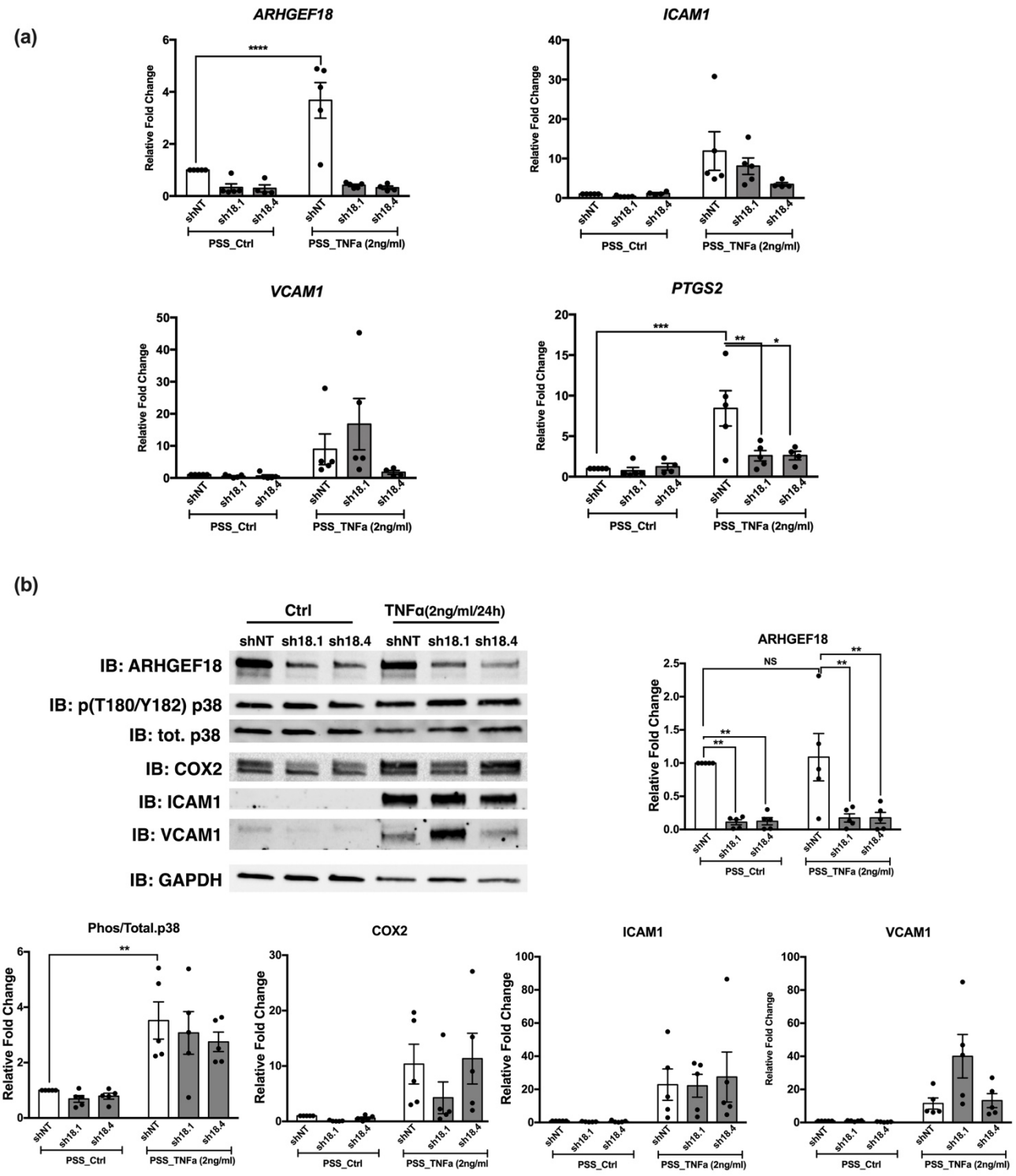

Figure 29: Effect of ARHGEF18 silencing on TNFα induced inflammatory molecules expression under shear stress

*Quantification of relative fold change in ARHGEF18, ICAM1, VCAM1, PTGS2 transcripts in HUVECs expressing either non-target (shNT) or ARHGEF18 specific shRNAs(sh18.1, sh18.4) subjected to physiological shear stress in the presence of TNFα (2ng/ml) for 24 h (a). Representative immunoblots and quantification of relative fold change in ARHGEF18, phospho-p38, COX2, ICAM1, VCAM1 from cell lysates of HUVECs expressing either non-target (shNT) or ARHGEF18 specific shRNAs (sh18.1, sh18.4) subjected to physiological shear stress in the presence of TNFα (2ng/ml) for 24 h (b). Quantification of relative fold change of ARHGEF18, phospho-p38, COX2, ICAM1, VCAM1blot. Data were expressed as mean+/-SEM. Statistical significance was calculated by 2way ANOVA followed by Tukey's or Sidak's multiple comparison test. *p<0.03, **<0.002, ***p<0.0002*

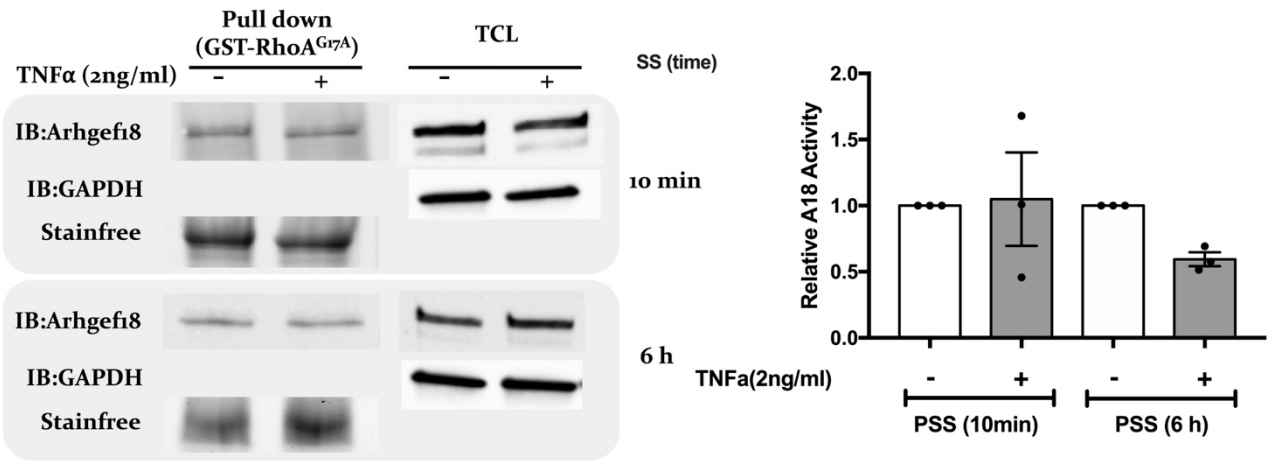

Figure 30: Effect of TNFα on ARHGEF18 activity under shear stress

Representative immunoblots of ARHGEF18 and GAPDH in GST-RhoA^{G17A} pulldown fractions and total cell lysates of HUVECs subjected physiological SS (PSS) in the presence of TNFα (2ng/ml) for 10 min and 6 h time points (left). Quantification of relative ARHGEF18 activity in HUVECs subjected physiological SS (PSS) in the presence of TNFα (2ng/ml) for 10 min and 6 h time points. Data were expressed as mean+/-SEM.

DISCUSSION

Small-GTPases are molecular switches that oscillates between active and inactive states which are tightly controlled by regulator molecules such as GEFs and GAPs. In various cell types, small-GTPases has been shown to regulate cytoskeletal organization and cellular functions such as migration, proliferation or permeability depending on external signals. In the vasculature, small-GTPases mediate ECs and VSMCs orientation, as well as contractile phenotype of VSMCs. In addition, they also regulate inflammatory and secretory phenotypes which are important for the physiological vascular response to the blood flow. Inability of vascular cells to respond to altered hemodynamics are one of the causative factors in many vascular diseases. In the same line, altered small-GTPase activation underlying vascular pathologies has been reported (Flentje et al., 2019), advocating for a mechanosensitivity for their regulator molecules. Using 3'SRP analysis screen, we have identified Arhgef18 in ECs which was important for RhoA and Rac1 activation, cell-cell junctional protein localization and SS mediated p38 signaling.

Identification of mechanosensitive GEF – a 3'SRP analysis

In 3'SRP analysis on *in-vitro* samples, only two GEFs (*ARHGEF18* and *ARHGEF40*) in ECs and one GEF (*Net-1*) in VSMCs were significantly regulated at the mRNA level by the mechanical force applied. Having very few GEFs with an expression associated with mechanical forces level was surprising but we ensured that this was not due to the inability of the experimental procedure to induce the appropriate mechanical stimulus, as we saw a change in the previously described mechano-regulated genes such as *KLF2* in ECs, and, *FN1, Col1A1 and IGF1* in VSMCs. As this analysis focused on RNA level, we cannot exclude that more GEF would have an expression at the protein level dependent on the mechanical forces applied. In fact, the transcription level of GEFs does not necessarily correlate with the protein level or the activity. Indeed, GEFs activity has been shown to be regulated through post-transcriptional modifications as well as through interacting protein partners (Fujishiro et al., 2008; Siesser et al., 2012). To have a full picture on GEFs status with changes in mechanical forces, an additional screening through active GEFs capture followed by mass-spectrometry analysis would help in identifying additional GEFs whose expression would not be altered by mechanical forces but their activity would. Interestingly, while *ARHGEF18* and *ARHGEF40* are expressed in most cell types, however we were unable to detect any change in the transcript level

in VSMCs *in-vitro* and in arteries *in-vivo*, indicating that the mechanosensitive expression of the GEFs is specific to endothelial cells. As arteries are mostly comprised of SMC, we were comforted by the identification of *Net-1 in-vivo* as a GEF with a significant transcript upregulation in SHR and SHR-SP mice compared to WKY mice.

Shear stress mediated expression and activity of *ARHGEF18*

In HUVECs, qRT-PCR analysis of *ARHGEF18* transcript confirmed the 3'SRP data and showed an inverse relationship to the SS applied. Interestingly, the activity of ARHGEF18 did not correlate with the RNA data and was decreased in both pathological SS conditions, low (3.6 dynes/cm^2) and high (36 dynes/cm^2), compared to physiological SS (16 dynes/cm^2). This could be due to dysfunctional signaling in ECs under pathological SS, which might downregulate endothelial protective ARHGEF18 activity. Moreover, at protein level, ARHGEF18 was more expressed in HUVECs subjected to pathological (low and high) SS compared to physiological SS condition. This discrepancy between activity and protein level might result from a compensatory mechanism that increases ARHGEF18 protein in response to the loss of its GEF activity. As the protein level is also different from the RNA level, this could not just "simply" go through modulation of the transcription. Several hypothesis can be considered, among them an increase in ARHGEF18 translation through mRNA caping mechanisms (Simpson et al., 2020) or a stabilization of ARHGEF18 by small heat-shock proteins (Collier & Benesch, 2020). In ECs under static and SS conditions, we demonstrated that ARHEF18 interacts with only RhoA but not with Rac1. On the other hand, we have observed a reduced activity of both RhoA and Rac1 in ARHGEF18 knockdown ECs under physiological SS. This was surprising as our experiments showed ARHGEF18 interaction with only RhoA and work done by Terry showed no effect on Rac1 activity upon ARHGEF18 knockdown. This could be explained by the RhoA and Rac1 signaling cross talk (Guilluy, Garcia-Mata, et al., 2011). One such cross talk has been described in 3T3 fibroblast cells, wherein RhoA effector mDia1 mediates Rac1 activation (Tsuji et al., 2002). Similar crosstalk between RhoA and Rac1 might exist in ECs under physiological SS which would be mediated through yet unknown effector of RhoA.

ARHGEF18 in ECs behavior and cell-cell junction

Arhgefi8-deficient ECs form denser networks without a significant alteration in total tube length compared to control ECs in an *in-vitro* matrigel assay. As no effect of ARHGEF18 silencing has been observed in ECs proliferation, increased network formation could be due to loss of planar cell polarity, similar to loss of apico-basal polarity and increased lumen formation in epithelial cells (Kim et al., 2015; Terry et al., 2011). Endothelial polarity, cytoskeletal organization and cell-cell communications are important for lumen formation (Lizama & Zovein, 2013), which is maintained by polarity proteins Par3&6, spatial activation of small-GTPases and cell junctions. In our experiments, decrease RhoA and Rac1 activity, altered cytoskeletal organization and defective cell junctions in ARHEF18 deficient ECs could affect the cells directionality, thereby resulting in multiple networks/lumen formation.

In our *in-vitro* experiment, ARHGEF18 silencing did not affect ECs permeability. This was surprising as ARHGEF18 silencing resulted in decreased junctional ZO1 and CLDN5, key molecules shown to be involved in tight junction stability and in permeability (Terry et al., 2011). One reason for not seeing any effect of ARHGEF18 silencing on permeability could be due to cell type specificity as CLDN5 controls barriers of HDMECs, but not HUVECs (Kluger et al., 2013). Moreover, CLDN5 knockout mice have a selective permeability for molecules of a size below 800 Daltons (Nitta et al., 2003) which is way less than the lowest molecular weight beads (3kDa) used in our experiments. On the other hand, junctional protein localization experiments were performed under SS conditions whereas permeability experiments were performed under static conditions. We have no evidence yet that ZO-1 and CLDN5 localization is also impaired under static condition. Furthermore, physiological SS is known to strengthen the cell-cell junctions compared to static condition. One possibility could be that under static condition permeability is not under the control of ARHGEF18 but the SS induced strengthening of the junction would be therefore a role of ARHGEF18 on barrier maintenance would be visible only under physiological SS. In this regard, localized activity of AHRGEF18 at junctions under physiological SS condition thanks to its physical interaction with ZO-1 and CLDN5 could play a role in the barrier maintenance.

ARHGEF18 in shear stress mediated signaling in ECs

Shear Stress modulates a wide variety of signaling networks. Of the signaling networks we analyzed, ARHGEF18 knockdown cells showed a dampened SS-induced p38 phosphorylation at 24 h timepoint. Eric *et al* (Gee et al., 2010), showed that inhibiting VEGFR2 impedes SS-mediated activation of p38 but not ERK1/2. On the other hand, Sumpio *et al* showed that knocking out PECAM1 did not alter SS-induced p38, AKT and ERK activation (Sumpio et al., 2005). Although, PECAM1 and VEGFR2 are a part of endothelial mechanosensory complex, it seems that SS-mediated p38 activation is mediated through VEGFR2 but not through PECAM1. Because both VEGFR2 and ARHGEF18 participate in p38 activity, one could hypothesize that ARHGEF18 could act downstream of VEGFR2. Future studies using combination of VEGFR2 inhibitors along with overexpression of GEF active ARHGEF18 mutants; and active GEF pulldown upon VEGF stimulation under SS would help to delineate if VEGFR2 could be the physical sensor upstream to ARHGEF18. Not to our surprise, SS-induced ARHGEF18 mediated p38 activation was dependent on GEF activity, as ECs overexpressing ARHGEF18^{Y260A} resulted in reduced SS-induced p38 phosphorylation similar to shRNA expressing cells. p38 MAPK signaling is important for multiple ECs functions such as cell alignment (Azuma et al., 2001) and inflammation (Schieven, 2005). In data from our lab and others, pharmacological inhibition of p38 resulted in mis-alignment of ECs to flow direction. This phenotype was similar to the one observed with shRNA and GEF mutant overexpressing cells. Taken together, these data strongly act in favor of an effect of ARHGEF18 on flow-mediated cytoskeletal arrangement through p38 signaling. Experimental approaches using GEF active mutants of ARHGEF18 in combination with p38 inhibitors could give us a clearer picture of the exact contribution of p38 to ARHGEF18-mediated flow-induced cell alignment. In addition to regulating the flow mediated cytoskeletal arrangement, p38 signaling also acts as a pro-inflammatory mediator. Using inflammatory cytokine such as TNFα, we showed that ARHGEF18 knockdown significantly downregulated the transcription of COX2 under physiological SS conditions while having no significant effect on ICAM1 or VCAM1 transcription level. This suggested the activation of a very specific pathway leading to only COX2 expression, and not other pro-inflammatory molecules, by ARHGEF18 following TNFα

stimulation. However, did not see any difference in COX2 expression at the protein level following TNFα stimulation between control and ARHGEF18 knockdown HUVECs. This could be due to a technical issue as serum was present in the medium during the SS experiments, which could activate multiple signaling mechanisms that ultimately leading to COX2 expression aside to TNFα. Another possibility could be the robust stability of COX2 protein. As the half-life of COX2 protein is longer compared to mRNA, 24h timepoint could be too short to see any such alterations in the COX2 protein in the absence of ARHGEF18. We also performed the experiments under physiological SS while in most of the vascular diseases, proinflammatory environment superimpose with altered hemodynamics. A second insult such as pathological SS might be therefore required to potentiate our observation. In this regard, low SS could be a right choice as it has been shown to induce COX2 expression in BAECs.

To conclude my research observations, we have identified ARHGEF18 in ECs as a mechanosensitive GEF whose expression is altered and activity is reduced under pathological shear stress conditions. ARHGEF18 activity is essential for ECs alignment to flow and may have a protective role in pathological shear stress induced EC inflammation.

Despite all of the information gathered from our *in-vitro* cell experiments, it only gives us a presumption on ARHGEF18 function *in-vivo*. For instance, as our *in-vitro* data suggests the involvement of ARHGEF18 in flow induced cytoskeletal organization, non-alignment of ECs in the region experiencing turbulent flow *in-vivo* may be due to minimal ARHGEF18 activity. Such minimal ARHGEF18 activity may not be sufficient to keep turbulent flow driven pathological signaling at check, and in long term this could result in dysfunctional endothelium and development of vascular diseases such as atherosclerosis. Although studying GEF activity in animal models is difficult, taking advantage of FRET based sensors previously used to study small GTPases activation (Wakayama et al., 2015; Yoo et al., 2010) could also be used to study the local activity of ARHGEF18 in an indirect way in an appropriate animal model such as the zebrafish. Recently, work done by Maria S. Balda's group showed that endothelial specific deletion of *ARHGEF18* using Tie2-Cre did not lead to embryonic death, which could infer an EC

dysfunction without drastic effect on the physiological function. This should be taken into account with caution, as deletion of ARHGEF18 at early stages of development could be compensated by other. More importantly, Maria S. Balda's group did not make any informative study on the effect of endothelial specific knockout of *ARHGEF18* in vascular network formation *in-vivo* as well as vascular function at adulthood.

Taken all of this into consideration, *in-vivo,* the effect of lack of ARHGEF18 in ECs may be subtle under physiological conditions and could require long time such as ageing result into vascular dysfunction and diseases. Lack of ARHGEF18 might also appeared only in a challenged environment such as hypertension, high fat diet or exacerbated pathological SS conditions. So far, we were the only group studied the role of ARHGEF18 under SS. We showed that ARHGEF18 activity was reduced under pathological shear stress conditions and therefore we hypothesize that ARHGEF18 might play an important role in vascular pathologies such as atherosclerosis and intracranial aneurysm wherein abnormal blood flow plays a crucial role.

Considering the *in-vitro* data, we could hypothesize that compromised ARHGEF18 activity at the sites of vasculature (aortic arch and vascular bifurcations) experiencing disturbed/altered SS could lead to localized vascular cell dysfunction, and maybe local increase in vascular permeability, and could result in vascular diseases in long term. Atherosclerosis and intracranial aneurysm animal models could be used to study ARHGEF18 activity in support of this hypothesis. Overexpression of ARHGEF18 in ECs resulted in mis-localization of ZO1 and CLDN5 into cytoplasm and we showed by co-immunoprecipitation a physical interaction between ARHGEF18 and ZO1/CLDN5. This suggests that ARHGEF18 could act as a structural component of tight junction, independent of its GEF activity. Such GEF independent effect of ARHGEF18 on tight junction proteins could further compromise vascular barrier properties and could result in immune cell extravasation thereby promoting the progression of vascular diseases such as atherosclerosis.

The remaining identified and uncharacterized GEFs such as NET1 and ARHGEF40 could also play important role in vascular cell physiology. Not chosen to be studied and little information available, *ARHGEF40* expression pattern is interesting as its transcript levels represents exactly opposite to *ARHGEF18* levels under shear stress conditions

tested. Like ARHGEEF18, ARHGEF40 has also been shown to be a RhoA specific GEF. It would be interesting to find out the effect of SS on ARHGEF40 and its involvement in SS mediated cytoskeletal organization and ECs physiology.

Although unpublished data from our lab showed no vascular defects in NET1 null mice (systemic vasculature), presence of high transcript number in cerebral arteries compared to mesenteric arteries could suggest a specific role of this GEF in the brain vasculature which have not been investigated. This function may not play crucial role during normal development and homeostasis, but may have important role in altered shear stress mediated vascular pathologies that are specific for brain such as cerebral aneurysms.

Understanding, how the expression and activity of GEFs in general or ARHGEF18 per se at the site of vascular lesions or malformations would help us to design therapeutic strategies to combat vascular diseases such as atherosclerosis and intracranial aneurysm.

REFERENCES

Abo, A., Boyhan, A., West, I., Thrasher, A. J., & Segal, A. W. (1992). Reconstitution of neutrophil NADPH oxidase activity in the cell-free system by four components: p67-phox, p47-phox, p21rac1, and cytochrome b-245. *Journal of Biological Chemistry*, *267*(24), 16767–16770. https://doi.org/10.1016/s0021-9258(18)41846-7

Aboualaiwi, W. A., Takahashi, M., Mell, B. R., Jones, T. J., Ratnam, S., Kolb, R. J., & Nauli, S. M. (2009). Ciliary polycystin-2 is a mechanosensitive calcium channel involved in nitric oxide signaling cascades. *Circulation Research*, *104*(7), 860–869. https://doi.org/10.1161/CIRCRESAHA.108.192765

Acharya, B. R., Nestor-Bergmann, A., Liang, X., Gupta, S., Duszyc, K., Gauquelin, E., Gomez, G. A., Budnar, S., Marcq, P., Jensen, O. E., Bryant, Z., & Yap, A. S. (2018). A Mechanosensitive RhoA Pathway that Protects Epithelia against Acute Tensile Stress. *Developmental Cell*, *47*(4), 439-452.e6. https://doi.org/10.1016/j.devcel.2018.09.016

Adam, R. M., Roth, J. A., Cheng, H. L., Rice, D. C., Khoury, J., Bauer, S. B., Peters, C. A., & Freeman, M. R. (2003). Signaling through P13K/AKT mediates stretch and PDGF-BBdependent DNA synthesis in bladder smooth muscle cells. *Journal of Urology*, *169*(6), 2388–2393. https://doi.org/10.1097/01.ju.0000063980.99368.35

Adams, R. H., & Alitalo, K. (2007). Molecular regulation of angiogenesis and lymphangiogenesis. *Nature Reviews Molecular Cell Biology*, *8*(6), 464–478. https://doi.org/10.1038/nrm2183

Albarrán-Juárez, J., Iring, A., Wang, S. P., Joseph, S., Grimm, M., Strilic, B., Wettschureck, N., Althoff, T. F., & Offermanns, S. (2018). Piezo1 and Gq/G11 promote endothelial inflammation depending on flow pattern and integrin activation. *Journal of Experimental Medicine*, *215*(10), 2655–2672. https://doi.org/10.1084/JEM.20180483

Alberts, A. S., & Treisman, R. (1998). Activation of RhoA and SAPK/JNK signalling pathways by the RhoA-specific exchange factor mNET1. *EMBO Journal*, *17*(14), 4075–4085. https://doi.org/10.1093/emboj/17.14.4075

Anderson, R. G. W. (1998). The caveolae membrane system. *Annual Review of Biochemistry*, *67*, 199–225. https://doi.org/10.1146/annurev.biochem.67.1.199

Aoki, T., Frosen, J., Fukuda, M., Bando, K., Shioi, G., Tsuji, K., Ollikainen, E., Nozaki, K., Laakkonen, J., & Narumiya, S. (2017). Prostaglandin E2-EP2-NF-κB signaling in macrophages as a potential therapeutic target for intracranial aneurysms. *Science Signaling*, *10*(465), 1–18. https://doi.org/10.1126/scisignal.aah6037

Aoki, T., Nishimura, M., Kataoka, H., Ishibashi, R., Nozaki, K., & Miyamoto, S. (2011). Complementary inhibition of cerebral aneurysm formation by eNOS and nNOS. *Laboratory Investigation*, *91*(4), 619–626. https://doi.org/10.1038/labinvest.2010.204

Arno, G., Carss, K. J., Hull, S., Zihni, C., Robson, A. G., Fiorentino, A., Black, G., Hall, G., Ingram, S., Gillespie, R., Manson, F., Sergouniotis, P., Inglehearn, C., Toomes, C., Ali, M., McKibbin, M., Poulter, J., Khan, K., Lord, E., … Yu, P. (2017). Biallelic Mutation of ARHGEF18, Involved in the Determination of Epithelial Apicobasal Polarity, Causes Adult-Onset Retinal Degeneration. *American Journal of Human Genetics*, *100*(2), 334–342. https://doi.org/10.1016/j.ajhg.2016.12.014

Arnold, W. P., Mittal, C. K., Katsuki, S., & Murad, F. (1977). Nitric oxide activates guanylate cyclase and increases guanosine 3':5'-cyclic monophosphate levels in various tissue preparations. *Proceedings of the National Academy of Sciences of the United States of America*, *74*(8), 3203–3207. https://doi.org/10.1073/pnas.74.8.3203

Ashraf, J. V., & Zen, A. A. H. (2021). Role of vascular smooth muscle cell phenotype switching in arteriogenesis. *International Journal of Molecular Sciences*, *22*(19). https://doi.org/10.3390/ijms221910585

Aspenström, P., Fransson, Å., & Saras, J. (2004). Rho GTPases have diverse effects on the organization of the actin filament system. *Biochemical Journal*, *377*(2), 327–337. https://doi.org/10.1042/BJ20031041

Astrof, S., & Hynes, R. O. (2009). Fibronectins in vascular morphogenesis. *Angiogenesis*, *12*(2), 165–175. https://doi.org/10.1007/s10456-009-9136-6

Awolesi, M. A., Sessa, W. C., & Sumpio, B. E. (1995). Cyclic strain upregulates nitric oxide synthase in cultured bovine aortic endothelial cells. *Journal of Clinical Investigation*, *96*(3), 1449–1454. https://doi.org/10.1172/JCI118181

Ayajiki, K., Kindermann, M., Hecker, M., Fleming, I., & Busse, R. (1996). *Intracellular pH and Tyrosine Phosphorylation but Not Calcium Determine Shear Stress-Induced Nitric Oxide Production in Native Endothelial Cells*. 750–758.

Azuma, N., Akasaka, N., Kito, H., Ikeda, M., Gahtan, V., Sasajima, T., & Sumpio, B. E. (2001). Role of p38 MAP kinase in endothelial cell alignment induced by fluid shear stress. *American Journal of Physiology - Heart and Circulatory Physiology*, *280*(1 49-1), 189–197. https://doi.org/10.1152/ajpheart.2001.280.1.h189

Baeriswyl, D. C., Prionisti, I., Peach, T., Tsolkas, G., Chooi, K. Y., Vardakis, J., Morel, S., Diagbouga, M. R., Bijlenga, P., Cuhlmann, S., Evans, P., Kwak, B. R., Ventikos, Y., & Krams, R. (2019). Disturbed flow induces a sustained, stochastic NF-κB activation which may support intracranial aneurysm growth in vivo. *Scientific Reports*, *9*(1), 1–14. https://doi.org/10.1038/s41598-019-40959-y

Baeyens, N., Bandyopadhyay, C., Coon, B. G., Yun, S., & Schwartz, M. A. (2016). Endothelial fluid

shear stress sensing in vascular health and disease. In *Journal of Clinical Investigation* (Vol. 126, Issue 3, pp. 821–828). American Society for Clinical Investigation. https://doi.org/10.1172/JCI83083

Baeyens, N., Nicoli, S., Coon, B. G., Ross, T. D., Van Den Dries, K., Han, J., Lauridsen, H. M., Mejean, C. O., Eichmann, A., Thomas, J. L., Humphrey, J. D., & Schwartz, M. A. (2015). Vascular remodeling is governed by a vegfr3-dependent fluid shear stress set point. *ELife*, *2015*(4), 1–35. https://doi.org/10.7554/eLife.04645

Balaban, N. Q., Schwarz, U. S., Riveline, D., Goichberg, P., Tzur, G., Sabanay, I., Mahalu, D., Safran, S., Bershadsky, A., Addadi, L., & Geiger, B. (2001). Force and focal adhesion assembly: a close relationship studied using elastic micropatterned substrates. *Nature*.

Baratchi, S., Khoshmanesh, K., Woodman, O. L., Potocnik, S., Peter, K., & McIntyre, P. (2017). Molecular Sensors of Blood Flow in Endothelial Cells. In *Trends in Molecular Medicine* (Vol. 23, Issue 9, pp. 850–868). Elsevier Ltd. https://doi.org/10.1016/j.molmed.2017.07.007

Bard, L., Boscher, C., Lambert, M., Mège, R. M., Choquet, D., & Thoumine, O. (2008). A molecular clutch between the actin flow and N-cadherin adhesions drives growth cone migration. *Journal of Neuroscience*, *28*(23), 5879–5890. https://doi.org/10.1523/JNEUROSCI.5331-07.2008

Barreiro, O., Yáñez-Mó, M., Serrador, J. M., Montoya, M. C., Vicente-Manzanares, M., Tejedor, R., Furthmayr, H., & Sánchez-Madrid, F. (2002). Dynamic interaction of VCAM-1 and ICAM-1 with moesin and ezrin in a novel endothelial docking structure for adherent leukocytes. *Journal of Cell Biology*, *157*(7), 1233–1245. https://doi.org/10.1083/jcb.200112126

Barry, D. M., Xu, K., Meadows, S. M., Zheng, Y., Norden, P. R., Davis, G. E., & Cleaver, O. (2015). Cdc42 is required for cytoskeletal support of endothelial cell adhesion during blood vessel formation in mice. *Development (Cambridge)*, *142*(17), 3058–3070. https://doi.org/10.1242/dev.125260

Beal, R., Alonso-Carriazo Fernandez, A., Grammatopoulos, D. K., Matter, K., & Balda, M. S. (2021). ARHGEF18/p114RhoGEF Coordinates PKA/CREB Signaling and Actomyosin Remodeling to Promote Trophoblast Cell-Cell Fusion During Placenta Morphogenesis. *Frontiers in Cell and Developmental Biology*, *9*. https://doi.org/10.3389/fcell.2021.658006

Bellanger, J. M., Lazaro, J. B., Diriong, S., Fernandez, A., Lamb, N., & Debant, A. (1998). The two guanine nucleotide exchange factor domains of Trio link the Rac1 and the RhoA pathways in vivo. *Oncogene*, *16*(2), 147–152. https://doi.org/10.1038/sj.onc.1201532

Bennett, M. R., Sinha, S., & Owens, G. K. (2016). Vascular Smooth Muscle Cells in Atherosclerosis. *Circulation Research*, *118*(4), 692–702.

https://doi.org/10.1161/CIRCRESAHA.115.306361

Billottet, C., Rottiers, P., Tatin, F., Varon, C., Reuzeau, E., Maître, J. L., Saltel, F., Moreau, V., & Génot, E. (2008). Regulatory signals for endothelial podosome formation. *European Journal of Cell Biology*, *87*(8–9), 543–554. https://doi.org/10.1016/j.ejcb.2008.02.006

Binnig, G., Quate' ', C. F., Gi, E. L., & Gerber, C. (n.d.). *Atomic Force Microscope*.

Birkenfeld, J., Nalbant, P., Yoon, S. H., & Bokoch, G. M. (2008). Cellular functions of GEF-H1, a microtubule-regulated Rho-GEF: is altered GEF-H1 activity a crucial determinant of disease pathogenesis? In *Trends in Cell Biology* (Vol. 18, Issue 5, pp. 210–219). https://doi.org/10.1016/j.tcb.2008.02.006

Birukov, K. G., Shirinsky, V. P., Stepanova, O. V., Tkachuk, V. A., Hahn, A. W. A., Resink, T. J., & Smirnov, V. N. (1995). Stretch affects phenotype and proliferation of vascular smooth muscle cells. *Molecular and Cellular Biochemistry*, *144*(2), 131–139. https://doi.org/10.1007/BF00944392

Birukova, A. A., Adyshev, D., Gorshkov, B., Bokoch, G. M., Birukov, K. G., & Verin, A. D. (2006). GEF-H1 is involved in agonist-induced human pulmonary endothelial barrier dysfunction. *American Journal of Physiology - Lung Cellular and Molecular Physiology*, *290*(3), 540–548. https://doi.org/10.1152/ajplung.00259.2005

Birukova, A. A., Fu, P., Xing, J., Yakubov, B., Cokic, I., & Birukov, K. G. (2010). Mechanotransduction by GEF-H1 as a novel mechanism of ventilator-induced vascular endothelial permeability. *American Journal of Physiology - Lung Cellular and Molecular Physiology*, *298*(6). https://doi.org/10.1152/ajplung.00263.2009

Bishop, A. L., & Hall, A. (2000). Rho GTPases and their effector proteins. *Biochemical Journal*, *348*(2), 241–255. https://doi.org/10.1042/0264-6021:3480241

Blomquist, A., Schwo $ Rer, G., Schablowski, H., Psoma, A., Lehnen, M., Jakobs, K. H., & Ru $ Menapp, U. (2000). Identification and characterization of a novel Rho-specific guanine nucleotide exchange factor. In *Biochem. J* (Vol. 352).

Boo, Y. C., & Jo, H. (2003). Flow-dependent regulation of endothelial nitric oxide synthase: Role of protein kinases. *American Journal of Physiology - Cell Physiology*, *285*(3 54-3). https://doi.org/10.1152/ajpcell.00122.2003

Boo, Y. C., Sorescu, G., Boyd, N., Shiojima, I., Walsh, K., Du, J., & Jo, H. (2002). Shear stress stimulates phosphorylation of endothelial nitric-oxide synthase at Ser 1179 by Akt-independent mechanisms. Role of protein kinase A. *Journal of Biological Chemistry*, *277*(5), 3388–3396. https://doi.org/10.1074/jbc.M108789200

Boon, L. M., Mulliken, J. B., & Vikkula, M. (2005). RASA1: Variable phenotype with capillary and

arteriovenous malformations. *Current Opinion in Genetics and Development*, *15*(3 SPEC. ISS.), 265–269. https://doi.org/10.1016/j.gde.2005.03.004

Boyd, N. L., Park, H., Yi, H., Boo, Y. C., Sorescu, G. P., Sykes, M., & Jo, H. (2003). Chronic shear induces caveolae formation and alters ERK and Akt responses in endothelial cells. *American Journal of Physiology - Heart and Circulatory Physiology*, *285*(3 54-3), 1113–1122. https://doi.org/10.1152/ajpheart.00302.2003

Brånén, L., Hovgaard, L., Nitulescu, M., Bengtsson, E., Nilsson, J., & Jovinge, S. (2004). Inhibition of tumor necrosis factor-α reduces atherosclerosis in apolipoprotein E knockout mice. *Arteriosclerosis, Thrombosis, and Vascular Biology*, *24*(11), 2137–2142. https://doi.org/10.1161/01.ATV.0000143933.20616.1b

Bretón-Romero, R., González De Orduña, C., Romero, N., Sánchez-Gómez, F. J., De Álvaro, C., Porras, A., Rodríguez-Pascual, F., Laranjinha, J., Radi, R., & Lamas, S. (2012). Critical role of hydrogen peroxide signaling in the sequential activation of p38 MAPK and eNOS in laminar shear stress. *Free Radical Biology and Medicine*, *52*(6), 1093–1100. https://doi.org/10.1016/j.freeradbiomed.2011.12.026

Bridges, E., Sheldon, H., Kleibeuker, E., Ramberger, E., Zois, C., Barnard, A., Harjes, U., Li, J. L., Masiero, M., MacLaren, R., & Harris, A. (2020). RHOQ is induced by DLL4 and regulates angiogenesis by determining the intracellular route of the Notch intracellular domain. *Angiogenesis*, *23*(3), 493–513. https://doi.org/10.1007/s10456-020-09726-w

Burridge, K. (2017). Focal adhesions: a personal perspective on a half century of progress. *FEBS Journal*, *284*(20), 3355–3361. https://doi.org/10.1111/febs.14195

Busse, R., & Mülsch, A. (1990). Calcium-dependent nitric oxide synthesis in endothelial cytosol is mediated by calmodulin. *FEBS Letters*, *265*(1–2), 133–136. https://doi.org/10.1016/0014-5793(90)80902-U

Camasão, D. B., & Mantovani, D. (2021). The mechanical characterization of blood vessels and their substitutes in the continuous quest for physiological-relevant performances. A critical review. *Materials Today Bio*, *10*(February). https://doi.org/10.1016/j.mtbio.2021.100106

Campinho, P., Vilfan, A., & Vermot, J. (2020). Blood Flow Forces in Shaping the Vascular System: A Focus on Endothelial Cell Behavior. In *Frontiers in Physiology* (Vol. 11). Frontiers Media S.A. https://doi.org/10.3389/fphys.2020.00552

Carbone, M. L., Brégeon, J., Devos, N., Chadeuf, G., Blanchard, A., Azizi, M., Pacaud, P., Jeunemaître, X., & Loirand, G. (2015). Angiotensin II Activates the RhoA Exchange Factor Arhgef1 in Humans. *Hypertension*, *65*(6), 1273–1278.

https://doi.org/10.1161/HYPERTENSIONAHA.114.05065

Carmeliet, P., & Jain, R. K. (2000). Angiogenesis in cancer and other diseases. *Nature*, *407*(6801), 249–257. https://doi.org/10.1038/35025220

Carvajal, J. A., Germain, A. M., Huidobro-Toro, J. P., & Weiner, C. P. (2000). Molecular mechanism of cGMP-mediated smooth muscle relaxation. *Journal of Cellular Physiology*, *184*(3), 409–420. https://doi.org/10.1002/1097-4652(200009)184:3<409::AID-JCP16>3.0.CO;2-K

Castro, M., Laviña, B., Ando, K., Álvarez-Aznar, A., Abu Taha, A., Brakebusch, C., Dejana, E., Betsholtz, C., & Gaengel, K. (2019). CDC42 Deletion Elicits Cerebral Vascular Malformations via Increased MEKK3-Dependent KLF4 Expression. *Circulation Research*, *124*(8), 1240–1252. https://doi.org/10.1161/CIRCRESAHA.118.314300

Cecchi, E., Giglioli, C., Valente, S., Lazzeri, C., Gensini, G. F., Abbate, R., & Mannini, L. (2011). Role of hemodynamic shear stress in cardiovascular disease. *Atherosclerosis*, *214*(2), 249–256. https://doi.org/10.1016/j.atherosclerosis.2010.09.008

Chachisvilis, M., Zhang, Y. L., & Frangos, J. A. (2006). G protein-coupled receptors sense fluid shear stress in endothelial cells. *Proceedings of the National Academy of Sciences of the United States of America*, *103*(42), 15463–15468. https://doi.org/10.1073/pnas.0607224103

Charpentier, E., Cornec, M., Dumont, S., Meistermann, D., Bordron, P., David, L., Redon, R., Bonnaud, S., & Bihoué, A. (2021). 3' RNA sequencing for robust and low-cost gene expression profiling. *Research Square*, 1–26. https://europepmc.org/article/ppr/ppr275255

Chen, K. Den, Li, Y. S., Kim, M., Li, S., Yuan, S., Chien, S., & Shyy, J. Y. J. (1999). Mechanotransduction in response to shear stress. Roles of receptor tyrosine kinases, integrins, and Shc. *Journal of Biological Chemistry*, *274*(26), 18393–18400. https://doi.org/10.1074/jbc.274.26.18393

Chen, Ji, Zhou, H., Li, Q., Qiu, M., Li, Z., Tang, Q., Liu, M., Zhu, Y., Huang, J., Lang, N., Liu, Z., Deng, Y., Zhang, S., & Bi, F. (2011). Epigenetic modification of RhoE expression in gastric cancer cells. *Oncology Reports*, *25*(1), 173–180. https://doi.org/10.3892/or_00001058

Chen, Jie, Green, J., Yurdagul, A., Albert, P., McInnis, M. C., & Orr, A. W. (2015). αvβ3 Integrins Mediate Flow-Induced NF-κB Activation, Proinflammatory Gene Expression, and Early Atherogenic Inflammation. *American Journal of Pathology*, *185*(9), 2575–2589. https://doi.org/10.1016/j.ajpath.2015.05.013

Chen, Q., Li, W., Quan, Z., & Sumpio, B. E. (2003). Modulation of vascular smooth muscle cell alignment by cyclic strain is dependent on reactive oxygen species and P38 mitogen-activated protein kinase. *Journal of Vascular Surgery*, *37*(3), 660–668.

https://doi.org/10.1067/mva.2003.95

Cheng, C., Haasdijk, R., Tempel, D., Van De Kamp, E. H. M., Herpers, R., Bos, F., Den Dekker, W. K., Blonden, L. A. J., De Jong, R., Bürgisser, P. E., Chrifi, I., Biessen, E. A. L., Dimmeler, S., Schulte-Merker, S., & Duckers, H. J. (2012). Endothelial cell-specific fgd5 involvement in vascular pruning defines neovessel fate in mice. *Circulation*, *125*(25), 3142–3158. https://doi.org/10.1161/CIRCULATIONAHA.111.064030

Cheng, J., & Du, J. (2007). Mechanical stretch simulates proliferation of venous smooth muscle cells through activation of the insulin-like growth factor-1 receptor. *Arteriosclerosis, Thrombosis, and Vascular Biology*, *27*(8), 1744–1751. https://doi.org/10.1161/ATVBAHA.107.147371

Chien, S. (2008). Effects of disturbed flow on endothelial cells. *Annals of Biomedical Engineering*, *36*(4), 554–562. https://doi.org/10.1007/s10439-007-9426-3

Chilibeck, P. D., Paterson, D. H., Cunningham, D. A., Taylor, A. W., & Noble, E. G. (1997). Muscle capillarization, O2 diffusion distance, and V̇O2 kinetics in old and young individuals. *Journal of Applied Physiology*, *82*(1), 63–69. https://doi.org/10.1152/jappl.1997.82.1.63

Chiu, C. Z., Wang, B. W., & Shyu, K. G. (2013). Effects of cyclic stretch on the molecular regulation of myocardin in rat aortic vascular smooth muscle cells. *Journal of Biomedical Science*, *20*(1), 1–12. https://doi.org/10.1186/1423-0127-20-50

Cizmecioglu, O., Ni, J., Xie, S., Zhao, J. J., & Roberts, T. M. (2016). Rac1-mediated membrane raft localization of PI3K/p110β is required for its activation by GPCRs or PTEN loss. *ELife*, *5*, 1–21. https://doi.org/10.7554/elife.17635

Collier, M. P., & Benesch, J. L. P. (2020). Small heat-shock proteins and their role in mechanical stress. *Cell Stress and Chaperones*, *25*(4), 601–613. https://doi.org/10.1007/s12192-020-01095-z

Corey, D. P., & Hudspeth, A. J. (1979). Response latency of vertebrate hair cells. *Biophysical Journal*, *26*(3), 499–506. https://doi.org/10.1016/S0006-3495(79)85267-4

Coso, O. A., Chiariello, M., Yu, J. C., Teramoto, H., Crespo, P., Xu, N., Miki, T., & Silvio Gutkind, J. (1995). The small GTP-binding proteins Rac1 and Cdc42regulate the activity of the JNK/SAPK signaling pathway. *Cell*, *81*(7), 1137–1146. https://doi.org/10.1016/S0092-8674(05)80018-2

Dajnowiec, D., & Langille, B. L. (2007). Arterial adaptations to chronic changes in haemodynamic function: Coupling vasomotor tone to structural remodelling. *Clinical Science*, *113*(1–2), 15–23. https://doi.org/10.1042/CS20060337

davies. (1997). Overview: Temporal and Spatial Relationships in Shear Stress-Mediated

Endothelial Signalling. *Journal of Vascular Research*.

Davies, P. F., Remuzzi, A., Gordon, E. J., Dewey, C. F., & Gimbrone, M. A. (1986). Turbulent fluid shear stress induces vascular endothelial cell turnover in vitro. *Proceedings of the National Academy of Sciences of the United States of America*, *83*(7), 2114–2117. https://doi.org/10.1073/pnas.83.7.2114

Davies, Peter F. (2009). Hemodynamic shear stress and the endothelium in cardiovascular pathophysiology. *Nature Clinical Practice Cardiovascular Medicine*, *6*(1), 16–26. https://doi.org/10.1038/ncpcardio1397

Davies, Peter F., Barbee, K. A., Volin, M. V., Robotewskyj, A., Chen, J., Joseph, L., Griem, M. L., Wernick, M. N., Jacobs, E., Polacek, D. C., DePaola, N., & Barakat, A. I. (1997). Spatial relationships in early signaling events of flow-mediated endothelial mechanotransduction. *Annual Review of Physiology*, *59*, 527–549. https://doi.org/10.1146/annurev.physiol.59.1.527

Davies, Peter F., Civelek, M., Fang, Y., & Fleming, I. (2013). The atherosusceptible endothelium: Endothelial phenotypes in complex haemodynamic shear stress regions in vivo. *Cardiovascular Research*, *99*(2), 315–327. https://doi.org/10.1093/cvr/cvt101

Davis, M. E., Cai, H., Drummond, G. R., & Harrison, D. G. (2001). Shear stress regulates endothelial nitric oxide synthase expression through c-Src by divergent signaling pathways. *Circulation Research*, *89*(11), 1073–1080. https://doi.org/10.1161/hh2301.100806

Davis, M. E., Grumbach, I. M., Fukai, T., Cutchins, A., & Harrison, D. G. (2004). Shear Stress Regulates Endothelial Nitric-oxide Synthase Promoter Activity through Nuclear Factor κB Binding. *Journal of Biological Chemistry*, *279*(1), 163–168. https://doi.org/10.1074/jbc.M307528200

Dejana, E., Orsenigo, F., & Lampugnani, M. G. (2008). The role of adherens junctions and VE-cadherin in the control of vascular permeability. *Journal of Cell Science*, *121*(13), 2115–2122. https://doi.org/10.1242/jcs.017897

Dekker, R. J., Van Soest, S., Fontijn, R. D., Salamanca, S., De Groot, P. G., VanBavel, E., Pannekoek, H., & Horrevoets, A. J. G. (2002). Prolonged fluid shear stress induces a distinct set of endothelial cell genes, most specifically lung Krüppel-like factor (KLF2). *Blood*, *100*(5), 1689–1698. https://doi.org/10.1182/blood-2002-01-0046

Dekker, R. J., Van Thienen, J. V., Rohlena, J., De Jager, S. C., Elderkamp, Y. W., Seppen, J., De Vries, C. J. M., Biessen, E. A. L., Van Berkel, T. J. C., Pannekoek, H., & Horrevoets, A. J. G. (2005). Endothelial KLF2 links local arterial shear stress levels to the expression of vascular tone-regulating genes. *American Journal of Pathology*, *167*(2), 609–618. https://doi.org/10.1016/S0002-9440(10)63002-7

Dela Paz, N. G., Melchior, B., & Frangos, J. A. (2017). Shear stress induces Gαq/11 activation independently of G protein-coupled receptor activation in endothelial cells. *American Journal of Physiology - Cell Physiology*, *312*(4), C428–C437. https://doi.org/10.1152/ajpcell.00148.2016

Dela Paz, N. G., Melchior, B., Shayo, F. Y., & Frangos, J. A. (2014). Heparan sulfates mediate the interaction between platelet endothelial cell adhesion molecule-1 (PECAM-1) and the Gαq/11 subunits of heterotrimeric G proteins. *Journal of Biological Chemistry*, *289*(11), 7413–7424. https://doi.org/10.1074/jbc.M113.542514

Demicheva, E., Hecker, M., & Korff, T. (2008). Stretch-induced activation of the transcription factor activator protein-1 controls monocyte chemoattractant protein-1 expression during arteriogenesis. *Circulation Research*, *103*(5), 477–484. https://doi.org/10.1161/CIRCRESAHA.108.177782

Deng, L., Blanco, F. J., Stevens, H., Lu, R., Caudrillier, A., McBride, M., McClure, J. D., Grant, J., Thomas, M., Frid, M., Stenmark, K., White, K., Seto, A. G., Morrell, N. W., Bradshaw, A. C., MacLean, M. R., & Baker, A. H. (2015). MicroRNA-143 Activation Regulates Smooth Muscle and Endothelial Cell Crosstalk in Pulmonary Arterial Hypertension. *Circulation Research*, *117*(10), 870–883. https://doi.org/10.1161/CIRCRESAHA.115.306806

Dérijard, B., Raingeaud, J., Barrett, T., Wu, I. H., Han, J., Ulevitch, R. J., & Davis, R. J. (1995). Independent human MAP kinase signal transduction pathways defined by MEK and MKK isoforms. *Science*, *267*(5198), 682–685. https://doi.org/10.1126/science.7839144

Dessalles, C. A., Leclech, C., Castagnino, A., & Barakat, A. I. (2021). Integration of substrate- and flow-derived stresses in endothelial cell mechanobiology. *Communications Biology*, *4*(1). https://doi.org/10.1038/s42003-021-02285-w

Diekmann, D., Abo, A., Johnston, C., Segal, A. W., & Hall, A. (1994). Interaction of Rac with p67phox and regulation of phagocytic NADPH oxidase activity. *Science*, *265*(5171), 531–533. https://doi.org/10.1126/science.8036496

Dimmeler, S., Assmus, B., Hermann, C., Haendeler, J., & Zeiher, A. M. (1998). Fluid Shear Stress Stimulates Phosphorylation of Akt in Human Endothelial Cells. *Circulation Research*, *83*(3), 334–341. https://doi.org/10.1161/01.RES.83.3.334

Dimmeler, S., Fleming, I., Fisslthaler, B., Hermann, C., Busse, R., & Zeiher, A. M. (1999). Activation of nitric oxide synthase in endothelial cells by Akt- dependent phosphorylation. *Nature*, *399*(6736), 601–605. https://doi.org/10.1038/21224

Dimmeler, S., Haendeler, J., Nehls, M., & Zeiher, A. M. (1997). Suppression of Apoptosis by Nitric Oxide via Inhibition of ICE-like and CPP-32-like Proteases. *Journal of Experimental*

Medicine, *185*(4), 601–607.

Dinsmore, C., & Reiter, J. F. (2016). Endothelial primary cilia inhibit atherosclerosis. *EMBO Reports*, *17*(2), 156–166. https://doi.org/10.15252/embr.201541019

Dragovich, M. A., Chester, D., Fu, B. M., Wu, C., Xu, Y., Goligorsky, M. S., & Zhang, X. F. (2016). Mechanotransduction of the endothelial glycocalyx mediates nitric oxide production through activation of TRP channels. *American Journal of Physiology - Cell Physiology*, *311*(6), C846–C853. https://doi.org/10.1152/ajpcell.00288.2015

Du, J., Ma, X., Shen, B., Huang, Y., Birnbaumer, L., & Yao, X. (2014). TRPV4, TRPC1, and TRPP2 assemble to form a flow-sensitive heteromeric channel. *FASEB Journal*, *28*(11), 4677–4685. https://doi.org/10.1096/fj.14-251652

Earley, S., & Brayden, J. E. (2015). Transient receptor potential channels in the vasculature. *Physiological Reviews*, *95*(2), 645–690. https://doi.org/10.1152/physrev.00026.2014

Eblen, S. T., Slack, J. K., Weber, M. J., & Catling, A. D. (2002). Rac-PAK Signaling Stimulates Extracellular Signal-Regulated Kinase (ERK) Activation by Regulating Formation of MEK1-ERK Complexes. *Molecular and Cellular Biology*, *22*(17), 6023–6033. https://doi.org/10.1128/mcb.22.17.6023-6033.2002

Echarri, A., & Del Pozo, M. A. (2015). Caveolae - mechanosensitive membrane invaginations linked to actin filaments. *Journal of Cell Science*, *128*(15), 2747–2758. https://doi.org/10.1242/jcs.153940

Egorova, A. D., van der Heiden, K., Poelmann, R. E., & Hierck, B. P. (2012). Primary cilia as biomechanical sensors in regulating endothelial function. *Differentiation*, *83*(2), S56–S61. https://doi.org/10.1016/j.diff.2011.11.007

Eguchi, S., Kawai, T., Scalia, R., & Rizzo, V. (2018). Understanding Angiotensin II type 1 receptor signaling in vascular pathophysiology. *Hypertension*, *71*(5), 804–810. https://doi.org/10.1161/HYPERTENSIONAHA.118.10266

El-Sibai, M., El Hajj, J., Al Haddad, M., El Baba, N., Al Saneh, M., Daoud Khatoun, W., Helaers, R., Vikkula, M., El Atat, O., Sabbagh, J., Abou Chebel, N., & Ghassibe-Sabbagh, M. (2021). Dysregulation of Rho GTPases in orofacial cleft patients-derived primary cells leads to impaired cell migration, a potential cause of cleft/lip palate development. *Cells & Development*, *165*, 203656. https://doi.org/10.1016/j.cdev.2021.203656

Elkhawad, M., Rudd, J. H. F., Sarov-Blat, L., Cai, G., Wells, R., Davies, L. C., Collier, D. J., Marber, M. S., Choudhury, R. P., Fayad, Z. A., Tawakol, A., Gleeson, F. V., Lepore, J. J., Davis, B., Willette, R. N., Wilkinson, I. B., Sprecher, D. L., & Cheriyan, J. (2012). Effects of p38 mitogen-activated protein kinase inhibition on vascular and systemic inflammation in

patients with atherosclerosis. *JACC: Cardiovascular Imaging*, *5*(9), 911–922. https://doi.org/10.1016/j.jcmg.2012.02.016

Etienne-Manneville, S., & Hall, A. (2002). Rho GTPases in cell biology. *Nature*, *420*(6916), 629–635. https://doi.org/10.1038/nature01148

Feaver, R. E., Gelfand, B. D., & Blackman, B. R. (2013). Human haemodynamic frequency harmonics regulate the inflammatory phenotype of vascular endothelial cells. *Nature Communications*, *4*, 1–11. https://doi.org/10.1038/ncomms2530

Fels, B., & Kusche-Vihrog, K. (2020). It takes more than two to tango: mechanosignaling of the endothelial surface. *Pflugers Archiv European Journal of Physiology*, *472*(4), 419–433. https://doi.org/10.1007/s00424-020-02369-2

Fine, N., Dimitriou, I. D., Rullo, J., Sandí, M. J., Petri, B., Haitsma, J., Ibrahim, H., La Rose, J., Glogauer, M., Kubes, P., Cybulsky, M., & Rottapel, R. (2016). GEF-H1 is necessary for neutrophil shear stress-induced migration during inflammation. *Journal of Cell Biology*, *215*(1). https://doi.org/10.1083/jcb.201603109

Fleming, I., & Busse, R. (1999). Signal transduction of eNOS activation. *Cardiovascular Research*, *43*(3), 532–541. https://doi.org/10.1016/S0008-6363(99)00094-2

Flentje, A., Kalsi, R., & Monahan, T. S. (2019). Small gtpases and their role in vascular disease. *International Journal of Molecular Sciences*, *20*(4), 1–16. https://doi.org/10.3390/ijms20040917

Florian, J. A., Kosky, J. R., Ainslie, K., Pang, Z., Dull, R. O., & Tarbell, J. M. (2003). Heparan sulfate proteoglycan is a mechanosensor on endothelial cells. *Circulation Research*, *93*(10). https://doi.org/10.1161/01.res.0000101744.47866.d5

Frauenstein, A., Ebner, S., Hansen, F. M., Sinha, A., Phulphagar, K., Swatek, K., Hornburg, D., Mann, M., & Meissner, F. (2021). Identification of covalent modifications regulating immune signaling complex composition and phenotype. *Molecular Systems Biology*, *17*(7). https://doi.org/10.15252/msb.202010125

Freeman, J. L., Abo, A., & David Lambeth, J. (1996). Rac "insert region" is a novel effector region that is implicated in the activation of NADPH oxidase, but not PAK65. *Journal of Biological Chemistry*, *271*(33), 19794–19801. https://doi.org/10.1074/jbc.271.33.19794

Fujishiro, S. hei, Tanimura, S., Mure, S., Kashimoto, Y., Watanabe, K., & Kohno, M. (2008). ERK1/2 phosphorylate GEF-H1 to enhance its guanine nucleotide exchange activity toward RhoA. *Biochemical and Biophysical Research Communications*, *368*(1), 162–167. https://doi.org/10.1016/j.bbrc.2008.01.066

Fujiwara, S., Ohashi, K., Mashiko, T., Kondo, H., & Mizuno, K. (2016). Interplay between Solo

and keratin filaments is crucial for mechanical forceinduced stress fiber reinforcement. *Molecular Biology of the Cell*, *27*(6), 954–966. https://doi.org/10.1091/mbc.E15-06-0417

Fukai, N., Kenagy, R. D., Chen, L., Gao, L., Daum, G., & Clowes, A. W. (2009). Syndecan-1: An inhibitor of arterial smooth muscle cell growth and intimal hyperplasia. *Arteriosclerosis, Thrombosis, and Vascular Biology*, *29*(9), 1356–1362. https://doi.org/10.1161/ATVBAHA.109.190132

Fukushima, Y., Okada, M., Kataoka, H., Hirashima, M., Yoshida, Y., Mann, F., Gomi, F., Nishida, K., Nishikawa, S. I., & Uemura, A. (2011). Sema3E-PlexinD1 signaling selectively suppresses disoriented angiogenesis in ischemic retinopathy in mice. *Journal of Clinical Investigation*, *121*(5), 1974–1985. https://doi.org/10.1172/JCI44900

Gambardella, L., Hemberger, M., Hughes, B., Zudaire, E., Andrews, S., & Vermeren, S. (2010). PI3K signaling through the dual GTPase-activating protein ARAP3 is essential for developmental angiogenesis. *Science Signaling*, *3*(145). https://doi.org/10.1126/scisignal.2001026

García-Cardeña, G., Fan, R., Shah, V., Sorrentino, R., Cirino, G., Papapetropoulos, A., & Sessa, W. C. (1998). Dynamic activation of endothelial nitric oxide synthase by Hsp90. *Nature*, *392*(6678), 821–824. https://doi.org/10.1038/33934

García-Cardeña, G., Fan, R., Stern, D. F., Liu, J., & Sessa, W. C. (1996). Endothelial nitric oxide synthase is regulated by tyrosine phosphorylation and interacts with caveolin-1. *Journal of Biological Chemistry*, *271*(44), 27237–27240. https://doi.org/10.1074/jbc.271.44.27237

García-Ponce, A., Schuster, K., Døskeland, S. O., Reed, R. K., Curry, F. R. E., Waschke, J., & Radeva, M. Y. (2020). Epac1 Is Crucial for Maintenance of Endothelial Barrier Function through A Mechanism Partly Independent of Rac1. *Cells*, *9*(10), 1–20. https://doi.org/10.3390/cells9102170

Garrett, T. A., Van Buul, J. D., & Burridge, K. (2007). VEGF-induced Rac1 activation in endothelial cells is regulated by the guanine nucleotide exchange factor Vav2. *Experimental Cell Research*, *313*(15), 3285–3297. https://doi.org/10.1016/j.yexcr.2007.05.027

Gavard, J., & Gutkind, J. S. (2006). VEGF Controls endothelial-cell permeability promoting β-arrestin-dependent Endocytosis VE-cadherin. *Nature Cell Biology*, *8*(11), 1223–1234. https://doi.org/10.1038/ncb1486

Gee, E., Milkiewicz, M., & Haas, T. L. (2010). p38 MAPK activity is stimulated by vascular endothelial growth factor receptor 2 activation and is essential for shear stress-induced angiogenesis. *Journal of Cellular Physiology*, *222*(1), 120–126. https://doi.org/10.1002/jcp.21924

Gertz, S. D., Mintz, Y., Beeri, R., Rubinstein, C., Gilon, D., Gavish, L., Berlatzky, Y., Appelbaum, L., & Gavish, L. (2013). Lessons from Animal Models of Arterial Aneurysm. *Aorta*, *1*(5), 244–254. https://doi.org/10.12945/j.aorta.2013.13-052

Ghosh, S., Gachhui, R., Crooks, C., Wu, C., Lisanti, M. P., & Stuehr, D. J. (1998). Interaction between caveolin-1 and the reductase domain of endothelial nitric-oxide synthase. Consequences for catalysis. *Journal of Biological Chemistry*, *273*(35), 22267–22271. https://doi.org/10.1074/jbc.273.35.22267

Giaid, A., & Saleh, D. (1995). Reduced Expression of Endothelial Nitric Oxide Synthase in the Lungs of Patients with Pulmonary Hypertension. *New England Journal of Medicine*, *333*(4), 214–221. https://doi.org/10.1056/NEJM199507273330403

Gimbrone, M. A., & García-Cardeña, G. (2016). Endothelial Cell Dysfunction and the Pathobiology of Atherosclerosis. *Circulation Research*, *118*(4), 620–636. https://doi.org/10.1161/CIRCRESAHA.115.306301

Girard, P. R., & Nerem, R. M. (1995). Shear stress modulates endothelial cell morphology and F-actin organization through the regulation of focal adhesion-associated proteins. *Journal of Cellular Physiology*, *163*(1), 179–193. https://doi.org/10.1002/jcp.1041630121

Goldschmidt, M. E., McLeod, K. J., & Taylor, W. R. (2001). Integrin-Mediated Mechanotransduction in Vascular Smooth Muscle Cells. *Circulation Research*, *88*(7), 674–680. https://doi.org/10.1161/hh0701.089749

Goumans, M. J., Liu, Z., & Ten Dijke, P. (2009). TGF-β signaling in vascular biology and dysfunction. *Cell Research*, *19*(1), 116–127. https://doi.org/10.1038/cr.2008.326

Gouverneur, M., Spaan, J. A. E., Pannekoek, H., Fontijn, R. D., & Vink, H. (2006). Fluid shear stress stimulates incorporation of hyaluronan into endothelial cell glycocalyx. *American Journal of Physiology - Heart and Circulatory Physiology*, *290*(1), 458–462. https://doi.org/10.1152/ajpheart.00592.2005

Green, D. J., Hopman, M. T. E., Padilla, J., Laughlin, M. H., & Thijssen, D. H. J. (2017). Vascular adaptation to exercise in humans: Role of hemodynamic stimuli. *Physiological Reviews*, *97*(2), 495–528. https://doi.org/10.1152/physrev.00014.2016

Gu, J., Zhang, X., Jiang, G., Li, Q., Wang, E., & Yu, J. (2022). ARHGEF40 promotes non-small cell lung cancer proliferation and invasion via the AKT-Wnt axis by binding to RhoA. *Molecular Carcinogenesis*, *April*, 1–15. https://doi.org/10.1002/mc.23457

Guilluy, C., Brégeon, J., Toumaniantz, G., Rolli-Derkinderen, M., Retailleau, K., Loufrani, L., Henrion, D., Scalbert, E., Bril, A., Torres, R. M., Offermanns, S., Pacaud, P., & Loirand, G. (2010). The Rho exchange factor Arhgefı mediates the effects of angiotensin II on vascular

tone and blood pressure. *Nature Medicine*, *16*(2), 183–190. https://doi.org/10.1038/nm.2079

Guilluy, C., Garcia-Mata, R., & Burridge, K. (2011). Rho protein crosstalk: Another social network? *Trends in Cell Biology*, *21*(12), 718–726. https://doi.org/10.1016/j.tcb.2011.08.002

Guilluy, C., Swaminathan, V., Garcia-Mata, R., O'Brien, E. T., Superfine, R., & Burridge, K. (2011). The Rho GEFs LARG and GEF-H1 regulate the mechanical response to force on integrins. *Nature Cell Biology*, *13*(6), 722–728. https://doi.org/10.1038/ncb2254

Guo, F., Tang, J., Zhou, Z., Dou, Y., Van Lonkhuyzen, D., Gao, C., & Huan, J. (2012). GEF-H1-RhoA signaling pathway mediates LPS-induced NF-κB transactivation and IL-8 synthesis in endothelial cells. *Molecular Immunology*, *50*(1–2), 98–107. https://doi.org/10.1016/j.molimm.2011.12.009

Guo, F., Xing, Y., Zhou, Z., Dou, Y., Tang, J., Gao, C., & Huan, J. (2012). Guanine-nucleotide exchange factor H1 mediates lipopolysaccharide-induced interleukin 6 and tumor necrosis factor α expression in endothelial cells via activation of nuclear factor κb. *Shock*, *37*(5), 531–538. https://doi.org/10.1097/SHK.0b013e31824caa96

Gupta, S., Duszyc, K., Verma, S., Budnar, S., Liang, X., Gomez, G. A., Marcq, P., Noordstra, I., & Yap, A. S. (2021). Enhanced RhoA signalling stabilizes E-cadherin in migrating epithelial monolayers. *Journal of Cell Science*, *134*(17). https://doi.org/10.1242/jcs.258767

Haas, A. J., Zihni, C., Ruppel, A., Hartmann, C., Ebnet, K., Tada, M., Balda, M. S., & Matter, K. (2020). Interplay between Extracellular Matrix Stiffness and JAM-A Regulates Mechanical Load on ZO-1 and Tight Junction Assembly. *Cell Reports*, *32*(3). https://doi.org/10.1016/j.celrep.2020.107924

Haga, J. H., Li, Y. S. J., & Chien, S. (2007). Molecular basis of the effects of mechanical stretch on vascular smooth muscle cells. In *Journal of Biomechanics* (Vol. 40, Issue 5, pp. 947–960). https://doi.org/10.1016/j.jbiomech.2006.04.011

Han, J., Lee, J. D., Jiang, Y., Li, Z., Feng, L., & Ulevitch, R. J. (1996). Characterization of the structure and function of a novel MAP kinase kinase (MKKG). *Journal of Biological Chemistry*, *271*(6), 2886–2891. https://doi.org/10.1074/jbc.271.6.2886

Harada, N., Masuda, M., & Fujiwara, K. (1995). Fluid Flow and Osmotic Stress Induce Tyrosine Phosphorylation of an Endothelial Cell 128-kDa Surface Glycoprotein. In *Biochemical and Biophysical Research Communications* (Vol. 214, Issue 1, pp. 69–74). https://doi.org/10.1006/bbrc.1995.2257

Hayakawa, K., Tatsumi, H., & Sokabe, M. (2008). Actin stress fibers transmit and focus force to activate mechanosensitive channels. *Journal of Cell Science*, *121*(4), 496–503. https://doi.org/10.1242/jcs.022053

Helmke, B. P., Thakker, D. B., Goldman, R. D., & Davies, P. F. (2001). Spatiotemporal analysis of flow-induced intermediate filament displacement in living endothelial cells. *Biophysical Journal*, *80*(1), 184–194. https://doi.org/10.1016/S0006-3495(01)76006-7

Herder, C., Swiercz, J. M., Müller, C., Peravali, R., Quiring, R., Offermanns, S., Wittbrodt, J., & Loosli, F. (2013). ArhGEF18 regulates RhoA-Rock2 signaling to maintain neuro-epithelial apico-basal polarity and proliferation. *Development (Cambridge)*, *140*(13), 2787–2797. https://doi.org/10.1242/dev.096487

Hikita, T., Mirzapourshafiyi, F., Barbacena, P., Riddell, M., Pasha, A., Li, M., Kawamura, T., Brandes, R. P., Hirose, T., Ohno, S., Gerhardt, H., Matsuda, M., Franco, C. A., & Nakayama, M. (2018). PAR -3 controls endothelial planar polarity and vascular inflammation under laminar flow . *EMBO Reports*, *19*(9), 1–19. https://doi.org/10.15252/embr.201745253

Hodge, R. G., & Ridley, A. J. (2016). Regulating Rho GTPases and their regulators. *Nature Reviews Molecular Cell Biology*, *17*(8), 496–510. https://doi.org/10.1038/nrm.2016.67

Hsieh, H.-J., Li, N.-Q., & Frangos, J. A. (1993). Pulsatile and steady flow induces c-fos expression in human endothelial cells. *Journal of Cellular Physiology*, *154*(1), 143–151. https://doi.org/10.1002/jcp.1041540118

Humphrey, J. D., & Schwartz, M. A. (2021). *Annual Review of Biomedical Engineering Vascular Mechanobiology: Homeostasis, Adaptation, and Disease*. https://doi.org/10.1146/annurev-bioeng-092419

Humphries, M. J. (2000). Integrin structure. *Biochemical Society Transactions*, *28*(4), 311–340. https://doi.org/10.1042/bst0280311

Huveneers, S., Oldenburg, J., Spanjaard, E., van der Krogt, G., Grigoriev, I., Akhmanova, A., Rehmann, H., & de Rooij, J. (2012). Vinculin associates with endothelial VE-cadherin junctions to control force-dependent remodeling. *Journal of Cell Biology*, *196*(5), 641–652. https://doi.org/10.1083/jcb.201108120

Huxley, A. F., & Niedergerke, R. (1954). Structural changes in muscle during contraction: Interference microscopy of living muscle fibres. *Nature*, *173*(4412), 971–973. https://doi.org/10.1038/173971a0

Huxley, H. E., & Hanson, J. (1954). Changes in the Cross-Striatins of Muscle during Contraction and Stretch and their Structural Interpretation. *Nature*.

Ilan, N., Cheung, L., Pinter, E., & Madri, J. A. (2000). Platelet-endothelial cell adhesion molecule-1 (CD31), a scaffolding molecule for selected catenin family members whose binding is mediated by different tyrosine and serine/threonine phosphorylation. *Journal of Biological Chemistry*, *275*(28), 21435–21443. https://doi.org/10.1074/jbc.M001857200

Ingber, D. E. (2006). Cellular mechanotransduction: putting all the pieces together again. *The FASEB Journal*, *20*(7), 811–827. https://doi.org/10.1096/fj.05-5424rev

Inoue, R., Jian, Z., & Kawarabayashi, Y. (2009). Mechanosensitive TRP channels in cardiovascular pathophysiology. *Pharmacology and Therapeutics*, *123*(3), 371–385. https://doi.org/10.1016/j.pharmthera.2009.05.009

Iomini, C., Tejada, K., Mo, W., Vaananen, H., & Piperno, G. (2004). Primary cilia of human endothelial cells disassemble under laminar shear stress. *Journal of Cell Biology*, *164*(6), 811–817. https://doi.org/10.1083/jcb.200312133

Iring, A., Jin, Y. J., Albarrán-Juárez, J., Siragusa, M., Wang, S. P., Dancs, P. T., Nakayama, A., Tonack, S., Chen, M., Künne, C., Sokol, A. M., Günther, S., Martínez, A., Fleming, I., Wettschureck, N., Graumann, J., Weinstein, L. S., & Offermanns, S. (2019). Shear stress-induced endothelial adrenomedullin signaling regulates vascular tone and blood pressure. *Journal of Clinical Investigation*, *129*(7), 2775–2791. https://doi.org/10.1172/JCI123825

Ishikawa, K.-I., Nagase, T., Suyama, M., Miyajima, N., Tanaka, A., Kotani, H., Nomura, N., & Ohara, O. (1998). Prediction of the Coding Sequences of Unidentified Human Genes. X. The Complete Sequences of 100 New cDNA Clones from Brain Which Can Code for Large Proteins in vitro. In *DNA RESEARCH* (Vol. 5). https://academic.oup.com/dnaresearch/article/5/3/169/379047

Jalali, S., Li, Y. S., Sotoudeh, M., Yuan, S., Li, S., Chien, S., & Shyy, J. Y. J. (1998). Shear stress activates p60src-Ras-MAPK signaling pathways in vascular endothelial cells. *Arteriosclerosis, Thrombosis, and Vascular Biology*, *18*(2), 227–234. https://doi.org/10.1161/01.ATV.18.2.227

Janota, C. S., Calero-Cuenca, F. J., & Gomes, E. R. (2020). The role of the cell nucleus in mechanotransduction. In *Current Opinion in Cell Biology* (Vol. 63, pp. 204–211). Elsevier Ltd. https://doi.org/10.1016/j.ceb.2020.03.001

Jeansson, M., Gawlik, A., Anderson, G., Li, C., Kerjaschki, D., Henkelman, M., & Quaggin, S. E. (2011). Angiopoietin-1 is essential in mouse vasculature during development and in response to injury. *Journal of Clinical Investigation*, *121*(6), 2278–2289. https://doi.org/10.1172/JCI46322

Jiang, Y., Chen, C., Li, Z., Guo, W., Gegner, J. A., Lin, S., & Han, J. (1996). Characterization of the structure and function of a new mitogen- activated protein kinase (p38β). *Journal of Biological Chemistry*, *271*(30), 17920–17926. https://doi.org/10.1074/jbc.271.30.17920

Jin, X., Mitsumata, M., Yamane, T., & Yoshida, Y. (2002). Induction of human inhibitor of apoptosis protein-2 by shear stress in endothelial cells. *FEBS Letters*, *529*(2–3), 286–292.

https://doi.org/10.1016/S0014-5793(02)03361-6

Jin, Z. G., Ueba, H., Tanimoto, T., Lungu, A. O., Frame, M. D., & Berk, B. C. (2003). Ligand-independent activation of vascular endothelial growth factor receptor 2 by fluid shear stress regulates activation of endothelial nitric oxide synthase. *Circulation Research*, *93*(4), 354–363. https://doi.org/10.1161/01.RES.0000089257.94002.96

Jong Lee, H., & Young Koh, G. (2003). Shear stress activates Tie2 receptor tyrosine kinase in human endothelial cells. *Biochemical and Biophysical Research Communications*, *304*(2), 399–404. https://doi.org/10.1016/S0006-291X(03)00592-8

Jou, L. Der, Lee, D. H., Morsi, H., & Mawad, M. E. (2008). Wall shear stress on ruptured and unruptured intracranial aneurysms at the internal carotid artery. *American Journal of Neuroradiology*, *29*(9), 1761–1767. https://doi.org/10.3174/ajnr.A1180

Kakogiannos, N., Ferrari, L., Giampietro, C., Scalise, A. A., Maderna, C., Ravà, M., Taddei, A., Lampugnani, M. G., Pisati, F., Malinverno, M., Martini, E., Costa, I., Lupia, M., Cavallaro, U., Beznoussenko, G. V., Mironov, A. A., Fernandes, B., Rudini, N., Dejana, E., & Giannotta, M. (2020). JAM-A Acts via C/EBP-α to Promote Claudin-5 Expression and Enhance Endothelial Barrier Function. *Circulation Research*, *127*(8), 1056–1073. https://doi.org/10.1161/CIRCRESAHA.120.316742

Kamiyama, M., Utsunomiya, K., Taniguchi, K., Yokota, T., Kurata, H., Tajima, N., & Kondo, K. (2003). Contribution of Rho A and Rho kinase to platelet-derived growth factor-BB-induced proliferation of vascular smooth muscle cells. *Journal of Atherosclerosis and Thrombosis*, *10*(2), 117–123. https://doi.org/10.5551/jat.10.117

Kanoldt, V., Fischer, L., & Grashoff, C. (2019). Unforgettable force-crosstalk and memory of mechanosensitive structures. *Biological Chemistry*, *400*(6), 687–698. https://doi.org/10.1515/hsz-2018-0328

Kanzaki, M., Watson, R. T., Hou, J. C., Stamnes, M., Saltiel, A. R., & Pessin, J. E. (2002). Small GTP-binding Protein TC10 Differentially Regulates Two Distinct Populations of Filamentous Actin in 3T3L1 Adipocytes. *Molecular Biology of the Cell*, *13*(7), 2334–2346. https://doi.org/10.1091/mbc.01-10-0490

Kataoka, C., Egashira, K., Inoue, S., Takemoto, M., Ni, W., Koyanagi, M., Kitamoto, S., Usui, M., Kaibuchi, K., Shimokawa, H., & Takeshita, A. (2002). Important role of Rho-kinase in the pathogenesis of cardiovascular inflammation and remodeling induced by long-term blockade of nitric oxide synthesis in rats. *Hypertension*, *39*(2 I), 245–250. https://doi.org/10.1161/hy0202.103271

Kather, J. N., & Kroll, J. (2013). Rho guanine exchange factors in blood vessels: Fine-tuners of

angiogenesis and vascular function. *Experimental Cell Research*, *319*(9), 1289–1297. https://doi.org/10.1016/j.yexcr.2012.12.015

Katsumi, A., Naoe, T., Matsushita, T., Kaibuchi, K., & Schwartz, M. A. (2005). Integrin activation and matrix binding mediate cellular responses to mechanical stretch. *Journal of Biological Chemistry*, *280*(17), 16546–16549. https://doi.org/10.1074/jbc.C400455200

Kauskot, A., Poirault-Chassac, S., Adam, F., Muczynski, V., Aymé, G., Casari, C., Bordet, J.-C., Soukaseum, C., Rothschild, C., Proulle, V., Pietrzyk-Nivau, A., Berrou, E., Christophe, O. D., Rosa, J.-P., Lenting, P. J., Bryckaert, M., Denis, C. V., & Baruch, D. (2016). LIM kinase/cofilin dysregulation promotes macrothrombocytopenia in severe von Willebrand disease-type 2B. *JCI Insight*, *1*(16). https://doi.org/10.1172/jci.insight.88643

Kilian, L. S., Voran, J., Frank, D., & Rangrez, A. Y. (2021). RhoA: a dubious molecule in cardiac pathophysiology. *Journal of Biomedical Science*, *28*(1), 1–21. https://doi.org/10.1186/s12929-021-00730-w

Kim, M., Shewan, A. M., Ewald, A. J., Werb, Z., & Mostov, K. E. (2015). p114RhoGEF governs cell motility and lumen formation during tubulogenesis through a ROCK-myosin-II pathway. *Journal of Cell Science*, *128*(23), 4317–4327. https://doi.org/10.1242/jcs.172361

Kluger, M. S., Clark, P. R., Tellides, G., Gerke, V., & Pober, J. S. (2013). Claudin-5 controls intercellular barriers of human dermal microvascular but not human umbilical vein endothelial cells. *Arteriosclerosis, Thrombosis, and Vascular Biology*, *33*(3), 489–500. https://doi.org/10.1161/ATVBAHA.112.300893

Ko, K. S., Arora, P. D., & McCulloch, C. A. G. (2001). Cadherins Mediate Intercellular Mechanical Signaling in Fibroblasts by Activation of Stretch-sensitive Calcium-permeable Channels. *Journal of Biological Chemistry*, *276*(38), 35967–35977. https://doi.org/10.1074/jbc.M104106200

Kofler, N. M., Shawber, C. J., Kangsamaksin, T., Reed, H. O., Galatioto, J., & Kitajewski, J. (2011). Notch Signaling in Developmental and Tumor Angiogenesis. *Genes and Cancer*, *2*(12), 1106–1116. https://doi.org/10.1177/1947601911423030

Kolega, J. (1986). Effects of mechanical tension on protrusive activity and microfilament and intermediate filament organization in an epidermal epithelium moving in culture. *Journal of Cell Biology*, *102*(4), 1400–1411. https://doi.org/10.1083/jcb.102.4.1400

Koller, A., & Kaley, G. (1991). Endothelial regulation of wall shear stress and blood flow in skeletal muscle microcirculation. *American Journal of Physiology - Heart and Circulatory Physiology*, *260*(3 29-3). https://doi.org/10.1152/ajpheart.1991.260.3.h862

Koller, A., Sun, D., Huang, A., & Kaley, G. (1994). Corelease of nitric oxide and prostaglandins

mediates flow-dependent dilation of rat gracilis muscle arterioles. *American Journal of Physiology - Heart and Circulatory Physiology*, *267*(1 36-1). https://doi.org/10.1152/ajpheart.1994.267.1.h326

Kozma, R., Ahmed, S., Best, A., & Lim, L. (1995). The Ras-related protein Cdc42Hs and bradykinin promote formation of peripheral actin microspikes and filopodia in Swiss 3T3 fibroblasts. *Molecular and Cellular Biology*, *15*(4), 1942–1952. https://doi.org/10.1128/mcb.15.4.1942

Kroon, J., Heemskerk, N., Kalsbeek, M. J. T., De Waard, V., Van Rijssel, J., & Van Buul, J. D. (2017). Flow-induced endothelial cell alignment requires the RhoGEF Trio as a scaffold protein to polarize active Rac1 distribution. *Molecular Biology of the Cell*, *28*(13), 1745–1753. https://doi.org/10.1091/mbc.E16-06-0389

Kurogane, Y., Miyata, M., Kubo, Y., Nagamatsu, Y., Kundu, R. K., Uemura, A., Ishida, T., Quertermous, T., Hirata, K. I., & Rikitake, Y. (2012). FGD5 mediates proangiogenic action of vascular endothelial growth factor in human vascular endothelial cells. *Arteriosclerosis, Thrombosis, and Vascular Biology*, *32*(4), 988–996. https://doi.org/10.1161/ATVBAHA.111.244004

Kuwahara, K., Saito, Y., Nakagawa, O., Kishimoto, I., Harada, M., Ogawa, E., Miyamoto, Y., Hamanaka, I., Kajiyama, N., Takahashi, N., Izumi, T., Kawakami, R., Tamura, N., Ogawa, Y., & Nakao, K. (1999). The effects of the selective ROCK inhibitor, Y27632, on ET-1-induced hypertrophic response in neonatal rat cardiac myocytes - Possible involvement of Rho/ROCK pathway in cardiac muscle cell hypertrophy. *FEBS Letters*, *452*(3), 314–318. https://doi.org/10.1016/S0014-5793(99)00680-8

Lacolley, P. (2004). Mechanical influence of cyclic stretch on vascular endothelial cells. *Cardiovascular Research*, *63*(4), 577–579. https://doi.org/10.1016/j.cardiores.2004.06.017

Laviña, B., Castro, M., Niaudet, C., Cruys, B., Álvarez-Aznar, A., Carmeliet, P., Bentley, K., Brakebusch, C., Betsholtz, C., & Gaengel, K. (2018). Defective endothelial cell migration in the absence of Cdc42 leads to capillary-venous malformations. *Development (Cambridge)*, *145*(13). https://doi.org/10.1242/dev.161182

Lee, D. L., Webb, R. C., & Jin, L. (2004). Hypertension and RhoA/Rho-kinase signaling in the vasculature: Highlights from the recent literature. *Hypertension*, *44*(6), 796–799. https://doi.org/10.1161/01.HYP.0000148303.98066.ab

Lessey-Morillon, E. C., Osborne, L. D., Monaghan-Benson, E., Guilluy, C., O'Brien, E. T., Superfine, R., & Burridge, K. (2014). The RhoA Guanine Nucleotide Exchange Factor, LARG, Mediates ICAM-1–Dependent Mechanotransduction in Endothelial Cells To Stimulate

Transendothelial Migration. *The Journal of Immunology*, *192*(7), 3390–3398. https://doi.org/10.4049/jimmunol.1302525

Levesque, M. J., & Nerem, R. M. (1985). The elongation and orientation of cultured endothelial cells in response to shear stress. *Journal of Biomechanical Engineering*, *107*(4), 341–347. https://doi.org/10.1115/1.3138567

Levesque, M. J., Nerem, R. M., & Sprague, E. A. (1990). Vascular endottielial cell proliferation in culture and the influence of flow. *Biomaterials*, *11*(9), 702–707. https://doi.org/10.1016/0142-9612(90)90031-K

Li, D., Sun, Y., Kong, X., Luan, C., Yu, Y., Chen, F., & Chen, P. (2018). Association between a single nucleotide polymorphism in the 3-UTR of ARHGEF18 and the risk of nonidiopathic pulmonary arterial hypertension in Chinese population. *Disease Markers*, *2018*. https://doi.org/10.1155/2018/2461845

Li, S., Chen, B. P. C., Azuma, N., Hu, Y. L., Wu, S. Z., Sumpio, B. E., Shyy, J. Y. J., & Chien, S. (1999). Distinct roles for the small GTPases Cdc42 and Rho in endothelial responses to shear stress. *Journal of Clinical Investigation*, *103*(8), 1141–1150. https://doi.org/10.1172/JCI5367

Li, X., Garcia-Elias, A., Benito, B., & Nattel, S. (2022). The effects of cardiac stretch on atrial fibroblasts: Analysis of the evidence and potential role in atrial fibrillation. *Cardiovascular Research*, *118*(2), 440–460. https://doi.org/10.1093/cvr/cvab035

Li, Y. S., Shyy, J. Y., Li, S., Lee, J., Su, B., Karin, M., & Chien, S. (1996). The Ras-JNK pathway is involved in shear-induced gene expression. *Molecular and Cellular Biology*, *16*(11), 5947–5954. https://doi.org/10.1128/mcb.16.11.5947

Li, Z., Dong, X., Wang, Z., Liu, W., Deng, N., Ding, Y., Tang, L., Hla, T., Zeng, R., Li, L., & Wu, D. (2005). Regulation of PTEN by Rho small GTPases. *Nature Cell Biology*, *7*(4), 399–404. https://doi.org/10.1038/ncb1236

Lin, K., Hsu, P. P., Chen, B. P., Yuan, S., Usami, S., Shyy, J. Y. J., Li, Y. S., & Chien, S. (2000). Molecular mechanism of endothelial growth arrest by laminar shear stress. *Proceedings of the National Academy of Sciences of the United States of America*, *97*(17), 9385–9389. https://doi.org/10.1073/pnas.170282597

Liu, M., Bi, F., Zhou, X., & Zheng, Y. (2012). Rho GTPase regulation by miRNAs and covalent modifications. *Trends in Cell Biology*, *22*(7), 365–373. https://doi.org/10.1016/j.tcb.2012.04.004

Liu, X., Liu, X., Li, M., Zhang, Y., Chen, W., Zhang, M., Zhang, C., & Zhang, M. (2021). Mechanical Stretch Induces Smooth Muscle Cell Dysfunction by Regulating ACE2 via P38/ATF3 and

Post-transcriptional Regulation by miR-421. *Frontiers in Physiology*, *11*(January), 1–14. https://doi.org/10.3389/fphys.2020.540591

Liu, Y., Yehl, K., Narui, Y., & Salaita, K. (2013). Tension sensing nanoparticles for mechano-imaging at the living/nonliving interface. *Journal of the American Chemical Society*, *135*(14), 5320–5323. https://doi.org/10.1021/ja401494e

Lizama, C. O., & Zovein, A. C. (2013). Polarizing pathways: Balancing endothelial polarity, permeability, and lumen formation. *Experimental Cell Research*, *319*(9), 1247–1254. https://doi.org/10.1016/j.yexcr.2013.03.028

Loie, E., Charrier, L. E., Sollier, K., Masson, J.-Y., & Laprise, P. (2015). CRB3A Controls the Morphology and Cohesion of Cancer Cells through Ehm2/p114RhoGEF-Dependent Signaling. *Molecular and Cellular Biology*, *35*(19), 3423–3435. https://doi.org/10.1128/mcb.00673-15

Loirand, G., Guérin, P., & Pacaud, P. (2006). Rho kinases in cardiovascular physiology and pathophysiology. *Circulation Research*, *98*(3), 322–334. https://doi.org/10.1161/01.RES.0000201960.04223.3c

Loot, A. E., Popp, R., Fisslthaler, B., Vriens, J., Nilius, B., & Fleming, I. (2008). Role of cytochrome P450-dependent transient receptor potential V4 activation in flow-induced vasodilatation. *Cardiovascular Research*, *80*(3), 445–452. https://doi.org/10.1093/cvr/cvn207

Love, M. I., Huber, W., & Anders, S. (2014). Moderated estimation of fold change and dispersion for RNA-seq data with DESeq2. *Genome Biology*, *15*(12), 1–21. https://doi.org/10.1186/s13059-014-0550-8

Lu, Y., Ye, Y., Bao, W., Yang, Q., Wang, J., Liu, Z., & Shi, S. (2017). Genome-wide identification of genes essential for podocyte cytoskeletons based on single-cell RNA sequencing. *Kidney International*, *92*(5), 1119–1129. https://doi.org/10.1016/j.kint.2017.04.022

Lysgaard Poulsen, J., Stubbe, J., & Lindholt, J. S. (2016). Animal Models Used to Explore Abdominal Aortic Aneurysms: A Systematic Review. *European Journal of Vascular and Endovascular Surgery*, *52*(4), 487–499. https://doi.org/10.1016/j.ejvs.2016.07.004

Madaule, P., & Axel, R. (1985). A novel ras-related gene family. *Cell*, *41*(1), 31–40. https://doi.org/10.1016/0092-8674(85)90058-3

Maisonpierre, P. C., Suri, C., Jones, P. F., Bartunkova, S., Wiegand, S. J., Radziejewski, C., Compton, D., McClain, J., Aldrich, T. H., Papadopoulos, N., Daly, T. J., Davis, S., Sato, T. N., & Yancopoulos, G. D. (1997). Angiopoietin-2, a Natural Antagonist for Tie2 That Disrupts in vivo Angiogenesis. *Science*, *277*(5322), 55–60. https://doi.org/10.1126/science.277.5322.55

Malek, A. M., & Izumo, S. (1996). Mechanism of endothelial cell shape change and cytoskeletal remodeling in response to fluid shear stress. *Journal of Cell Science*, *109*(4), 713–726. https://doi.org/10.1242/jcs.109.4.713

Marinković, G., Hibender, S., Hoogenboezem, M., Van Broekhoven, A., Girigorie, A. F., Bleeker, N., Hamers, A. A. J., Stap, J., Van Buul, J. D., De Vries, C. J. M., & De Waard, V. (2013). Immunosuppressive drug azathioprine reduces aneurysm progression through inhibition of Rac1 and c-Jun-Terminal-N-Kinase in endothelial cells. *Arteriosclerosis, Thrombosis, and Vascular Biology*, *33*(10), 2380–2388. https://doi.org/10.1161/ATVBAHA.113.301394

Marinković, G., Kroon, J., Hoogenboezem, M., Hoeben, K. A., Ruiter, M. S., Kurakula, K., Otermin Rubio, I., Vos, M., de Vries, C. J. M., van Buul, J. D., & de Waard, V. (2014). Inhibition of GTPase Rac1 in Endothelium by 6-Mercaptopurine Results in Immunosuppression in Nonimmune Cells: New Target for an Old Drug. *The Journal of Immunology*, *192*(9), 4370–4378. https://doi.org/10.4049/jimmunol.1302527

Marivin, A., Morozova, V., Walawalkar, I., Leyme, A., Kretov, D. A., Cifuentes, D., Dominguez, I., & Garcia-Marcos, M. (2019). GPCR-independent activation of G proteins promotes apical cell constriction in vivo. *Journal of Cell Biology*, *218*(5), 1743–1763. https://doi.org/10.1083/jcb.201811174

Marziano, C., Genet, G., & Hirschi, K. K. (2021). Vascular endothelial cell specification in health and disease. *Angiogenesis*, *24*(2), 213–236. https://doi.org/10.1007/s10456-021-09785-7

Maurya, M. R., Gupta, S., Li, J. Y. S., Ajami, N. E., Chen, Z. B., Shyy, J. Y. J., Chien, S., & Subramaniam, S. (2021). Longitudinal shear stress response in human endothelial cells to atheroprone and atheroprotective conditions. *Proceedings of the National Academy of Sciences of the United States of America*, *118*(4), 2–9. https://doi.org/10.1073/pnas.2023236118

Mederos Y Schnitzler, M., Storch, U., & Gudermann, T. (2011). AT1 receptors as mechanosensors. *Current Opinion in Pharmacology*, *11*(2), 112–116. https://doi.org/10.1016/j.coph.2010.11.003

Meng, H., Tutino, V. M., Xiang, J., & Siddiqui, A. (2014). High WSS or Low WSS? Complex interactions of hemodynamics with intracranial aneurysm initiation, growth, and rupture: Toward a unifying hypothesis. *American Journal of Neuroradiology*, *35*(7), 1254–1262. https://doi.org/10.3174/ajnr.A3558

Mikelis, C. M., Simaan, M., Ando, K., Fukuhara, S., Sakurai, A., Amornphimoltham, P., Masedunskas, A., Weigert, R., Chavakis, T., Adams, R. H., Offermanns, S., Mochizuki, N., Zheng, Y., & Gutkind, J. S. (2015). RhoA and ROCK mediate histamine-induced vascular leakage and anaphylactic shock. *Nature Communications*, *6*.

https://doi.org/10.1038/ncomms7725

Minden, A., Lin, A., Claret, F. X., Abo, A., & Karin, M. (1995). Selective activation of the JNK signaling cascadeand c-Jun transcriptional activity by the small GTPases Rac and Cdc42Hs. *Cell*, *81*(7), 1147–1157. https://doi.org/10.1016/S0092-8674(05)80019-4

Miralles, F., Posern, G., Zaromytidou, A. I., & Treisman, R. (2003). Actin dynamics control SRF activity by regulation of its coactivator MAL. *Cell*, *113*(3), 329–342. https://doi.org/10.1016/S0092-8674(03)00278-2

Mochizuki, S., Vink, H., Hiramatsu, O., Kajita, T., Shigeto, F., Spaan, J. A. E., & Kajiya, F. (2003). Role of hyaluronic acid glycosaminoglycans in shear-induced endothelium-derived nitric oxide release. *American Journal of Physiology - Heart and Circulatory Physiology*, *285*(2 54-2), 722–726. https://doi.org/10.1152/ajpheart.00691.2002

Mohammadi, M. T., & Dehghani, G. A. (2014). Acute hypertension induces brain injury and blood-brain barrier disruption through reduction of claudins mRNA expression in rat. *Pathology Research and Practice*, *210*(12), 985–990. https://doi.org/10.1016/j.prp.2014.05.007

Morello, F., Perino, A., & Hirsch, E. (2009). Phosphoinositide 3-kinase signalling in the vascular system. *Cardiovascular Research*, *82*(2), 261–271. https://doi.org/10.1093/cvr/cvn325

Morrow, D., Sweeney, C., Birney, Y. A., Cummins, P. M., Walls, D., Redmond, E. M., & Cahill, P. A. (2005). Cyclic strain inhibits notch receptor signaling in vascular smooth muscle cells in vitro. *Circulation Research*, *96*(5), 567–575. https://doi.org/10.1161/01.RES.0000159182.98874.43

Mostowy, S., & Cossart, P. (2012). Septins: The fourth component of the cytoskeleton. *Nature Reviews Molecular Cell Biology*, *13*(3), 183–194. https://doi.org/10.1038/nrm3284

Mukai, Y. (2002). Involvement of Rho-kinase in hypertensive vascular disease--a novel therapeutic target in hypertension. *Fukuoka Acta Medica*, *93*(8), 129–134. https://doi.org/10.1096/fsb2fj000735fje

Mukaro, V. R., Quach, A., Gahan, M. E., Boog, B., Huang, Z. H., Gao, X., Haddad, C., Mahalingam, S., Hii, C. S., & Ferrante, A. (2018). Small tumor necrosis factor receptor biologics inhibit the tumor necrosis factor-p38 signalling axis and inflammation. *Nature Communications*, *9*(1). https://doi.org/10.1038/s41467-018-03640-y

Muller, J. M., Chilian, W. M., & Davis, M. J. (1997). Integrin signaling transduces shear stress-dependent vasodilation of coronary arterioles. *Circulation Research*, *80*(3), 320–326. https://doi.org/10.1161/01.RES.80.3.320

Nagata, K. I., & Inagaki, M. (2005). Cytoskeletal modification of Rho guanine nucleotide

exchange factor activity: Identification of a Rho guanine nucleotide exchange factor as a binding partner for Sept9b, a mammalian septin. *Oncogene*, *24*(1), 65–76. https://doi.org/10.1038/sj.onc.1208101

Nagel, T., Resnick, N., Dewey, C. F., & Gimbrone, M. A. (1999). Vascular endothelial cells respond to spatial gradients in fluid shear stress by enhanced activation of transcription factors. *Arteriosclerosis, Thrombosis, and Vascular Biology*, *19*(8), 1825–1834. https://doi.org/10.1161/01.ATV.19.8.1825

Nakajima, H., & Tanoue, T. (2011). Lulu2 regulates the circumferential actomyosin tensile system in epithelial cells through p114rhoGEF. *Journal of Cell Biology*, *195*(2), 245–261. https://doi.org/10.1083/jcb.201104118

Nakajima, N., Nagahiro, S., Sano, T., Satomi, J., & Satoh, K. (2000). Phenotypic modulation of smooth muscle cells in human cerebral aneurysmal walls. *Acta Neuropathologica*, *100*(5), 475–480. https://doi.org/10.1007/s004010000220

Nam, D., Ni, C. W., Rezvan, A., Suo, J., Budzyn, K., Llanos, A., Harrison, D., Giddens, D., & Jo, H. (2009). Partial carotid ligation is a model of acutely induced disturbed flow, leading to rapid endothelial dysfunction and atherosclerosis. *American Journal of Physiology - Heart and Circulatory Physiology*, *297*(4), 1535–1543. https://doi.org/10.1152/ajpheart.00510.2009

Nauli, S. M., Jin, X., Aboualaiwi, W. A., El-Jouni, W., Su, X., & Zhou, J. (2013). Non-motile primary cilia as fluid shear stress mechanosensors. In *Methods in Enzymology* (1st ed., Vol. 525). Elsevier Inc. https://doi.org/10.1016/B978-0-12-397944-5.00001-8

Nauli, S. M., Kawanabe, Y., Kaminski, J. J., Pearce, W. J., Ingber, D. E., & Zhou, J. (2008). Endothelial cilia are fluid shear sensors that regulate calcium signaling and nitric oxide production through polycystin-1. *Circulation*, *117*(9), 1161–1171. https://doi.org/10.1161/CIRCULATIONAHA.107.710111

Neudauer, C. L., Joberty, G., Tatsis, N., & Macara, I. G. (1998). Distinct cellular effects and interactions of the Rho-family GTPase TC10. *Current Biology*, *8*(21), 1151–1161. https://doi.org/10.1016/s0960-9822(07)00486-1

Nishimura, R., Kato, K., Fujiwara, S., Ohashi, K., & Mizuno, K. (2018). Solo and keratin filaments regulate epithelial tubule morphology. *Cell Structure and Function*, *43*(1), 95–105. https://doi.org/10.1247/csf.18010

Nitta, T., Hata, M., Gotoh, S., Seo, Y., Sasaki, H., Hashimoto, N., Furuse, M., & Tsukita, S. (2003). Size-selective loosening of the blood-brain barrier in claudin-5-deficient mice. *Journal of Cell Biology*, *161*(3), 653–660. https://doi.org/10.1083/jcb.200302070

Niu, J., Profirovic, J., Pan, H., Vaiskunaite, R., & Voyno-Yasenetskaya, T. (2003). G Protein βγ

Subunits Stimulate p114RhoGEF, a Guanine Nucleotide Exchange Factor for RhoA and Rac1: Regulation of Cell Shape and Reactive Oxygen Species Production. *Circulation Research*, *93*(9), 848–856. https://doi.org/10.1161/01.RES.0000097607.14733.0C

Obi, S., Yamamoto, K., Shimizu, N., Kumagaya, S., Masumura, T., Sokabe, T., Asahara, T., & Ando, J. (2009). Fluid shear stress induces arterial differentiation of endothelial progenitor cells. *Journal of Applied Physiology*, *106*(1), 203–211. https://doi.org/10.1152/japplphysiol.00197.2008

Okuda, M., Takahashi, M., Suero, J., Murry, C. E., Traub, O., Kawakatsu, H., & Berk, B. C. (1999). Shear stress stimulation of p130(cas) tyrosine phosphorylation requires calcium-dependent c-Src activation. *Journal of Biological Chemistry*, *274*(38), 26803–26809. https://doi.org/10.1074/jbc.274.38.26803

Olesen, S. P., Claphamt, D. E., & Davies, P. F. (1988). Haemodynamic shear stress activates a K+ current in vascular endothelial cells. *Nature*, *331*(6152), 168–170. https://doi.org/10.1038/331168a0

Oliver, T., Jacobson, K., & Dembo, M. (1995). Traction forces in locomoting cells. *Cell Motility and the Cytoskeleton*, *31*(3), 225–240. https://doi.org/10.1002/cm.970310306

Orr, A. W., Sanders, J. M., Bevard, M., Coleman, E., Sarembock, I. J., & Schwartz, M. A. (2005). The subendothelial extracellular matrix modulates NF-κB activation by flow: A potential role in atherosclerosis. *Journal of Cell Biology*, *169*(1), 191–202. https://doi.org/10.1083/jcb.200410073

Orsenigo, F., Giampietro, C., Ferrari, A., Corada, M., Galaup, A., Sigismund, S., Ristagno, G., Maddaluno, L., Koh, G. Y., Franco, D., Kurtcuoglu, V., Poulikakos, D., Baluk, P., McDonald, D., Grazia Lampugnani, M., & Dejana, E. (2012). Phosphorylation of VE-cadherin is modulated by haemodynamic forces and contributes to the regulation of vascular permeability in vivo. *Nature Communications*, *3*. https://doi.org/10.1038/ncomms2199

Osawa, M., Masuda, M., Kusano, K. I., & Fujiwara, K. (2002). Evidence for a role of platelet endothelial cell adhesion molecule-1 in endothelial cell mechanosignal transduction: Is it a mechanoresponsive molecule? *Journal of Cell Biology*, *158*(4), 773–785. https://doi.org/10.1083/jcb.200205049

Osborn, E. A., Rabodzey, A., Dewey, C. F., & Hartwig, J. H. (2006). Endothelial actin cytoskeleton remodeling during mechanostimulation with fluid shear stress. *American Journal of Physiology - Cell Physiology*, *290*(2), 444–452. https://doi.org/10.1152/ajpcell.00218.2005

Otte, L. A., Bell, K. S., Loufrani, L., Yeh, J. C., Melchior, B., Dao, D. N., Stevens, H. Y., White, C. R., & Frangos, J. A. (2009). Rapid changes in shear stress induce dissociation of a Gαq/11-

platelet endothelial cell adhesion molecule-1 complex. *Journal of Physiology*, *587*(10), 2365–2373. https://doi.org/10.1113/jphysiol.2009.172643

Papaioannou, T. G., & Stefanadis, C. (2005). Vascular wall shear stress: basic principles and methods. *Hellenic Journal of Cardiology : HJC = Hellenike Kardiologike Epitheorese*, *46*(1), 9–15. http://www.ncbi.nlm.nih.gov/pubmed/15807389

Park, H., Go, Y. M., Darji, R., Choi, J. W., Lisanti, M. P., Maland, M. C., & Jo, H. (2000). Caveolin-1 regulates shear stress-dependent activation of extracellular signal-regulated kinase. *American Journal of Physiology - Heart and Circulatory Physiology*, *278*(4 47-4), 1285–1293. https://doi.org/10.1152/ajpheart.2000.278.4.h1285

Paul, F., Zauber, H., Von Berg, L., Rocks, O., Daumke, O., & Selbach, M. (2017). Quantitative gtpase affinity purification identifies rho family protein interaction partners. *Molecular and Cellular Proteomics*, *16*(1), 73–85. https://doi.org/10.1074/mcp.M116.061531

Persat, A. (2017). Bacterial mechanotransduction. In *Current Opinion in Microbiology* (Vol. 36, pp. 1–6). Elsevier Ltd. https://doi.org/10.1016/j.mib.2016.12.002

Petsophonsakul, P., Furmanik, M., Forsythe, R., Dweck, M., Schurink, G. W., Natour, E., Reutelingsperger, C., Jacobs, M., Mees, B., & Schurgers, L. (2019). Role of vascular smooth muscle cell phenotypic switching and calcification in aortic aneurysm formation involvement of Vitamin K-dependent processes. *Arteriosclerosis, Thrombosis, and Vascular Biology*, *39*(7), 1351–1368. https://doi.org/10.1161/ATVBAHA.119.312787

Planas-Paz, L., Strilić, B., Goedecke, A., Breier, G., Fässler, R., & Lammert, E. (2012). Mechanoinduction of lymph vessel expansion. *EMBO Journal*, *31*(4), 788–804. https://doi.org/10.1038/emboj.2011.456

Polacheck, W. J., Kutys, M. L., Yang, J., Eyckmans, J., Wu, Y., Vasavada, H., Hirschi, K. K., & Chen, C. S. (2017). A non-canonical Notch complex regulates adherens junctions and vascular barrier function. *Nature*, *552*(7684), 258–262. https://doi.org/10.1038/nature24998

Qi, Y. X., Yao, Q. P., Huang, K., Shi, Q., Zhang, P., Wang, G. L., Han, Y., Bao, H., Wang, L., Li, H. P., Shen, B. R., Wang, Y., Chien, S., & Jiang, Z. L. (2016). Nuclear envelope proteins modulate proliferation of vascular smooth muscle cells during cyclic stretch application. *Proceedings of the National Academy of Sciences of the United States of America*, *113*(19), 5293–5298. https://doi.org/10.1073/pnas.1604569113

Raftopoulou, M., & Hall, A. (2004). Cell migration: Rho GTPases lead the way. *Developmental Biology*, *265*(1), 23–32. https://doi.org/10.1016/j.ydbio.2003.06.003

Rampersad, S. N., Freitag, S. I., Hubert, F., Brzezinska, P., Butler, N., Umana, M. B., Wudwud, A. R., & Maurice, D. H. (2016). EPAC1 promotes adaptive responses in human arterial

endothelial cells subjected to low levels of laminar fluid shear stress: Implications in flow-related endothelial dysfunction. *Cellular Signalling*, *28*(6), 606–619. https://doi.org/10.1016/j.cellsig.2016.02.016

Ranade, S. S., Qiu, Z., Woo, S. H., Hur, S. S., Murthy, S. E., Cahalan, S. M., Xu, J., Mathur, J., Bandell, M., Coste, B., Li, Y. S. J., Chien, S., & Patapoutian, A. (2014). Piezo1, a mechanically activated ion channel, is required for vascular development in mice. *Proceedings of the National Academy of Sciences of the United States of America*, *111*(28), 10347–10352. https://doi.org/10.1073/pnas.1409233111

Rateri, D. L., Moorleghen, J. J., Balakrishnan, A., Owens, A. P., Howatt, D. A., Subramanian, V., Poduri, A., Charnigo, R., Cassis, L. A., & Daugherty, A. (2011). Endothelial cell-specific deficiency of ang II type 1a receptors attenuates ang II-induced ascending aortic aneurysms in LDL Receptor-/- mice. *Circulation Research*, *108*(5), 574–581. https://doi.org/10.1161/CIRCRESAHA.110.222844

Reitsma, S., Slaaf, D. W., Vink, H., Van Zandvoort, M. A. M. J., & Oude Egbrink, M. G. A. (2007). The endothelial glycocalyx: Composition, functions, and visualization. *Pflugers Archiv European Journal of Physiology*, *454*(3), 345–359. https://doi.org/10.1007/s00424-007-0212-8

Retailleau, K., Duprat, F., Arhatte, M., Ranade, S. S., Peyronnet, R., Martins, J. R., Jodar, M., Moro, C., Offermanns, S., Feng, Y., Demolombe, S., Patel, A., & Honoré, E. (2015). Piezo1 in Smooth Muscle Cells Is Involved in Hypertension-Dependent Arterial Remodeling. *Cell Reports*, *13*(6), 1161–1171. https://doi.org/10.1016/j.celrep.2015.09.072

Reusch, H. P., Chan, G., Ives, H. E., & Nemenoff, R. A. (1997). Activation of JNK/SAPK and ERK by mechanical strain in vascular smooth muscle cells depends on extracellular matrix composition. *Biochemical and Biophysical Research Communications*, *237*(2), 239–244. https://doi.org/10.1006/bbrc.1997.7121

Richards, M., Hetheridge, C., & Mellor, H. (2015). The Formin FMNL3 Controls Early Apical Specification in Endothelial Cells by Regulating the Polarized Trafficking of Podocalyxin. *Current Biology*, *25*(17), 2325–2331. https://doi.org/10.1016/j.cub.2015.07.045

Ridley, A. J., & Hall, A. (1992). The small GTP-binding protein rho regulates the assembly of focal adhesions and actin stress fibers in response to growth factors. *Cell*, *70*(3), 389–399. https://doi.org/10.1016/0092-8674(92)90163-7

Ridley, A. J., Paterson, H. F., Johnston, C. L., Diekmann, D., & Hall, A. (1992). The small GTP-binding protein rac regulates growth factor-induced membrane ruffling. *Cell*, *70*(3), 401–410. https://doi.org/10.1016/0092-8674(92)90164-8

Rizzo, V., McIntosh, D. P., Oh, P., & Schnitzer, J. E. (1998). In situ flow activates endothelial nitric oxide synthase in luminal caveolae of endothelium with rapid caveolin dissociation and calmodulin association. *Journal of Biological Chemistry*, *273*(52), 34724–34729. https://doi.org/10.1074/jbc.273.52.34724

Rizzo, V., Morton, C., DePaola, N., Schnitzer, J. E., & Davies, P. F. (2003). Recruitment of endothelial caveolae into mechanotransduction pathways by flow conditioning in vitro. *American Journal of Physiology - Heart and Circulatory Physiology*, *285*(4 54-4), 1720–1729. https://doi.org/10.1152/ajpheart.00344.2002

Rooprai, J., Boodhwani, M., Beauchesne, L., Chan, K. L., Dennie, C., Wells, G. A., & Coutinho, T. (2022). Central Hypertension in Patients With Thoracic Aortic Aneurysms: Prevalence and Association With Aneurysm Size and Growth. *American Journal of Hypertension*, *35*(1), 79–86. https://doi.org/10.1093/ajh/hpaa183

Roux, E., Bougaran, P., Dufourcq, P., & Couffinhal, T. (2020). Fluid Shear Stress Sensing by the Endothelial Layer. In *Frontiers in Physiology* (Vol. 11). Frontiers Media S.A. https://doi.org/10.3389/fphys.2020.00861

Schaefer, A., Reinhard, N. R., & Hordijk, P. L. (2014). Toward understanding RhoGTPase specificity: Structure, function and local activation. *Small GTPases*, *5*(2), 1–11. https://doi.org/10.4161/21541248.2014.968004

Schell, C., Rogg, M., Suhm, M., Helmstädter, M., Sellung, D., Yasuda-Yamahara, M., Kretz, O., Küttner, V., Suleiman, H., Kollipara, L., Zahedi, R. P., Sickmann, A., Eimer, S., Shaw, A. S., Kramer-Zucker, A., Hirano-Kobayashi, M., Abe, T., Aizawa, S., Grahammer, F., … Huber, T. B. (2017). The FERM protein EPB41L5 regulates actomyosin contractility and focal adhesion formation to maintain the kidney filtration barrier. *Proceedings of the National Academy of Sciences of the United States of America*, *114*(23), E4621–E4630. https://doi.org/10.1073/pnas.1617004114

Schermuly, R. T., Stasch, J. P., Pullamsetti, S. S., Middendorff, R., Müller, D., Schlüter, K. D., Dingendorf, A., Hackemack, S., Kolosionek, E., Kaulen, C., Dumitrascu, R., Weissmann, N., Mittendorf, J., Klepetko, W., Seeger, W., Ghofrani, H. A., & Grimminger, F. (2008). Expression and function of soluble guanylate cyclase in pulmonary arterial hypertension. *European Respiratory Journal*, *32*(4), 881–891. https://doi.org/10.1183/09031936.00114407

Schieven, G. (2005). The Biology of p38 Kinase: A Central Role in Inflammation. *Current Topics in Medicinal Chemistry*, *5*(10), 921–928. https://doi.org/10.2174/1568026054985902

Schnoor, M., Lai, F. P. L., Zarbock, A., Kläver, R., Polaschegg, C., Schulte, D., Weich, H. A., Oelkers, J. M., Rottner, K., & Vestweber, D. (2011). Cortactin deficiency is associated with

reduced neutrophil recruitment but increased vascular permeability in vivo. *Journal of Experimental Medicine*, *208*(18), 1721–1735. https://doi.org/10.1084/jem.20101920

Schumacher, S., Vazquez Nunez, R., Biertümpfel, C., & Mizuno, N. (2021). Bottom-up reconstitution of focal adhesion complexes. *FEBS Journal*, *289*, 3360–3373. https://doi.org/10.1111/febs.16023

Sedding, D. G., Hermsen, J., Seay, U., Eickelberg, O., Kummer, W., Schwencke, C., Strasser, R. H., Tillmanns, H., & Braun-Dullaeus, R. C. (2005). Caveolin-1 facilitates mechanosensitive protein kinase B (Akt) signaling in vitro and in vivo. *Circulation Research*, *96*(6), 635–642. https://doi.org/10.1161/01.RES.0000160610.61306.0f

Seki, T., Yokoshiki, H., Sunagawa, M., Nakamura, M., & Sperelakis, N. (1999). Angiotensin II stimulation of Ca2+-channel current in vascular smooth muscle cells is inhibited by lavendustin-A and LY-294002. *Pflugers Archiv European Journal of Physiology*, *437*(3), 317–323. https://doi.org/10.1007/s004240050785

Seko, T., Ito, M., Kureishi, Y., Okamoto, R., Moriki, N., Onishi, K., Isaka, N., Hartshorne, D. J., & Nakano, T. (2003). Activation of RhoA and inhibition of myosin phosphatase as important components in hypertension in vascular smooth muscle. *Circulation Research*, *92*(4), 411–418. https://doi.org/10.1161/01.RES.0000059987.90200.44

SenBanerjee, S., Lin, Z., Atkins, G. B., Greif, D. M., Rao, R. M., Kumar, A., Feinberg, M. W., Chen, Z., Simon, D. I., Luscinskas, F. W., Michel, T. M., Gimbrone, M. A., García-Cardeña, G., & Jain, M. K. (2004). KLF2 is a novel transcriptional regulator of endothelial proinflammatory activation. *Journal of Experimental Medicine*, *199*(10), 1305–1315. https://doi.org/10.1084/jem.20031132

Shay-Salit, A., Shushy, M., Wolfovitz, E., Yahav, H., Breviario, F., Dejana, E., & Resnick, N. (2002). VEGF receptor 2 and the adherens junction as a mechanical transducer in vascular endothelial cells. *Proceedings of the National Academy of Sciences of the United States of America*, *99*(14), 9462–9467. https://doi.org/10.1073/pnas.142224299

Sheetz, M. P., & Singer, S. J. (1974). Biological membranes as bilayer couples. A molecular mechanism of drug erythrocyte interactions. *Proceedings of the National Academy of Sciences of the United States of America*, *71*(11), 4457–4461. https://doi.org/10.1073/pnas.71.11.4457

Shesely, E. G., Maeda, N., Kim, H. S., Desai, K. M., Krege, J. H., Laubach, V. E., Sherman, P. A., Sessa, W. C., & Smithies, O. (1996). Elevated blood pressures in mice lacking endothelial nitric oxide synthase. *Proceedings of the National Academy of Sciences of the United States of America*, *93*(23), 13176–13181. https://doi.org/10.1073/pnas.93.23.13176

Shi, F., Deng, T., Mo, J., Wang, H., & Lu, J. (2021). An immune-related gene-based signature as prognostic tool in ovarian serous cystadenocarcinoma. *International Journal of General Medicine*, *14*, 4095–4104. https://doi.org/10.2147/IJGM.S313791

Shi, Z. D., Ji, X. Y., Qazi, H., & Tarbell, J. M. (2009). Interstitial flow promotes vascular fibroblast, myofibroblast, and smooth muscle cell motility in 3-D collagen I via upregulation of MMP-1. *American Journal of Physiology - Heart and Circulatory Physiology*, *297*(4). https://doi.org/10.1152/ajpheart.00369.2009

Shyy, Y. J., Hsieh, H. J., Usami, S., & Chien, S. (1994). Fluid shear stress induces a biphasic response of human monocyte chemotactic protein 1 gene expression in vascular endothelium. *Proceedings of the National Academy of Sciences of the United States of America*, *91*(11), 4678–4682. https://doi.org/10.1073/pnas.91.11.4678

Siesser, P. F., Motolese, M., Walker, M. P., Goldfarb, D., Gewain, K., Yan, F., Kulikauskas, R. M., Chien, A. J., Wordeman, L., & Major, M. B. (2012). FAM123A binds to microtubules and inhibits the guanine nucleotide exchange factor ARHGEF2 to decrease actomyosin contractility. *Science Signaling*, *5*(240), 1–15. https://doi.org/10.1126/scisignal.2002871

Simons, M., Gordon, E., & Claesson-Welsh, L. (2016). Mechanisms and regulation of endothelial VEGF receptor signalling. *Nature Reviews Molecular Cell Biology*, *17*(10), 611–625. https://doi.org/10.1038/nrm.2016.87

Simpson, L. J., Reader, J. S., & Tzima, E. (2020). Mechanical Regulation of Protein Translation in the Cardiovascular System. *Frontiers in Cell and Developmental Biology*, *8*(January), 1–13. https://doi.org/10.3389/fcell.2020.00034

Song, C., Gao, Y., Tian, Y., Han, X., Chen, Y., & Tian, D. L. (2013). Expression of p114RhoGEF predicts lymph node metastasis and poor survival of squamous-cell lung carcinoma patients. *Tumor Biology*, *34*(3), 1925–1933. https://doi.org/10.1007/s13277-013-0737-8

Song, J. tao, Hu, B., Qu, H. yan, Bi, C. long, Huang, X. zhen, & Zhang, M. (2012). Mechanical Stretch Modulates MicroRNA 21 Expression, Participating in Proliferation and Apoptosis in Cultured Human Aortic Smooth Muscle Cells. *PLoS ONE*, *7*(10), 1–10. https://doi.org/10.1371/journal.pone.0047657

Song, Y., Wu, Y., Su, X., Zhu, Y., Liu, L., Pan, Y., Zhu, B., Yang, L., Gao, L., & Li, M. (2016). Activation of AMPK inhibits PDGF-induced pulmonary arterial smooth muscle cells proliferation and its potential mechanisms. *Pharmacological Research*, *107*, 117–124. https://doi.org/10.1016/j.phrs.2016.03.010

Sotoudeh, M., Li, Y. S., Yajima, N., Chang, C. C., Tsou, T. C., Wang, Y., Usami, S., Ratcliffe, A., Chien, S., & Shyy, J. Y. J. (2002). Induction of apoptosis in vascular smooth muscle cells by

mechanical stretch. *American Journal of Physiology - Heart and Circulatory Physiology*, *282*(5 51-5), 1709–1716. https://doi.org/10.1152/ajpheart.00744.2001

Spittell, J. A. (1983). Hypertension and arterial aneurysm. *Journal of the American College of Cardiology*, *1*(2), 533–540. https://doi.org/10.1016/S0735-1097(83)80085-0

Stabley, D. R., Jurchenko, C., Marshall, S. S., & Salaita, K. S. (2012). Visualizing mechanical tension across membrane receptors with a fluorescent sensor. *Nature Methods*, *9*(1), 64–67. https://doi.org/10.1038/nmeth.1747

Stalcup, S. A., Davidson, D., & Mellins, R. B. (1982). ENDOTHELIAL CELL FUNCTIONS IN THE HEMODYNAMIC RESPONSES TO STRESS. *Annals of the New York Academy of Sciences*, *401*(1 Endothelium), 117–131. https://doi.org/10.1111/j.1749-6632.1982.tb25712.x

Stockton, R., Reutershan, J., Scott, D., Sanders, J., Ley, K., & Schwartz, M. A. (2007). Induction of vascular permeability: beta PIX and GIT1 scaffold the activation of extracellular signal-regulated kinase by PAK. *Molecular Biology of the Cell*, *18*(6), 2346–2355. https://doi.org/10.1091/mbc.e06-07-0584

Stoner, L., Erickson, M. L., Young, J. M., Fryer, S., Sabatier, M. J., Faulkner, J., Lambrick, D. M., & McCully, K. K. (2012). There's more to flow-mediated dilation than nitric oxide. *Journal of Atherosclerosis and Thrombosis*, *19*(7), 589–600. https://doi.org/10.5551/jat.11973

Strange, F., Gruter, B. E., Fandino, J., & Marbacher, S. (2020). Preclinical intracranial aneurysm models: A systematic review. *Brain Sciences*, *10*(3). https://doi.org/10.3390/brainsci10030134

Sulciner, D. J., Irani, K., Yu, Z. X., Ferrans, V. J., Goldschmidt-Clermont, P., & Finkel, T. (1996). rac1 regulates a cytokine-stimulated, redox-dependent pathway necessary for NF-kappaB activation. *Molecular and Cellular Biology*, *16*(12), 7115–7121. https://doi.org/10.1128/mcb.16.12.7115

Sullivan, G. W., Sarembock, I. J., & Linden, J. (2000). The role of inflammation in vascular diseases. *Journal of Leukocyte Biology*, *67*(5), 591–602. https://doi.org/10.1002/jlb.67.5.591

Sumimoto, H. (2008). Structure, regulation and evolution of Nox-family NADPH oxidases that produce reactive oxygen species. *FEBS Journal*, *275*(13), 3249–3277. https://doi.org/10.1111/j.1742-4658.2008.06488.x

Sumpio, B. E., Yun, S., Cordova, A. C., Haga, M., Zhang, J., Koh, Y., & Madri, J. A. (2005). MAPKs (ERK1/2, p38) and AKT can be phosphorylated by shear stress independently of platelet endothelial cell adhesion molecule-1 (CD31) in vascular endothelial cells. *Journal of Biological Chemistry*, *280*(12), 11185–11191. https://doi.org/10.1074/jbc.M414631200

Sundararaman, A., Fukushima, Y., Norman, J. C., Uemura, A., & Mellor, H. (2020). RhoJ

Regulates α5β1 Integrin Trafficking to Control Fibronectin Remodeling during Angiogenesis. *Current Biology*, *30*(11), 2146-2155.e5. https://doi.org/10.1016/j.cub.2020.03.042

Suri, C., Jones, P. F., Patan, S., Bartunkova, S., Maisonpierre, P. C., Davis, S., Sato, T. N., & Yancopoulos, G. D. (1996). Requisite role of angiopoietin-1, a ligand for the TIE2 receptor, during embryonic angiogenesis. *Cell*, *87*(7), 1171–1180. https://doi.org/10.1016/S0092-8674(00)81813-9

Swift, M. R., & Weinstein, B. M. (2009). Arterial-venous specification during development. *Circulation Research*, *104*(5), 576–588. https://doi.org/10.1161/CIRCRESAHA.108.188805

Taba, Y., Miyagi, M., Miwa, Y., Inoue, H., Takahashi-yanaga, F., Morimoto, S., Sasaguri, T., & Mori-, S. (2003). stress stabilize c-IAP1 in vascular endothelial cells. *Apoptosis*, 38–46.

Tada, S., & Tarbell, J. M. (2002). Flow through internal elastic lamina affects shear stress on smooth muscle cells (3D simulations). *American Journal of Physiology - Heart and Circulatory Physiology*, *282*(2 51-2), 1589–1597. https://doi.org/10.1152/ajpheart.00751.2001

Tada, Y., Wada, K., Shimada, K., Makino, H., Liang, E. I., Murakami, S., Kudo, M., Kitazato, K. T., Nagahiro, S., & Hashimoto, T. (2014). Roles of Hypertension in the Rupture of Intracranial Aneurysms. *Stroke*, *45*(2), 579–586. https://doi.org/10.1161/STROKEAHA.113.003072

Taddei, A., Giampietro, C., Conti, A., Orsenigo, F., Breviario, F., Pirazzoli, V., Potente, M., Daly, C., Dimmeler, S., & Dejana, E. (2008). Endothelial adherens junctions control tight junctions by VE-cadherin-mediated upregulation of claudin-5. *Nature Cell Biology*, *10*(8), 923–934. https://doi.org/10.1038/ncb1752

Takagi, H., & Umemoto, T. (2017). Association of Hypertension with Abdominal Aortic Aneurysm Expansion. *Annals of Vascular Surgery*, *39*, 74–89. https://doi.org/10.1016/j.avsg.2016.04.019

Takahashi, M., & Berk, B. C. (1996). Mitogen-activated protein kinase (ERK1/2) activation by shear stress and adhesion in endothelial cells. Essential role for a herbimycin-sensitive kinase. *Journal of Clinical Investigation*, *98*(11), 2623–2631. https://doi.org/10.1172/JCI119083

Takuji Tsuji, * Yusaku Ohta,*† Yuya Kanno,* Kenzo Hirose,† Kazumasa Ohashi,* and Kensaku Mizuno*. (2010). Involvement of p114-RhoGEF and Lfc in Wnt-3a– and Dishevelled-Induced RhoA Activation and Neurite Retraction in N1E-115 Mouse Neuroblastoma Cells. *Molecular Biology of the Cell* , *21*, 3590–3600.

Tan, J. L., Tien, J., Pirone, D. M., Gray, D. S., Bhadriraju, K., & Chen, C. S. (2003). Cells lying on a bed of microneedles: An approach to isolate mechanical force. *Proceedings of the*

National Academy of Sciences of the United States of America, *100*(4), 1484–1489. https://doi.org/10.1073/pnas.0235407100

Taylor, C. L., Yuan, Z., Selman, W. R., Ratcheson, R. A., & Rimm, A. A. (1995). Cerebral arterial aneurysm formation and rupture in 20,767 elderly patients: Hypertension and other risk factors. *Journal of Neurosurgery*, *83*(5), 812–819. https://doi.org/10.3171/jns.1995.83.5.0812

Teramoto, H., Crespo, P., Coso, O. A., Igishi, T., Xu, N., & Gutkind, J. S. (1996). The small GTP-binding protein Rho activates c-Jun N-terminal kinases/stress-activated protein kinases in human kidney 293T cells. Evidence for a Pak-independent signaling pathway. *Journal of Biological Chemistry*, *271*(42), 25731–25734. https://doi.org/10.1074/jbc.271.42.25731

Terry, S. J., Elbediwy, A., Zihni, C., Harris, A. R., Bailly, M., Charras, G. T., Balda, M. S., & Matter, K. (2012). Stimulation of Cortical Myosin Phosphorylation by p114RhoGEF Drives Cell Migration and Tumor Cell Invasion. *PLoS ONE*, *7*(11). https://doi.org/10.1371/journal.pone.0050188

Terry, S. J., Zihni, C., Elbediwy, A., Vitiello, E., San, I. V. L. C., Balda, M. S., & Matter, K. (2011). Spatially restricted activation of RhoA signalling at epithelial junctions by p114RhoGEF drives junction formation and morphogenesis. *Nature Cell Biology*, *13*(2), 159–166. https://doi.org/10.1038/ncb2156

Thompson, D. W. (1917). On Growth and Form. *Cambridge University Press*, *42*(20), 557. https://doi.org/10.2307/2019330

Timmerman, I., Heemskerk, N., Kroon, J., Schaefer, A., van Rijssel, J., Hoogenboezem, M., Unen, J. van, Goedhart, J., Gadella, T. W. J., Yin, T., Wu, Y., Huveneers, S., & van Buul, J. D. (2015). Correction to "A local VE-cadherin and Trio-based signaling complex stabilizes endothelial junctions through Rac1" [J. Cell Sci., 128, (2015), 3041-3054]. *Journal of Cell Science*, *128*(18), 3514. https://doi.org/10.1242/jcs.179424

Toppert, J. N., Cai, J., Qiu, Y., Anderson, K. R., Xu, Y. Y., Deeds, J. D., Feeley, R., Gimeno, C. J., Woolf, E. A., Tayber, O., Mays, G. G., Sampson, B. A., Schoen, F. J., Gimbrone, M. A., & Falb, D. (1997). Vascular MADs: Two novel MAD-related genes selectively inducible by flow in human vascular endothelium. *Proceedings of the National Academy of Sciences of the United States of America*, *94*(17), 9314–9319. https://doi.org/10.1073/pnas.94.17.9314

Tornavaca, O., Chia, M., Dufton, N., Almagro, L. O., Conway, D. E., Randi, A. M., Schwartz, M. A., Matter, K., & Balda, M. S. (2015). ZO-1 controls endothelial adherens junctions, cell-cell tension, angiogenesis, and barrier formation. *Journal of Cell Biology*, *208*(6), 821–838. https://doi.org/10.1083/jcb.201404140

Tse, S. W., Broderick, J. A., Wei, M. L., Luo, M. H., Smith, D., McCaffery, P., Stamm, S., &

Andreadis, A. (2005). Identification, expression analysis, genomic organization and cellular location of a novel protein with a RhoGEF domain. *Gene*, *359*(1–2), 63–72. https://doi.org/10.1016/j.gene.2005.06.025

Tseng, H., Peterson, T. E., & Berk, B. C. (1995). Fluid shear stress stimulates mitogen-activated protein kinase in endothelial cells. *Circulation Research*, *77*(5), 869–878. https://doi.org/10.1161/01.RES.77.5.869

Tsuji, T., Ishizaki, T., Okamoto, M., Higashida, C., Kimura, K., Furuyashiki, T., Arakawa, Y., Birge, R. B., Nakamoto, T., Hirai, H., & Narumiya, S. (2002). ROCK and mDia1 antagonize in Rho-dependent Rac activation in Swiss 3T3 fibroblasts. *Journal of Cell Biology*, *157*(5), 819–830. https://doi.org/10.1083/jcb.200112107

Tu, T. Y., & Chao, P. C. P. (2018). Continuous blood pressure measurement based on a neural network scheme applied with a cuffless sensor. *Microsystem Technologies*, *24*(11), 4539–4549. https://doi.org/10.1007/s00542-018-3957-4

Turton, K. B., Wilkerson, E. M., Hebert, A. S., Fogerty, F. J., Schira, H. M., Botros, F. E., Coon, J. J., & Mosher, D. F. (2018). Expression of novel "LOCGEF" isoforms of ARHGEF18 in eosinophils. *Journal of Leukocyte Biology*, *104*(1), 135–145. https://doi.org/10.1002/JLB.2MA1017-418RR

Tzima, E. (2006). Role of small GTPases in endothelial cytoskeletal dynamics and the shear stress response. In *Circulation Research* (Vol. 98, Issue 2, pp. 176–185). https://doi.org/10.1161/01.RES.0000200162.94463.d7

Tzima, E., Angel, M., Pozo, D., Kiosses, W. B., Mohamed, S. A., Li, S., Chien, S., & Schwartz, M. A. (2002). Activation of Rac1 by shear stress in endothelial cells mediates both cytoskeletal reorganization and effects on gene expression. *EMBO Journal*, *21*(24), 6791–6800.

Tzima, E., Del Pozo, M. A., Shattil, S. J., Chien, S., & Schwartz, M. A. (2001). Activation of integrins in endothelial cells by fluid shear stress mediates Rho-dependent cytoskeletal alignment. *EMBO Journal*, *20*(17), 4639–4647. https://doi.org/10.1093/emboj/20.17.4639

Tzima, E., Irani-Tehrani, M., Kiosses, W. B., Dejana, E., Schultz, D. A., Engelhardt, B., Cao, G., DeLisser, H., & Schwartz, M. A. (2005). A mechanosensory complex that mediates the endothelial cell response to fluid shear stress. *Nature*, *437*(7057), 426–431. https://doi.org/10.1038/nature03952

Tzima, E., Kiosses, W. B., Del Pozo, M. A., & Schwartz, M. A. (2003). Localized Cdc42 activation, detected using a novel assay, mediates microtubule organizing center positioning in endothelial cells in response to fluid shear stress. *Journal of Biological Chemistry*, *278*(33), 31020–31023. https://doi.org/10.1074/jbc.M301179200

Urade, R., Chiu, Y. H., Chiu, C. C., & Wu, C. Y. (2022). Small GTPases and Their Regulators: A Leading Road toward Blood Vessel Development in Zebrafish. *International Journal of Molecular Sciences*, *23*(9). https://doi.org/10.3390/ijms23094991

Uray, I. P., & Uray, K. (2021). Mechanotransduction at the plasma membrane-cytoskeleton interface. In *International Journal of Molecular Sciences* (Vol. 22, Issue 21). MDPI. https://doi.org/10.3390/ijms222111566

Van Buul, J. D., Allingham, M. J., Samson, T., Meller, J., Boulter, E., García-Mata, R., & Burridge, K. (2007). RhoG regulates endothelial apical cup assembly downstream from ICAM1 engagement and is involved in leukocyte trans-endothelial migration. *Journal of Cell Biology*, *178*(7), 1279–1293. https://doi.org/10.1083/jcb.200612053

Van Buul, J. D., Geerts, D., & Huveneers, S. (2014). Rho GAPs and GEFs: Controling switches in endothelial cell adhesion. *Cell Adhesion and Migration*, *8*(2), 108–124. https://doi.org/10.4161/cam.27599

Van Den Berg, B. M., Spaan, J. A. E., Rolf, T. M., & Vink, H. (2006). Atherogenic region and diet diminish glycocalyx dimension and increase intima-to-media ratios at murine carotid artery bifurcation. *American Journal of Physiology - Heart and Circulatory Physiology*, *290*(2), 915–920. https://doi.org/10.1152/ajpheart.00051.2005

van Rijssel, J., Hoogenboezem, M., Wester, L., Hordijk, P. L., & van Buul, J. D. (2012). The N-terminal DH-PH domain of trio induces cell spreading and migration by regulating lamellipodia dynamics in a Rac1-dependent fashion. *PLoS ONE*, *7*(1), 1–13. https://doi.org/10.1371/journal.pone.0029912

Van Rijssel, J., Kroon, J., Hoogenboezem, M., Van Alphen, F. P. J., De Jong, R. J., Kostadinova, E., Geerts, D., Hordijk, P. L., & Van Buul, J. D. (2012). The Rho-guanine nucleotide exchange factor Trio controls leukocyte transendothelial migration by promoting docking structure formation. *Molecular Biology of the Cell*, *23*(15), 2831–2844. https://doi.org/10.1091/mbc.E11-11-0907

VanderLaan, P. A., Reardon, C. A., & Getz, G. S. (2004). Site Specificity of Atherosclerosis: Site-Selective Responses to Atherosclerotic Modulators. *Arteriosclerosis, Thrombosis, and Vascular Biology*, *24*(1), 12–22. https://doi.org/10.1161/01.ATV.0000105054.43931.f0

Vartiainen, M. K., Guettler, S., Larijani, B., & Treisman, R. (2007). Nuclear actin regulates dynamic subcellular localization and activity of the SRF cofactor MAL. *Science*, *316*(5832), 1749–1752. https://doi.org/10.1126/science.1141084

Vega, F. M., & Ridley, A. J. (2008). Rho GTPases in cancer cell biology. *FEBS Letters*, *582*(14), 2093–2101. https://doi.org/10.1016/j.febslet.2008.04.039

Vigil, D., Cherfils, J., Rossman, K. L., & Der, C. J. (2010). Ras superfamily GEFs and GAPs: Validated and tractable targets for cancer therapy? *Nature Reviews Cancer*, *10*(12), 842–857. https://doi.org/10.1038/nrc2960

Vion, A. (2022). *ARHGEF26 : a new player in vascular endothelial growth factor receptor 2 traf fi cking*. 1–2. https://doi.org/10.1093/cvr/cvab344.3.

Vion, A. C., Alt, S., Klaus-Bergmann, A., Szymborska, A., Zheng, T., Perovic, T., Hammoutene, A., Oliveira, M. B., Bartels-Klein, E., Hollfinger, I., Rautou, P. E., Bernabeu, M. O., & Gerhardt, H. (2018). Primary cilia sensitize endothelial cells to BMP and prevent excessive vascular regression. *Journal of Cell Biology*, *217*(5), 1651–1665. https://doi.org/10.1083/jcb.201706151

Wakayama, Y., Fukuhara, S., Ando, K., Matsuda, M., & Mochizuki, N. (2015). Cdc42 mediates Bmp - Induced sprouting angiogenesis through Fmnl3-driven assembly of endothelial filopodia in zebrafish. *Developmental Cell*, *32*(1), 109–122. https://doi.org/10.1016/j.devcel.2014.11.024

Wang, W. Bin, Li, H. P., Yan, J., Zhuang, F., Bao, M., Liu, J. T., Qi, Y. X., & Han, Y. (2019). CTGF regulates cyclic stretch-induced vascular smooth muscle cell proliferation via microRNA-19b-3p. *Experimental Cell Research*, *376*(1), 77–85. https://doi.org/10.1016/j.yexcr.2019.01.015

Wang, D., Paria, B. C., Zhang, Q., Karpurapu, M., Li, Q., Gerthoffer, W. T., Nakaoka, Y., & Rao, G. N. (2009). A role for Gab1/SHP2 in thrombin activation of PAK1: Gene transfer of kinase-dead pak1 inhibits injury-induced restenosis. *Circulation Research*, *104*(9), 1066–1075. https://doi.org/10.1161/CIRCRESAHA.109.196691

Wang, J., Jiang, J., Yang, X., Zhou, G., Wang, L., & Xiao, B. (2022). Tethering Piezo channels to the actin cytoskeleton for mechanogating via the cadherin-β-catenin mechanotransduction complex. *Cell Reports*, *38*(6), 110342. https://doi.org/10.1016/j.celrep.2022.110342

Wang, N., Butler, J. P., & Ingber, D. E. (1993). Mechanotransduction across the cell surface and through the cytoskeleton. *Science (New York, N.Y.)*, *260*(5111), 1124–1127. https://doi.org/10.1126/science.7684161

Wang, S. P., Chennupati, R., Kaur, H., Iring, A., Wettschureck, N., & Offermanns, S. (2016). Endothelial cation channel PIEZO1 controls blood pressure by mediating flow-induced ATP release. *Journal of Clinical Investigation*, *126*(12), 4527–4536. https://doi.org/10.1172/JCI87343

Wang, Y., Martin-McNulty, B., da Cunha, V., Vincelette, J., Lu, X., Feng, Q., Halks-Miller, M., Mahmoudi, M., Schroeder, M., Subramanyam, B., Tseng, J.-L., Deng, G. D., Schirm, S.,

Johns, A., Kauser, K., Dole, W. P., & Light, D. R. (2005). Fasudil, a Rho-Kinase Inhibitor, Attenuates Angiotensin II–Induced Abdominal Aortic Aneurysm in Apolipoprotein E–Deficient Mice by Inhibiting Apoptosis and Proteolysis. *Circulation*, *111*(17), 2219–2226. https://doi.org/10.1161/01.CIR.0000163544.17221.BE

Wei, S., Ning, G., Li, L., Yan, Y., Yang, S., Cao, Y., & Wang, Q. (2017). A GEF activity-independent function for nuclear Net1 in Nodal signal transduction and mesendoderm formation. *Journal of Cell Science*, *130*(18), 3072–3082. https://doi.org/10.1242/jcs.204917

Wessel, F., Winderlich, M., Holm, M., Frye, M., Rivera-Galdos, R., Vockel, M., Linnepe, R., Ipe, U., Stadtmann, A., Zarbock, A., Nottebaum, A. F., & Vestweber, D. (2014). Leukocyte extravasation and vascular permeability are each controlled in vivo by different tyrosine residues of VE-cadherin. *Nature Immunology*, *15*(3), 223–230. https://doi.org/10.1038/ni.2824

Wirth, A., Benyó, Z., Lukasova, M., Leutgeb, B., Wettschureck, N., Gorbey, S., Orsy, P., Horváth, B., Maser-Gluth, C., Greiner, E., Lemmer, B., Schütz, G., Gutkind, S., & Offermanns, S. (2008). G12-G13-LARG-mediated signaling in vascular smooth muscle is required for salt-induced hypertension. *Nature Medicine*, *14*(1), 64–68. https://doi.org/10.1038/nm1666

Witmer, A. N., Dai, J., Weich, H. A., Vrensen, G. F. J. M., & Schlingemann, R. O. (2002). Expression of vascular endothelial growth factor receptors 1, 2, and 3 in quiescent endothelia. *Journal of Histochemistry and Cytochemistry*, *50*(6), 767–777. https://doi.org/10.1177/002215540205000603

Wojciak-Stothard, B., & Ridley, A. J. (2003). Shear stress-induced endothelial cell polarization is mediated by Rho and Rac but not Cdc42 or PI 3-kinases. *Journal of Cell Biology*, *161*(2), 429–439. https://doi.org/10.1083/jcb.200210135

Wolfrum, S., Dendorfer, A., Rikitake, Y., Stalker, T. J., Gong, Y., Scalia, R., Dominiak, P., & Liao, J. K. (2004). Inhibition of Rho-kinase leads to rapid activation of phosphatidylinositol 3-kinase/protein kinase Akt and cardiovascular protection. *Arteriosclerosis, Thrombosis, and Vascular Biology*, *24*(10), 1842–1847. https://doi.org/10.1161/01.ATV.0000142813.33538.82

Wood, K. C., Cortese-Krott, M. M., Kovacic, J. C., Noguchi, A., Liu, V. B., Wang, X., Raghavachari, N., Boehm, M., Kato, G. J., Kelm, M., & Gladwin, M. T. (2013). Circulating blood endothelial nitric oxide synthase contributes to the regulation of systemic blood pressure and nitrite homeostasis. *Arteriosclerosis, Thrombosis, and Vascular Biology*, *33*(8), 1861–1871. https://doi.org/10.1161/ATVBAHA.112.301068

Wu, T., Hu, E., Xu, S., Chen, M., Guo, P., Dai, Z., Feng, T., Zhou, L., Tang, W., Zhan, L., Fu, X., Liu, S., Bo, X., & Yu, G. (2021). clusterProfiler 4.0: A universal enrichment tool for

interpreting omics data. *The Innovation*, *2*(3), 100141. https://doi.org/10.1016/j.xinn.2021.100141

Xanthis, I., Souilhol, C., Serbanovic-Canic, J., Roddie, H., Kalli, A. C., Fragiadaki, M., Wong, R., Shah, D. R., Askari, J. A., Canham, L., Akhtar, N., Feng, S., Ridger, V., Waltho, J., Pinteaux, E., Humphries, M. J., Bryan, M. T., & Evans, P. C. (2019). B1 Integrin Is a Sensor of Blood Flow Direction. *Journal of Cell Science*, *132*(11). https://doi.org/10.1242/JCS.229542

Xie, Z., Nagarajan, V., Sturdevant, D. E., Iwaki, S., Chan, E., Wisch, L., Young, M., Nelson, C. M., Porcella, S. F., & Druey, K. M. (2013). Genome-wide SNP analysis of the Systemic Capillary Leak Syndrome (Clarkson disease). *Rare Diseases*, *1*(1), e27445. https://doi.org/10.4161/rdis.27445

Xiong, L., Kou, F., Yang, Y., & Wu, J. (2007). A novel role for IGF-1R in p53-mediated apoptosis through translational modulation of the p53-Mdm2 feedback loop. *Journal of Cell Biology*, *178*(6), 995–1007. https://doi.org/10.1083/jcb.200703044

Xu, J., Mathur, J., Vessières, E., Hammack, S., Nonomura, K., Favre, J., Grimaud, L., Petrus, M., Francisco, A., Li, J., Lee, V., Xiang, F. li, Mainquist, J. K., Cahalan, S. M., Orth, A. P., Walker, J. R., Ma, S., Lukacs, V., Bordone, L., … Patapoutian, A. (2018). GPR68 Senses Flow and Is Essential for Vascular Physiology. *Cell*, *173*(3), 762-775.e16. https://doi.org/10.1016/j.cell.2018.03.076

Xu, X., Jin, D., Durgan, J., & Hall, A. (2013). LKB1 Controls Human Bronchial Epithelial Morphogenesis through p114RhoGEF-Dependent RhoA Activation. *Molecular and Cellular Biology*, *33*(14), 2671–2682. https://doi.org/10.1128/mcb.00154-13

Yamawaki, H., Lehoux, S., & Berk, B. C. (2003). Chronic physiological shear stress inhibits tumor necrosis factor-induced proinflammatory responses in rabbit aorta perfused ex vivo. *Circulation*, *108*(13), 1619–1625. https://doi.org/10.1161/01.CIR.0000089373.49941.C4

Yanazume, T., Hasegawa, K., Wada, H., Morimoto, T., Abe, M., Kawamura, T., & Sasayama, S. (2002). Rho/ROCK pathway contributes to the activation of extracellular signal-regulated kinase/GATA-4 during myocardial cell hypertrophy. *Journal of Biological Chemistry*, *277*(10), 8618–8625. https://doi.org/10.1074/jbc.M107924200

Yang, B., & Rizzo, V. (2013). Shear stress activates eNOS at the endothelial apical surface through β1 containing integrins and caveolae. *Cellular and Molecular Bioengineering*, *6*(3), 346–354. https://doi.org/10.1007/s12195-013-0276-9

Yang, N., Higuchi, O., Ohashi, K., Nagata, K., Wada, A., Kangawa, K., Nishida, E., & Mizuno, K. (1998). Cofflin phosphorylation by LIM-kinase 1 and its role in Rac-mediated actin reorganization. *Nature*, *393*(6687), 809–812. https://doi.org/10.1038/31735

Yang, X., Li, J., Fang, Y., Zhang, Z., Jin, D., Chen, X., Zhao, Y., Li, M., Huan, L., Kent, T. A., Dong, J. F., Jiang, R., Yang, S., Jin, L., Zhang, J., Zhong, T. P., & Yu, F. (2018a). Rho Guanine Nucleotide Exchange Factor ARHGEF17 Is a Risk Gene for Intracranial Aneurysms. *Circulation. Genomic and Precision Medicine*, *11*(7), e002099. https://doi.org/10.1161/CIRCGEN.117.002099

Yang, X., Li, J., Fang, Y., Zhang, Z., Jin, D., Chen, X., Zhao, Y., Li, M., Huan, L., Kent, T. A., Dong, J. F., Jiang, R., Yang, S., Jin, L., Zhang, J., Zhong, T. P., & Yu, F. (2018b). Rho Guanine Nucleotide Exchange Factor ARHGEF17 Is a Risk Gene for Intracranial Aneurysms. *Circulation. Genomic and Precision Medicine*, *11*(7), e002099. https://doi.org/10.1161/CIRCGEN.117.002099

Ye, G. J. C., Nesmith, A. P., & Parker, K. K. (2014). The role of mechanotransduction on vascular smooth muscle myocytes cytoskeleton and contractile function. *Anatomical Record*, *297*(9), 1758–1769. https://doi.org/10.1002/ar.22983

Yeh, J. C., Otte, L. A., & Frangos, J. A. (2008). Regulation of G protein-coupled receptor activities by the platelet-endothelial cell adhesion molecule, PECAM-1. *Biochemistry*, *47*(34), 9029–9039. https://doi.org/10.1021/bi8003846

Yoo, S. K., Deng, Q., Cavnar, P. J., Wu, Y. I., Hahn, K. M., & Huttenlocher, A. (2010). Differential Regulation of Protrusion and Polarity by PI(3)K during Neutrophil Motility in Live Zebrafish. *Developmental Cell*, *18*(2), 226–236. https://doi.org/10.1016/j.devcel.2009.11.015

Yoon, Y. S., Choo, J. H., Yoo, T., Kang, K., & Chung, J. H. (2007). RhoB is epigenetically regulated in an age- and tissue-specific manner. *Biochemical and Biophysical Research Communications*, *362*(1), 164–169. https://doi.org/10.1016/j.bbrc.2007.08.002

Yoshida, Y., Yamada, A., Akimoto, Y., Abe, K., Matsubara, S., Hayakawa, J., Tanaka, J., Kinoshita, M., Kato, T., Ogata, H., Sakashita, A., Mishima, K., Kubota, Y., Kawakami, H., Kamijo, R., & Iijima, T. (2021). Cdc42 has important roles in postnatal angiogenesis and vasculature formation. *Developmental Biology*, *477*(February 2019), 64–69. https://doi.org/10.1016/j.ydbio.2021.05.002

Yu, G., Wang, L. G., Han, Y., & He, Q. Y. (2012). ClusterProfiler: An R package for comparing biological themes among gene clusters. *OMICS A Journal of Integrative Biology*, *16*(5), 284–287. https://doi.org/10.1089/omi.2011.0118

Yu, J., Bergaya, S., Murata, T., Alp, I. F., Bauer, M. P., Lin, M. I., Drab, M., Kurzchalia, T. V., Stan, R. V., & Sessa, W. C. (2006). Direct evidence for the role of caveolin-1 and caveolae in mechanotransduction and remodeling of blood vessels. *Journal of Clinical Investigation*, *116*(5), 1284–1291. https://doi.org/10.1172/JCI27100

Yuan, L., Sacharidou, A., Stratman, A. N., Le Bras, A., Zwiers, P. J., Spokes, K., Bhasin, M., Shih, S. C., Nagy, J. A., Molema, G., Aird, W. C., Davis, G. E., & Oettgen, P. (2011). RhoJ is an endothelial cell-restricted Rho GTPase that mediates vascular morphogenesis and is regulated by the transcription factor ERG. *Blood*, *118*(4), 1145–1153. https://doi.org/10.1182/blood-2010-10-315275

Yzaguirre, A. D., Padmanabhan, A., De Groh, E. D., Engleka, K. A., Li, J., Speck, N. A., & Epstein, J. A. (2015). Loss of neurofibromin Ras-GAP activity enhances the formation of cardiac blood islands in murine embryos. *ELife*, *4*(OCTOBER2015), 1–19. https://doi.org/10.7554/eLife.07780

Zaritsky, A., Tseng, Y. Y., Rabadán, M. A., Krishna, S., Overholtzer, M., Danuser, G., & Hall, A. (2017). Diverse roles of guanine nucleotide exchange factors in regulating collective cell migration. *Journal of Cell Biology*, *216*(6), 1543–1556. https://doi.org/10.1083/jcb.201609095

Zhang, M., Ren, Y., Wang, Y., Wang, R., Zhou, Q., Peng, Y., Li, Q., Yu, M., & Jiang, Y. (2015). Regulation of Smooth Muscle Contractility by Competing Endogenous mRNAs in Intracranial Aneurysms. *Journal of Neuropathology and Experimental Neurology*, *74*(5), 411–424. https://doi.org/10.1097/NEN.0000000000000185

Zhang, S., Han, J., Sells, M. A., Chernoff, J., Knaus, U. G., Ulevitch, R. J., & Bokoch, G. M. (1995). Rho family GTPases regulate p38 mitogen-activated protein kinase through the downstream mediator Pak1. *Journal of Biological Chemistry*, *270*(41), 23934–23936. https://doi.org/10.1074/jbc.270.41.23934

Zhang, Y., Xia, P., Zhang, W., Yan, M., Xiong, X., Yu, W., & Song, E. (2017). Short interfering RNA targeting Net1 reduces the angiogenesis and tumor growth of in vivo cervical squamous cell carcinoma through VEGF down-regulation. *Human Pathology*, *65*, 113–122. https://doi.org/10.1016/j.humpath.2017.04.021

Zhao, J., Nishimura, Y., Kimura, A., Ozawa, K., Kondo, T., Tanaka, T., & Yoshizumi, M. (2017). Chemokines protect vascular smooth muscle cells from cell death induced by cyclic mechanical stretch. *Scientific Reports*, *7*(1), 1–9. https://doi.org/10.1038/s41598-017-15867-8

Zhao, Q., Zhang, K., Li, Z., Zhang, H., Fu, F., Fu, J., Zheng, M., & Zhang, S. (2021). High Migration and Invasion Ability of PGCCs and Their Daughter Cells Associated With the Nuclear Localization of S100A10 Modified by SUMOylation. *Frontiers in Cell and Developmental Biology*, *9*. https://doi.org/10.3389/fcell.2021.696871

Zhao, Y., Vanhoutte, P. M., & Leung, S. W. S. (2015a). Vascular nitric oxide: Beyond eNOS. *Journal of Pharmacological Sciences*, *129*(2), 83–94. https://doi.org/10.1016/j.jphs.2015.09.002

Zhao, Y., Vanhoutte, P. M., & Leung, S. W. S. (2015b). Vascular nitric oxide: Beyond eNOS. *Journal of Pharmacological Sciences*, *129*(2), 83–94. https://doi.org/10.1016/j.jphs.2015.09.002

Zhao, Y. Y., Zhao, Y. D., Mirza, M. K., Huang, J. H., Potula, H. H. S. K., Vogel, S. M., Brovkovych, V., Yuan, J. X. J., Wharton, J., & Malik, A. B. (2009). Persistent eNOS activation secondary to caveolin-1 deficiency induces pulmonary hypertension in mice and humans through PKG nitration. *Journal of Clinical Investigation*, *119*(7), 2009–2018. https://doi.org/10.1172/JCI33338

Zholdybayeva, E. V., Medetov, Y. Z., Aitkulova, A. M., Makhambetov, Y. T., Akshulakov, S. K., Kaliyev, A. B., Talzhanov, Y. A., Kulmambetova, G. N., Iskakova, A. N., & Ramankulov, Y. M. (2018). Genetic Risk Factors for Intracranial Aneurysm in the Kazakh Population. *Journal of Molecular Neuroscience*, *66*(1), 135–145. https://doi.org/10.1007/s12031-018-1134-y

Zhu, L., Yang, H., Chao, Y., Gu, Y., Zhang, J., Wang, F., Yu, W., Ye, P., Chu, P., Kong, X., & Chen, S. (2021). Akt phosphorylation regulated by IKKε in response to low shear stress leads to endothelial inflammation via activating IRF3. *Cellular Signalling*, *80*(September 2020), 109900. https://doi.org/10.1016/j.cellsig.2020.109900

Zhu, Q. M., MacDonald, B. T., Mizoguchi, T., Chaffin, M., Leed, A., Arduini, A., Malolepsza, E., Lage, K., Kaushik, V. K., Kathiresan, S., & Ellinor, P. T. (2021). Endothelial ARHGEF26 is an angiogenic factor promoting VEGF signalling. *Cardiovascular Research*, 1–14. https://doi.org/10.1093/cvr/cvab344

Zinn, A., Goicoechea, S. M., Kreider-Letterman, G., Maity, D., Awadia, S., Cedeno-Rosario, L., Chen, Y., & Garcia-Mata, R. (2019). The small GTPase RhoG regulates microtubule-mediated focal adhesion disassembly. *Scientific Reports*, *9*(1), 1–15. https://doi.org/10.1038/s41598-019-41558-7

Zou, Y., Akazawa, H., Qin, Y., Sano, M., Takano, H., Minamino, T., Makita, N., Iwanaga, K., Zhu, W., Kudoh, S., Toko, H., Tamura, K., Kihara, M., Nagai, T., Fukamizu, A., Umemura, S., Iiri, T., Fujita, T., & Komuro, I. (2004). Mechanical stress activates angiotensin II type 1 receptor without the involvement of angiotensin II. *Nature Cell Biology*, *6*(6), 499–506. https://doi.org/10.1038/ncb1137

DOCTORAT BIOLOGIE BRETAGNE SANTE LOIRE

Nantes Université

Titre : Identification des facteurs d'échange de guanine-nucléotides (GEF) mécanosensibles : Rôle dans l'homéostasie vasculaire

Mots clés : Hémodynamique, Cellules Vasculaires, Arhgef18, GEF

Résumé : Les forces hémodynamiques jouent un rôle important dans le développement et l'homéostasie du réseau vasculaire. Les cellules endothéliales (CE) et les cellules musculaires lisses (VSMC), composant la paroi vasculaire, répondent à ces forces en réorganisant leur cytosquelette. Une altération des forces hémodynamiques provoque une alteration de ce cytosquelette et conduit à la survenue de pathologies vasculaires tels que l'athérosclérose et les anévrismes. Les facteurs d'échange de nucléotides de guanine (GEFs) médient l'activation spatio-temporelle des petites GTPases (RhoA, Rac1, Cdc42), acteurs clés de la dynamique du cytosquelette. L'identification des GEFs mécano-sensibles pourrait donc fournir de nouvelles cibles thérapeutiques dans les pathologies vasculaires. Un séquençage ARN effectuée sur des CE et des VSMC soumises à différentes forces hémodynamiques a permis d'identifier ARHGEF18 et ARHGEF40 dans les CE ainsi que NET1 dans les VSMCs comme des GEFs mecano-sensibles potentiels. Dans les CE, les contraintes de cisaillement pathologiques (3,6 et 36 dynes/cm2) réduisent l'activité d'Arhgef18 en comparaison aux contraintes de cisaillement physiologiques (16 dynes/cm2). De plus, Arhegf18 interagit uniquement avec RhoA mais l'extinction d'Arhgef18 réduit à la fois l'activité de RhoA et de Rac1. Les CEs déficientes en Arhgef18 ont une adhésion et une migration réduite en comparaison aux CEs contrôle. Sous contraintes de cisaillement physiologiques, l'extinction d'Arhgef18 altère l'alignement des CE dans le sens du flux et la localisation de ZO-1 et Claudin5 aux jonctions. Enfin, l'extinction d'Arhgef18 réduit de manière significative l'expression de COX2 médiée par TNFα. Ces résultats identifient Arhgef18 comme un GEF mécano-sensible qui joue un rôle important dans la physiologie des CEs et la prévention de l'inflammation et pourrait donc prévenir la survenue de pathologies vasculaires.

Title : Identification of Mechanosensitive Guanine Nucleotide Exchange Factors (GEFs): Role in Vascular Homeostasis

Keywords : Hemodynamics, Vascular cells, Arhgef18, GEF.

Abstract : Hemodynamic forces play an important role in the vascular network development and homeostasis. Altered hemodynamic forces have been shown to associate with vascular disorders such as atherosclerosis and aneurysms. Cytoskeletal rearrangement is the primary response of vascular cells such as endothelial cells (ECs) and smooth muscle cells (VSMCs) to hemodynamic forces and irregular cytoskeletal arrangements has been observed in areas prone to vascular disorders in vivo. Guanine nucleotide exchange factors (GEFs) mediate spatio-temporal activation of small-GTPases (RhoA, Rac1, Cdc42), which are key players of cytoskeletal dynamics. Identifying mechanosensitive GEFs may provide new potential therapeutic targets to treat vascular disorders. RNA sequencing performed on ECs and VSMCs subjected to various shear stress and cyclic stretch levels respectively, identified ARHGEF18, ARHGEF40 in ECs and NET1 in VSMCs as potential mechanosensitive GEFs. In ECs, pathological (3.6 & 36 dynes/cm^2) shear stress reduced Arhgef18 activity compared to physiological (16 dynes/cm^2) shear stress. In our hands, Arhgef18 interact with RhoA only but knocking down of Arhgef18 reduces both RhoA and Rac1 activity. Moreover, ECs silenced for Arhgef18 showed reduced adhesion and migration under static conditions. Under physiological shear stress conditions, loss of Arhgef18 altered cell alignment and junctional protein localization. Furthermore, knockdown of Arhgef18 significantly reduced TNFα mediated COX2 expression. These findings Identified Arhgef18 as a potential mechanosensitive GEF that plays important role in ECs physiology and inflammation thereby vascular diseases.